



HAL
open science

THE UNIFIED MODEL OF ELECTROWEAK INTERACTIONS AND APPLICATION TO NEUTRINO PHENOMENOLOGY

P. Aurenche, J. Ph. Guillet

► **To cite this version:**

P. Aurenche, J. Ph. Guillet. THE UNIFIED MODEL OF ELECTROWEAK INTERACTIONS AND APPLICATION TO NEUTRINO PHENOMENOLOGY. Doctoral. France. 2018. hal-02477889

HAL Id: hal-02477889

<https://cel.hal.science/hal-02477889>

Submitted on 13 Feb 2020

HAL is a multi-disciplinary open access archive for the deposit and dissemination of scientific research documents, whether they are published or not. The documents may come from teaching and research institutions in France or abroad, or from public or private research centers.

L'archive ouverte pluridisciplinaire **HAL**, est destinée au dépôt et à la diffusion de documents scientifiques de niveau recherche, publiés ou non, émanant des établissements d'enseignement et de recherche français ou étrangers, des laboratoires publics ou privés.

**THE UNIFIED MODEL OF ELECTROWEAK INTERACTIONS
AND APPLICATION TO NEUTRINO PHENOMENOLOGY**

P. Aurenche^a, J. Ph. Guillet^b

LAPTh, Univ. Grenoble Alpes, USMB, CNRS, F-74000 Annecy, France

Abstract

The unified model of electroweak interactions (Glashow-Weinberg-Salam model) is constructed step by step. As an application, the phenomenology of neutrino mixing, in the framework of the three-family model, is discussed in detail. Numerous formulae for appearance or disappearance of neutrinos in vacuum or in matter are derived. These notes should provide a self-contained introduction to the GWS model and to neutrino mixing and oscillations. Recent experimental results on neutrino oscillations are briefly reviewed.

^a aurenche@lapth.cnrs.fr

^b guillet@lapth.cnrs.fr

The following notes are rather detailed so that a student who does not have a proper academic environment in particle physics can find them self-sufficient. The prerequisite is a course on advanced quantum mechanics and some knowledge on the notion of invariant scattering amplitudes and Feynman rules for fermions and bosons.

These notes are available at the following URL : https://lectures.lapth.cnrs.fr/standard_model where some exercices on the calculation of particle production and decay can be found.

We thank Pasquale Serpico for very informative discussions on neutrinos and astrophysics and for carefully reading the corresponding chapters.

Contents

1	Introduction	6
2	The Fermi theory and its extensions	8
2.1	Contact interactions	8
2.2	Vector boson mediated interactions	11
2.3	Still more problems!	13
3	Fermions, chirality, helicity	18
3.1	Fermions : chirality	18
3.2	Fermions : positive and negative energy solutions	18
3.3	Fermions : helicity	20
4	The global $SU(2)_L \otimes U(1)_Y$ gauge invariance : conserved currents	26
4.1	Global gauge invariance and Noether theorem	26
4.2	The lagrangian density	28
4.3	The global $SU(2)_L$ gauge invariance	28
4.4	The global $U(1)_Y$ gauge invariance	29
5	The local $SU(2)_L \otimes U(1)_Y$ gauge invariance : interactions	32
5.1	Fermion-boson interactions, construction of the photon and the Z boson	35
5.2	Gauge bosons and their self-interactions	38
5.3	Progress status and problems	41
6	Spontaneous symmetry breaking under a global phase change	43
6.1	Global symmetry breaking	43
6.2	The Goldstone theorem	44
7	Spontaneous local $U(1)$ symmetry breaking	47
7.1	Unitary gauge	47
7.2	Renormalisable gauges : 't Hooft R_ξ gauges	49
7.3	Fermion masses	51
7.4	Gauge invariance at the Born level: an exemple	52

8	The broken $SU(2)_L \otimes U(1)_Y$ symmetry	55
8.1	Local symmetry breaking and the Brout-Englert-Higgs mechanism	56
8.2	The Higgs and gauge bosons sector : masses and couplings	56
8.3	The Yukawa lagrangian \mathcal{L}_Y and fermion masses and couplings	60
8.4	The Higgs boson discovery	62
8.5	Conclusions	64
9	Exercise : study of the reaction proton + proton \rightarrow H + X	65
9.1	The gluon-gluon fusion mechanism	65
9.2	Function Li_2	71
9.3	Different rewriting of the function $J(z)$	72
10	Exercises: Higgs boson decays	75
10.1	Kinematics	75
10.2	Higgs decay into a fermion anti-fermion pair	75
10.3	Higgs decay into a $W^+ W^-$ pair	76
10.4	Higgs decay in a $\gamma \gamma$ pair	77
	10.4.1 W boson loop	77
	10.4.2 Fermion loops	82
10.5	Final result	82
11	Family mixing and the Kobayashi-Maskawa matrix	84
12	Neutrinos and the Pontecorvo-Maki-Nakagawa-Sakata matrix	89
12.1	Neutrino survival and oscillation	91
12.2	Summary of results	93
12.3	Survival probabilities in vacuum	95
12.4	Oscillation in vacuum, \mathcal{CP} asymmetries, mass hierarchy and δ	96
13	Neutrinos interactions with matter	100
13.1	Incoherent scattering	101
13.2	Coherent scattering	101
13.3	Matter of constant density	103
13.4	Matter of varying density: ν_e in the sun	105
13.5	Neutrinos through the earth	108

14 Neutrino experiments	113
14.1 Nuclear reactors : KamLAND, Double-Chooz, Daya Bay, RENO	114
14.1.1 Long baseline: KamLAND, $\delta\mathbf{m}_{21}^2, \theta_{12}$	114
14.1.2 Short baseline: Double-Chooz, Daya Bay, RENO, $\delta\mathbf{m}_{31}^2, \theta_{13}$	115
14.2 Neutrinos from accelerators: T2K, NO ν A and OPERA ; $\delta\mathbf{m}_{32}^2, \theta_{23}, \delta$	116
14.3 Atmospheric neutrinos: Super-Kamiokande ; $\delta\mathbf{m}_{32}^2, \theta_{23}, \delta$	120
14.4 Solar neutrinos: SNO ; $\delta\mathbf{m}_{12}^2, \theta_{12}$	124
14.5 Ultra-high energy or cosmic neutrinos	129
14.6 Problems?	135
14.7 Neutrinos: conclusions	137
15 Majorana neutrinos	140
15.1 Majorana mass term for neutrinos	140
15.2 Neutrino masses and the see-saw mechanism	142
16 Conclusions	146
Appendix A Properties of γ^μ matrices	148
Appendix B Charge conjugation \mathcal{C}, space reflection \mathcal{P}, time reversal \mathcal{T}	150
B.1 Charge conjugation \mathcal{C}	150
B.2 Space reflection \mathcal{P}	152
B.3 Variance and invariance of the lagrangien under \mathcal{C} and \mathcal{CP}	154
B.4 Time reflection \mathcal{T}	155
Appendix C Feynman rules of the Glashow-Weinberg-Salam model	157
C.1 Propagators	157
C.2 Vertices	157

1 Introduction

From the experimental point of view the world of “elementary particles” consists in:

– *leptons*: they have spin $\frac{1}{2}$ and come in three doublets, (e^-, ν_e) the electron and its associated neutrino, (μ^-, ν_μ) the muon and its neutrino, (τ^-, ν_τ) the tau and its neutrino.

– *vector bosons*: they have spin 1 and there is a massless boson, the photon, and three massive ones, the W^+ , W^- and the Z .

– *hadrons*: one distinguishes mesons of integer spin ($S = 0, 1, \dots$) from baryons of half-integer spin ($S = \frac{1}{2}, \frac{3}{2}, \dots$). The *hadrons* have been known for a long time to have a finite size (typically of the order of 1 fm) and there exist so many hadrons (about 150 mesons and 120 baryons) that they cannot be considered as elementary. At high energy they appear as composite objects made up of quasi-free point-like fields : the quarks and the gluons. Like the *leptons* and the *vector bosons*, the quarks and the gluons are structureless down to a scale of about 10^{-3} to 10^{-4} fermi, *i.e.* 10^{-18} to 10^{-19} m according to the most recent experimental results obtained at the CERN Large Hadron Collider (LHC). They are treated as elementary fields appearing in the lagrangian which describes the dynamics of their interactions.

Three types of forces have been identified acting on these fields: the strong force which affects only the quarks and the gluons, and the electromagnetic and weak forces. The basic principle which guides the construction of models of particle physics is that of local gauge invariance according to which the physical properties do not depend on the phases of the fields. The Standard Model is a (highly successful) example of a minimal model based on the local gauge group

$$SU(3) \otimes SU(2)_L \otimes U(1)_Y$$

i.e. the direct product of three simple groups. The main features of these groups are :

– The $SU(3)$ gauge group or colour group is the symmetry group of strong interactions. This group acts on the quarks and the interaction force is mediated by the gluons which are the gauge bosons of the group. The quarks and the gluons are coloured fields. The “coupling” (fine structure constant) between quarks and gluons is denoted by α_s which can be large. Under some conditions, however, α_s becomes very small and perturbation theory applies. The $SU(3)$ colour symmetry is exact and consequently the gluons are massless. The theory of strong interactions based on colour $SU(3)$ is called Quantum Chromodynamics ;

– The $SU(2)_L \otimes U(1)_Y$ is the gauge group of the unified weak and electromagnetic interactions, where $SU(2)_L$ is the weak isospin group, acting on left-handed fermions, and $U(1)_Y$ is the hypercharge group. At “low” energy, below 250 GeV, the $SU(2)_L \otimes U(1)_Y$ symmetry is “spontaneously” broken

and the residual group is $U(1)_{\text{em}}$ whose generator is a linear combination of the $U(1)_Y$ generator and a generator of $SU(2)_L$: the corresponding gauge boson is of course the photon and the associated “coupling” is $\alpha \simeq \frac{1}{137}$. Symmetry breaking implies that the other gauge bosons acquire a mass: they are the heavy W^\pm, Z bosons discovered at CERN in the mid ’80’s. The symmetry breaking mechanism is associated to the names of Brout, Englert, Higgs, Guralnik, Hagen, Kibble and Sudarshan and it is known now as the BEH mechanism after the names of the authors (Brout, Englert, Higgs) who published their results first. Higgs emphasized the existence of a massive scalar field as a consequence of the spontaneously broken symmetry and this field is traditionally referred to as the Higgs boson, but it is sometimes called also the “BEH boson” or simply the “massive scalar boson”. Unlike the strong and electromagnetic interactions, the weak interactions violate parity. The electroweak theory, based on spontaneously broken $SU(2)_L \otimes U(1)_Y$ gauge invariance, is known as the Glashow-Salam-Weinberg (GSW) model.

A specific feature of the electroweak model is the generation mixing occurring at the Born level independently for the quark and the lepton sectors. The corresponding formalism is associated to the Cabibbo-Kobayashi-Maskawa (CKM) matrix for the quarks and the Pontecorvo-Maki-Nakagawa-Sakata (PMNS) matrix for the leptons. In the latter case the consequences are neutrino oscillations the phenomenology of which will be the object of the second part of these notes.

Before entering the description of the unified theory of electroweak interactions, based on broken gauge invariance, it is useful to briefly review the Fermi theory of weak interactions and its phenomenological extensions: this will serve to motivate the choice of the gauge group $SU(2)_L \otimes U(1)_Y$ as well as illustrate the features related to the presence of massive gauge bosons.

2 The Fermi theory and its extensions

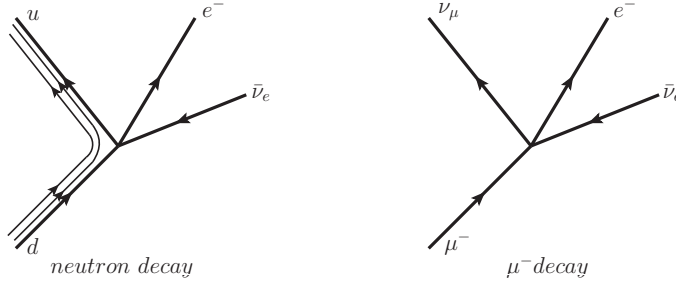
At the beginning was the Fermi theory of muon decay :

$$\mu^- \rightarrow e^- \bar{\nu}_e \nu_\mu.$$

and neutron decay :

$$n \rightarrow p e^- \bar{\nu}_e.$$

In the latter case we work in the quark/parton model where we assume the nucleon is made of three quarks : neutron = (udd) and proton = (uud) . For neutron decay, charge conservation allows only the transition $d \rightarrow u e^- \bar{\nu}_e$, the other two quarks being spectators.



2.1 Contact interactions

These transitions are described by a local current-current (4 fermion) interaction parameterised by the Lagrangian:

$$\mathcal{L} = \frac{G_F}{\sqrt{2}} J^\nu(x) J_\nu^\dagger(x). \quad (2.1)$$

The current has a leptonic part and a hadronic part, $J_\nu(x) = l_\nu(x) + h_\nu(x)$,

$$\begin{aligned} l_\nu(x) &= \bar{\psi}_e \gamma_\nu (1 - \gamma_5) \psi_{\nu_e} + \bar{\psi}_\mu \gamma_\nu (1 - \gamma_5) \psi_{\nu_\mu} + \bar{\psi}_\tau \gamma_\nu (1 - \gamma_5) \psi_{\nu_\tau} \\ h_\nu(x) &= \bar{\psi}_d \gamma_\nu (1 - \gamma_5) \psi_u + \bar{\psi}_s \gamma_\nu (1 - \gamma_5) \psi_c + \bar{\psi}_b \gamma_\nu (1 - \gamma_5) \psi_t, \end{aligned} \quad (2.2)$$

where, for simplicity, the argument of the fermion fields are not shown, ψ_e instead $\psi_e(x)$, \dots . The γ_5 matrix anticommutes with all γ_ν 's (see the appendix for the properties of the γ_5 matrix). The particular $V - A$ (vector (γ_ν) - axial ($\gamma_\nu \gamma_5$)) form of the current is dictated by experiment, in particular the angular distribution of particles in the final state¹. The Fermi constant G_F is universal,

¹The $\gamma_\nu \gamma_5$ interaction breaks parity maximally, see sec.B.2 in the appendix.

i.e. it is the same for the hadronic sector and the leptonic sector and its value has been measured to be :

$$G_F = 1.6639(2)10^{-5} \text{ GeV}^{-2}. \quad (2.3)$$

Thus the transition matrix element for μ decay is an element in $(G/\sqrt{2})l^\nu(x)l_\nu^\dagger(x)$ constructed from the first two terms of $l^\nu(x)$:

$$\begin{aligned} \mathcal{M} &= \frac{G_F}{\sqrt{2}}(\bar{\psi}_e\gamma_\nu(1-\gamma_5)\psi_{\nu_e})(\bar{\psi}_\mu\gamma^\nu(1-\gamma_5)\psi_{\nu_\mu})^\dagger \\ &= \frac{G_F}{\sqrt{2}}(\bar{\psi}_e\gamma_\nu(1-\gamma_5)\psi_{\nu_e})(\bar{\psi}_{\nu_\mu}\gamma^\nu(1-\gamma_5)\psi_\mu) \end{aligned} \quad (2.4)$$

and that of neutron decay (d quark decay) is an element of $(G/\sqrt{2})l^\nu(x)h_\nu^\dagger(x)$:

$$\begin{aligned} \mathcal{M} &= \frac{G_F}{\sqrt{2}}(\bar{\psi}_e\gamma_\nu(1-\gamma_5)\psi_{\nu_e})(\bar{\psi}_d\gamma^\nu(1-\gamma_5)\psi_u)^\dagger \\ &= \frac{G_F}{\sqrt{2}}(\bar{\psi}_e\gamma_\nu(1-\gamma_5)\psi_{\nu_e})(\bar{\psi}_u\gamma^\nu(1-\gamma_5)\psi_d). \end{aligned} \quad (2.5)$$

Introducing the expansion of a spinor ψ_i in terms of plane waves with annihilation operators $b_i^{(\alpha)}(p)$ and $d_i^{(\alpha)}(p)$ for a positive energy and negative energy particle respectively (α is the polarisation index):

$$\begin{aligned} \psi_i(x) &= \int \frac{d^3p}{(2\pi)^3 2\omega} \psi_i(p, x) \\ &= \int \frac{d^3p}{(2\pi)^3 2\omega} \sum_\alpha \left[b_i^{(\alpha)}(p) u_{i\alpha}(p) e^{-ip \cdot x} + d_i^{(\alpha)\dagger}(p) v_{i\alpha}(p) e^{ip \cdot x} \right], \quad p \cdot x = \omega t - \mathbf{p} \cdot \mathbf{x}, \end{aligned} \quad (2.6)$$

where the $u_{i\alpha}(p)$ and $v_{i\alpha}(p)$ are, respectively, the wave functions of the annihilated fermion (positive energy) and the created antifermion (negative energy). Injecting eq. (2.6) into the matrix element above, we see that eq. (2.5) describes several processes related by crossing symmetry such as: $d \rightarrow u e^- \bar{\nu}_e$ (term in $\bar{u}_u \cdots u_d \bar{u}_e \cdots v_{\nu_e}$) or $d \bar{u} \rightarrow e^- \bar{\nu}_e$ (term in $\bar{v}_u \cdots u_d \bar{u}_e \cdots v_{\nu_e}$) or $\nu_e d \rightarrow e^- u$ (term in $\bar{u}_u \cdots u_d \bar{u}_e \cdots u_{\nu_e}$) or \cdots . Considering the last process which is the dominant mechanism for the deep inelastic scattering of a neutrino on a proton one can easily calculate the cross section at the partonic level. Defining the momenta by $\nu_e(p_1) d(p_2) \rightarrow e^-(p_3) u(p_4)$, the invariants are

$$(p_1 + p_2)^2 = s, \quad (p_1 - p_3)^2 = t = q^2 = (s/2)(1 - \cos \theta), \quad (p_1 - p_4)^2 = u = (s/2)(1 + \cos \theta). \quad (2.7)$$

Supposing all fermions massless, the matrix element is (ignoring the polarisation indices):

$$\mathcal{M} = \frac{G_F}{\sqrt{2}} [\bar{u}_e(p_3)\gamma^\mu(1-\gamma_5)u_{\nu_e}(p_1)] [\bar{u}_u(p_4)\gamma_\mu(1-\gamma_5)u_d(p_2)], \quad (2.8)$$

and the matrix element squared summed/averaged over polarisation is

$$\begin{aligned}\bar{\Sigma}|\mathcal{M}|^2 &= \frac{1}{4} \frac{G_F^2}{2} 4 \operatorname{Tr}(\not{p}_3 \gamma^\mu \not{p}_1 \gamma^\nu (1 - \gamma_5)) \operatorname{Tr}(\not{p}_4 \gamma_\mu \not{p}_2 \gamma_\nu (1 - \gamma_5)) \\ &= \frac{G_F^2}{2} [\operatorname{Tr}(\not{p}_3 \gamma^\mu \not{p}_1 \gamma^\nu) \operatorname{Tr}(\not{p}_4 \gamma_\mu \not{p}_2 \gamma_\nu) + \operatorname{Tr}(\not{p}_3 \gamma^\mu \not{p}_1 \gamma^\nu \gamma_5) \operatorname{Tr}(\not{p}_4 \gamma_\mu \not{p}_2 \gamma_\nu \gamma_5)].\end{aligned}\quad (2.9)$$

The traces and their product can be easily evaluated using eqs. (A.9) and (A.10) in appendix A. There is no mixing between the trace with a γ_5 matrix and that without since the former is antisymmetric in $\mu\nu$ and the latter is symmetric. After reduction the result is simple:

$$\bar{\Sigma}|\mathcal{M}|^2 = 4 G_F^2 [(s^2 + u^2) + (s^2 - u^2)] = 8 G_F^2 s^2, \quad (2.10)$$

where the first term in the square brackets corresponds to the first term ($V - A$ interaction) in eq. (2.9). The differential cross section is²:

$$\begin{aligned}\frac{d\sigma^{\nu_e d \rightarrow e^- u}}{d\Omega} &= \frac{1}{2s} \int \frac{d^3 p_3}{(2\pi)^3 2E_3} \frac{d^3 p_4}{(2\pi)^3 2E_4} (2\pi)^4 \delta^{(4)}(p_1 + p_2 - p_3 - p_4) (\bar{\Sigma}|\mathcal{M}|^2) \\ &= \left\{ \frac{1}{(2\pi)^2} \frac{1}{16s} \right\} (8 G_F^2 s^2) \\ &= \frac{G_F^2}{8\pi^2} s,\end{aligned}\quad (2.11)$$

independent of the polar angle. This result is in agreement with the data at not too high s . It is also interesting to consider in the Fermi model the diffusion of antineutrinos on the proton. In the quark/parton model, because of charge conservation, the $\bar{\nu}_e$ interacts only with the u quarks via the transition $\bar{\nu}_e(p_1) u(p_2) \rightarrow e^+(p_3) d(p_4)$. The matrix element can easily be constructed and it is:

$$\mathcal{M} = \frac{G_F}{\sqrt{2}} [\bar{v}_{\nu_e}(p_1) \gamma^\mu (1 - \gamma_5) v_e(p_3)] [\bar{u}_d(p_4) \gamma_\mu (1 - \gamma_5) u_u(p_2)]. \quad (2.12)$$

Taking the square of the matrix element one obtains eq. (2.9) with p_1 and p_3 interchanged. Because $\operatorname{Tr}(\not{p}_3 \gamma^\mu \not{p}_1 \gamma^\nu)$ is symmetric and $\operatorname{Tr}(\not{p}_3 \gamma^\mu \not{p}_1 \gamma^\nu \gamma_5)$ antisymmetric under this interchange, one sees immediately that $\bar{\Sigma}|\mathcal{M}|^2 = 4 G_F^2 [(s^2 + u^2) - (s^2 - u^2)] = 8 G_F^2 u^2$ and consequently the differential cross section is found to be:

$$\frac{d\sigma^{\bar{\nu}_e u \rightarrow e^+ d}}{d\Omega} = \frac{G_F^2}{8\pi^2} \frac{u^2}{s} = \frac{G_F^2}{8\pi^2} \frac{s}{4} (1 + \cos\theta)^2 \quad (2.13)$$

also in agreement with experimental observations where the positron is produced mainly in the direction of the initial $\bar{\nu}_e$ quark.

²The term in $\{\dots\}$ is the phase space factor for massless particles.

If instead of the $V - A$ form of the currents we had used only the vector part the results would be in disagreement with data since for both cross sections above, eqs (2.11) and (2.13), the result would have been :

$$\frac{d\sigma}{d\Omega} = \frac{G_F^2}{64\pi^2} \frac{s^2 + u^2}{s}, \quad (2.14)$$

a prediction not supported by experiments because of the wrong angular distribution for both reactions. If one had tried "scalar currents" of the form:

$$\begin{aligned} l(x) &= \bar{\psi}_e \psi_{\nu_e} + \bar{\psi}_\mu \psi_{\nu_\mu} + \dots \\ h(x) &= \bar{\psi}_d \psi_u + \bar{\psi}_s \psi_c + \dots, \end{aligned} \quad (2.15)$$

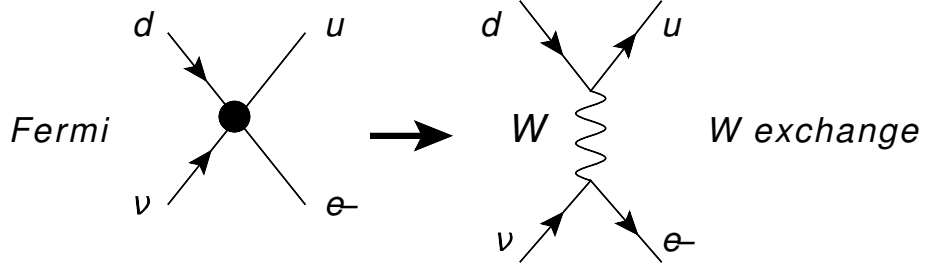
both ν and $\bar{\nu}$ cross sections would have been proportional to s : this prediction is correct for $\nu_e d \rightarrow e^- u$ but incorrect for $\bar{\nu}_e u \rightarrow e^+ d$. In summary, all low energy data support the $V - A$ form to describe weak interactions.

However the Fermi theory is not satisfactory at high energy. Indeed, from eq. (2.11) one obtains for the total cross section $\sigma^{\nu_e d \rightarrow e^- u} = G_F^2 s / 2\pi$. However such a rapid rise of the cross section with energy cannot be asymptotically true as it violates the famous Froissart unitarity bound which requires $\sigma \leq \ln^2 s$ as $s \rightarrow \infty$. Note that the linear rise in s of a $2 \rightarrow 2$ cross section integrated over all final state variables could have easily been guessed on dimensional grounds. Indeed, in Fermi theory, such a cross section is proportional to G_F^2 of dimension GeV^{-4} but a cross section³ is measured in units of GeV^{-2} . Since, after integrating over the final state phase space, the only scale available in the problem is s , of dimension GeV^2 , one necessarily has $\sigma \propto G_F^2 s$.

2.2 Vector boson mediated interactions

The rapid rise of cross sections is related to the locality of the current-current interaction. One can make the 4-fermion interaction nonlocal by postulating a massive charged particle coupling to the $J_\mu(x)$ current similarly to the coupling of a photon to the fermionic current $\bar{\psi}(x)\gamma_\mu\psi(x)$ to mediate the interaction between the currents. It must be a vector particle because of the γ_μ coupling in eq. (2.2) as shown below

³We work in the system where $\hbar = c = 1$.



Denoting M_W the mass of this particle and g_W its dimensionless coupling to the currents, the matrix element eq. (2.5) becomes :

$$\mathcal{M} = g_W^2 [\bar{\psi}_e \gamma_\mu (1 - \gamma_5) \psi_{\nu_e}] \frac{g^{\mu\nu} - q^\mu q^\nu / M_W^2}{q^2 - M_W^2} [\bar{\psi}_u \gamma_\nu (1 - \gamma_5) \psi_d] \quad (2.16)$$

where q is the momentum transfer from the d quark to the u quark. Coming back to the reaction $\nu_e(p_1) d(p_2) \rightarrow e(p_3) u(p_4)$ studied above, the matrix element eq. (2.8), in momentum space is (we do not write explicitly the polarisation index of the fermions):

$$\begin{aligned} \mathcal{M} &= g_W^2 [\bar{u}_e(p_3) \gamma_\mu (1 - \gamma_5) u_{\nu_e}(p_1)] \frac{g^{\mu\nu} - q^\mu q^\nu / M_W^2}{q^2 - M_W^2} [\bar{u}_u(p_4) \gamma_\nu (1 - \gamma_5) u_d(p_2)] \\ &= \frac{g_W^2}{q^2 - M_W^2} [\bar{u}_e(p_3) \gamma_\mu (1 - \gamma_5) u_{\nu_e}(p_1)] [\bar{u}_u(p_4) \gamma^\mu (1 - \gamma_5) u_d(p_2)], \end{aligned} \quad (2.17)$$

with $q = p_1 - p_3 = p_4 - p_2$ and where we have used Dirac equation for massless fields $\not{p}_i u(p_i) = 0$. This equation is identical to eq (2.8) provided we make the substitution:

$$\frac{G_F}{\sqrt{2}} = \frac{g_W^2}{q^2 - M_W^2} \rightarrow \frac{g_W^2}{M_W^2} \quad \text{when } q^2 \rightarrow 0, \quad (2.18)$$

which allows to obtain the matrix element squared summed/averaged over polarisation from eq. (2.8):

$$\overline{\Sigma} |\mathcal{M}|^2 = 16 g_W^4 \frac{s^2}{(q^2 - M_W^2)^2}, \quad (2.19)$$

and the differential cross section :

$$\frac{d\sigma^{\nu_e d \rightarrow e^- u}}{d\Omega} = \frac{g_W^4}{4\pi^2} \frac{s}{(q^2 - M_W^2)^2}, \quad (2.20)$$

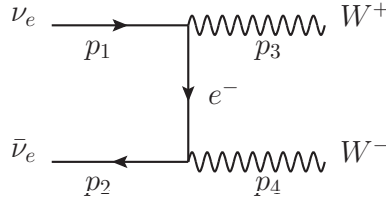
with $q^2 = -s(1 - \cos \theta)/2$. The integrated cross section is easily calculated to be:

$$\sigma^{\nu_e d \rightarrow e^- u} = \frac{1}{\pi} \frac{g_W^4}{M_W^2} \frac{s}{s + M_W^2}. \quad (2.21)$$

At low energy we recover the Fermi model prediction provided, $g_W^2/M_W^2 = G_F \sqrt{2}$, while at high energy the Froissart bound is satisfied.

2.3 Still more problems!

However this is not the end of the story ! The W particle can be produced, and has been produced at LEP2, in the reaction $e^- e^+ \rightarrow W^- W^+$ but the corresponding cross section, in our model, violates Froissart bound. To see this, let us consider instead the unrealistic, but simpler, case⁴ of the scattering $\nu_e(p_1) \bar{\nu}_e(p_2) \rightarrow W^+(p_3) W^-(p_4)$ the amplitude of which is given by only one Feynman diagram with the exchange of an electron:



To illustrate the problem we first define the kinematics and make some comments on the polarisation states of a massive vector particle. We work at very high energy in the center of mass frame of the $e^- e^+$ system :

$$(p_1 + p_2)^\mu = (\sqrt{s}, \mathbf{0}), \quad p_1^\mu = \left(\frac{\sqrt{s}}{2}, 0, 0, \frac{\sqrt{s}}{2}\right), \quad p_2^\mu = \left(\frac{\sqrt{s}}{2}, 0, 0, -\frac{\sqrt{s}}{2}\right). \quad (2.22)$$

We take p_3 and p_4 in the xOz plane:

$$p_3^\mu = (E_3, p_3 \sin \theta, 0, p_3 \cos \theta), \quad E_3 = \sqrt{s}/2, \quad p_3 = \sqrt{s/4 - M_W^2} \quad (2.23)$$

Unlike the photon which has two transverse polarisation states the W particle being massive has three degrees of polarisation.

• Polarisation of a massive spin 1 particle

In the rest frame of a massive particle, $p = (M, \mathbf{0})$ the polarisation is described by space-like vectors. A basis of such vectors is given by

$$\varepsilon^{(1)\mu} = (0, 1, 0, 0), \quad \varepsilon^{(2)\mu} = (0, 0, 1, 0), \quad \varepsilon^{(3)\mu} = (0, 0, 0, 1), \quad (2.24)$$

satisfying $\varepsilon^{(i)} \cdot \varepsilon^{(j)} = -\delta^{ij}$ as well as $p \cdot \varepsilon^{(i)} = 0$ for $i, j = 1, 2, \text{ or } 3$.

⁴For $e^- e^+$ there are two diagrams , and this complicates the discussion.

Important remark

For a boson W with momentum p , the polarisation vectors become functions of p , $\varepsilon^{(i)\mu}(p)$, satisfying the same conditions as above, namely $\varepsilon^{(i)}(p) \cdot \varepsilon^{(j)}(p) = -\delta^{ij}$ as well as $p \cdot \varepsilon^{(i)}(p) = 0$. One often needs, in the propagator for example,

$$\mathcal{P}^{\mu\nu} = \sum_i \varepsilon^{(i)\mu}(p) \varepsilon^{(i)\nu}(p) = - \left(g^{\mu\nu} - \frac{p^\mu p^\nu}{M_W^2} \right). \quad (2.25)$$

The last equality is easily derived knowing that the rank 2 tensor $\mathcal{P}^{\mu\nu}$ depends only on the vector p^μ so that it is of the form $ag^{\mu\nu} + bp^\mu p^\nu$: the conditions $p^2 = M_W^2$, $p_\mu \mathcal{P}^{\mu\nu} = p_\nu \mathcal{P}^{\mu\nu} = 0$ and $\mathcal{P}^\mu{}_\mu = -3$ then determine a and b as given in eq. (2.25).

If the boson W has its momentum along the z -axis, $p = (E, 0, 0, p)$ the polarisation vectors are boosted to:

$$\varepsilon^{(1)\mu} = (0, 1, 0, 0), \quad \varepsilon^{(2)\mu} = (0, 0, 1, 0) \quad \text{transverse polarisations} \quad (2.26)$$

$$\varepsilon^{(3)\mu} = \frac{1}{M_W}(p, 0, 0, E) \quad \text{longitudinal polarisation.} \quad (2.27)$$

For a boson W with a momentum making an angle θ in the zOx plane one simply has to make a rotation around the Oy axis, $p = (E, p \sin \theta, 0, p \cos \theta)$, and the polarisation vectors become:

$$\varepsilon^{(1)\mu}(p) = (0, \cos \theta, 0, -\sin \theta), \quad \varepsilon^{(2)\mu}(p) = (0, 0, 1, 0) \quad \text{transverse polarisations} \quad (2.28)$$

$$\varepsilon^{(3)\mu}(p) = \frac{1}{M_W}(p, p \sin \theta, 0, E \cos \theta) \quad \text{longitudinal polarisation.} \quad (2.29)$$

In the high energy limit, in the frame of eqs. (2.22), $E \simeq p \simeq \sqrt{s}/2 \gg M_W$, the longitudinal polarisation vector simplifies to:

$$\varepsilon^{(3)\mu}(p) \approx \frac{1}{M_W}(\sqrt{s}/2, \sqrt{s}/2 \sin \theta, 0, \sqrt{s}/2 \cos \theta) \approx \frac{p^\mu}{M_W}. \quad (2.30)$$

We use this approximation in the calculation below. For convenience we introduce the notation

$$\varepsilon^{(1)\mu} \text{ or } \varepsilon^{(2)\mu} = \varepsilon_T^\mu, \quad \text{and } \varepsilon^{(3)\mu} = \varepsilon_L^\mu.$$

In contrast, we recall that a massless spin 1 particle has only two states of transverse polarisation.

• **Production of massive vector bosons**

After all these kinematic preliminaries we turn to the evaluation of the matrix element. Remembering

the $\gamma_\mu(1 - \gamma_5)$ coupling of the W boson to the fermions, the matrix element for the diagram above with the electron exchange is:

$$\mathcal{M}^{ij} = -2ig_w^2 \frac{\bar{v}(p_2) \not{\epsilon}^{(j)}(p_4)(\not{p}_1 - \not{p}_3) \not{\epsilon}^{(i)}(p_3)(1 - \gamma_5)u(p_1)}{(p_1 - p_3)^2} \quad (2.31)$$

where we have pushed the $(1 - \gamma_5)$ factors to the right, hence the factor 2. Without doing the calculation explicitly one can guess that the matrix element squared will contain terms of the form :

$$|\mathcal{M}^{ij}|^2 \propto \frac{g_w^4}{((p_1 - p_3)^2)^2} \{ (p_1 \cdot \epsilon^{(i)}(p_3) p_2 \cdot \epsilon^{(j)}(p_4))^2, \dots, (p_k \cdot p_l) (p_1 \cdot \epsilon^{(j)}(p_3))^2 \epsilon^{(j)2}(p_4), \dots, (p_k \cdot p_l) (p_m \cdot p_n) (\epsilon^{(i)}(p_3) \cdot \epsilon^{(j)}(p_4))^2, \dots \}, \quad (2.32)$$

with p_k, p_l, \dots any of the external momenta. In the limit $\sqrt{s} \gg M_w$, it is easy to see that, if both polarisation vectors are transverse, all expressions such as:

$$p_1 \cdot \epsilon_T(p_3) p_2 \cdot \epsilon_T(p_4) \propto (p_1 \cdot \epsilon_T(p_3))^2 \propto s, \quad (2.33)$$

since all components of the transverse polarisation vectors are of order 1 and the momenta are generically of order \sqrt{s} . If, on the contrary, both W 's are longitudinally polarised, the components of the polarisation vectors being of $\mathcal{O}(\sqrt{s}/M_w)$ one finds:

$$p_1 \cdot \epsilon_L(p_3) p_2 \cdot \epsilon_L(p_4) \propto ((p_1 \cdot \epsilon_L(p_3))^2) \propto \frac{s^2}{M_w^2}. \quad (2.34)$$

In consequence ($p_1 \cdot p_3 \propto s$),

$$|\mathcal{M}_{TT}|^2 \propto g_w^4, \quad \text{and} \quad |\mathcal{M}_{LL}|^2 \propto g_w^4 \frac{s^2}{M_w^4}. \quad (2.35)$$

Asymptotically the matrix element squared for the production of longitudinal bosons grows very fast while it is bounded in the case of transverse bosons. Since integrating over phase space to obtain the total cross section brings a factor $1/s$ (see eq. (2.11)) we expect the production of two longitudinal W 's to violate unitarity. To calculate effectively this cross section, one has to be a bit more refined and to go back to eq. (2.31) using the form eq. (2.30) for the polarisation vectors:

$$\mathcal{M}_{LL} = -i \frac{g_w^2}{M_w^2} \bar{v}(p_2) \not{p}_4 \left[\frac{\not{p}_4 - \not{p}_2}{(p_2 - p_4)^2} + \frac{\not{p}_1 - \not{p}_3}{(p_1 - p_3)^2} \right] \not{p}_3 (1 - \gamma_5) u(p_1), \quad (2.36)$$

where we have used the trivial equality $p_1 - p_3 = p_4 - p_2$. Anticommuting the matrices so as to bring \not{p}_1 close to $u(p_1)$ and use the Dirac equation $\not{p}_1 u(p_1) = 0$ and similarly for \not{p}_2 and $\bar{v}(p_2)$ we end up

with:

$$\begin{aligned}
\mathcal{M}_{LL} &= -i \frac{g_W^2}{M_W^2} \bar{v}(p_2) \left[\frac{M_W^2 - 2p_2 \cdot p_4}{(p_2 - p_4)^2} \not{p}_3 + \not{p}_4 \frac{2p_1 \cdot p_3 - M_W^2}{(p_1 - p_3)^2} \right] (1 - \gamma_5) u(p_1) \\
&= -i \frac{g_W^2}{M_W^2} \bar{v}(p_2) [\not{p}_3 - \not{p}_4] (1 - \gamma_5) u(p_1)
\end{aligned} \tag{2.37}$$

Averaging on the initial polarisations one finds:

$$\begin{aligned}
\overline{|\mathcal{M}_{LL}|^2} &= \frac{1}{4} \frac{g_W^4}{M_W^4} 2 \text{Tr}(\not{p}_2 (\not{p}_3 - \not{p}_4) \not{p}_1 (\not{p}_3 - \not{p}_4) (1 - \gamma_5)) \\
&= 2 \frac{g_W^4}{M_W^4} \text{Tr}(\not{p}_2 \not{p}_3 \not{p}_1 \not{p}_3 (1 - \gamma_5)) \\
&= 16 \frac{g_W^4}{M_W^4} p_1 \cdot p_3 p_2 \cdot p_3 = \frac{g_W^4}{M_W^4} s^2 (1 - \cos^2 \theta),
\end{aligned} \tag{2.38}$$

in the limit $s \gg M_W^2$. It is then easy to obtain the differential cross section using the phase space factor of eq. (2.11) and then the integrated cross section for $\nu_e \bar{\nu}_e \rightarrow W_L W_L$:

$$\sigma(\nu_e \bar{\nu}_e \rightarrow W_L^+ W_L^-) = \frac{g_W^4}{24\pi} \frac{s}{M_W^4}. \tag{2.39}$$

In contrast one can estimate the cross section of $\nu_e \bar{\nu}_e \rightarrow W_T W_T$ (but it is more tedious and is left as an exercise):

$$\sigma(\nu_e \bar{\nu}_e \rightarrow W_T^+ W_T^-) \propto \frac{g_W^4}{M_W^2} \quad \text{when } s \rightarrow \infty. \tag{2.40}$$

We thus find that the production of longitudinally polarised vector bosons violates the unitarity limit while that of transverse bosons is well behaved at high energies. Several ways have been tried to cure this problem: among them one can mention the hypothesis of a new heavy lepton (fig. 1b) and choose its couplings to enforce a proper behaviour of the cross section at high energies. It turns out that

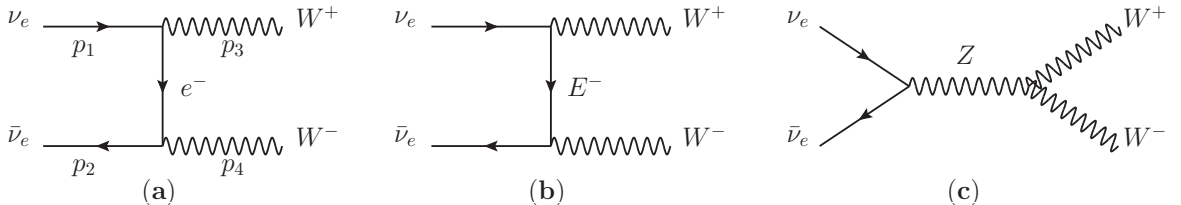


Figure 1: Possible Feynman diagrams for $\nu_e \bar{\nu}_e \rightarrow W^+ W^-$ scattering. **(a)**: e exchange; **(b)** hypothetical heavy electron E exchange; **(c)** neutral vector boson Z exchange.

another possibility, namely that of a heavy neutral vector boson, denoted Z (fig. 1c), is realised in

Nature. Assuming the Z coupling to the fermions of type $g_Z \gamma_\mu (a - b \gamma_5)$ and to the charged W bosons of type⁵ $g'_Z (p_{W^+}^\rho - p_{W^-}^\rho) g^{\mu\nu} + \dots$, they can be chosen to make cross sections such as $\nu_e \bar{\nu}_e \rightarrow W^+ W^-$, $e^+ e^- \rightarrow W^+ W^-$, \dots asymptotically well behaved. However, this patch up job is not yet sufficient to have a satisfactory model. Indeed, keeping fermion masses and considering for example $e^+ e^- \rightarrow Z Z$ scattering one finds an interference piece in the cross section $\sim g^4 m_e \sqrt{s} / M_Z^4$ which again violates unitarity! Similar problems arise in the $W W$ scattering process, *e.g.* $W^+ W^- \rightarrow W^+ W^-$ which are studied at LHC or will be in the future $e^+ e^-$ high energy linear colliders: the cross sections for these processes diverge linearly in s . These problems can be solved by supposing the existence of a scalar particle which interacts with the bosons as well as the fermions with appropriately chosen couplings.

One can thus construct a viable electroweak theory in the pedestrian way described above, carefully choosing masses and couplings of the newly introduced particles so as to ensure the correct behaviour of all cross sections. It is more instructive however to assume that these relations among masses and couplings arise from some symmetry property. This is what is done next. Before doing that, one should discuss the implications of the $\gamma_\mu (1 - \gamma_5)$ coupling in the weak interactions compared to the γ_μ coupling of electrodynamics. Then we describe in some details the symmetry group assuming global then local gauge invariance. At this level, the chosen group requires all fields to be massless. The theory is renormalisable (well behaved at asymptotic energies) being a non-abelian field theory. Then, by the mechanism of “spontaneous symmetry breaking” whereby the symmetry of the lagrangian is preserved but the choice of a ground state breaks the symmetry, fermions and gauge bosons acquire a mass. After symmetry breaking, the theory remains renormalisable as a consequence of the underlying gauge invariance which imposes the required relations between couplings. One is left however with a large number of parameters (at least 18 for the Standard Model with massless neutrinos and 25 with massive neutrinos) which gives a motivation for a (still unsuccessful!) search of a deeper symmetry.

⁵Dimensional arguments and gauge invariance lead to such a choice.

3 Fermions, chirality, helicity

3.1 Fermions : chirality

We saw that the Fermi model involves charged transitions such as $\bar{\psi}_d \gamma_\mu (1 - \gamma_5) \psi_u$ ou $\bar{\psi}_e \gamma_\mu (1 - \gamma_5) \psi_{\nu_e}$, *i.e.* charged currents of a particular type : the fermion interacts only through the combination $(1 - \gamma_5)\psi$. We can always write :

$$\psi = \psi_- + \psi_+, \quad \text{with} \quad \psi_- = \frac{1 - \gamma_5}{2} \psi, \quad \psi_+ = \frac{1 + \gamma_5}{2} \psi \quad (3.1)$$

The spinors ψ_- and ψ_+ have a definite *chirality* defined by their transformation when applying γ_5 :

$$\gamma_5 \psi_- = -\psi_-, \quad \gamma_5 \psi_+ = \psi_+. \quad (3.2)$$

ψ_- , ψ_+ have *negative*, *positive chirality* respectively. The combinations

$$P^- = \frac{1 - \gamma_5}{2}, \quad P^+ = \frac{1 + \gamma_5}{2} \quad (3.3)$$

are projection operators satisfying:

$$P^+ + P^- = 1, \quad P^+ P^- = 0, \quad (P^+)^2 = P^+, \quad (P^-)^2 = P^-. \quad (3.4)$$

Only negative chirality fermions are sensitive to the weak interactions. It is useful to note that:

$$\overline{\psi_-} = \bar{\psi} \frac{1 + \gamma_5}{2}, \quad \overline{\psi_+} = \bar{\psi} \frac{1 - \gamma_5}{2}. \quad (3.5)$$

3.2 Fermions : positive and negative energy solutions

When using the plane wave decomposition of the spinor, eq. (2.6), the free Dirac equation $(i\cancel{\partial} - m)\psi = 0$ implies:

$$(\cancel{p} - m) u_\alpha(p) = 0, \quad (\cancel{p} + m) v_\alpha(p) = 0 \quad (3.6)$$

on the positive ($u_\alpha \exp(-ipx)$, see eq. (2.6)) and negative ($v_\alpha \exp(ipx)$) energy component respectively.

At rest, $\mathbf{p} = \mathbf{0}$, and using the Dirac representation of γ_μ matrices given in appendix, they reduce to:

$$\begin{aligned} m(\gamma^0 - 1)u_\alpha &\Rightarrow \begin{pmatrix} 0 & 0 \\ 0 & -2\mathbb{1}_2 \end{pmatrix} \begin{pmatrix} \chi_\alpha \\ 0 \end{pmatrix} = 0 \\ m(\gamma^0 + 1)v_\alpha &\Rightarrow \begin{pmatrix} 2\mathbb{1}_2 & 0 \\ 0 & 0 \end{pmatrix} \begin{pmatrix} 0 \\ \chi_\alpha \end{pmatrix} = 0 \end{aligned} \quad (3.7)$$

where we have introduced the 2-component spinors :

$$\chi_1 = \begin{pmatrix} 1 \\ 0 \end{pmatrix}, \quad \chi_2 = \begin{pmatrix} 0 \\ 1 \end{pmatrix} \quad \text{and} \quad u_\alpha = \begin{pmatrix} \chi_\alpha \\ 0 \end{pmatrix}, \quad v_\alpha = \begin{pmatrix} 0 \\ \chi_\alpha \end{pmatrix}, \quad \alpha = 1, 2. \quad (3.8)$$

Since one has $\tau^3 \chi_1 = \chi_1$, $\tau^3 \chi_2 = -\chi_2$ one says that χ_1 has spin up and χ_2 spin down and⁶

$$\frac{1 + \tau^3}{2} \quad \text{and} \quad \frac{1 - \tau^3}{2} \quad (3.9)$$

are respectively the spin up and spin down projection operators for the 2-component spinors. When $\mathbf{p} \neq \mathbf{0}$, to obtain the spinors $u_\alpha(p)$ and $v_\alpha(p)$ one can apply a Lorentz boost to the solution in the rest frame or, more simply, observe that:

$$\boxed{u_\alpha(p) = \frac{1}{\sqrt{\omega + m}}(\not{p} + m)u_\alpha, \quad v_\alpha(p) = \frac{1}{\sqrt{\omega + m}}(-\not{p} + m)v_\alpha,} \quad (3.10)$$

satisfy eqs. (3.6) respectively. The factor $1/\sqrt{\omega + m}$ is the chosen normalisation factor such that:

$$\begin{aligned} \bar{u}_\alpha(p) u_\beta(p) &= 2m \delta_{\alpha\beta}, & u_\alpha^\dagger(p) u_\beta(p) &= 2\omega \delta_{\alpha\beta}, \\ \bar{v}_\alpha(p) v_\beta(p) &= -2m \delta_{\alpha\beta}, & v_\alpha^\dagger(p) v_\beta(p) &= 2\omega \delta_{\alpha\beta}. \end{aligned} \quad (3.11)$$

Explicitly, one has in terms of two component spinors:

$$\boxed{u_\alpha(p) = \frac{1}{\sqrt{\omega + m}} \begin{pmatrix} (\omega + m) \chi_\alpha \\ \mathbf{p} \cdot \boldsymbol{\tau} \chi_\alpha \end{pmatrix}, \quad v_\alpha(p) = \frac{1}{\sqrt{\omega + m}} \begin{pmatrix} \mathbf{p} \cdot \boldsymbol{\tau} \chi_\alpha \\ (\omega + m) \chi_\alpha \end{pmatrix}.} \quad (3.12)$$

The solution $u_\alpha(p)$ is the positive energy spinor while $v_\alpha(p)$ is called the negative energy one with momentum $(-\omega, -\mathbf{p})$. In particular, for a boost of magnitude η in the z direction, the positive energy spinors have momentum $p = (\omega, 0, 0, p_z)$, with $\omega = m \cosh \eta$, $p_z = m \sinh \eta$, and they become:

$$u_\alpha(p) = \frac{1}{\sqrt{\omega + m}} \begin{pmatrix} (\omega + m) \chi_\alpha \\ p_z \tau^3 \chi_\alpha \end{pmatrix} \Rightarrow u_1(p) = \frac{1}{\sqrt{\omega + m}} \begin{pmatrix} \omega + m \\ 0 \\ p_z \\ 0 \end{pmatrix}, \quad u_2(p) = \frac{1}{\sqrt{\omega + m}} \begin{pmatrix} 0 \\ \omega + m \\ 0 \\ -p_z \end{pmatrix}, \quad (3.13)$$

while the negative energy solutions with momentum $-p$ are:

$$v_\alpha(p) = \frac{1}{\sqrt{\omega + m}} \begin{pmatrix} p_z \tau^3 \chi_\alpha \\ (\omega + m) \chi_\alpha \end{pmatrix} \Rightarrow v_1(p) = \frac{1}{\sqrt{\omega + m}} \begin{pmatrix} p_z \\ 0 \\ \omega + m \\ 0 \end{pmatrix}, \quad v_2(p) = \frac{1}{\sqrt{\omega + m}} \begin{pmatrix} 0 \\ -p_z \\ 0 \\ \omega + m \end{pmatrix}. \quad (3.14)$$

In general, it is useful to introduce operators which project out positive and negative energy states. They are defined by:

$$\Lambda_\pm = \frac{\pm \not{p} + m}{2m}, \quad (3.15)$$

⁶The Pauli matrices τ^i are given in appendix A.

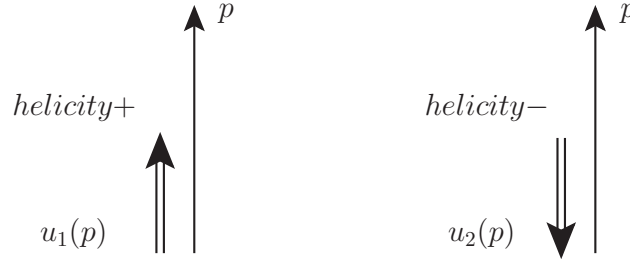
and they satisfy the required relations:

$$\Lambda_-(p) + \Lambda_+(p) = 1, \quad \Lambda_-(p)\Lambda_+(p) = \Lambda_+(p)\Lambda_-(p) = 0, \quad (\Lambda_-(p))^2 = \Lambda_-(p), \quad (\Lambda_+(p))^2 = \Lambda_+(p). \quad (3.16)$$

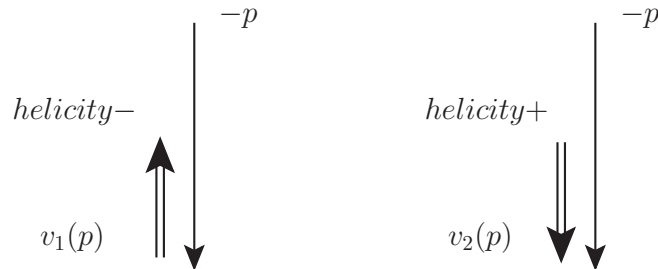
Thus $\Lambda_{\pm}\psi(p, x)$ respectively project the positive and negative energy solutions of $\psi(x)$ in eq. (2.6). We discuss in appendix B.1 the interpretation of the negative energy solution as a positive energy antiparticle.

3.3 Fermions : helicity

When applying a boost along the z -axis one does not change the orientation of the fermion spin, as shown in the figure below, so that the projection of the fermion spin along the momentum is positive for $u_1(p)$ (spin up) and negative for $u_2(p)$ (spin down) : one says that $u_1(p)$ has *positive helicity* or is *right-handed* and is denoted by $u_R(p)$, while $u_2(p)$ has *negative helicity* or is *left-handed* and is denoted by $u_L(p)$.



For the negative energy solutions the situation is opposite and $v_1(p) = v_L(p)$ has *negative helicity* or is *left-handed* and $v_2(p) = v_R(p)$ has *positive helicity* or is *right-handed* as shown below



For a spinor of momentum \mathbf{p} one defines the helicity projection operator

$$\mathcal{S}^{\pm}(\hat{\mathbf{p}}) = \frac{1 \pm \boldsymbol{\tau} \cdot \hat{\mathbf{p}}}{2}, \quad \boldsymbol{\tau} = \begin{pmatrix} \tau & 0 \\ 0 & \tau \end{pmatrix}, \quad \hat{\mathbf{p}} = \frac{\mathbf{p}}{|\mathbf{p}|} \quad (3.17)$$

with $\hat{\mathbf{p}}$ the unit vector in the direction of the momentum. Applying these operators to the positive energy spinors one finds $((\boldsymbol{\tau}\hat{\mathbf{p}})^2 = 1)$:

$$\mathcal{S}^\pm(\hat{\mathbf{p}})u_\alpha(p) = \frac{1}{2\sqrt{\omega+m}} \begin{pmatrix} (\omega+m)(1 \pm \boldsymbol{\tau}\hat{\mathbf{p}})\chi_\alpha \\ p(\pm 1 + \boldsymbol{\tau}\hat{\mathbf{p}})\chi_\alpha \end{pmatrix}. \quad (3.18)$$

If $\hat{\mathbf{p}}$ is in the direction of Oz , the helicity projection operators applied on the spinors reduce to

$$\mathcal{S}^\pm(\hat{\mathbf{p}})u_\alpha(p) = \frac{1}{2\sqrt{\omega+m}} \begin{pmatrix} (\omega+m)(1 \pm \tau_3)\chi_\alpha \\ p(\pm 1 + \tau_3)\chi_\alpha \end{pmatrix}, \quad (3.19)$$

showing that $u_1(p)$ is right-handed, and $u_2(p)$ is left-handed as found before. For negative energy spinors, since they have momentum $-\mathbf{p}$, $\mathcal{S}^+(-\hat{\mathbf{p}})$ projects out positive helicity and $\mathcal{S}^-(-\hat{\mathbf{p}})$ projects out negative helicity. The operators S^\pm are helicity projection operators and satisfy:

$$(S^\pm(\mathbf{p}))^2 = S^\pm(\mathbf{p}), \quad S^+(\mathbf{p})S^-(\mathbf{p}) = 0, \quad S^+(\mathbf{p}) + S^-(\mathbf{p}) = \mathbb{1}_2 \quad (3.20)$$

• Massless spinors : helicity and chirality

In the Standard Model, at high energy, quarks of light flavours and neutrinos are often treated as massless. Considering massless spinors with a generic momentum p one has:

$$\boxed{u_\alpha(p) = \sqrt{\omega} \begin{pmatrix} \chi_\alpha \\ \hat{\mathbf{p}} \cdot \boldsymbol{\tau} \chi_\alpha \end{pmatrix}, \quad v_\alpha(p) = \sqrt{\omega} \begin{pmatrix} \hat{\mathbf{p}} \cdot \boldsymbol{\tau} \chi_\alpha \\ \chi_\alpha \end{pmatrix}, \quad \alpha = 1 \text{ or } 2.} \quad (3.21)$$

When acting on positive energy spinors $u_\alpha(p)$, the helicity projection operator and P^\pm , the chirality projection operators of eq. (3.3), give the same result:

$$\mathcal{S}^\pm(\hat{\mathbf{p}})u_\alpha(p) = P^\pm u_\alpha(p) = \frac{\sqrt{\omega}}{2} \begin{pmatrix} (1 \pm \boldsymbol{\tau}\hat{\mathbf{p}})\chi_\alpha \\ (\pm 1 + \boldsymbol{\tau}\hat{\mathbf{p}})\chi_\alpha \end{pmatrix}, \quad \alpha = 1, 2,$$

This shows that positive chirality and right-handed helicity are the same and likewise for negative chirality and left-handed helicity. For spinors $v_\alpha(p)$ one finds instead:

$$\mathcal{S}^\pm(-\hat{\mathbf{p}})v_\alpha(p) = P^\mp v_\alpha(p) = \frac{\sqrt{\omega}}{2} \begin{pmatrix} (\mp 1 + \boldsymbol{\tau}\hat{\mathbf{p}})\chi_\alpha \\ (1 \mp \boldsymbol{\tau}\hat{\mathbf{p}})\chi_\alpha \end{pmatrix}, \quad \alpha = 1, 2,$$

thus a right-handed negative energy spinor has negative chirality and a left-handed one positive chirality. Thus if one constructs a massless spinor $u(p)$ as a linear combination of $u_\alpha, \alpha = 1, 2$, then $u_L(p) = \frac{(1-\gamma_5)}{2} u(p)$ and $u_R(p) = \frac{(1+\gamma_5)}{2} u(p)$ are respectively left-handed and right-handed spinors, while $v_L(p) = \frac{(1+\gamma_5)}{2} v(p)$ is left-handed and $v_R(p) = \frac{(1-\gamma_5)}{2} v(p)$ right-handed, so helicity = chirality for positive energy spinors but helicity = - chirality for negative energy ones .

To summarise, in the massless case, from the definition of $\psi(x)$ in eq. (2.6), the combination

$$\psi_L(x) = \frac{1 - \gamma_5}{2} \psi(x) \quad (3.22)$$

- destroys a left-handed fermion, with wave function $u_L(p)$ and creates a right-handed antifermion with wave function $v_R(p)$, eqs. (3.28), (3.30),

$$\psi_L(x) = \int \frac{d^3p}{(2\pi)^3 2\omega} \left[b_L(p) u_L(p) e^{-ip \cdot x} + d_R^\dagger(p) v_R(p) e^{ip \cdot x} \right] \quad (3.23)$$

and *mutatis mutandis*:

$$\psi_R(x) = \frac{1 + \gamma_5}{2} \psi(x) \quad (3.24)$$

- destroys a right-handed fermion, with wave function $u_R(p)$ and creates a left-handed antifermion with wave function $v_L(p)$.

$$\psi_R(x) = \int \frac{d^3p}{(2\pi)^3 2\omega} \left[b_R(p) u_R(p) e^{-ip \cdot x} + d_L^\dagger(p) v_L(p) e^{ip \cdot x} \right] \quad (3.25)$$

Thus, the Fermi interaction, discussed in the previous section, concerns only left-handed fermions and right-handed antifermions.

• Massless chiral spinors

It is easy and amusing (as well as useful for neutrino physics) to find the explicit form of massless chiral spinors of arbitrary momentum. For instance, for positive energy spinors one has, using expressions (3.12) :

$$\begin{aligned} \gamma_5 u_R(p) = u_R(p) & \quad \Rightarrow \quad \hat{\mathbf{p}} \cdot \boldsymbol{\tau} \chi_R = \chi_R \\ \gamma_5 u_L(p) = -u_L(p) & \quad \Rightarrow \quad \hat{\mathbf{p}} \cdot \boldsymbol{\tau} \chi_L = -\chi_L, \end{aligned} \quad (3.26)$$

for right-handed and left-handed spinors respectively. Solving for $\hat{\mathbf{p}} \cdot \boldsymbol{\tau} \chi = \pm \chi$, we get the 2-component spinors after proper normalisation:

$$\chi_R = \begin{pmatrix} \cos \frac{\theta}{2} e^{-i\frac{\phi}{2}} \\ \sin \frac{\theta}{2} e^{i\frac{\phi}{2}} \end{pmatrix} \quad \chi_L = \begin{pmatrix} -\sin \frac{\theta}{2} e^{-i\frac{\phi}{2}} \\ \cos \frac{\theta}{2} e^{i\frac{\phi}{2}} \end{pmatrix}, \quad (3.27)$$

and thus,

$$u_R(p) = \sqrt{\omega} \begin{pmatrix} \chi_R \\ \chi_R \end{pmatrix} \quad u_L(p) = \sqrt{\omega} \begin{pmatrix} \chi_L \\ -\chi_L \end{pmatrix}, \quad (3.28)$$

One follows the same procedure for negative energy spinors, but since their momentum is $-p$ they satisfy

$$\gamma_5 v_R(p) = -v_R(p), \quad \gamma_5 v_L(p) = v_L(p) \quad (3.29)$$

and, compared to the $u(p)$ spinors, the role of χ_R and χ_L is interchanged so that:

$$v_R(p) = \sqrt{\omega} \begin{pmatrix} -\chi_L \\ \chi_L \end{pmatrix} \quad v_L(p) = -\sqrt{\omega} \begin{pmatrix} \chi_R \\ \chi_R \end{pmatrix}, \quad (3.30)$$

The relations $\chi_R^\dagger \chi_R = \chi_L^\dagger \chi_L = 1, \chi_R^\dagger \chi_L = \chi_L^\dagger \chi_R = 0$ ensure that eqs. (3.11) are satisfied.

• **Massive spinors : helicity and chirality**

In general, if in the rest-frame of the fermion the polarisation direction is given by the vector $s = (0, \mathbf{s})$ with $s^2 = -1, s.p = 0$, the spin projection operators along or opposite \mathbf{s} are given, in a covariant form, by

$$\Sigma^\pm(s) = \frac{1 \pm \gamma_5 \not{s}}{2}. \quad (3.31)$$

Specifying to the helicity, the spin projection along or opposite the fermion momentum, one defines

$$s = \left(\frac{p}{m}, \frac{\omega}{m} \hat{\mathbf{p}} \right), \quad \text{with } p = |\mathbf{p}| \quad \text{and} \quad \hat{\mathbf{p}} = \frac{\mathbf{p}}{p}, \quad (3.32)$$

(which satisfies the conditions $s^2 = -1, s.p = 0$) and $\Sigma^\pm(s)$ takes the form:

$$\Sigma^\pm(s) = \frac{1}{2m} \begin{pmatrix} m \pm \omega \hat{\mathbf{p}} \cdot \boldsymbol{\tau} & \mp p \\ \pm p & m \mp \omega \hat{\mathbf{p}} \cdot \boldsymbol{\tau} \end{pmatrix}. \quad (3.33)$$

The form of the projectors $\Sigma^\pm(s)$ is different from the helicity projection operators defined in eq. (3.17) but when acting on positive energy spinors $u(p)$, one shows that:

$$\Sigma^\pm(s) u_\alpha(p) = \mathcal{S}^\pm(\hat{\mathbf{p}}) u_\alpha(p), \quad \alpha = 1, 2 \quad (3.34)$$

Thus, for positive energy spinors, Σ^+ projects out right-handed states and Σ^- the left-handed ones. Similarly, when acting on negative energy spinors $v(p)$, one finds that,

$$\Sigma^\pm(s) v_\alpha(p) = \mathcal{S}^\pm(-\hat{\mathbf{p}}) v_\alpha(p), \quad \alpha = 1, 2 \quad (3.35)$$

related to the fact that negative energy spinors carry momentum $-p$. Thus, again, Σ^+ projects out the right-handed helicity state and Σ^- the left-handed ones.

For massive spinors at very high energy if one uses $(1 \pm \gamma_5)/2$ as helicity projection operators rather than $\Sigma^\pm(s)$, with s as defined in eq. (3.32), the error made is of $\mathcal{O}(m/\omega)$ ⁷.

⁷A negative chirality massive fermion at very high energy will be mainly left-handed with a small admixture, of $\mathcal{O}(m/\omega)$, of the right-handed component, and vice-versa.

In summary, it is easy to see that the fermion wave-functions:

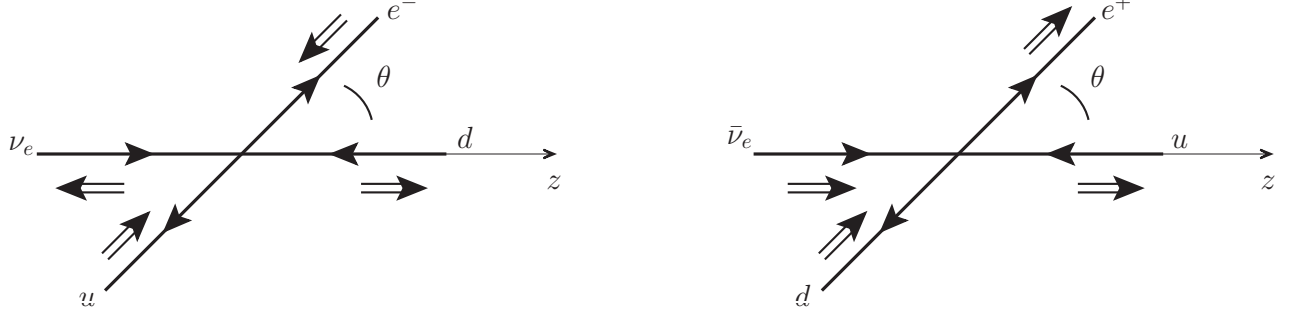
$$\begin{aligned}
\psi_R^f(p, x) &= \Sigma^+(s) \frac{\not{p} + m}{2m} \psi(p, x) && \text{destroys a right-handed fermion} \\
\psi_L^f(p, x) &= \Sigma^-(s) \frac{\not{p} + m}{2m} \psi(p, x) && \text{destroys a left-handed fermion} \\
\psi_R^{\bar{f}}(p, x) &= \Sigma^+(s) \frac{-\not{p} + m}{2m} \psi(p, x) && \text{creates a right-handed antifermion} \\
\psi_L^{\bar{f}}(p, x) &= \Sigma^-(s) \frac{-\not{p} + m}{2m} \psi(p, x) && \text{creates a left-handed antifermion.} \tag{3.36}
\end{aligned}$$

This summary will prove useful when discussing \mathcal{C} and \mathcal{CP} violation later.

Application

The helicity arguments above and conservation of angular momentum are useful to understand/predict the angular dependence of a process governed by the $\gamma_\mu(1 - \gamma_5)$ interaction which carries total angular momentum 1 ($L = 0, S = 1$). For example, coming back to the processes $\nu_e d \rightarrow e^- u$ and $\bar{\nu}_e u \rightarrow e^+ d$, eqs. (2.8) and (2.12), the leptonic transition is given by $\bar{\psi}_e \gamma_\mu(1 - \gamma_5)\psi_{\nu_e} = 2 \bar{\psi}_{eL} \gamma_\mu \psi_{\nu_eL}$ or its hermitian conjugate $\bar{\psi}_{\nu_e} \gamma_\mu(1 - \gamma_5)\psi_e = 2 \bar{\psi}_{\nu_eL} \gamma_\mu \psi_{eL}$. From eq. (3.23), we see that these transitions involve only left-handed leptons or right-handed antileptons. Likewise, from the $\bar{\psi}_d \gamma_\mu(1 - \gamma_5)\psi_u$ or $\bar{\psi}_u \gamma_\mu(1 - \gamma_5)\psi_d$ interactions, only left-handed quarks or right-handed antiquarks are allowed. In the scattering $\nu_e d \rightarrow e^- u$ only left-handed leptons and quarks are involved. If θ denotes the angle between the incoming and outgoing leptons in the νd center of mass frame, the spin projection of the system along the axis of motion of the particles is 0 because each particle has a negative helicity and they move in opposite directions (see the figure). Therefore we expect no angular dependence for the cross section, in agreement with eq. (2.11). On the contrary, for the scattering $\bar{\nu}_e u \rightarrow e^+ d$ the antileptons being right-handed and the quarks left-handed the spin projection of the antilepton-quark system along the direction of motion of the antilepton is always 1 : for a forward produced e^+ the angular momentum projection along the z axis is 1 for both initial and final states and thus is conserved while for a backward produced e^+ ($\theta = \pi$) the spin projection of the final system along the z axis is -1, and angular momentum is not conserved, consequently the matrix element vanishes. From Clebsh-Gordan tables⁸ the associated angular distribution is proportional to $d_{11}^1(\theta) \simeq 1 + \cos \theta$, in agreement with eq. (2.13).

⁸See, *Clebsh-Gordan coefficients, spherical harmonics and d-functions* in Particle Data group, C. Patrignani *et. al.*, Chin. Phys. **C40** (2016) 100001 (<http://pdg.lbl.gov>).



Similar arguments can be applied to $\nu/\bar{\nu}$ scattering on quarks or antiquarks and, then, one can easily derive eqs. (2.11), (2.13).

We note the useful relations :

$$\begin{aligned}
 \bar{\psi}_L \gamma_\mu \psi_L &= \frac{1}{2} \bar{\psi} \gamma_\mu (1 - \gamma_5) \psi & \bar{\psi}_L \gamma_\mu \psi_R &= \bar{\psi}_R \gamma_\mu \psi_L = 0 \\
 \bar{\psi} \gamma_\mu \psi &= \bar{\psi}_L \gamma_\mu \psi_L + \bar{\psi}_R \gamma_\mu \psi_R, & \bar{\psi}_R \psi_R &= \bar{\psi}_L \psi_L = 0. \\
 \bar{\psi} \psi &= \bar{\psi}_R \psi_L + \bar{\psi}_L \psi_R, & &
 \end{aligned} \tag{3.37}$$

4 The global $SU(2)_L \otimes U(1)_Y$ gauge invariance : conserved currents

Before entering the details of the model it is useful to recall the relation between rigid (global) gauge transformations and conserved currents since, as we shall see, the construction of the Weinberg-Salam model is made more transparent when using this notion. The choice of $SU(2)_L$ is motivated by the structure of currents building up the Fermi interaction. For massless particles these currents are conserved, hence from Noether theorem, they are the consequences of a global $SU(2)$ invariance. The assumed $U(1)_Y$ global invariance is the minimal group necessary to construct the electromagnetic current : indeed by an appropriate choice of the hypercharges Y , one constructs the electromagnetic current as the sum of the neutral $SU(2)$ one and the $U(1)$ current. Following the spectacular success of QED the $SU(2)_L \otimes U(1)_Y$ invariance is made local to generate the interactions. It works !

4.1 Global gauge invariance and Noether theorem

One starts from the lagrangian density $\mathcal{L}(\psi(x), \partial_\mu \psi(x))$, which is a fonction of the field and its first derivatives, and from the action defined by

$$S = \int d^4x \mathcal{L}(\psi(x), \partial_\mu \psi(x)).$$

The action has no dimension. The Maupertuis principle (least action principle) states that, "in Nature", the action is stationary under a variation of the field and this leads to the Euler-Lagrange equations

$$\frac{\delta \mathcal{L}}{\delta \psi(x)} - \partial_\mu \frac{\delta \mathcal{L}}{\delta \partial_\mu \psi(x)} = 0 \quad (4.1)$$

Now, assume that the lagrangian density is invariant under the rigid transformation

$$\begin{aligned} \psi(x) &\rightarrow e^{i\alpha} \psi(x) \\ \bar{\psi}(x) &\rightarrow e^{-i\alpha} \bar{\psi}(x), \end{aligned} \quad (4.2)$$

where α is a real arbitrary constant, independent of the space-time coordinate x . Considering rather an infinitesimal transformation

$$\begin{aligned} \delta \psi(x) &= i\alpha \psi(x) \\ \delta \bar{\psi}(x) &= -i\alpha \bar{\psi}(x), \end{aligned} \quad (4.3)$$

the variation of the lagrangian is⁹ (note the relative position of the derivative term such as $\delta \mathcal{L}/\delta \psi$ and the $\delta \psi$)

$$\delta \mathcal{L}(\psi, \partial_\mu \psi) = \frac{\delta \mathcal{L}}{\delta \psi} \delta \psi + \frac{\delta \mathcal{L}}{\delta \partial_\mu \psi} \delta \partial_\mu \psi + \delta \bar{\psi} \frac{\delta \mathcal{L}}{\delta \bar{\psi}} + (\delta \partial_\mu \bar{\psi}) \frac{\delta \mathcal{L}}{\delta \partial_\mu \bar{\psi}}. \quad (4.4)$$

⁹To lighten the notation and when no ambiguity arises one simply writes in the following ψ for $\psi(x)$ and $\delta \psi$ for $\delta \psi(x)$.

But, $\delta\partial_\mu\psi = \partial_\mu\delta\psi = i\alpha\partial_\mu\psi$, $\delta\partial_\mu\bar{\psi} = \partial_\mu\delta\bar{\psi} = -i\alpha\partial_\mu\bar{\psi}$, and using the Euler-Lagrange equations to eliminate $\delta\mathcal{L}/\delta\psi$ and $\delta\mathcal{L}/\delta\bar{\psi}$ one finds

$$\delta\mathcal{L}(\psi, \partial_\mu\psi) = i\alpha\partial_\mu\left(\frac{\delta\mathcal{L}}{\delta\partial_\mu\psi}\psi - \bar{\psi}\frac{\delta\mathcal{L}}{\delta\partial_\mu\bar{\psi}}\right). \quad (4.5)$$

Since $\delta\mathcal{L}(\psi, \partial_\mu\psi) = 0$ under the variation of the fields, eqs. (4.3), the current defined by

$$\boxed{J^\mu(x) = \frac{\delta\mathcal{L}}{\delta\partial_\mu\psi}\psi - \bar{\psi}\frac{\delta\mathcal{L}}{\delta\partial_\mu\bar{\psi}}} \quad (4.6)$$

is conserved, *i.e.* $\boxed{\partial_\mu J^\mu(x) = 0}$. For a fermion field with the langrangien density

$$\mathcal{L}(\psi, \partial_\mu\psi) = \bar{\psi}(i\partial\!\!\!/ - m)\psi$$

the conserved current is simply

$$J^\mu(x) = \bar{\psi}\gamma^\mu\psi. \quad (4.7)$$

One defines the charge by the space integration of the 0th component of the current, and specifying $x = (t, \mathbf{x})$, $d^4x = dt d^3x$, one has

$$\boxed{Q(t) = \int d^3x J^0(t, \mathbf{x}) = \int d^3x \psi^\dagger(t, \mathbf{x})\psi(t, \mathbf{x})}. \quad (4.8)$$

Using current conservation, $\partial_\mu J^\mu(x) \equiv \partial_t J^0(t, \mathbf{x}) + \nabla \cdot \mathbf{J}(t, \mathbf{x}) = 0$, it is easy to prove that the charge is time independent since

$$\frac{dQ(t)}{dt} = - \int_\Omega d^3x \nabla \cdot \mathbf{J}(t, \mathbf{x}) = - \int_{\partial\Omega} \mathbf{ds} \cdot \mathbf{J}(t, \mathbf{x}) = 0, \quad (4.9)$$

where the last equality is realised when we assume the fields are suppressed at infinity.

Thus the Noether theorem states that to an invariance under a set of continuous transformations corresponds a conserved current. The results eqs. (4.6), (4.7) are easily extended to the case of non abelian symmetries such as $SU(2), \dots, SU(N)$ or to a lagrangian density involving several fields ψ_i . Then if

$$\mathcal{L}(\psi, \partial_\mu\psi) = \sum_i \bar{\psi}_i(i\partial\!\!\!/ - m_i)\psi_i \quad (4.10)$$

is invariant under the set of transformations

$$\begin{aligned} \delta\psi_i &= i\alpha y_i \psi_i, & \forall i \\ \delta\bar{\psi}_i &= -i\alpha y_i \bar{\psi}_i, & \forall i, \end{aligned} \quad (4.11)$$

with α a common real parameter and y_i the charge of field ψ_i , the conserved current is

$$\boxed{J^\mu(x) = \sum_i y_i \bar{\psi}_i \gamma^\mu \psi_i}, \quad (4.12)$$

a result to be used later. The charge of fermion ψ_i is then defined as y_i .

4.2 The lagrangian density

As discussed above, the weak interactions induce a transition between left-handed fermions of different charges. It is then natural to group them into doublets

$$\underbrace{\begin{pmatrix} \nu_{e_L} \\ e_L^- \end{pmatrix}, \begin{pmatrix} \nu_{\mu_L} \\ \mu_L^- \end{pmatrix}, \begin{pmatrix} \nu_{\tau_L} \\ \tau_L^- \end{pmatrix}}_{\text{leptons}}; \underbrace{\begin{pmatrix} u_L \\ d_L \end{pmatrix}, \begin{pmatrix} c_L \\ s_L \end{pmatrix}, \begin{pmatrix} t_L \\ b_L \end{pmatrix}}_{\text{quarks}} \quad (4.13)$$

We introduce the left handed doublets:

$$\Psi_{e_L} = \begin{pmatrix} \nu_{e_L} \\ e_L^- \end{pmatrix}, \dots \quad \Psi_{q_L} = \begin{pmatrix} u_L \\ d_L \end{pmatrix}, \dots, \quad (4.14)$$

and the right-handed singlets $\psi_{e_R} = e_R, \dots, \psi_{q_R} = q_R, \dots$. We assume all fermions are massless. The free massless fermion lagrangian is then written,

$$-i\mathcal{L}_F = \bar{e} \not{\partial} e + \bar{\nu}_{e_L} \not{\partial} \nu_{e_L} + \bar{u} \not{\partial} u + \bar{d} \not{\partial} d \quad (4.15)$$

where we have kept the first family of fermions ν_e, e, u, d only and where we have ignored the right-handed neutrino ν_{e_R} not observed experimentally. Using the second of eq. (3.37) and regrouping the members of a doublet one finds

$$-i\mathcal{L}_F = \bar{\Psi}_{e_L} \not{\partial} \Psi_{e_L} + \bar{\Psi}_{q_L} \not{\partial} \Psi_{q_L} + \bar{e}_R \not{\partial} e_R + \bar{u}_R \not{\partial} u_R + \bar{d}_R \not{\partial} d_R \quad (4.16)$$

For massless fermions the charged current introduced by Fermi, eq. (2.2), is conserved so it is tempting to introduce a global symmetry associated to this current.

4.3 The global $SU(2)_L$ gauge invariance

It is obvious that the lagrangian above is invariant under a global $SU(2)$ phase change of the left handed fermion fields, *i.e.* under the transformation,

$$\Psi_L \rightarrow e^{i\alpha \cdot \tau / 2} \Psi_L, \quad \bar{\Psi}_L \rightarrow \bar{\Psi}_L e^{-i\alpha \cdot \tau / 2} \quad (4.17)$$

where the 2×2 Pauli matrices $\boldsymbol{\tau} = (\tau_1, \tau_2, \tau_3)$ satisfy the algebra

$$\left[\frac{\tau_i}{2}, \frac{\tau_j}{2} \right] = i \epsilon_{ijk} \frac{\tau_k}{2}, \quad (4.18)$$

and have the following properties

$$\boldsymbol{\tau} = \boldsymbol{\tau}^\dagger, \quad \text{Tr}(\tau_i \tau_j) = 2\delta_{ij} \quad (4.19)$$

The parameter $\boldsymbol{\alpha} = (\alpha_1, \alpha_2, \alpha_3)$ is a set of 3 arbitrary constants. As discussed above to a global symmetry is associated a conserved current. The $SU(2)$ group has three generators and there are three conserved currents. Following the reasoning leading to eq. (4.6) they are identified to

$$\boxed{J_i^\mu(x) = \bar{\Psi}_{e_L} \gamma^\mu \frac{\tau_i}{2} \Psi_{e_L} + \bar{\Psi}_{q_L} \gamma^\mu \frac{\tau_i}{2} \Psi_{q_L}.} \quad (4.20)$$

They are called the "weak isospin currents". The first two, $J_1^\mu(x)$, $J_2^\mu(x)$, are related to the currents introduced by E. Fermi to describe the weak interaction: for example, using the first of the eq. (3.37) identities, $J_1^\mu(x)$ is written

$$\begin{aligned} J_1^\mu(x) &= \frac{1}{2}(\bar{e}_L \gamma^\mu \nu_{e_L} + \bar{d}_L \gamma^\mu u_L + \text{h.c.}), \\ &= \frac{1}{4}(\bar{e} \gamma^\mu (1 - \gamma_5) \nu_e + \bar{d} \gamma^\mu (1 - \gamma_5) u + \text{h.c.}), \end{aligned}$$

which together with $J_2^\mu(x)$ allows to reconstruct eq. (2.2). The third one is new, it is a neutral current,

$$J_3^\mu(x) = \frac{1}{2}[\bar{\nu}_{e_L} \gamma^\mu \nu_{e_L} - \bar{e}_L \gamma^\mu e_L + \bar{u}_L \gamma^\mu u_L - \bar{d}_L \gamma^\mu d_L]. \quad (4.21)$$

The corresponding weak isopin charge is given by,

$$I_3 = \int d^3x J_3^0(x) = \frac{1}{2} \int d^3x (\nu_{e_L}^\dagger \nu_{e_L} - e_L^\dagger e_L + u_L^\dagger u_L - d_L^\dagger d_L), \quad (4.22)$$

which allows to assign a charge $I_3 = +1/2$ to the neutrino and the u quark and $I_3 = -1/2$ to the electron and the d quark. Obviously $J_3^\mu(x)$ cannot be the current coupling to the photon field otherwise the neutrino would interact with the photon ! $J_3^\mu(x)$ is a neutral current since it does not change the charge of the fermion.

4.4 The global $U(1)_Y$ gauge invariance

The lagrangian \mathcal{L}_F of eq. (4.15) is invariant under a $U(1)$ global transformation acting on all fields, left and right. It is called called the $U(1)_Y$ group, where Y refers to the hypercharge. A transformation

is defined by :

$$\begin{aligned}
\Psi_{e_L} &\rightarrow e^{i\beta y_L^e/2} \Psi_{e_L}, & \Psi_{q_L} &\rightarrow e^{i\beta y_L^q/2} \Psi_{q_L} \\
e_R &\rightarrow e^{i\beta y_R^e/2} e_R, \\
u_R &\rightarrow e^{i\beta y_R^u/2} u_R, & d_R &\rightarrow e^{i\beta y_R^d/2} d_R,
\end{aligned} \tag{4.23}$$

where the $y_L^e, y_L^q, y_R^e, y_R^u, y_R^d$ are the hypercharges of the corresponding fields. The associated conserved current writes (see eq. (4.12))

$$\boxed{J_Y^\mu(x) = y_L^e \bar{\Psi}_{e_L} \gamma^\mu \Psi_{e_L} + y_L^q \bar{\Psi}_{q_L} \gamma^\mu \Psi_{q_L} + y_R^e \bar{e}_R \gamma^\mu e_R + y_R^u \bar{u}_R \gamma^\mu u_R + y_R^d \bar{d}_R \gamma^\mu d_R.} \tag{4.24}$$

Since the sum of conserved currents is also a conserved current we can construct the electromagnetic current,

$$\boxed{J_{\text{emg}}^\mu(x) = e_e \bar{e} \gamma^\mu e + e_u \bar{u} \gamma^\mu u + e_d \bar{d} \gamma^\mu d,} \tag{4.25}$$

as the sum of the weak isospin and hypercharge currents¹⁰ :

$$\boxed{J_{\text{emg}}^\mu(x) = J_3^\mu(x) + \frac{J_Y^\mu(x)}{2},} \tag{4.26}$$

with the hypercharges of the fields chosen so as to construct their correct electric charges (which are normalised here to the charge of the proton). For the lepton sector, for exemple, one finds -1 for the left-handed doublet and -2 for the right-handed electron partner to get a charge of -1 for both left-handed and right-handed component of the electron and 0 for the neutrino. The results are summarised in the following table :

	I	I_3	Y	Q
ν_e	$1/2$	$1/2$	-1	0
e_L	$1/2$	$-1/2$	-1	-1
e_R	0	0	-2	-1
u_L	$1/2$	$1/2$	$1/3$	$2/3$
d_L	$1/2$	$-1/2$	$1/3$	$-1/3$
u_R	0	0	$4/3$	$2/3$
d_R	0	0	$-2/3$	$-1/3$

(4.27)

which shows that the relation between the charge, hypercharge and weak isospin satisfies, by construction, the famous Gell-Mann/Nishijima relation :

$$\boxed{Q = I_3 + \frac{Y}{2}} \tag{4.28}$$

¹⁰the facteur $1/2$ associated to the hypercharge current is historically conventional.

• **Application**

In general, for a $SU(2)$ doublet $\Phi^T = (\phi_1, \phi_2)$ of fields of hypercharge y_Φ and electric charges (e_1, e_2) , the Gell-Mann/Nishijima relation yields

$$e_1 - e_2 = 1 \quad \text{and} \quad y_\Phi = e_1 + e_2, \quad (4.29)$$

Thus the charges of the members of a doublet always differ by one unit of charge while the hypercharge is the sum of the electric charges. For a field singlet under $SU(2)$ the relation between hypercharge and electric charge is simply

$$e_\phi = \frac{y_\phi}{2}. \quad (4.30)$$

5 The local $SU(2)_L \otimes U(1)_Y$ gauge invariance : interactions

The local $SU(2)$ transformation, acting on the left-handed doublets only, is defined by

$$\Psi'_L \rightarrow U(x)\Psi_L = e^{ig\boldsymbol{\alpha}(x)\cdot\boldsymbol{\tau}/2}\Psi_L \quad , \quad \overline{\Psi}'_L \rightarrow \overline{\Psi}_L U^\dagger(x) = \overline{\Psi}_L e^{-ig\boldsymbol{\alpha}(x)\cdot\boldsymbol{\tau}/2}, \quad (5.1)$$

with $UU^\dagger = 1$, or, for an infinitesimal transformation,

$$\delta\Psi_L = ig\boldsymbol{\alpha}(x) \cdot \frac{\boldsymbol{\tau}}{2}\Psi_L \quad , \quad \delta\overline{\Psi}_L = -ig\overline{\Psi}_L \boldsymbol{\alpha}(x) \cdot \frac{\boldsymbol{\tau}}{2}, \quad (5.2)$$

where the 3 components of the real parameter $\boldsymbol{\alpha}(x)$ are functions of the space-time coordinates. We have introduced a coupling g associated to this transformation. Under the local transformation the lagrangian density (4.15) is no longer invariant because of the derivative term in $\partial^\mu\boldsymbol{\alpha}(x)$

$$\delta\mathcal{L}_F = \overline{\Psi}_{e_L} \{-g(\partial^\mu\boldsymbol{\alpha}(x)) \cdot \frac{\boldsymbol{\tau}}{2}\}\gamma_\mu\Psi_{e_L} + \overline{\Psi}_{q_L} \{-g(\partial^\mu\boldsymbol{\alpha}(x)) \cdot \frac{\boldsymbol{\tau}}{2}\}\gamma_\mu\Psi_{q_L} \quad (5.3)$$

To recover the invariance of \mathcal{L}_F under this transformation one introduces a multiplet (a triplet) of gauge vector fields $\mathbf{W}^\mu(x) = (W_1^\mu(x), W_2^\mu(x), W_3^\mu(x))$ and defines the covariant derivative operating only on the left-handed fields :

$$D_L^\mu = \partial^\mu - ig\mathcal{W}^\mu(x), \quad \text{with} \quad \mathcal{W}^\mu(x) = \frac{\boldsymbol{\tau}}{2} \cdot \mathbf{W}^\mu(x). \quad (5.4)$$

The transformation properties of $\mathbf{W}^\mu(x)$ are chosen such that the lagrangian density

$$\mathcal{L}_F = \overline{\Psi}_{e_L} \not{D}_L \Psi_{e_L} + \overline{\Psi}_{q_L} \not{D}_L \Psi_{q_L} + \overline{\psi}_{e_R} \not{\partial} \psi_{e_R} + \overline{\psi}_{u_R} \not{\partial} \psi_{u_R} + \overline{\psi}_{d_R} \not{\partial} \psi_{d_R} \quad (5.5)$$

is invariant under an $SU(2)$ transformation. Since the right-handed fields are not affected by the transformation it is enough to impose that $D_L^\mu\Psi(x)$ transforms as $\Psi(x)$ to achieve the invariance of the lagrangian:

$$(D_L^\mu\Psi(x))' = U(x)(D_L^\mu\Psi(x)). \quad (5.6)$$

Therefore,

$$(D_L^\mu\Psi(x))' = (D_L^\mu)'U(x)\Psi(x) = U(x)D_L^\mu\Psi(x), \quad (5.7)$$

implies

$$(D_L^\mu)' = U(x)D_L^\mu U^{-1}(x), \quad (5.8)$$

since it should hold for all $\Psi(x)$. Consequently, using $\partial^\mu U^{-1}(x) = (\partial^\mu U^{-1}(x)) + U^{-1}(x)\partial^\mu$, one finds

$$(D_L^\mu)' = \partial^\mu + U(x)(\partial^\mu U^{-1}(x)) - igU(x)\mathcal{W}^\mu(x)U^{-1}(x), \quad (5.9)$$

which can be written as $(D_L^\mu)' = \partial^\mu - ig\mathcal{W}^\mu(x)$ with

$$\mathcal{W}^\mu(x) = \frac{i}{g}U(x)(\partial^\mu U^{-1}(x)) + U(x)\mathcal{W}^\mu(x)U^{-1}(x) \quad (5.10)$$

Restricting to the infinitesimal transformations eq. (5.2), one obtains

$$\boxed{\mathcal{W}'^\mu(x) - \mathcal{W}^\mu(x) = \delta\mathcal{W}^\mu(x) = \partial^\mu \boldsymbol{\alpha}(x) \cdot \frac{\boldsymbol{\tau}}{2} + ig [\boldsymbol{\alpha}(x) \cdot \frac{\boldsymbol{\tau}}{2}, \mathcal{W}^\mu(x)],} \quad (5.11)$$

which, in terms of $SU(2)$ components, is equivalent to

$$\boxed{\delta W_i^\mu(x) = \partial^\mu \alpha_i(x) - g \epsilon_{ijk} \alpha_j(x) W_k^\mu(x).} \quad (5.12)$$

spinor we have $D_L'^\mu U = U D_L^\mu$, hence eq. (5.8).

To construct the kinetic term of the gauge bosons $W_i^\mu(x)$ we first consider, as in QED, the tensor

$$\mathcal{F}^{\mu\nu}(x) = [D_L^\mu(x), D_L^\nu(x)] \quad (5.13)$$

Using Leibnitz rule $\partial_\mu W_i^\nu(x) = (\partial_\mu W_i^\nu(x)) + W_i^\nu(x)\partial_\mu$ it is easy to show that the tensor is given by

$$\mathcal{F}^{\mu\nu}(x) = \partial^\mu \mathcal{W}^\nu(x) - \partial^\nu \mathcal{W}^\mu(x) - ig[\mathcal{W}^\mu(x), \mathcal{W}^\nu(x)] \quad (5.14)$$

or in components

$$\boxed{F_i^{\mu\nu}(x) = \partial^\mu W_i^\nu(x) - \partial^\nu W_i^\mu(x) + g \epsilon_{ijk} W_j^\mu(x) W_k^\nu(x).} \quad (5.15)$$

The transformation property of $\mathcal{F}^{\mu\nu}(x)$ is obviously the same as that of D_L^μ , eq. (5.8), and we have then $\mathcal{F}'^{\mu\nu}(x) = U\mathcal{F}^{\mu\nu}(x)U^{-1}$ so that

$$\text{Tr}\mathcal{F}^{\mu\nu}(x)\mathcal{F}_{\mu\nu}(x) = \frac{1}{2}F_i^{\mu\nu}(x)F_{i\mu\nu}(x) \quad (5.16)$$

is a Lorentz scalar invariant under a gauge transformation by the property of cyclicity of the trace. Furthermore it has the right dimension to be the kinetic term of the W_i^μ bosons. The lagrangian of left-handed fields becomes then :

$$\mathcal{L}_{FL} = -\frac{1}{4} F_i^{\mu\nu}(x)F_{i\mu\nu}(x) + \bar{\Psi}_{eL} iD_L^\mu \gamma_\mu \Psi_{eL} + \bar{\Psi}_{qL} iD_L^\mu \gamma_\mu \Psi_{qL}. \quad (5.17)$$

where each of the three terms is invariant under a local $SU(2)$ transformation. We note at this point the perfect analogy between the construction of the “weak” lagrangian with that of QCD: the differences are in the choice of group which requires here only three vector bosons while for $SU(3)$ symmetry eight bosons had to be introduced. Also, the $SU(2)$ group acts only on the left handed components

of the fields and consequently the $W_i^\mu(x)$ gauge bosons do not couple to the right handed fermion components.

We now make the $U(1)_Y$ gauge transformation local. It is defined by

$$\begin{aligned}\delta\Psi_{e_L} &= ig' \frac{y_L^e}{2} \beta(x) \Psi_{e_L}, & \delta\Psi_{q_L} &= ig' \frac{y_L^q}{2} \beta(x) \Psi_{q_L} \\ \delta e_R &= ig' \frac{y_R^e}{2} \beta(x) e_R, \\ \delta u_R &= ig' \frac{y_R^u}{2} \beta(x) u_R, & \delta d_R &= ig' \frac{y_R^d}{2} \beta(x) d_R,\end{aligned}\quad (5.18)$$

with g' the coupling associated to the $U(1)$ transformation. To keep the invariance of the lagrangien requires the introduction of another vector boson $B_\mu(x)$ to which are associated covariant derivatives generating couplings of $B_\mu(x)$ to fermions. Because the fermions carry different hypercharges we introduce covariant derivatives appropriate for each right-handed field : acting on field ψ_R ($\psi = e, u, d$) it is¹¹

$$\boxed{D_{\psi_R}^\mu = \partial^\mu - i g' \frac{y^{\psi_R}}{2} B^\mu}, \quad (5.19)$$

while for the left handed fields the covariant derivative eq. (5.4) acquires a new piece and becomes :

$$\boxed{D_{\psi_L}^\mu = \partial^\mu - i g \frac{\boldsymbol{\tau}}{2} \cdot \mathbf{W}^\mu - i g' \frac{y^{\psi_L}}{2} B^\mu}. \quad (5.20)$$

The stress-energy tensor of the new vector field is simply :

$$\boxed{\mathcal{K}^{\mu\nu}(x) = \partial^\mu B^\nu(x) - \partial^\nu B^\mu(x)} \quad (\text{abelian field}). \quad (5.21)$$

In summary, the initial free lagrangian eq. (4.15) becomes, after imposing a $SU(2)$ local symmetry on the left-handed fields and an appropriate $U(1)$ invariance on both the left-handed fields and a right-handed ones,

$$\boxed{\begin{aligned}\mathcal{L} = \mathcal{L}_G + \mathcal{L}_F &= -\frac{1}{4} F_{i\mu\nu}(x) F_i^{\mu\nu}(x) - \frac{1}{4} \mathcal{K}_{\mu\nu}(x) \mathcal{K}^{\mu\nu}(x) \\ &+ \bar{\Psi}_{e_L} i \not{D}_{e_L} \Psi_{e_L} + \bar{\Psi}_{q_L} i \not{D}_{q_L} \Psi_{q_L} + \\ &+ \bar{e}_R i \not{D}_{e_R} e_R + \bar{u}_R i \not{D}_{u_R} u_R + \bar{d}_R i \not{D}_{d_R} d_R\end{aligned}} \quad (5.22)$$

where only the (e, ν_e) and (u, d) quark family has been specified. It is important to point out that the $SU(2)_L \otimes U(1)_Y$ invariance imposes that all fermions are massless. Indeed a fermion mass term

¹¹The left and right covariant derivatives generically defined as D_L^μ, D_R^μ are now denoted $D_{\psi_L}^\mu, D_{\psi_R}^\mu$ since they depend on the quantum numbers of the fermion fields ψ_L, ψ_R .

in the lagrangian would have the form

$$\mathcal{L}_{mass} = m \bar{\psi}\psi = m(\bar{\Psi}_L \psi_R + \bar{\psi}_R \Psi_L). \quad (5.23)$$

But since Ψ_L is a doublet and $\bar{\psi}_R$ a singlet under $SU(2)$, the mass term cannot be invariant under a gauge transformation!

It is useful to separate the lagrangian density eq. (5.22) into a free part

$$\begin{aligned} \mathcal{L}_{0F} + \mathcal{L}_{0G} = & \bar{\Psi}_{e_L} i \not{\partial} \Psi_{e_L} + \bar{\Psi}_{q_L} i \not{\partial} \Psi_{q_L} + \bar{e}_R i \not{\partial} e_R + \bar{u}_R i \not{\partial} u_R + \bar{d}_R i \not{\partial} d_R \\ & - \frac{1}{4} [(\partial_\mu \mathbf{W}_\nu(x) - \partial_\nu \mathbf{W}_\mu(x)) \cdot (\partial^\mu \mathbf{W}^\nu(x) - \partial^\nu \mathbf{W}^\mu(x)) + (\partial_\mu B_\nu(x) - \partial_\nu B_\mu(x)) (\partial^\mu B^\nu(x) - \partial^\nu B^\mu(x))], \end{aligned} \quad (5.24)$$

and an interacting part containing all terms depending on the couplings g and g' . It contains two classes of terms : one describing the fermion-gauge bosons interactions (which can be expressed very easily in terms of the currents introduced above) and the other the W boson self interactions

$$\begin{aligned} \mathcal{L}_{IF} + \mathcal{L}_{IG} = & g \mathbf{J}^\mu(x) \cdot \mathbf{W}_\mu(x) + g' \frac{J_Y^\mu(x)}{2} B_\mu(x) \\ & - \frac{g}{2} \epsilon_{ijk} (\partial_\mu W_{i\nu}(x) - \partial_\nu W_{i\mu}(x)) W_j^\mu(x) W_k^\nu(x) - \frac{g^2}{4} \epsilon_{ijk} W_{j\mu}(x) W_{k\nu}(x) \epsilon_{ilm} W_l^\mu(x) W_m^\nu(x) \end{aligned} \quad (5.25)$$

with \mathbf{J}^μ the weak isospin current of eq. (4.20) and J_Y^μ the hypercharge current of eq. (4.24). One recognizes in the sum of these two terms the expression which lead to the construction of the electromagnetic current in eq. (4.25).

5.1 Fermion-boson interactions, construction of the photon and the Z boson

We turn first to the fermion- \mathbf{W}^μ interaction. It is read off from \mathcal{L}_{IF} and is simply

$$g \mathbf{J}^\mu(x) \cdot \mathbf{W}_\mu(x) = \frac{g}{2} (\bar{\Psi}_{e_L} \gamma^\mu \tau_i \Psi_{e_L} + \bar{\Psi}_{q_L} \gamma^\mu \tau_i \Psi_{q_L}) W_{i\mu}. \quad (5.26)$$

Defining the charged vector fields

$$(W^\pm)^\mu(x) = \frac{(W_1^\mu(x) \mp i W_2^\mu(x))}{\sqrt{2}}, \quad \text{with} \quad (W^{+*})^\mu(x) = (W^-)^\mu(x) \quad (5.27)$$

their interaction with the fermions can be easily obtained from the charge changing part of the currents ($J_1^\mu(x), J_2^\mu(x)$) in eq. (5.26) and we find

$$\mathcal{L}_{IF}(\text{charged current}) = \frac{g}{\sqrt{2}} (\bar{\nu}_{e_L} \gamma^\mu e_L W_\mu^+ + \bar{u}_L \gamma^\mu d_L W_\mu^+ + \text{h.c.}) \quad (5.28)$$

$$= \frac{g}{2\sqrt{2}} (\bar{\nu}_e \gamma^\mu (1 - \gamma_5) e W_\mu^+ + \bar{u} \gamma^\mu (1 - \gamma_5) d W_\mu^+ + \text{h.c.}), \quad (5.29)$$

which is now expressed in terms of the usual fermion fields ν_e, e, u, d . One can thus read off the W^\pm coupling to fermions : using standard techniques it is found to be $-i(g/2\sqrt{2})\gamma_\mu(1 - \gamma_5)$, coupling with the same strength to all fermion species. (Note the relation $g/2\sqrt{2} = g_W$ of eq. (2.16)).

Turning now to the neutral vector bosons sector one has two pieces : one originates from the $SU(2)_L$ invariance, namely $gJ_3^\mu W_{3\mu}$ contained in eq. (5.26), and the other one from the $U(1)_Y$ invariance, $g'J_Y^\mu B_\mu$. From eq. (5.25) we can read off the neutral current interaction lagrangian which is

$$\mathcal{L}_{IF}(\text{neutral currents}) = gJ_3^\mu W_{3\mu} + g'\frac{1}{2}J_Y^\mu B_\mu \quad (5.30)$$

Note that the photon cannot be identified to the $W_{3\mu}$ field because of the γ_5 term in the coupling nor to the B_μ boson because of the different charge assignment for the left and right component of a fermion field. The photon will be constructed as a linear combination of both. Thus, introducing the fields A_μ and Z_μ such that

$$\begin{aligned} B^\mu &= \cos\theta A^\mu - \sin\theta Z^\mu \\ W_3^\mu &= \sin\theta A^\mu + \cos\theta Z^\mu, \end{aligned} \quad (5.31)$$

with θ an adjustable parameter, one finds

$$\mathcal{L}_{IF}(\text{neutral currents}) = (g \sin\theta J_3^\mu + g' \cos\theta \frac{1}{2} J_Y^\mu) A_\mu + (g \cos\theta J_3^\mu - g' \sin\theta \frac{1}{2} J_Y^\mu) Z_\mu. \quad (5.32)$$

To construct the field A_μ as the photon field we should adjust the parameters to be such that

$$g \sin\theta J_3^\mu + g' \cos\theta \frac{1}{2} J_Y^\mu = e J_{\text{emg}}^\mu \quad (5.33)$$

where, by convention, e is taken as the charge of the proton. This can be achieved if we choose

$$\boxed{g \sin\theta = g' \cos\theta = e} \quad (5.34)$$

since, then, we recover eq. (4.26) which lead to eq. (4.25) for J_{emg}^μ . With this choice, we have $J_Y^\mu/2 = J_{\text{emg}}^\mu - J_3^\mu$ which is used to eliminate in the coefficient of Z_μ the hypercharge current so that the interaction lagrangien reads

$$\mathcal{L}_{IF}(\text{neutral currents}) = e J_{\text{emg}}^\mu A_\mu + \frac{e}{\sin\theta \cos\theta} (J_3^\mu - \sin^2\theta J_{\text{emg}}^\mu) Z_\mu, \quad (5.35)$$

defining the couplings of the photon $A_\mu(x)$ and the neutral $Z_\mu(x)$ boson to the fermions. Concerning the Z_μ couplings we can be more explicit and derive them for a pair of fermions ψ_1, ψ_2 of charge

e_1, e_2 (normalised to the proton charge e) respectively, such that (ψ_{1L}, ψ_{2L}) forms a $SU(2)$ doublet ($I = 1/2$) and ψ_{1R}, ψ_{2R} are singlets ($I = 0$). Writing explicitly the currents J_3^μ and J_{emg}^μ , we have from eq. (5.35):

$$\begin{aligned}
& \frac{e}{\sin \theta \cos \theta} \left[(\bar{\psi}_{1L} \bar{\psi}_{2L}) \begin{pmatrix} 1/2 - e_1 \sin^2 \theta & 0 \\ 0 & -1/2 - e_2 \sin^2 \theta \end{pmatrix} \not{Z} \begin{pmatrix} \psi_{1L} \\ \psi_{2L} \end{pmatrix} \right. \\
& \quad \left. + (\bar{\psi}_{1R} \bar{\psi}_{2R}) \begin{pmatrix} -e_1 \sin^2 \theta & 0 \\ 0 & -e_2 \sin^2 \theta \end{pmatrix} \not{Z} \begin{pmatrix} \psi_{1R} \\ \psi_{2R} \end{pmatrix} \right] \\
&= \frac{e}{\sin \theta \cos \theta} \left[(\bar{\psi}_1 \bar{\psi}_2) \begin{pmatrix} 1/2 - e_1 \sin^2 \theta & 0 \\ 0 & -1/2 - e_2 \sin^2 \theta \end{pmatrix} \not{Z} \frac{(1 - \gamma_5)}{2} \begin{pmatrix} \psi_1 \\ \psi_2 \end{pmatrix} \right. \\
& \quad \left. + (\bar{\psi}_1 \bar{\psi}_2) \begin{pmatrix} -e_1 \sin^2 \theta & 0 \\ 0 & -e_2 \sin^2 \theta \end{pmatrix} \not{Z} \frac{(1 + \gamma_5)}{2} \begin{pmatrix} \psi_1 \\ \psi_2 \end{pmatrix} \right] \\
&= \frac{e}{\sin \theta \cos \theta} \left[(\bar{\psi}_1 \bar{\psi}_2) \begin{pmatrix} 1/4 - e_1 \sin^2 \theta & 0 \\ 0 & -1/4 - e_2 \sin^2 \theta \end{pmatrix} \not{Z} \begin{pmatrix} \psi_1 \\ \psi_2 \end{pmatrix} \right. \\
& \quad \left. - (\bar{\psi}_1 \bar{\psi}_2) \begin{pmatrix} 1/4 & 0 \\ 0 & -1/4 \end{pmatrix} \not{Z} \gamma_5 \begin{pmatrix} \psi_1 \\ \psi_2 \end{pmatrix} \right] \tag{5.36}
\end{aligned}$$

The full neutral current interaction lagrangian density eq. (5.35) can then be written for one generation of quarks and leptons

$$\begin{aligned}
\mathcal{L}_{IF}(\text{neutral currents}) &= -e \bar{e} \not{A} e + \frac{e}{\sin \theta \cos \theta} \sum_{l=\nu, e} \bar{l} \not{Z} (a_l - b_l \gamma_5) l \\
& \quad + e \sum_{q=u, d} e_q \bar{q} \not{A} q + \frac{e}{\sin \theta \cos \theta} \sum_{q=u, d} \bar{q} \not{Z} (a_q - b_q \gamma_5) q
\end{aligned} \tag{5.37}$$

with

$$\boxed{a_i = \frac{I_3}{2} - e_i \sin^2 \theta, \quad b_i = \frac{I_3}{2}.} \tag{5.38}$$

Contrary to the photon which has a purely vector coupling to the fermions, the neutral gauge boson Z_μ has both vector and axial-vector couplings. We recall that with the choice of $g = e/\cos \theta$ the charged W_μ couplings are

$$\boxed{\mathcal{L}_{IF}(\text{charged current}) = \frac{e}{2\sqrt{2}\sin \theta} (\bar{\nu}_e \gamma^\mu (1 - \gamma_5) e W_\mu^+ + \bar{u} \gamma^\mu (1 - \gamma_5) d W_\mu^+ + \text{h.c.}),} \tag{5.39}$$

These couplings are in agreement with those of the physical Z boson once the "weak mixing" or Weinberg angle θ (in fact introduced by Glashow!) is taken from experiment to be :

$$\sin^2 \theta \sim .2313 . \tag{5.40}$$

We hereafter denote the weak mixing angle by θ_w .

• **The covariant derivative in terms of the A_μ, Z_μ, W_μ^\pm fields**

It is useful, for later use, to have an explicit representation of the covariant derivatives eqs. (5.19) and (5.20) in terms of the W_μ^\pm, A_μ and Z_μ gauge bosons. Although they can be read off the previous discussion based on defining the electromagnetic current we construct them directly. For instance, the covariant derivative eq. (5.20) acting on a $SU(2)$ doublet of fields with hypercharge y_ϕ , the components of which having electric charge (ee_1, ee_2) , contains the piece

$$-ig\frac{\tau_3}{2}W_{3\mu} - ig'y_\phi\frac{B_\mu}{2} = -i\left[(g\sin\theta_w\frac{\tau_3}{2} + g'\cos\theta_w\frac{y_\phi}{2})A_\mu + (g\cos\theta_w\frac{\tau_3}{2} - g'\sin\theta_w\frac{y_\phi}{2})Z_\mu\right] \quad (5.41)$$

For A_μ to be the photon one imposes the conditions

$$\begin{aligned} \frac{1}{2}(g\sin\theta_w + g'y_\phi\cos\theta_w) = ee_1 & \quad \Rightarrow \quad g'y_\phi\cos\theta_w = e(e_1 + e_2) & \quad \Rightarrow \quad g'\cos\theta_w = e \\ \frac{1}{2}(-g\sin\theta_w + g'y_\phi\cos\theta_w) = ee_2 & \quad \Rightarrow \quad g\sin\theta_w = e(e_1 - e_2) = e & \quad \Rightarrow \quad g\sin\theta_w = e, \end{aligned} \quad (5.42)$$

where the rightmost equalities are a consequence, eq. (4.29), of the Gell-Mann/Nishijima relation. Eliminating g, g', y_ϕ in favour of e, θ_w and the charges one finds

$$-ig\frac{\tau_3}{2}W_{3\mu} - ig'y_\phi\frac{B_\mu}{2} = -ie\begin{pmatrix} e_1A_\mu & 0 \\ 0 & e_2A_\mu \end{pmatrix} - \frac{ie}{\sin\theta_w\cos\theta_w}\begin{pmatrix} \frac{1}{2} - e_1\sin^2\theta_w & 0 \\ 0 & -\frac{1}{2} - e_2\sin^2\theta_w \end{pmatrix} Z_\mu$$

Going back to the full expression, eq. (5.20), including the W_μ^\pm contribution, the covariant derivative on a doublet field is

$$\boxed{D_\mu = \partial_\mu - i\frac{e}{\sqrt{2}\sin\theta_w}\begin{pmatrix} 0 & W_\mu^+ \\ W_\mu^- & 0 \end{pmatrix} - ie\begin{pmatrix} e_1A_\mu & 0 \\ 0 & e_2A_\mu \end{pmatrix} - i\frac{e}{\sin\theta_w\cos\theta_w}\begin{pmatrix} (\frac{1}{2} - e_1\sin^2\theta_w)Z_\mu & 0 \\ 0 & (-\frac{1}{2} - e_2\sin^2\theta_w)Z_\mu \end{pmatrix}} \quad (5.43)$$

Since, by definition, $W_\mu^{-*} = W_\mu^+$, from now on we use the notation $W_\mu^- = W_\mu$ and $W_\mu^+ = W_\mu^*$ to respectively represent the wave functions of the W^- and W^+ gauge bosons.

The covariant derivative acting on a singlet ϕ is simply

$$\boxed{D_\mu = \partial_\mu - ig'y_\phi\frac{B_\mu}{2} = \partial_\mu - ie e_\phi A_\mu + i\frac{e e_\phi \sin^2\theta_w}{\sin\theta_w\cos\theta_w}Z_\mu} \quad (5.44)$$

5.2 Gauge bosons and their self-interactions

We already identified in eq. (5.24) the free gauge boson pieces \mathcal{L}_{0G} and in eq. (5.25) the interacting terms \mathcal{L}_{IG} . We now reformulate these expressions in terms of the "physical" fields W_μ^*, W_μ, Z_μ and

A_μ . For this purpose we rewrite \mathcal{L}_{0G} by doing an integration by part and neglecting, as usual, the terms which are total derivatives, we find

$$\mathcal{L}_{0G} = \frac{1}{2}W_{i\mu}(x)\mathcal{D}^{\mu\nu}W^{i\nu}(x) + \frac{1}{2}B_\mu(x)\mathcal{D}^{\mu\nu}B_\nu(x), \quad (5.45)$$

with $\mathcal{D}^{\mu\nu} = \square g^{\mu\nu} - \partial^\mu \partial^\nu$. This is rewritten in a matrix form

$$\mathcal{L}_{0G} = \frac{1}{2}(W_{1\mu} \ W_{2\mu}) \begin{pmatrix} \mathcal{D}^{\mu\nu} & 0 \\ 0 & \mathcal{D}^{\mu\nu} \end{pmatrix} \begin{pmatrix} W_{1\mu} \\ W_{2\mu} \end{pmatrix} + \frac{1}{2}(W_{3\mu} \ B_\mu) \begin{pmatrix} \mathcal{D}^{\mu\nu} & 0 \\ 0 & \mathcal{D}^{\mu\nu} \end{pmatrix} \begin{pmatrix} W_{3\mu} \\ B_\mu \end{pmatrix}. \quad (5.46)$$

We go from the $W_{3\mu}, B_\mu$ coordinates to the A_μ, Z_μ coordinates by a rotation matrix \mathcal{R} , eq. (5.31), and since $\mathcal{R}^T \mathcal{R} = 1$, we can immediately replace $(W_{3\mu} \ B_\mu)$ by $(A_\mu \ Z_\mu)$ in the equation above. Now we go from the $W_{1\mu}, W_{2\mu}$ components to the charged W 's ones via the matrix \mathcal{O} defined by

$$\begin{pmatrix} W_{1\mu} \\ W_{2\mu} \end{pmatrix} = \begin{pmatrix} \frac{1}{\sqrt{2}} & \frac{1}{\sqrt{2}} \\ \frac{i}{\sqrt{2}} & \frac{-i}{\sqrt{2}} \end{pmatrix} \begin{pmatrix} W_\mu^* \\ W_\mu \end{pmatrix}, \quad (5.47)$$

which satisfies $\mathcal{O}^T \mathcal{O} = \begin{pmatrix} 0 & 1 \\ 1 & 0 \end{pmatrix}$ so that we can immediately write

$$\begin{aligned} \mathcal{L}_{0G} &= \frac{1}{2}[W_\mu^*(x)\mathcal{D}^{\mu\nu}W_\nu(x) + W_\mu(x)\mathcal{D}^{\mu\nu}W_\nu^*(x)] + \frac{1}{2}Z_\mu(x)\mathcal{D}^{\mu\nu}Z_\nu(x) + \frac{1}{2}A_\mu(x)\mathcal{D}^{\mu\nu}A_\nu(x) \\ &= -\frac{1}{4}\mathcal{K}_{\mu\nu}^*\mathcal{K}^{\mu\nu} - \frac{1}{4}\mathcal{K}_{\mu\nu}\mathcal{K}^{*\mu\nu} - \frac{1}{4}\mathcal{K}_{Z\mu\nu}\mathcal{K}_Z^{\mu\nu} - \frac{1}{4}\mathcal{K}_{A\mu\nu}\mathcal{K}_A^{\mu\nu}, \end{aligned} \quad (5.48)$$

where in the last line we have dropped a total derivative and where the $\mathcal{K}^{*\mu\nu}, \mathcal{K}^{\mu\nu}, \mathcal{K}_Z^{\mu\nu}, \mathcal{K}_A^{\mu\nu}$ are respectively the abelian-like stress-energy tensors, eq. (5.21), of the W^\pm, Z, A gauge bosons.

We turn now to the interaction lagrangian density \mathcal{L}_{IG} eq. (5.25). Permuting $\mu \leftrightarrow \nu, j \leftrightarrow k$ in the term $\epsilon_{ijk}\partial_\nu W_{i\mu}(x)W_j^\mu(x)W_k^\nu(x)$ one obtains

$$\mathcal{L}_{IG} = -g \epsilon_{ijk}\partial_\mu W_{i\nu}(x)W_j^\mu(x)W_k^\nu(x) - \frac{g^2}{4}\epsilon_{ijk}W_{j\mu}(x)W_{k\nu}(x) \epsilon_{ilm}W_l^\mu(x)W_m^\nu(x). \quad (5.49)$$

The term linear in g can be written

$$-g \det \begin{vmatrix} \partial_\mu W_{1\nu} & W_1^\mu & W_1^\nu \\ \partial_\mu W_{2\nu} & W_2^\mu & W_2^\nu \\ \partial_\mu W_{3\nu} & W_3^\mu & W_3^\nu \end{vmatrix}. \quad (5.50)$$

Adding $i \times$ the second line to the first one to reconstruct W_μ^* and taking into account the fact that a determinant is invariant when adding or subtracting lines (eventually multiplied by a constant factor)

one obtains for the expression (5.50)

$$\begin{aligned}
-g \det \begin{vmatrix} \sqrt{2}\partial_\mu W_\nu^* & \sqrt{2}W^{*\mu} & \sqrt{2}W^{*\nu} \\ \partial_\mu W_{2\nu} & W_2^\mu & W_2^\nu \\ \partial_\mu W_{3\nu} & W_3^\mu & W_3^\nu \end{vmatrix} &= -\frac{g}{2i} \det \begin{vmatrix} \sqrt{2}\partial_\mu W_\nu^* & \sqrt{2}W^{*\mu} & \sqrt{2}W^{*\nu} \\ 2i\partial_\mu W_{2\nu} & 2iW_2^\mu & 2iW_2^\nu \\ \partial_\mu W_{3\nu} & W_3^\mu & W_3^\nu \end{vmatrix} \\
&= ig \det \begin{vmatrix} \partial_\mu W_\nu^* & W^{*\mu} & W^{*\nu} \\ \partial_\mu W_\nu & W^\mu & W^\nu \\ \partial_\mu W_{3\nu} & W_3^\mu & W_3^\nu \end{vmatrix}. \tag{5.51}
\end{aligned}$$

The last equality is obtained by subtracting the first line from the second. Then using $W_{3\nu} = \sin\theta_W A_\nu + \cos\theta_W Z_\nu$ and the relation $e = g \sin\theta_W$ (eq. (5.34)), the above expression becomes

$$ie \det \begin{vmatrix} \partial_\mu W_\nu^* & W^{*\mu} & W^{*\nu} \\ \partial_\mu W_\nu & W^\mu & W^\nu \\ \partial_\mu A_\nu & A^\mu & A^\nu \end{vmatrix} + ie \frac{\cos\theta_W}{\sin\theta_W} \det \begin{vmatrix} \partial_\mu W_\nu^* & W^{*\mu} & W^{*\nu} \\ \partial_\mu W_\nu & W^\mu & W^\nu \\ \partial_\mu Z_\nu & Z^\mu & Z^\nu \end{vmatrix}. \tag{5.52}$$

Expanding the determinant we find for the $\gamma W^+ W^-$ vertex

$$-i e [\partial_\mu W_\nu^* (W^\mu A^\nu - A^\mu W^\nu) - \partial_\mu W_\nu (W^{*\mu} A^\nu - A^\mu W^{*\nu}) + \partial_\mu A_\nu (W^{*\mu} W^\nu - W^{-\mu} W^{*\nu})], \tag{5.53}$$

By assigning a definite index to each field, *e.g.* $A^\lambda, W^\rho, W^{*\sigma}$, the expression takes the usual form

$$ie [A^\lambda g^{\rho\sigma} (W_\rho \partial_\lambda W_\sigma^* - W_\sigma^* \partial_\lambda W_\rho) + W^\rho g^{\sigma\lambda} (W_\sigma^* \partial_\rho A_\lambda - A_\lambda \partial_\rho W_\sigma^*) + W^{*\sigma} g^{\lambda\rho} (A_\lambda \partial_\sigma W_\rho - W_\rho \partial_\sigma A_\lambda)], \tag{5.54}$$

and similarly for the $ZW^+ W^-$ vertex with the coupling $e \cos\theta_W / \sin\theta_W$ instead of e . This defines all tri-linear couplings among gauge bosons.

The term in g^2 in the interaction lagrangian density eq. (5.49) is rather boring to expand. Using the relation $\epsilon_{ijk}\epsilon_{ilm} = \delta_{jl}\delta_{km} - \delta_{jm}\delta_{kl}$, it becomes

$$\begin{aligned}
&-\frac{e^2}{4\sin^2\theta_W} [\mathbf{W}^\mu(x) \cdot \mathbf{W}_\mu(x) \mathbf{W}^\nu(x) \cdot \mathbf{W}_\nu(x) - \mathbf{W}^\mu(x) \cdot \mathbf{W}_\nu(x) \mathbf{W}^\nu(x) \cdot \mathbf{W}_\mu(x)] \\
&= -\frac{e^2}{4\sin^2\theta_W} [W_i^\mu W_{i\rho} W_j^\nu W_{j\sigma}] [g_\mu^\rho g_\nu^\sigma - g_\mu^\sigma g_\nu^\rho] \tag{5.55}
\end{aligned}$$

with the notation $\mathbf{W}^\mu \cdot \mathbf{W}_\nu = \Sigma_i W_i^\mu W_{i\nu}$. One obtains the vertex for the physical fields using

$$\mathbf{W}^\mu(x) \cdot \mathbf{W}_\rho(x) = W^\mu W_\rho^* + W^{*\mu} W_\rho + (\sin\theta_W A^\mu + \cos\theta_W Z^\mu)(\sin\theta_W A_\rho + \cos\theta_W Z_\rho), \tag{5.56}$$

so that eq. (5.55) becomes

$$-\frac{e^2}{2\sin^2\theta_W} [W_\mu W_\rho^* W_\sigma W_\nu^* + W_\mu W_\rho^* (\sin\theta_W A_\sigma + \cos\theta_W Z_\sigma)(\sin\theta_W A_\nu + \cos\theta_W Z_\nu)] [g^{\mu\rho} g^{\nu\sigma} - g^{\mu\sigma} g^{\nu\rho}]$$

The antisymmetry of the $[g^{\mu\rho} g^{\nu\sigma} - g^{\mu\sigma} g^{\nu\rho}]$ tensor combination kills the terms with only photons and/or Z bosons. The self-couplings of gauge bosons are thus given by

$$\begin{aligned}
\mathcal{L}_{IG} = & \\
& -i e [A^\lambda g^{\rho\sigma} (W_\rho \partial_\lambda W_\sigma^* - W_\sigma^* \partial_\lambda W_\rho) + W^\rho g^{\sigma\lambda} (W_\sigma^* \partial_\rho A_\lambda - A_\lambda \partial_\rho W_\sigma^*) + W^{*\sigma} g^{\lambda\rho} (A_\lambda \partial_\sigma W_\rho - W_\rho \partial_\sigma A_\lambda)] \\
& + \{A_\lambda \rightarrow Z_\lambda, \quad e \rightarrow e \cos \theta_w / \sin \theta_w\} \tag{5.57} \\
& - \frac{e^2}{2 \sin^2 \theta_w} [W_\mu W_\rho^* W_\sigma W_\nu^* + W_\mu W_\rho^* (\sin \theta_w A_\sigma + \cos \theta_w Z_\sigma) (\sin \theta_w A_\nu + \cos \theta_w Z_\nu)] [g^{\mu\rho} g^{\nu\sigma} - g^{\mu\sigma} g^{\nu\rho}]
\end{aligned}$$

In conclusion, from eq. (5.49) one has two three-boson vertices $W^-W^+\gamma$, W^-W^+Z with derivative couplings and four four-boson vertices $W^-W^+W^-W^+$, $W^-W^+\gamma\gamma$, W^-W^+ZZ , $W^-W^+\gamma Z$. The absence of vertices involving only γ 's and/or Z 's has its origin in the fact that they would arise from the term $g^2 \epsilon_{i33} W_{3\mu}(x) W_{3\nu}(x) \epsilon_{i33} W_3^\rho(x) W_3^\sigma(x)$, in eq. (5.49), which is of course 0. Using "standard methods" one can, from the expressions above, extract the Feynman rules for the couplings between fermions and gauge bosons. It will not be done here as they can be found in books.

To summarize this rather technical section we count at this point 15 couplings in the model (for one generation of fermions). One has:

- 9 fermion-fermion-boson vertices: $\bar{e}e\gamma$, $\bar{e}eZ$, $\bar{\nu}_e\nu_e Z$, $\bar{\nu}_e e W^+$, $\bar{u}u\gamma$, $\bar{u}uZ$, $\bar{d}d\gamma$, $\bar{d}dZ$, $\bar{u}dW^+$
- 2 trilinear gauge bosons vertices : $W^+W^-\gamma$, W^+W^-Z
- 4 quadrilinear gauge bosons vertices : $W^-W^+W^-W^+$, $W^-W^+\gamma\gamma$, W^-W^+ZZ , $W^-W^+\gamma Z$.

They depend only on two parameters e and θ_w (and, of course, the fermion charges). It is obvious that the symmetry properties of the lagrangien is quite constraining. The important fact is that the relations between couplings derived above will be preserved by the mechanism of "spontaneous symmetry breaking" we are going to discuss. This is an important difference with a mechanism of explicit symmetry breaking where these relations would have been lost.

5.3 Progress status and problems

Considering what has been achieved until now, one finds that the model based on the $SU(2)_L \otimes U(1)_Y$ symmetry contains four gauge bosons: two charged ones with $(V - A)$ couplings to fermions and two neutral ones with couplings such that these bosons can be interpreted as the photon and the Z boson. The "only" difference with the real world is that in the present state of development of the model the gauge bosons are massless, because of the assumed exact gauge invariance and the fermions are also massless because of the left-right asymmetry of the gauge group. Counting the bosonic degrees

of freedom of the model one realizes that three degrees of freedom are “missing”, associated to the longitudinal polarisation states of the heavy vector bosons as summarised in the table.

	<u>Model</u>			<u>Real World</u>	
	degrees of freedom			degrees of freedom	
	transverse	longitudinal		transverse	longitudinal
W^-	2	0	W^-	2	1
W^+	2	0	W^+	2	1
Z	2	0	Z	2	1
γ	2	0	γ	2	0

In order to complete the model one should therefore introduce at least three new fields in the lagrangian. This will be done through a multiplet of scalar fields and it will be seen that, by the mechanism of spontaneous symmetry breaking of local gauge invariance, some of the scalar fields become the longitudinal polarisation states and correlatively the vector bosons acquire a mass.

6 Spontaneous symmetry breaking under a global phase change

We proceed in steps and discuss, first, the case of a global symmetry and state the Goldstone theorem. In the next sections we deal with the case of a spontaneously broken local $U(1)$ symmetry, leading to a massive gauge boson, and then we turn to the Glashow-Weinberg-Salam model based on a broken $SU(2)_L \otimes U(1)_Y$ symmetry.

6.1 Global symmetry breaking

Consider the very simple case of a complex scalar field

$$\varphi = \frac{1}{\sqrt{2}}(\varphi_1 + i\varphi_2) \quad (6.1)$$

which has two degrees of freedom $\varphi_1(x), \varphi_2(x)$. The lagrangian

$$\mathcal{L} = \partial_\mu \varphi^* \partial^\mu \varphi - V(\varphi) \text{ with the potential } V(\varphi) = -\mu^2 |\varphi|^2 + h |\varphi|^4. \quad (6.2)$$

is invariant under a rigid $U(1)$ phase transformation $\varphi(x) \rightarrow e^{i\alpha} \varphi(x)$ where α is constant. The potential has the well-known ‘‘Mexican hat’’ or ‘‘cul-de-bouteille’’ shape (depending on your cultural background!). The hamiltonian is

$$\begin{aligned} H &= \pi \partial_0 \varphi - \mathcal{L}, \text{ with } \pi = \frac{\delta \mathcal{L}}{\delta \partial_0 \varphi} = \partial_0 \varphi^* \\ &= \underbrace{|\vec{\nabla} \varphi|^2}_{H_{\text{kinetic}}} + V(\varphi). \end{aligned} \quad (6.3)$$

The (positive) kinetic part vanishes for static configurations and the full hamiltonian is minimal for constant values of the field given by

$$|\varphi_0| = \frac{\mu}{\sqrt{2h}} = \frac{v}{\sqrt{2}} \quad (6.4)$$

which defines the so-called vacuum expectation value v of the field φ in terms of the parameters of the lagrangian. Indeed, the quantum theory should be constructed from the lowest energy classical state which, in this case, is characterised by having its norm constrained by the above equation. One immediately notices that the vacuum is degenerate since the application of a gauge transformation (phase change) does not affect the norm of the state. There is an infinite number of classical vacuum states, namely all states of type $|\varphi_0| e^{i\alpha}$. However to construct the quantum theory one needs to choose a particular vacuum, by imposing, for example, the classical vacuum field to be real *i.e.*

$$\varphi_0 = \frac{v}{\sqrt{2}} \quad (6.5)$$

This obviously amounts to breaking the symmetry of the vacuum since φ_0 is no more invariant under a gauge transformation, but the dynamical laws are still unbroken because they are given by the gauge invariant lagrangian eq. (6.2). This is the basis of “spontaneous symmetry breaking” in contradistinction to “explicit symmetry breaking” where the lagrangian itself would lose gauge invariance. To study the theory, we translate the original field by its vacuum expectation value

$$\varphi(x) = \frac{1}{\sqrt{2}}(v + \varphi_1(x) + i\varphi_2(x)) \quad (6.6)$$

and, neglecting constant terms, the lagrangian becomes

$$\begin{aligned} \mathcal{L} = & \frac{1}{2}(\partial_\mu\varphi_1)^2 - hv^2\varphi_1^2 + \frac{1}{2}(\partial_\mu\varphi_2)^2 \\ & - hv\varphi_1(\varphi_1^2 + \varphi_2^2) - \frac{h}{4}(\varphi_1^2 + \varphi_2^2)^2 \end{aligned} \quad (6.7)$$

After spontaneous symmetry breaking, we are left with a model of two interacting real fields φ_1 and φ_2 . The free theory is given by the first line of the equation above which shows that φ_1 has a mass $m_{\varphi_1} = \sqrt{2hv^2}$ while φ_2 is massless: φ_2 is called the Goldstone boson. The interaction part is all contained in the second line of eq. (6.7) and there are cubic and quartic interactions between φ_1 and φ_2 . Since, the initial lagrangian contained only two parameters, there are necessarily relations between the three parameters m_{φ_1} , the coefficient of the cubic coupling term g_3 and the coefficient of the quartic coupling g_4 e.g.

$$g_3^2 = 2m_{\varphi_1}^2 g_4. \quad (6.8)$$

Such a relation reflects the symmetry property of the lagrangian density. These features are a simple illustration of very general properties of spontaneous breaking of larger (non-abelian) group symmetry. They are a particular case of the Goldstone theorem.

6.2 The Goldstone theorem

This theorem reads :

When a global symmetry is spontaneously broken there appear as many massless scalar modes (called the Goldstone bosons) as there are broken degrees of symmetry.

A proof of this theorem is now sketched. Consider φ , a collection of n scalar fields φ_i , $i = 1, \dots, n$ written as a column vector so that

$$\varphi^T = (\varphi_1, \dots, \varphi_n) \quad (6.9)$$

The lagrangian density is formally written as

$$\mathcal{L} = \mathcal{L}(\varphi, \partial_\mu \varphi)_{\text{kin}} - V(\varphi). \quad (6.10)$$

The vacuum of the model is defined by the conditions

$$\frac{\delta V}{\delta \varphi_i} = 0, \Rightarrow \text{vacuum: } \varphi^{0T} = (\varphi_1^0, \dots, \varphi_n^0) \quad (6.11)$$

One perturbs around the vacuum state

$$\varphi = \varphi^0 + \varphi', \quad \text{i.e. } \varphi_i = \varphi_i^0 + \varphi'_i \quad (6.12)$$

so that the lagrangian (neglecting constant terms) is re-written

$$\mathcal{L} = \mathcal{L}(\varphi', \partial_\mu \varphi')_{\text{kin}} - \frac{1}{2} \sum_{ij} \left. \frac{\delta V}{\delta \varphi_i \delta \varphi_j} \right|_{\varphi^0} \varphi'_i \varphi'_j \oplus (\varphi'^3) \oplus (\varphi'^4) \quad (6.13)$$

where it is not necessary for our present purposes to specify the cubic nor the quartic couplings. By construction, there are no terms linear in the fields because we are expanding around the minimum of the potential. The quantity of interest is the quadratic term which defines the mass matrix

$$m_{ij}^2 = \left. \frac{\delta V}{\delta \varphi_i \delta \varphi_j} \right|_{\varphi^0}. \quad (6.14)$$

Consider now the action of an infinitesimal global gauge transformation. Its action on the fields is

$$\delta \varphi = i \alpha^J T^J \varphi, \quad J = 1, \dots, N, \quad (6.15)$$

where the T^J are the N generators ($n \times n$ matrices) of the group and the α^J are the N associated arbitrary parameters. If for some field configuration φ we have for a particular generator T^J ,

$$T^J \varphi = 0, \Rightarrow \delta \varphi = i \alpha^J T^J \varphi = 0, \quad (6.16)$$

then we say that this configuration φ is invariant under the sub-group generated by T^J : the corresponding symmetry is unbroken. If, on the contrary, $T^J \varphi \neq 0$ the corresponding degree of symmetry is said to be spontaneously broken. Let us suppose now that the vacuum satisfies

$$\begin{aligned} T^J \varphi^0 &\neq 0 && \text{for } J = 1, \dots, N' \\ T^J \varphi^0 &= 0 && \text{for } J = N' + 1, \dots, N, \end{aligned} \quad (6.17)$$

i.e. that the vacuum state breaks N' degrees of symmetry. The invariance of the potential $V(\varphi)$ under the gauge transformation $\delta \varphi_i = i \alpha^J T_{ik}^J \varphi_k$ yields

$$\delta V(\varphi) = \frac{\delta V}{\delta \varphi_i} \delta \varphi_i = i \alpha^J \frac{\delta V}{\delta \varphi_i} T_{ik}^J \varphi_k = 0. \quad (6.18)$$

Since this true for any α^J one has

$$\frac{\delta V}{\delta \varphi_i} T_{ik}^J \varphi_k = 0. \quad (6.19)$$

Taking the derivative of this relation at $\varphi = \varphi^0$, it comes out

$$\frac{\delta^2 V}{\delta \varphi_j \delta \varphi_i} \Big|_{\varphi^0} T_{ik}^J \varphi_k^0 + \frac{\delta V}{\delta \varphi_i} \Big|_{\varphi^0} T_{ik}^J \delta_{kj} = 0 \Rightarrow m_{ji}^2 T_{ik}^J \varphi_k^0 = 0, \quad (6.20)$$

where the last equality is true because φ^0 defines the minimum of the potential. Since this relation is automatically satisfied for $J = N' + 1, \dots, N$ one concludes that the mass matrix must have N' vanishing eigenvalues. Thus, N' fields φ'_i will be massless which are the Golstone bosons associated to the N' degrees of broken symmetry (*qed*).

7 Spontaneous local U(1) symmetry breaking

We impose now that the lagrangian density eq. (6.2) is invariant under the local phase change $\varphi(x) \rightarrow e^{ig\alpha(x)}\varphi(x)$. For this purpose we introduce a vector field $B_\mu(x)$ and a covariant derivative $D_\mu = \partial_\mu - igB_\mu(x)$ such that $D_\mu\varphi(x) \rightarrow ig\alpha(x)D_\mu\varphi(x)$ under an infinitesimal phase change. This is realised if $B_\mu(x)$ transforms as $B_\mu(x) \rightarrow B_\mu(x) + g\partial_\mu\alpha(x)$. Since $D_\mu\varphi^*(x) \rightarrow -ig\alpha(x)D_\mu\varphi^*(x)$ the locally invariant version of the scalar field lagrangian density is

$$\mathcal{L}_S + \mathcal{L}_G = D_\mu\varphi^*D_\mu\varphi + \mu^2\varphi^*\varphi - h(\varphi^*\varphi)^2 - \frac{1}{4}\mathcal{K}_{\mu\nu}\mathcal{K}^{\mu\nu} \quad (7.1)$$

where we have also included the kinetic term, see eq. (5.21), of the gauge boson $B_\mu(x)$. As in the study of the breaking of the global symmetry we choose as the lowest energy state $\varphi_0 = v/\sqrt{2}$, (eq. (6.5)), and we expand the field around this vacuum expectation value as in eq. (6.6).

7.1 Unitary gauge

We take advantage of the freedom of choice of the gauge to find a function $\alpha(x)$ such that $e^{ig\alpha(x)}$ applied to eq. (6.6) gives

$$\varphi(x) = \frac{1}{\sqrt{2}}(v + H(x)), \quad (7.2)$$

i.e. we absorb the imaginary part in a change of phase and we are left with one real field $H(x)$. This choice defines the unitary gauge. Applying the covariant derivative on $\varphi(x)$ one obtains

$$D_\mu\varphi(x) = \frac{1}{\sqrt{2}}\partial_\mu H(x) - igB_\mu(x)\frac{1}{\sqrt{2}}(v + H(x)) \quad (7.3)$$

Injecting this in the lagrangian density, taking the potential part from eq. (6.7) with $\varphi_1 = H$, $\varphi_2 = 0$, and reshuffling the terms we find

$$\boxed{\begin{aligned} \mathcal{L}_S + \mathcal{L}_G = & \left[\frac{1}{2}(\partial_\mu H(x))^2 - hv^2 H^2(x) \right] + \left[-\frac{1}{4}\mathcal{K}_{\mu\nu}(x)\mathcal{K}^{\mu\nu}(x) + \frac{g^2 v^2}{2}B_\mu(x)B^\mu(x) \right] \\ & + g^2 v H(x)B_\mu(x)B^\mu(x) + \frac{g^2}{2}H^2(x)B_\mu(x)B^\mu(x) - hvH^3(x) - \frac{h}{4}H^4(x). \end{aligned}} \quad (7.4)$$

The terms in the first line are those from which we build the propagators of the H and B_μ fields respectively, while the second line contains the couplings between the fields. Applying the Euler-Lagrange equation (4.1) we obtain for the H field ($\partial_\mu\partial^\mu = \square$)

$$(-\square - 2hv^2)H(x) = 3hvH^2(x) + hH^3(x) - g^2 v B_\mu(x)B^\mu(x) - g^2 H(x)B_\mu(x)B^\mu(x), \quad (7.5)$$

and for the gauge boson

$$(\square g_{\mu\nu} - \partial_\mu \partial_\nu + (gv)^2) B^\nu(x) = -g^2 H^2(x) B_\mu(x) - 2g^2 v H B_\mu(x). \quad (7.6)$$

To get the free propagators one solves the Green's functions

$$\begin{aligned} (-\square - 2hv^2) G(x-y) &= i\delta^{(4)}(x-y) \\ (\square g_{\mu\rho} - \partial_\mu \partial_\rho + (gv)^2 g_{\mu\rho}) G^{\rho\nu}(x-y) &= ig'_\mu{}^\nu \delta^{(4)}(x-y), \end{aligned} \quad (7.7)$$

in Fourier space. For the scalar field one parameterises $G(x-y) = \int (d^4k/(2\pi)^4) \exp(-ik(x-y)) G(k)$ and one easily get the H field propagator

$$\boxed{G(k) = \frac{i}{k^2 - M_H^2 + i\epsilon} \quad \text{with} \quad M_H = v\sqrt{2h},} \quad (7.8)$$

with the $i\epsilon$ prescription required by causality. Similarly, for the gauge field we write $G^{\mu\nu}(x-y) = \int (d^4k/(2\pi)^4) \exp(-ik(x-y)) G^{\mu\nu}(k)$ to get

$$(-k^2 g_{\mu\rho} + k_\mu k_\rho + (gv)^2 g_{\mu\rho}) G^{\rho\nu}(k) = ig'_\mu{}^\nu. \quad (7.9)$$

We look for the solution under the form $G^{\rho\nu}(k) = ag^{\rho\nu} + bk^\rho k^\nu$ which is the most general rank 2 tensor which can be constructed from a vector k^μ . One obtains finally

$$\boxed{G_{\mu\nu}(k) = \frac{-i}{k^2 - M_B^2 + i\epsilon} \left(g_{\mu\nu} - \frac{k_\mu k_\nu}{M_B^2} \right) \quad \text{with} \quad M_B = gv.} \quad (7.10)$$

The mass of the scalar H field is $M_H = \sqrt{2h}v$ and the mass of the gauge field $M_B = gv$: both are proportional to the vacuum expectation value of the scalar field but the latter is proportional to the gauge coupling while the former depends on the quartic coupling in the potential. The term giving rise to the gauge boson mass originates from the covariant derivative acting on $\varphi(x)$ after symmetry breaking while the mass of the H field comes from the potential $V(\varphi)$.

• **Remark on the polarisation of a massive vector boson**

The propagator of $B_\mu(x)$ is that of a massive scalar field which has three states of polarisation. Indeed one can easily verify, from eq. (2.25), that the numerator of eq. (7.10) is

$$-\left(g_{\mu\nu} - \frac{k_\mu k_\nu}{M_B^2} \right) = \sum_i \varepsilon_\mu^{(i)}(k) \varepsilon_\nu^{(i)}(k), \quad (7.11)$$

the trace of which is -3.

Counting the degrees of freedom in the model we have after symmetry breaking one real scalar field $H(x)$ and the three polarisation states of the gauge boson while before symmetry breaking one had two scalar fields $\varphi_1(x), \varphi_2(x)$ and the two polarisation states of the massless gauge boson : it appears that the massless Goldstone boson $\varphi_2(x)$ has become the longitudinal polarisation of $B_\mu(x)$. The gauge used in this derivation is called the unitary gauge. With this choice the vector boson propagator may lead, as we have seen, to divergences when calculating Feynman diagrams because of the $k_\mu k_\nu / m_B^2$ term and therefore may ruin the renormalisability of the model.

7.2 Renormalisable gauges : 't Hooft R_ξ gauges

To study this in more detail we go back to the lagrangian density eq. (7.1) with the general form, eq. (6.6), of the scalar field after symmetry breaking. The covariant derivative is then

$$\begin{aligned} D_\mu \phi(x) &= (\partial_\mu - igB_\mu(x)) \frac{1}{\sqrt{2}} (v + \phi_1(x) + i\phi_2(x)) \\ &= \frac{1}{\sqrt{2}} [\partial_\mu \phi_1(x) + gB_\mu(x)\phi_2(x)] + \frac{i}{\sqrt{2}} [\partial_\mu \phi_2(x) - gB_\mu(x)(v + \phi_1(x))] \end{aligned} \quad (7.12)$$

The lagrangian density takes then the form, keeping explicitly only the terms quadratic in the fields,

$$\boxed{\mathcal{L}_S + \mathcal{L}_G = \left[\frac{1}{2} (\partial_\mu \phi_1(x))^2 - hv^2 \phi_1^2(x) \right] + \left[-\frac{1}{4} \mathcal{K}_{\mu\nu}(x) \mathcal{K}^{\mu\nu}(x) + \frac{g^2 v^2}{2} B_\mu(x) B^\mu(x) \right] + \left[\frac{1}{2} (\partial_\mu \phi_2(x))^2 - gvB_\mu(x) \partial^\mu \phi_2(x) \right] + \mathcal{L}_{\text{int}}.} \quad (7.13)$$

The first line is identical to that of eq. (7.4) with a massive scalar field $\phi_1(x)$ ($\phi_1(x) = H(x)$ is the Higgs field) and a massive gauge boson. In the second line one has the massless $\phi_2(x)$ scalar (the Goldstone boson) coupling to the gauge field. The function \mathcal{L}_{int} ,

$$\mathcal{L}_{\text{int}} = g(\varphi_2 \overleftrightarrow{\partial}_\mu \varphi_1) B^\mu + g^2 v \varphi_1 B_\mu B^\mu + \frac{g^2}{2} (\varphi_1^2 + \varphi_2^2) B_\mu B^\mu - hv\varphi_1 (\varphi_1^2 + \varphi_2^2) - \frac{h}{4} (\varphi_1^2 + \varphi_2^2)^2, \quad (7.14)$$

contains the couplings between ϕ_1, ϕ_2 and B_μ .

Clearly $\phi_2(x)$ is not independent on $B_\mu(x)$ since it oscillates into the gauge boson with a derivative coupling as can be seen from eq. (7.13). In fact if we consider the polarisation tensor of the B_μ field, treating both the mass term and the $B_\mu \partial^\mu \phi_2$ as vertices we find ($gv = M_B$)

$$\begin{array}{c} \text{wavy line} \text{---} \text{grey circle} \text{---} \text{wavy line} \\ \text{---} \text{wavy line} \text{---} \text{black circle} \text{---} \text{wavy line} \\ \text{---} \text{wavy line} \text{---} \text{black dot} \text{---} \text{arrow} \text{---} \text{black dot} \text{---} \text{wavy line} \end{array} = \begin{array}{c} \text{wavy line} \text{---} \text{black circle} \text{---} \text{wavy line} \\ \text{---} \text{wavy line} \text{---} \text{black dot} \text{---} \text{arrow} \text{---} \text{black dot} \text{---} \text{wavy line} \end{array} + \begin{array}{c} \text{wavy line} \text{---} \text{black dot} \text{---} \text{arrow} \text{---} \text{black dot} \text{---} \text{wavy line} \\ \text{---} \text{wavy line} \text{---} \text{black dot} \text{---} \text{arrow} \text{---} \text{black dot} \text{---} \text{wavy line} \end{array}$$

$$iM_B^2 g_{\mu\nu} \qquad \qquad \qquad -M_B k_\mu \qquad \qquad \qquad M_B k_\nu$$

$$iM_B^2 g^{\mu\nu} + (-M_B k^\mu) \frac{i}{k^2} M_B k^\nu = iM_B^2 (g^{\mu\nu} - \frac{k^\mu k^\nu}{k^2}) \quad (7.15)$$

which is transverse as it should be. From eq. (2.25) one sees that the tensor structure is equivalent to summing over transverse and longitudinal polarisations of B_μ : this shows that $\phi_2(x)$ builds up the longitudinal polarisation of the originally transverse $B_\mu(x)$ field. One may suspect that iterating the self-energy bubble on the B_μ field propagator will reconstruct the propagator of a massive field. This is discussed more precisely below.

We follow here a procedure familiar from QED. To quantise QED, it is necessary to break the gauge invariance and this is done by adding to the lagrangian a ‘‘gauge fixing’’ term. Here the gauge fixing term is chosen to be

$$\mathcal{L}_{GF} = -\frac{1}{2\xi} (\partial_\mu B^\mu(x) + \xi gv \phi_2(x))^2. \quad (7.16)$$

This choice (instead of the traditional term $-(\partial_\mu B^\mu(x))^2/2\xi$ of QED) is made to eliminate the mixed term $gvB_\mu(x)\partial^\mu\phi_2(x)$ in the lagrangian. This class of gauge conditions is known under the name of ‘t Hooft’s gauges or R_ξ gauges where ξ is an arbitrary real number. One considers the new lagrangian density $\mathcal{L}_S + \mathcal{L}_G + \mathcal{L}_{GF}$ which then becomes

$$\boxed{\mathcal{L}_S + \mathcal{L}_G + \mathcal{L}_{GF} = \left[\frac{1}{2} (\partial_\mu \phi_1(x))^2 - hv^2 \phi_1^2(x) \right] + \frac{1}{2} [(\partial_\mu \phi_2(x))^2 - \xi (gv)^2 \phi_2^2(x)] + \left[-\frac{1}{4} \mathcal{K}_{\mu\nu} \mathcal{K}^{\mu\nu} + \frac{(gv)^2}{2} B_\mu(x) B^\mu(x) \right] + \frac{1}{2\xi} (\partial_\mu B^\mu(x))^2 + \mathcal{L}_{\text{int}}} \quad (7.17)$$

By the specific choice of the gauge condition the mixed term in $B_\mu \partial^\mu \phi_2$ in $\mathcal{L}_S + \mathcal{L}_G$ combines with the term $\phi_2 \partial^\mu B_\mu$ in \mathcal{L}_{GF} to give a total derivative which can be safely ignored in perturbation theory. However the Goldstone boson acquires a mass from the gauge fixing lagrangian density. Following the procedure used when working in the unitary gauge one derives the Green’s equation for the fields ϕ_i and B_μ , the solution of which gives the free propagators. Thus one obtains

$$\begin{aligned} (-\square - 2hv^2)G_{\phi_1}(x-y) &= i\delta^{(4)}(x-y) \\ (-\square - \xi(gv)^2)G_{\phi_2}(x-y) &= i\delta^{(4)}(x-y) \\ (\square g_{\mu\nu} - (1 - \frac{1}{\xi})\partial_\mu\partial_\nu + (gv)^2 g_{\mu\nu})G^{\nu\rho}(x-y) &= ig_\mu^\rho \delta^{(4)}(x-y). \end{aligned} \quad (7.18)$$

For the scalar fields we obtain easily

$$\text{for the field } \phi_1 = H \quad \boxed{G_H(k) = \frac{i}{k^2 - M_H^2 + i\epsilon} \quad \text{with } M_H = v\sqrt{2h}} \quad (7.19)$$

$$\text{for the Goldstone field } \phi_2 \quad \boxed{G_{\phi_2}(k) = \frac{-i}{k^2 - \xi M_B^2 + i\epsilon} \quad \text{with } M_B = gv} \quad (7.20)$$

For the gauge fields, introducing $G^{\nu\rho}(x-y) = \int (d^4k/(2\pi)^4) \exp(-ik(x-y))G^{\nu\rho}(k)$ one has to solve

$$(k^2 g_{\mu\nu} - (1 - \frac{1}{\xi})k_\mu k_\nu - M_B^2 g_{\mu\nu})G^{\nu\rho}(k) = -i g_\mu^\rho \quad (7.21)$$

One looks for the solution in the form of $a^{\nu\rho} + b k^\nu k^\rho$ and one finds

$$\boxed{G_{\nu\rho}(k) = -\frac{i}{k^2 - M_B^2 + i\epsilon} \left(g_{\nu\rho} - (1 - \xi) \frac{k_\nu k_\rho}{k^2 - \xi M_B^2} \right)}. \quad (7.22)$$

One observes that for any value of ξ finite all propagators have the right asymptotic behavior *i.e.* they behave like $1/k^2, k^2 \rightarrow \infty$ which is a necessary condition for the model to be renormalisable. However both the Goldstone and the gauge boson propagators have a spurious pole at $k^2 - \xi m_B^2$ which should cancel when calculating a physical process. It is interesting to compare the gauge boson propagator in the general 't Hooft gauge with its form in the unitary gauge. One proves easily

$$-\frac{i}{k^2 - M_B^2 + i\epsilon} \left(g_{\nu\rho} - (1 - \xi) \frac{k_\nu k_\rho}{k^2 - \xi M_B^2} \right) = -\frac{i}{k^2 - M_B^2 + i\epsilon} \left(g_{\nu\rho} - \frac{k_\nu k_\rho}{M_B^2} \right) - \frac{i}{M_B^2} \frac{k_\nu k_\rho}{k^2 - \xi M_B^2} \quad (7.23)$$

One recognises on the right-hand side the propagator in the unitary gauge, eq. (7.10), plus a term which has the the same pole structure as the Goldstone boson. An exemple will be given later, on how such a cancellation occurs between this extra piece and the Goldstone contribution.

Special choices of ξ can be made:

- $\xi = 0$ (Landau gauge) : the Goldstone boson is massless and the gauge boson propagator is transverse *i.e.* $k^\nu G_{\nu\rho} = 0$;
- $\xi = 1$ (Feynman gauge) : the Goldstone boson has the same mass as the gauge boson but one loses the transversity property of the gauge boson propagator;
- $\xi \rightarrow \infty$: the Goldstone boson does not propagate and one keeps only the physical degrees of freedom in the model: one recovers the unitary gauge already considered.

7.3 Fermion masses

We now include a fermion in our toy model. We assume one massless fermion $\psi(x)$ and impose a local $U(1)$ gauge invariance only on the left-handed component of $\psi(x)$: $\delta\psi_L(x) = ig\alpha(x)\psi_L(x)$, $\delta\psi_R(x) = 0$. The fermion part of the lagrangian density takes the form

$$\mathcal{L}_F = \bar{\psi}_L i \mathcal{D} \psi_L + \bar{\psi}_R i \not{\partial} \psi_R, \quad (7.24)$$

with the covariant derivative acting on $\psi_L(x)$ defined by

$$\mathcal{D} \psi_L = (\not{\partial} - ig \not{B}) \psi_L. \quad (7.25)$$

We parameterise the $U(1)$ invariant interaction between the scalar field and the fermion by the Yukawa type lagrangian density

$$\mathcal{L}_Y = -\lambda_f(\bar{\psi}_L\phi\psi_R + \bar{\psi}_R\phi^*\psi_L). \quad (7.26)$$

After symmetry breaking, using the parameterisation eq. (6.6) of the scalar field, only \mathcal{L}_Y is affected

$$\begin{aligned} \mathcal{L}_Y &= -\frac{\lambda_f}{\sqrt{2}}(v + H)(\bar{\psi}_L\psi_R + \bar{\psi}_R\psi_L) - i\frac{\lambda_f}{\sqrt{2}}\phi_2(\bar{\psi}_L\psi_R - \bar{\psi}_R\psi_L) \\ &= -\frac{\lambda_f v}{\sqrt{2}}\bar{\psi}\psi - \frac{\lambda_f}{\sqrt{2}}H\bar{\psi}\psi - i\frac{\lambda_f}{\sqrt{2}}\phi_2\bar{\psi}\gamma^5\psi, \end{aligned} \quad (7.27)$$

where we have recombined the left-handed and right-handed fields. Regrouping all fermion terms we have

$$\mathcal{L}_F + \mathcal{L}_Y = \bar{\psi}(i\not{\partial} - \frac{\lambda_f v}{\sqrt{2}})\psi + \frac{g}{2}\bar{\psi}\not{B}(1 - \gamma^5)\psi - \frac{\lambda_f}{\sqrt{2}}H\bar{\psi}\psi - i\frac{\lambda_f}{\sqrt{2}}\phi_2\bar{\psi}\gamma^5\psi. \quad (7.28)$$

We read off the fermion mass

$$m_f = \frac{\lambda_f v}{\sqrt{2}} \quad (7.29)$$

and the couplings of the fermion

- to the gauge field : $-i(g/2)\gamma_\mu(1 - \gamma^5)$;
- to the Higgs field : $i\lambda_f/\sqrt{2}$;
- to the Goldstone boson : $(\lambda_f/\sqrt{2})\gamma^5$.

The coupling of the Higgs to the fermion can be written in terms of "physical parameters", masses and the gauge coupling, and one finds

$$\text{coupling Higgs-fermion-fermion : } i\lambda_f/\sqrt{2} = i g \frac{m_f}{M_B}, \quad (7.30)$$

which illustrates an important feature of spontaneous symmetry breaking, namely that the coupling is proportional to the fermion mass.

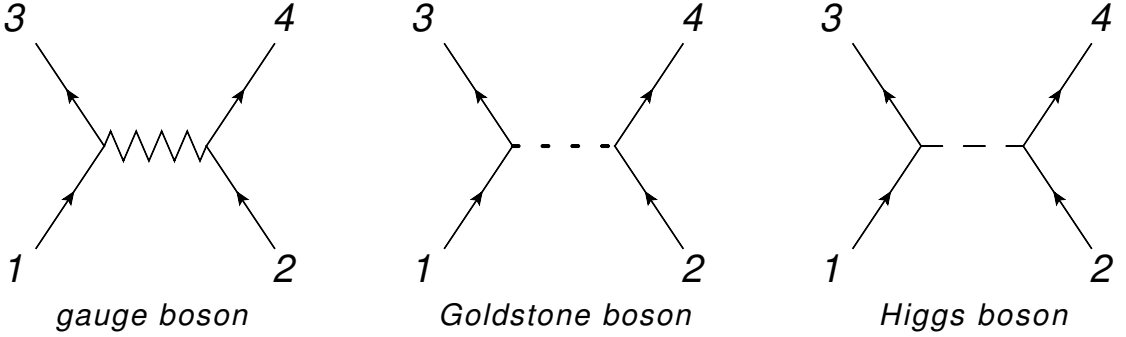
In the unitary gauge, the Higgs and gauge boson couplings to the fermion are as above, while the Goldstone boson ϕ_2 is absorbed by the gauge choice and does not couple to the fermion.

7.4 Gauge invariance at the Born level: an exemple

Putting everything together, the lagrangien density of our model in a general R_ξ gauge is

$$\mathcal{L}_S + \mathcal{L}_G + \mathcal{L}_{GF} + \mathcal{L}_F + \mathcal{L}_Y \quad (7.31)$$

with $\mathcal{L}_S + \mathcal{L}_G + \mathcal{L}_{GF}$ from eq. (7.17) and $\mathcal{L}_F + \mathcal{L}_Y$ from eq. (7.28). We are now in a position to calculate the scattering amplitude for the collision $\psi_1 + \psi_2 \rightarrow \psi_3 + \psi_4$. The diagrams to be considered are



The point is to check that the first two diagrams lead to a gauge independent contribution since the Higgs exchange diagram is independent of the gauge choice ξ . Using the decomposition eq. (7.23) of the gauge boson propagator in the general 't Hooft gauge it is enough to prove that the rightmost term in eq. (7.23) is cancelled by the Goldstone exchange diagram. From the gauge boson exchange we have

$$-\frac{g^2}{4}\bar{\psi}_3\gamma_\mu(1-\gamma^5)\psi_1(-i)\frac{k^\mu k^\nu}{M_B^2(k^2-\xi M_B^2)}\bar{\psi}_4\gamma_\nu(1-\gamma^5)\psi_2. \quad (7.32)$$

Using Dirac equation this term can be considerably simplified. For instance with $k^\mu = p_1^\mu - p_3^\mu$

$$\begin{aligned} \bar{\psi}_3\gamma_\mu(1-\gamma^5)\psi_1 k^\mu &= \bar{\psi}_3(\not{p}_1 - \not{p}_3)\psi_1 + \bar{\psi}_3\gamma^5\not{p}_1\psi_1 + \bar{\psi}_3\not{p}_3\gamma^5\psi_1 \\ &= 2m_f\bar{\psi}_3\gamma^5\psi_1, \end{aligned} \quad (7.33)$$

where to obtain the last line we have used Dirac equation $\not{p}_1\psi_1 = m_f\psi_1$ and $\bar{\psi}_3\not{p}_3 = m_f\bar{\psi}_3$. The same trick can be used at the other vertex to obtain

$$\begin{aligned} \bar{\psi}_4\gamma_\mu(1-\gamma^5)\psi_2 k^\mu &= \bar{\psi}_4(\not{p}_4 - \not{p}_2)\psi_2 - \bar{\psi}_4\not{p}_4\gamma^5\psi_2 - \bar{\psi}_4\gamma^5\not{p}_2\psi_2 \\ &= -2m_f\bar{\psi}_4\gamma^5\psi_2. \end{aligned} \quad (7.34)$$

This shows that after symmetry breaking the axial current $\bar{\psi}\gamma_\mu\gamma_5\psi$ is not conserved since, when contracted with the gauge field momentum, it gives a term proportional to the mass of the fermion. Thus eq. (7.32) reduces to

$$-\frac{g^2 m_f^2}{M_B^2} \frac{i}{k^2 - \xi M_B^2} \bar{\psi}_3 \gamma^5 \psi_1 \bar{\psi}_4 \gamma^5 \psi_2 \quad (7.35)$$

The contribution of the Goldstone boson exchange is simply

$$\frac{\lambda_F^2}{2} \frac{i}{k^2 - \xi M_B^2} \bar{\psi}_3 \gamma^5 \psi_1 \bar{\psi}_4 \gamma^5 \psi_2 \quad (7.36)$$

Using the relation $g^2 m_f^2 / M_B^2 = \lambda_F^2 / 2$, eq. (7.30), one easily verifies the compensation of the ξ dependent part of the gauge propagator by the Goldstone boson. Needless to say that, for this to occur, the

mass term of the gauge boson and that of the fermion should have the same origin and be both related to the vacuum expectation value v . The gauge invariance can be checked on other processes notably those involving the triple gauge couplings, however the discussion is more tricky since it implies the coupling of the Goldstone field to the vector boson as given in (7.14).

8 The broken $SU(2)_L \otimes U(1)_Y$ symmetry

In this case, the generators of the symmetry group will be $T^J = (\tau_1, \tau_2, \tau_3, Y)$, *i.e.* the generators of the weak isospin group and of the $U(1)_Y$ hypercharge gauge group. We introduce a complex scalar field $\Phi(x)$, which is a doublet of $SU(2)$ ($I_\Phi = \frac{1}{2}$),

$$\Phi = \frac{1}{\sqrt{2}} \begin{pmatrix} \varphi_1 - i \varphi_2 \\ \varphi_3 - i \varphi_4 \end{pmatrix} \quad (8.1)$$

and the standard scalar lagrangian

$$\mathcal{L}_S = \partial_\mu \Phi^\dagger \partial^\mu \Phi - V(\Phi), \quad V(\Phi) = -\mu^2 \Phi^\dagger \Phi + h (\Phi^\dagger \Phi)^2. \quad (8.2)$$

which is invariant under the rigid transformation

$$\Phi \rightarrow \Phi' = e^{i\tau \cdot \alpha/2} e^{iy_\Phi \beta/2} \Phi. \quad (8.3)$$

The minimum of the potential is obtained for (see eq. (6.4))

$$\Phi^\dagger \Phi = |\Phi|^2 = \frac{\mu^2}{2h} = \frac{v^2}{2}. \quad (8.4)$$

There is an infinite number of vacua states : all states with the norm $v/\sqrt{2}$ obtained by a gauge transformation. We choose the physical vacuum to be

$$\boxed{\Phi_0 = \begin{pmatrix} 0 \\ \frac{v}{\sqrt{2}} \end{pmatrix} \quad \text{with} \quad v = \frac{\mu}{\sqrt{h}}.} \quad (8.5)$$

Since we require the electric charge to be conserved after symmetry breaking, following the reasoning in sec. 6.2, we have to enforce that the charge generator acting on the vacuum state should vanish.

Using the Gell-Mann/Nishijima relation eq. (4.28) the charge operator acting on Φ_0 is

$$Q \Phi_0 = (I_3 + \frac{Y}{2}) \Phi_0 = \frac{1}{2} (\tau_3 + Y) \Phi_0 = \begin{pmatrix} \frac{1}{2} + \frac{y_\Phi}{2} & 0 \\ 0 & -\frac{1}{2} + \frac{y_\Phi}{2} \end{pmatrix} \begin{pmatrix} 0 \\ \frac{v}{\sqrt{2}} \end{pmatrix} = 0 \quad (8.6)$$

implying that the hypercharge of the scalar field must be $y_\Phi = 1$ to ensure charge conservation in the broken theory: the charge of the classical vacuum is 0. As in the abelian case, we can study the system around the classical minimum and expand the scalar field around its vacuum expectation value

$$\Phi = \begin{pmatrix} \frac{1}{\sqrt{2}}(\omega_1(x) - i\omega_2(x)) \\ \frac{1}{\sqrt{2}}(v + \omega_0(x) - i\omega_3(x)) \end{pmatrix} = \begin{pmatrix} \omega^*(x) \\ \frac{1}{\sqrt{2}}(v + \omega_0(x) - i\omega_3(x)) \end{pmatrix}. \quad (8.7)$$

The complex field ω^* has a positive electric charge while ω_0 and ω_3 are neutral. In terms of the new variables the scalar potential $V(\Phi)$ becomes

$$V(\Phi) = hv^2\omega_0^2 + hv\omega_0(\omega_0^2 + \omega^2) + \frac{h}{4}(\omega_0^2 + \omega^2)^2 \quad (8.8)$$

showing that the triplet ω of ω_i fields is massless while the neutral ω_0 field acquires a mass

$$\boxed{M_{\omega_0} = \sqrt{2}hv}. \quad (8.9)$$

All these fields are coupled together with a strength which can be read off the equation above.

Thus, in our model, in agreement with Noether theorem, three degrees of freedom are broken leading to three massless Goldstone bosons, and the vacuum is still left invariant under the combination $Q = I_3 + Y/2$. There is still an abelian symmetry left, namely the $U(1)_{\text{emg}}$ group.

8.1 Local symmetry breaking and the Brout-Englert-Higgs mechanism

Armed with this lengthy preliminaries we now turn to spontaneous breaking of the local gauge symmetry $SU(2)_L \otimes U(1)_Y$ down to $U(1)_{\text{emg}}$ in the framework of the Standard Model. Let us state the results before diving into an ocean of technicalities. The case of a global symmetry has just been analysed and led to the appearance of three massless (Goldstone) bosons and a massive one. When the symmetry is made local these massless bosons turn out to be unphysical (two charged ones, ω and ω^* , and a neutral one ω_3), in the sense that they can be gotten rid off by a gauge transformation, but instead, three gauge bosons (a neutral one and the two charged ones) become massive and therefore acquire longitudinal polarisation states which are the Goldstone modes in disguise.

To implement the breaking of the local $SU(2)_L \otimes U(1)_Y$ symmetry we first have to extend the electroweak lagrangian eq. (5.22) to include the scalar field contribution \mathcal{L}_S eq. (8.2) in its locally gauge invariant form (see eq. (8.12) below) as well as the interaction of the scalar field with the fermions \mathcal{L}_Y (where Y stands for Yukawa; see eq. (8.26) below) so that the complete electroweak lagrangian density is

$$\mathcal{L} = \mathcal{L}_F + \mathcal{L}_G + \mathcal{L}_S + \mathcal{L}_Y. \quad (8.10)$$

In the following we work in the unitary gauge.

8.2 The Higgs and gauge bosons sector : masses and couplings

We concentrate for the moment on \mathcal{L}_S which drives the spontaneous breaking of the local electroweak symmetry. Only neutral scalar fields can acquire a vacuum expectation value : other fields, such

as fermions or gauge bosons, cannot do so otherwise the physical vacuum would have some angular momentum or other non-vanishing quantum numbers. We impose now the invariance of \mathcal{L}_S under a change of the local phases

$$\Phi(x) \rightarrow \Phi'(x) = e^{ig\alpha(x)\cdot\tau/2} e^{ig'y_\Phi\beta(x)/2} \Phi(x). \quad (8.11)$$

To keep gauge invariance requires substituting the covariant derivative to the partial derivative in \mathcal{L}_S which then takes the form

$$\boxed{\mathcal{L}_S = D_\mu \Phi^\dagger D_\mu \Phi - \mu^2 \Phi^\dagger \Phi + h(\Phi^\dagger \Phi)^2} \quad (8.12)$$

with the definition, eq. (5.20),

$$D_\mu = \partial^\mu - i g \frac{\boldsymbol{\tau}}{2} \cdot \mathbf{W}^\mu - i \frac{1}{2} g' B^\mu \quad (8.13)$$

and the choice, eq. (8.6), $y_\Phi = 1$ for the hypercharge. This can be easily checked using the same line of reasoning as used in sec. 5.

To study the system around the classical vacuum we parameterise the scalar field as in eq. (8.7). However we note that by an appropriate gauge transformation we can find $\alpha(x)$, $\beta(x)$ such that :

$$e^{ig'y_\Phi\beta(x)/2} e^{ig\tau\cdot\alpha(x)/2} \Phi(x) = \begin{pmatrix} 0 \\ \frac{v+H(x)}{\sqrt{2}} \end{pmatrix}, \quad (8.14)$$

showing that the fields $\omega_i(x)$ can be removed from the lagrangian altogether and therefore are not physical. Of course, explicit gauge invariance of the vacuum state will be lost since a particular gauge has been chosen. To analyse the effects of symmetry breaking we work with the ‘‘physical’’ A_μ and Z_μ fields of eq. (5.31) rather than with $W_{3\mu}$ and B_μ . For this purpose we use the expression eq. (5.43) for the covariant derivative which, applied to the form eq. (8.14) of Φ (with $e_1 = 1, e_2 = 0$), yields

$$\begin{aligned} D_\mu \begin{pmatrix} 0 \\ \frac{v+H(x)}{\sqrt{2}} \end{pmatrix} &= \left[\partial_\mu - i \frac{e}{\sqrt{2} \sin \theta_W} \begin{pmatrix} 0 & W_\mu^* \\ W_\mu & 0 \end{pmatrix} - ie \begin{pmatrix} A_\mu & 0 \\ 0 & 0 \end{pmatrix} \right. \\ &\quad \left. - i \frac{e}{\sin \theta_W \cos \theta_W} \begin{pmatrix} \frac{1}{2} - \sin^2 \theta_W Z_\mu & 0 \\ 0 & -\frac{1}{2} Z_\mu \end{pmatrix} \right] \begin{pmatrix} 0 \\ \frac{v+H(x)}{\sqrt{2}} \end{pmatrix} \\ &= \begin{pmatrix} -i \frac{e}{2 \sin \theta_W} W_\mu^* (v + H(x)) \\ \partial_\mu \frac{H(x)}{\sqrt{2}} + i \frac{e}{2\sqrt{2} \sin \theta_W \cos \theta_W} Z_\mu (v + H(x)) \end{pmatrix} \end{aligned} \quad (8.15)$$

It is then trivial to get $D_\mu \Phi^\dagger D_\mu \Phi$ and write the scalar lagrangian density \mathcal{L}_S

$$\boxed{\mathcal{L}_S = \frac{1}{2} (\partial_\mu H(x))^2 + \frac{e^2}{4 \sin^2 \theta_W} (v + H(x))^2 W_\mu^* W^\mu + \frac{e^2}{8 \sin^2 \theta_W \cos^2 \theta_W} (v + H(x))^2 Z_\mu Z^\mu - hv^2 H^2 - hv H^3 - \frac{h}{4} H^4} \quad (8.16)$$

In the last line we have used eq. (8.8) for the scalar potential dropping of course the spurious $\omega(x)$ fields which have been gauged away. The above equation contains a lot of information since it gives masses to the gauge and the Higgs fields as well as defines the couplings between them.

• **Masses**

Combining the terms proportional to v^2 in the equation above with the stress-energy terms of \mathcal{L}_{0G} , eq. (5.48), we have the pieces in the lagrangien density which lead to the free propagators of the H and gauge bosons,

$$\begin{aligned} \mathcal{L}_{OS} + \mathcal{L}_{OG} &= \frac{1}{2}(\partial_\mu H(x))^2 - hv^2 H^2 - \frac{1}{4}\mathcal{K}_{A\mu\nu}\mathcal{K}_A^{\mu\nu} \\ &\quad - \frac{1}{2}\mathcal{K}_{\mu\nu}^*\mathcal{K}^{\mu\nu} + \frac{e^2 v^2}{4\sin^2\theta_W}W_\mu^*W^\mu \\ &\quad - \frac{1}{4}\mathcal{K}_{Z\mu\nu}\mathcal{K}_Z^{\mu\nu} + \frac{e^2 v^2}{8\sin^2\theta_W\cos^2\theta_W}Z_\mu Z^\mu \end{aligned} \quad (8.17)$$

Using the same method as in sec. 7.1 we can derive the propagators of the H scalar and the gauge bosons

$$\begin{aligned} G(k) &= \frac{i}{k^2 - M_H^2 + i\epsilon} \\ G_A^{\mu\nu}(k) &= \frac{-i}{k^2 + i\epsilon} g^{\mu\nu} \\ G_W^{\mu\nu}(k) &= \frac{-i}{k^2 - M_W^2 + i\epsilon} (g^{\mu\nu} - k^\mu k^\nu / M_W^2) \\ G_Z^{\mu\nu}(k) &= \frac{-i}{k^2 - M_Z^2 + i\epsilon} (g^{\mu\nu} - k^\mu k^\nu / M_Z^2) \end{aligned} \quad (8.18)$$

We recover a massive H field with $M_H = \sqrt{2h} v$ as in eq. (7.8), while the W and Z bosons acquire the masses

$$\boxed{M_W = \frac{ev}{2\sin\theta_W}, \quad M_Z = \frac{ev}{2\sin\theta_W\cos\theta_W}}, \quad (8.19)$$

and the photon remains massless as no quadratic term in A_μ appears in the lagrangian. The vanishing of the photon mass is a consequence of the surviving exact gauge symmetry $U(1)_{\text{emg}}$. Note the important relation

$$\boxed{M_W = M_Z \cos\theta_W} \quad (8.20)$$

We have the relation $v = \sin\theta_W M_W / \sqrt{\pi\alpha}$ between the vacuum expectation value of the scalar field and the physical parameters and, plugging in numerical values, we find $v \sim 250$ GeV, which is the

basis for the claim, made in the introduction, that the non-abelian symmetry is broken at the scale of 250 GeV.

• Couplings

We consider now all the terms of \mathcal{L}_S , eq. (8.16), not contained in \mathcal{L}_{0S} to define the interaction lagrangian of the Higgs boson

$$\begin{aligned}\mathcal{L}_{IS} = & \frac{e^2 v}{2 \sin^2 \theta_W} H W_\mu^* W^\mu + \frac{e^2}{4 \sin^2 \theta_W} H^2 W_\mu^* W^\mu \\ & + \frac{e^2 v}{4 \sin^2 \theta_W \cos^2 \theta_W} H Z_\mu Z^\mu + \frac{e^2}{8 \sin^2 \theta_W \cos^2 \theta_W} H^2 Z_\mu Z^\mu \\ & - h v H^3 - \frac{h}{4} H^4\end{aligned}\quad (8.21)$$

One notes that the trilinear couplings of the H boson to a pair of gauge bosons have the dimension of a mass, proportional to the vacuum expectation value v , while the quadrilinear couplings are dimensionless proportional to e^2 . One can show that, in terms of Feynman diagrams,

$$\begin{aligned}- \text{ the vertex } HW^+W^- \text{ is : } & -i \frac{e^2 v}{2 \sin^2 \theta_W} = -i \frac{e}{\sin \theta_W} M_W; \\ - \text{ the vertex } HZZ \text{ is : } & -i \frac{e^2 v}{2 \sin^2 \theta_W \cos^2 \theta_W} = -i \frac{e}{\sin \theta_W \cos \theta_W} M_Z; \\ - \text{ the vertex } H^2W^+W^- \text{ is : } & -i \frac{e^2}{2 \sin^2 \theta_W} \\ - \text{ the vertex } H^2ZZ \text{ is : } & -i \frac{e^2}{2 \sin^2 \theta_W \cos^2 \theta_W}.\end{aligned}\quad (8.22)$$

There are furthermore the H boson self-couplings proportional respectively to $h v$ and h . These variables are easily eliminated in favour of the observables M_W, M_H and one finds,

$$\begin{aligned}- \text{ the vertex } H^3: & i 6 h v = i \frac{3}{2} \frac{e}{\sin \theta_W} \frac{M_H^2}{M_W} \\ - \text{ the vertex } H^4: & i 6 h = i \frac{3}{4} \frac{e^2}{\sin^2 \theta_W} \frac{M_H^2}{M_W^2}.\end{aligned}\quad (8.23)$$

It is interesting to remark that the triple and the quartic H boson vertices vary as the square of the Higgs boson mass (for fixed W mass). As an indication of the strength of the Higgs boson couplings one finds 0.2 for the vertex $H^2W^+W^-$ and 0.12 for the quartic H^4 term.

To complete this section we recall the gauge boson self-couplings defined in \mathcal{L}_{IG} , eq. (5.57) : they are not affected by the spontaneous breaking of the symmetry, eventhough three gauge bosons have acquired a mass.

8.3 The Yukawa lagrangian \mathcal{L}_Y and fermion masses and couplings

The scalar field Φ couples to fermions. The requirement for such couplings to exist is that the corresponding terms in the lagrangian density be Lorentz invariant as well as invariant under a $SU(2)_L \otimes U(1)_Y$ transformation, before the spontaneous breaking of this symmetry is implemented. Let us recall that Ψ_{e_L} and Ψ_{q_L} of eq. (4.14) and Φ of eq. (8.1) are $\mathbf{2}$ under $SU(2)$ *i.e.* they transform as

$$\delta\Phi = i \frac{\tau}{2} \alpha \Phi, \dots, \quad \delta\Psi = i \frac{\tau}{2} \alpha \Psi, \dots, \quad \delta\bar{\Psi} = -i \bar{\Psi} \frac{\tau}{2} \alpha, \dots \quad (8.24)$$

so that $\bar{\Psi}_{e_L} \Phi$, $\bar{\Psi}_{q_L} \Phi$ are invariant under a $SU(2)_L$ transformation and so are the hermitian conjugates $\gamma^0 \Phi^\dagger \Psi_{e_L}$, $\gamma^0 \Phi^\dagger \Psi_{q_L}$. Considering now the transformation properties under $U(1)_Y$: the combination $\bar{\Psi}_{e_L} \Phi$ has hypercharge 2 and $\bar{\Psi}_{q_L} \Phi$ hypercharge 2/3 so that $\bar{\Psi}_{e_L} \Phi e_R$ and $\bar{\Psi}_{q_L} \Phi d_R$ (see table eq. (4.27) for the hypercharge assignments) are invariant under a $SU(2)_L \otimes U(1)_Y$ gauge transformation. Their hermitian conjugates are : $\bar{e}_R \Phi^\dagger \Psi_{e_L}$ and $\bar{d}_R \Phi^\dagger \Psi_{q_L}$. Since these terms are also Lorentz invariants they satisfy all criteria to enter \mathcal{L}_Y .

One can construct another type of group invariant with the help of $\tilde{\Phi} = i\tau_2 \Phi^*$ which is a $SU(2)$ doublet : indeed one can show

$$\delta\tilde{\Phi} \equiv \delta(i\tau_2 \Phi^*) = i\tau_2 \delta\Phi^* = i\tau_2 (-i \frac{\tau^*}{2} \alpha) \Phi^* = (i \frac{\tau}{2} \alpha) \tilde{\Phi} \quad (8.25)$$

where one has used for the last equality the property $i\tau_2 \tau^* = -\tau(i\tau_2)$. The combinations $\bar{\Psi}_{e_L} i\tau_2 \Phi^*$ and $\bar{\Psi}_{q_L} i\tau_2 \Phi^*$ are invariant under a $SU(2)_L$ transformation and have hypercharge 0 and -4/3 ($y_{\Phi^*} = -y_\Phi = -1$), respectively. Thus $\bar{\Psi}_{q_L} i\tau_2 \Phi^* u_R = \bar{\Psi}_{q_L} \tilde{\Phi} u_R$ is invariant under a group transformation. Had we included a right-handed neutrino the contribution $\bar{\Psi}_{e_L} i\tau_2 \Phi^* \nu_R = \bar{\Psi}_{e_L} \tilde{\Phi} \nu_R$ would satisfy the conditions but we will ignore it here (see sec. 12). Thus the Yukawa lagrangian then takes the form

$$\boxed{\mathcal{L}_Y = - c_d \bar{\Psi}_{q_L} \Phi d_R - c_u \bar{\Psi}_{q_L} \tilde{\Phi} u_R - c_e \bar{\Psi}_{e_L} \Phi e_R + \text{h.c.} + \text{other families},} \quad (8.26)$$

where we have explicitly written out the terms involving the first family of fermions ($\nu, e; u, d$). Six other parameters should be similarly introduced for the couplings of the second and third families so that nine new parameters appear in the model.

Implementing spontaneous symmetry breaking, in the unitary gauge, *i.e.* substituting in \mathcal{L}_Y the expression of Φ as given in the right-hand side of eq. (8.14), we derive

$$\boxed{\mathcal{L}_Y = - c_d \frac{v+H}{\sqrt{2}} \bar{d}d - c_u \frac{v+H}{\sqrt{2}} \bar{u}u - c_e \frac{v+H}{\sqrt{2}} \bar{e}e + \text{other families.}} \quad (8.27)$$

From this expression we relate the mass of a fermion f to the vacuum expectation value v via

$$\boxed{m_f = c_f \frac{v}{\sqrt{2}}}. \quad (8.28)$$

This is not a prediction of the theory since the parameters c_f are unknown and will be adjusted so as to obtain the “physical” mass of the corresponding fermion. Furthermore, no relation is expected between the masses of partners of a given family since one parameter is introduced for each of the fermion type in a family. One may remark that the only “prediction” is that the neutrino remains massless as a consequence of the absence a right-handed neutrino. On the other hand, the Higgs couplings to the fermions are predicted, if the fermion masses are known,

$$\boxed{g_f = \frac{c_f}{\sqrt{2}} = \frac{m_f}{v} = \frac{e}{2 \sin \theta_W} \frac{m_f}{M_W}}, \quad (8.29)$$

where eqs. (8.28) and (8.19) have been used: the Higgs particle couples to a fermion flavour in proportion to the fermion mass, implying that the top quark could play a major role in the production and/or decay of the Higgs particle ($m_t \sim 175$ GeV) while the electron and light fermion contributions can be safely neglected. It is a puzzle why one observes such a large spectrum of masses from $m_e = .511 \cdot 10^{-3}$ GeV to $m_t = 173.21$ GeV! No model naturally “explains” this fact.

• **Remark**

In sec. 2.3 we mentioned a problem related to massive gauge bosons namely the bad asymptotic behavior of the cross section of W pair production in $e^- e^+$ colliders. This was illustrated on the simpler case $\nu \bar{\nu} \rightarrow W^- W^+$ showing that the longitudinal polarisation states yield a cross section violating the Froissart bound if one keeps only the neutrino exchange diagram. Coming back to $e^- e^+ \rightarrow W^- W^+$ we leave it to the reader to check that, keeping fermion mass terms and including all diagrams in the unitary gauge, as shown in Fig. 2, the corresponding cross section is asymptotically finite. At higher orders, loop diagrams involve massive gauge boson propagators: in the unitary gauge

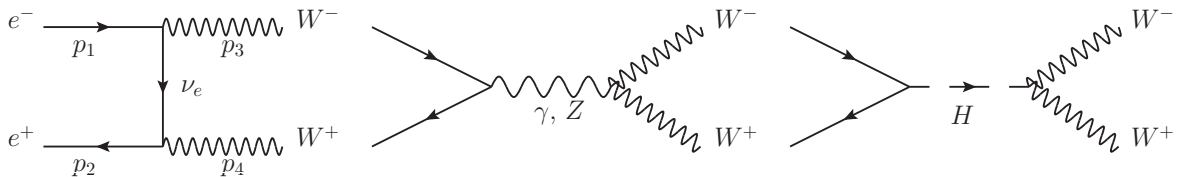


Figure 2: *The $e^- e^+ \rightarrow W^- W^+$ diagrams at lowest order in the unitary gauge.*

they do not converge to 0 when $k^2 \rightarrow \infty$ and this leads to an apparently non-renormalisable theory.

As explained in detail for the abelian case, the way out is to work in a “renormalisable” gauge (the ‘t Hooft gauges) where the gauge boson propagators have the form eq. (7.22) and the Goldstone modes ω are explicitly kept in the calculation.

8.4 The Higgs boson discovery

As an application we consider Higgs production in proton-proton colliders at the LHC at a center of mass energy $\sqrt{s} = 7, 8$ or 13 TeV. The Higgs boson could be produced in the annihilation of light

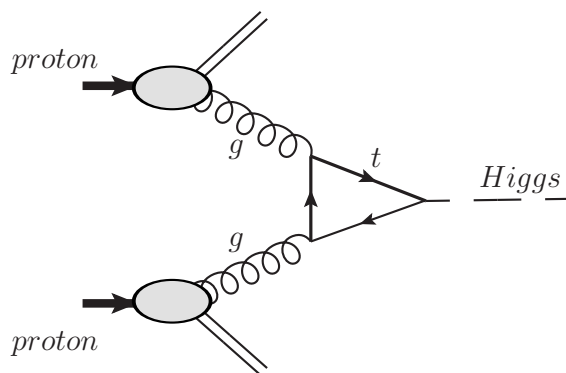


Figure 3: *Higgs production mechanism at hadron-hadron colliders : the dominant contribution arises from the subprocess where two gluons couple to the Higgs via a top quark loop. Another diagram with the fermion arrow reversed should be added.*

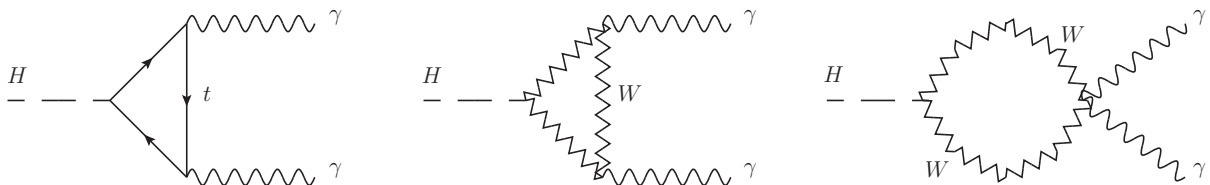


Figure 4: *Higgs decay mechanism into two photons: The dominant contributions arises from top quark loops and W boson loops. The final photons should be symmetrised in the first two diagrams.*

quarks and antiquarks of the initial hadrons, $q + \bar{q} \rightarrow H$, but such a coupling, eq. (8.29), is suppressed by a factor $m_f/v \simeq m_f/250$ with m_f , the mass of the quark, measured in GeV. The direct process $t\bar{t} \rightarrow H$ is possible but it is, of course, suppressed because of the negligibly small density of top quarks in the proton. For a Higgs mass below about 500 GeV it turns out that the dominant process is gluon-gluon fusion where the effective Higgs coupling to the gluon-gluon system is *via* a top quark loop as indicated in Fig. 3. The discovery channels of the Higgs boson have been $H \rightarrow Z Z^* \rightarrow 4$

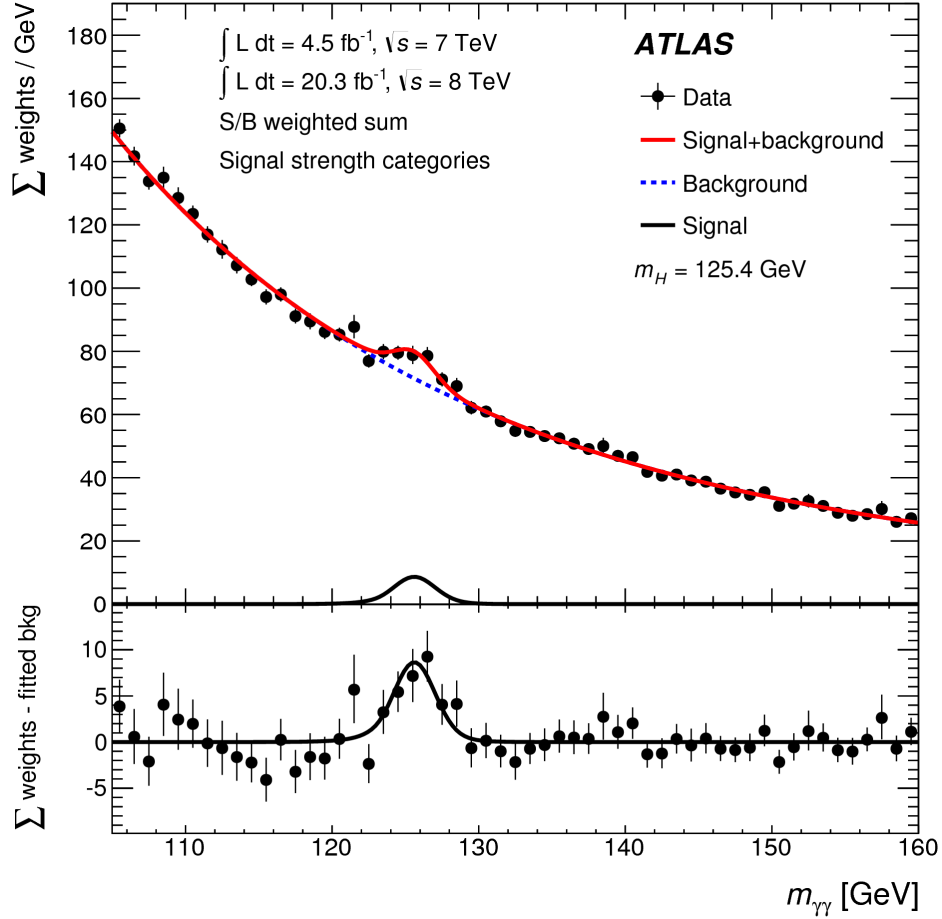


Figure 5: *ATLAS (Phys. Rev. D90 (2014) 112015) results on Higgs observation through its decay into 2 photons.*

charged leptons (direct HZZ coupling $\propto e M_Z$) and $H \rightarrow \gamma \gamma$. As shown in fig. 4 the two photon channel involves again a virtual top loop as well as W^\pm loops. The results of the ATLAS and CMS collaborations are shown in Figs. 5 and 6: they illustrate the difficulty to extract the small $H \rightarrow \gamma \gamma$ signal from a huge background, essentially $q \bar{q} \rightarrow \gamma \gamma$ and its large associated QCD corrections. The H boson, of mass $M_H = 125.09$ GeV, cannot decay in a top pair of mass $2 * 173.21$ GeV but can decay into a bottom-antibottom pair. However the background in this channel is too large to be able to extract the Higgs signal, but the decay $H \rightarrow b + \bar{b}$, with H produced in association with a vector boson, has been studied by ATLAS¹² and CMS¹³. Other decay channels which have been considered and will be studied at the High Luminosity LHC and the High Energy (27 GeV) LHC are $H \rightarrow WW^* \rightarrow l\nu l'\nu'$,

¹²ATLAS Collaboration, M. Aaboud et al., Phys. Lett. **B786** (2018) 59, arXiv:1808.08238 [hep-ex].

¹³CMS Collaboration, Phys. Rev. Lett. **121** (2018) 121801, arXiv:1808.08242 [hep-ex].

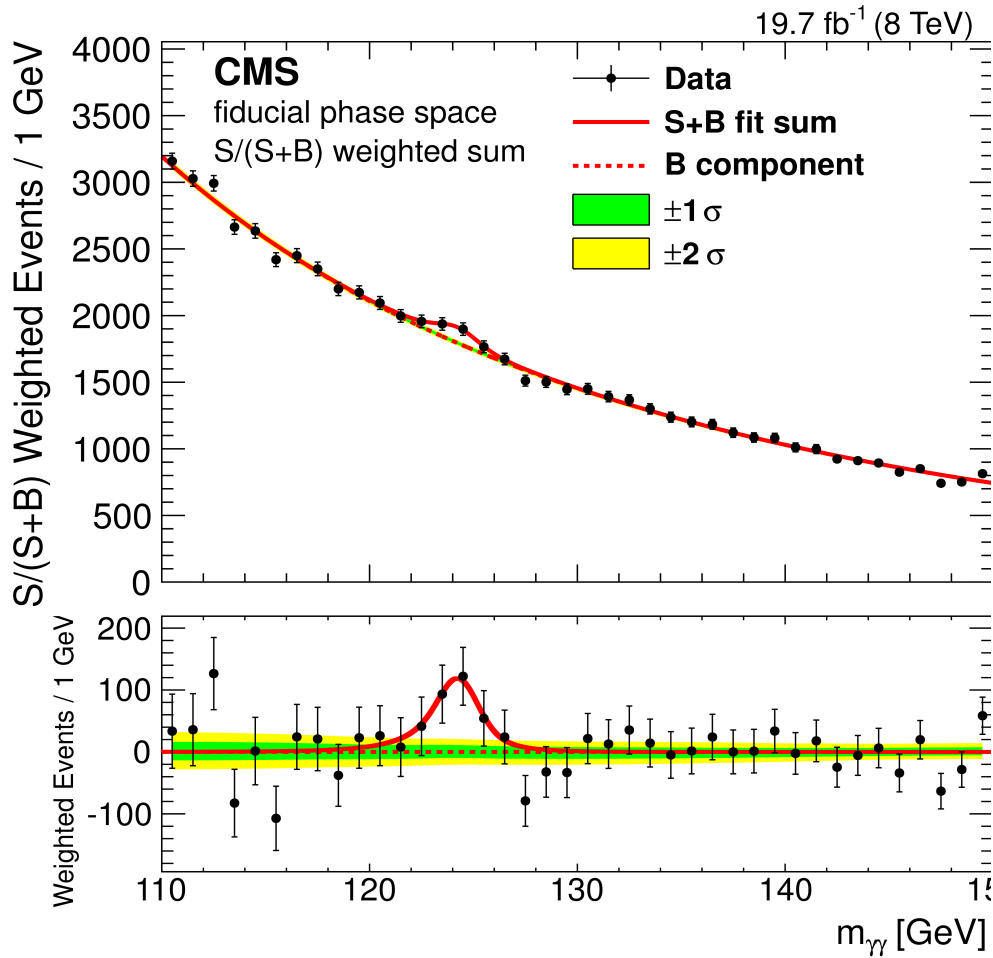


Figure 6: *CMS (Eur. Phys. J. C76 (2016) 13) results on Higgs observation through its decay into 2 photons.*

$H \rightarrow \tau^- \tau^+$ with the τ 's decaying leptonically or hadronically and $H \rightarrow \mu^- \mu^+$.¹⁴

The next two sections are devoted to a discussion of important production and decay mechanisms of the Higgs boson. Other exercises on the Standard Model can be found at https://lectures.lapth.cnrs.fr/standard_model/cours/exo_en.pdf.

8.5 Conclusions

At this point one has, in a first approximation, a complete model for the electroweak interactions. It contains a massive scalar particle, a massless and three massive gauge bosons, with propagators as in eqs. (8.18). All couplings between bosons and bosons to fermions are given assuming no mixing between the three generations of matter fields. The generation mixing is dealt with in sec. 11.

¹⁴Higgs Physics at the HL-LHC and HE-LHC, arXiv:1902.00134, [hep-ph].

9 Exercise : study of the reaction proton + proton \rightarrow H + X

The mass of the Higgs boson is large enough to justify the use of the parton model and perturbative QCD to study the production of a Higgs boson in proton-proton collisions.

9.1 The gluon-gluon fusion mechanism

In this framework, considering only the dominant process via gluon-gluon fusion, the hadronic cross section of the inclusive reaction $p(k_1) + p(k_2) \rightarrow H(p_3) + X$ can be written as:

$$\sigma_H = \int_0^1 dx_1 \int_0^1 dx_2 F_g^P(x_1, M^2) F_g^P(x_2, M^2) \hat{\sigma}_{g g \rightarrow H}, \quad (9.1)$$

where $F_g^P(x, M^2)$ stands for the gluon density in the proton, the gluon carrying a fraction x of the proton four-momentum, evolved at the factorisation scale M . The quantity $\hat{\sigma}_{g g \rightarrow H}$ is the cross section of the partonic reaction $g(p_1) + g(p_2) \rightarrow H(p_3)$. The 4-momenta of the initial gluons are such that $p_1 = x_1 k_1$ and $p_2 = x_2 k_2$. The partonic cross section itself is given by:

$$\hat{\sigma}_{g g \rightarrow H} = \frac{1}{4 p_1 \cdot p_2} \int \frac{d^3 p_3}{(2\pi)^3 2 E_3} (2\pi)^4 \delta^4(p_1 + p_2 - p_3) |\bar{T}|^2, \quad (9.2)$$

with $|\bar{T}|^2$ the matrix element squared averaged over initial polarisations and colours. Transforming $d^3 p_3 / (2 E_3)$ in $d^4 p_3 \delta^+(p_3^2 - M_H^2)$, the integration on p_3 can be performed easily with the Dirac distribution and we get:

$$\hat{\sigma}_{g g \rightarrow H} = \frac{1}{2 x_1 x_2 S} (2\pi) \delta^+(x_1 x_2 S - M_H^2) |\bar{T}|^2, \quad (9.3)$$

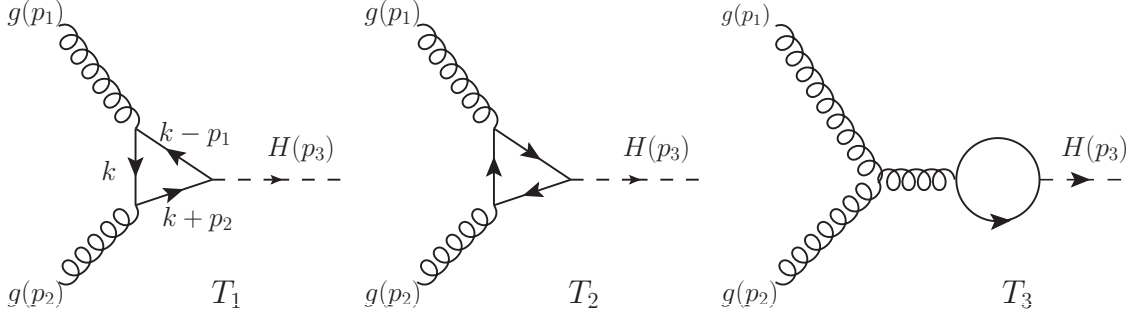
with the total energy squared $S = (k_1 + k_2)^2 = 2 k_1 \cdot k_2$ (the proton mass is neglected). Injecting eq. (9.3) in eq. (9.1), we get for the hadronic cross section:

$$\sigma_H = \int_0^1 \frac{dx_1}{x_1} \int_0^1 \frac{dx_2}{x_2} F_g^P(x_1, M^2) F_g^P(x_2, M^2) \frac{\pi}{S} \delta^+(x_1 x_2 S - M_H^2) |\bar{T}|^2. \quad (9.4)$$

The integration over x_2 can be performed with the help of the remaining Dirac distribution to find:

$$\sigma_H = \frac{\pi}{M_H^2 S} \int_{M_H^2/S}^1 \frac{dx_1}{x_1} F_g^P(x_1, M^2) F_g^P\left(\frac{M_H^2}{x_1 S}, M^2\right) |\bar{T}|^2 \quad (9.5)$$

The bounds on integration are obtained from the constraints $0 < x_1, x_2 \leq 1$ and $M_H^2/S \leq x_1 x_2 \leq 1$ which lead to $M_H^2/(x_1 S) \leq x_2 \leq 1$ and $M_H^2/S \leq x_1 \leq 1$. We compute now $|\bar{T}|^2$. At the lowest order, three diagrams contribute to the partonic process $g(p_1) + g(p_2) \rightarrow H(p_3)$:



The amplitude T_3 vanishes because it is proportional to $\text{Tr}[T^a]$, T^a traceless, a generator of the $SU(3)$ colour algebra. Applying the Feynman rules in $n \neq 4$ dimensions to tame potential ultraviolet divergencies (μ is the arbitrary mass introduced when going to n dimensions) and taking into account the factor -1 for a fermion loop, the amplitude T_1 is given by:

$$\begin{aligned}
T_1 &= -g_s^2 \frac{m_q}{v} \text{Tr}[T^a T^b] \mu^{4-n} \int \frac{d^n k}{(2\pi)^n} \text{Tr} \left[\gamma^\nu \frac{(\not{k} + m_q)}{k^2 - m_q^2 + i\epsilon} \gamma^\mu \frac{(\not{k} - \not{p}_1 + m_q)}{(k - p_1)^2 - m_q^2 + i\epsilon} \frac{(\not{k} + \not{p}_2 + m_q)}{(k + p_2)^2 - m_q^2 + i\epsilon} \right] \\
&\quad \times \epsilon_\mu^a(p_1) \epsilon_\nu^b(p_2) \\
&= -\frac{g_s^2 e m_q}{4 \sin \theta_w M_W} \mu^{4-n} \delta^{ab} \epsilon_\mu^a(p_1) \epsilon_\nu^b(p_2) \int \frac{d^n k}{(2\pi)^n} \\
&\quad \times \frac{\text{Tr} [\gamma^\nu (\not{k} + m_q) \gamma^\mu (\not{k} - \not{p}_1 + m_q) (\not{k} + \not{p}_2 + m_q)]}{(k^2 - m_q^2 + i\epsilon) ((k - p_1)^2 - m_q^2 + i\epsilon) ((k + p_2)^2 - m_q^2 + i\epsilon)} \quad (9.6)
\end{aligned}$$

where $g_s T^a$ is the strong interaction coupling of a gluon of colour a to a quark, m_q/v (see eq. (8.29)), the coupling of the quarks to the Higgs boson. In the second equation the relation $1/v = e/2 \sin \theta_w M_W$, eq. (8.19) is used and $\text{Tr} [T^a T^b] = \delta_{ab}/2$ takes care of the sum on the quark colours in the loop. Setting

$$N^{\mu\nu}(k) = \text{Tr} [\gamma^\nu (\not{k} + m_q) \gamma^\mu (\not{k} - \not{p}_1 + m_q) (\not{k} + \not{p}_2 + m_q)]$$

and computing the trace on the Dirac matrices as usual, we get:

$$\begin{aligned}
N^{\mu\nu}(k) &= 4 m_q \{ g^{\mu\nu} (k - p_1) \cdot (k + p_2) + (k + p_2)^\nu (k - p_1)^\mu - (k - p_1)^\nu (k + p_2)^\mu + k^\nu (k + p_2)^\mu \\
&\quad + (k + p_2)^\nu k^\mu - g^{\mu\nu} k \cdot (k + p_2) + k^\nu (k - p_1)^\mu + k^\mu (k - p_1)^\nu - g^{\mu\nu} k \cdot (k - p_1) + m_q^2 g^{\mu\nu} \} \\
&= 4 m_q \{ g^{\mu\nu} (m_q^2 - k^2 - p_1 \cdot p_2) + 4 k^\mu k^\nu - 2 k^\nu p_1^\mu + 2 k^\mu p_2^\nu + p_1^\nu p_2^\mu - p_2^\nu p_1^\mu \} . \quad (9.7)
\end{aligned}$$

In eq. (9.7), all the terms proportional to p_1^μ and p_2^ν can be dropped because they will vanish after contraction with the gluon polarisation vectors. The quantity $N^{\mu\nu}(k)$ becomes:

$$N^{\mu\nu}(k) = 4 m_q \{ g^{\mu\nu} (m_q^2 - k^2 - p_1 \cdot p_2) + 4 k^\mu k^\nu + p_1^\nu p_2^\mu \} . \quad (9.8)$$

Then, two Feynman parameters x and y are introduced to linearize the denominator:

$$\begin{aligned}
T_1 &= 2 K_{\mu\nu} \int_0^1 dy y \int_0^1 dx \int \frac{d^n k}{(2\pi)^n} N^{\mu\nu}(k) \\
&\quad \times [(1-y)(k^2 - m_q^2 + i\epsilon) + xy((k-p_1)^2 - m_q^2 + i\epsilon) + (1-x)y((k+p_2)^2 - m_q^2 + i\epsilon)]^{-3} \\
&= 2 K_{\mu\nu} \int_0^1 dy y \int_0^1 dx \int \frac{d^n k}{(2\pi)^n} N^{\mu\nu}(k) \\
&\quad \times [(k + (p_2(1-x) - p_1x)y)^2 + 2y^2x(1-x)p_1.p_2 - m_q^2 + i\epsilon]^{-3}
\end{aligned} \tag{9.9}$$

with

$$K_{\mu\nu} = -\frac{g_s^2 e m_q}{4 \sin \theta_w M_w} \mu^{4-n} \delta^{ab} \epsilon_\mu^a(p_1) \epsilon_\nu^b(p_2)$$

We shift the loop four-momentum $k = l - (p_2(1-x) - p_1x)y$. The factor $N^{\mu\nu}(k)$ contains terms of the type k^2 and $k^\mu k^\nu$ which transform under the shift as:

$$\begin{aligned}
k^2 &\simeq l^2 - 2y^2x(1-x)p_1.p_2 \\
k^\mu k^\nu &\simeq g^{\mu\nu}/n l^2 - y^2x(1-x)p_2^\mu p_1^\nu
\end{aligned}$$

All odd powers of l will vanish after the integration over l , so they have been removed. Eq. (9.8) becomes:

$$N^{\mu\nu}(k) = 4m_q \left\{ g^{\mu\nu} \left[\left(\frac{4}{n} - 1 \right) l^2 + m_q^2 + 2p_1.p_2 \left(y^2x(1-x) - \frac{1}{2} \right) \right] + p_1^\nu p_2^\mu (1 - 4y^2x(1-x)) \right\} \tag{9.10}$$

The amplitude T_1 is then:

$$T_1 = 2 K_{\mu\nu} \int_0^1 dy y \int_0^1 dx \int \frac{d^n l}{(2\pi)^n} 4m_q \frac{(A_1 l^2 + A_2) g^{\mu\nu} + B p_1^\nu p_2^\mu}{(l^2 - R^2 + i\epsilon)^3} \tag{9.11}$$

with:

$$\begin{aligned}
R^2 &= m_q^2 - 2y^2x(1-x)p_1.p_2 \\
A_1 &= 4/n - 1 \\
A_2 &= 2m_q^2 - p_1.p_2 - R^2 \\
B &= 1 - 4y^2x(1-x) = 1 - 2(m_q^2 + R^2)/p_1.p_2
\end{aligned}$$

The integration over the four-momentum l yields the following result¹⁵:

$$\begin{aligned}
T_1 &= \frac{i}{(4\pi)^{n/2}} 4m_q K_{\mu\nu} \int_0^1 dy y \int_0^1 dx \left[\frac{n}{2} \frac{4-n}{n} \Gamma\left(2 - \frac{n}{2}\right) (R^2 - i\epsilon)^{-2+n/2} g^{\mu\nu} \right. \\
&\quad \left. - \Gamma\left(3 - \frac{n}{2}\right) (R^2 - i\epsilon)^{-3+n/2} (A_2 g^{\mu\nu} + B p_1^\nu p_2^\mu) \right]
\end{aligned} \tag{9.12}$$

¹⁵The general formula is:

$$\begin{aligned}
\int \frac{d^n k}{(2\pi)^n} \frac{k^{2r}}{[k^2 - R^2 + i\epsilon]^m} &= i (R^2 - i\epsilon)^{r-m+\frac{n}{2}} \frac{(-1)^{r-m}}{(4\pi)^{\frac{n}{2}}} \frac{\Gamma(r + \frac{n}{2})}{\Gamma(\frac{n}{2})} \frac{\Gamma(m-r-\frac{n}{2})}{\Gamma(m)} \\
&= i \frac{(-1)^{r-m}}{(4\pi)^2} \left(\frac{4\pi}{R^2 - i\epsilon} \right)^\epsilon (R^2)^{2+r-m} \frac{\Gamma(2+r-\epsilon)}{\Gamma(2-\epsilon)} \frac{\Gamma(m-r-2+\epsilon)}{\Gamma(m)}
\end{aligned}$$

The coefficient in front of the ultraviolet divergence $\Gamma\left(2 - \frac{n}{2}\right)$ vanishes for $n = 4$, more precisely:

$$\frac{n}{2} \frac{4-n}{n} \Gamma\left(2 - \frac{n}{2}\right) = \left(2 - \frac{n}{2}\right) \Gamma\left(2 - \frac{n}{2}\right) = \Gamma\left(3 - \frac{n}{2}\right)$$

So, actually, there is no divergence in this amplitude and we can now take safely $n = 4$ so that $\Gamma\left(3 - \frac{n}{2}\right)$ reduces to 1. In addition, using $p_1.p_2 = M_H^2/2$, we get:

$$T_1 = \frac{i}{(4\pi)^2} 4m_q K_{\mu\nu} \left(g^{\mu\nu} - \frac{2p_1^\nu p_2^\mu}{M_H^2} \right) \int_0^1 dy y \int_0^1 dx \times \left[2 + \frac{M_H^2}{2} \left(1 - \frac{4m_q^2}{M_H^2} \right) \frac{1}{m_q^2 - y^2 x(1-x)M_H^2 - i\epsilon} \right] \quad (9.13)$$

To perform the integration on the Feynman parameters, let us introduce the function:

$$J(z) = \int_0^1 dx \int_0^1 dy y \frac{1}{1 - y^2 x(1-x)/z - i\epsilon} \quad (9.14)$$

with $z = m_q^2/M_H^2$ positive. The integration over y can be easily performed to get:

$$\begin{aligned} J(z) &= -\frac{z}{2} \int_0^1 dx \frac{1}{x(1-x)} \ln \left(1 - \frac{x(1-x)}{z} - i\epsilon \right) \\ &= -\frac{z}{2} \int_0^1 dx \left[\frac{1}{x} + \frac{1}{(1-x)} \right] \ln \left(1 - \frac{x(1-x)}{z} - i\epsilon \right) \\ &= -z \int_0^1 \frac{dx}{x} \ln \left(1 - \frac{x(1-x)}{z} - i\epsilon \right) . \end{aligned} \quad (9.15)$$

The roots of the argument of the logarithm are given by:

$$\begin{aligned} 0 < z < \frac{1}{4} \quad x_{1,2} &= \frac{1}{2} \pm \frac{1}{2} \sqrt{1 - 4z} \pm i\epsilon \\ z > \frac{1}{4} \quad x_{1,2} &= \frac{1}{2} \pm \frac{i}{2} \sqrt{4z - 1} , \end{aligned}$$

so

$$\ln \left(1 - \frac{x(1-x)}{z} - i\epsilon \right) = \ln \left(\frac{1}{z} \right) + \ln(x - x_1) + \ln(x - x_2) ,$$

but $\ln(1/z) = -\ln(x_1 x_2) = -\ln(-x_1) - \ln(-x_2)$ because x_1 and x_2 are complex conjugate. The two terms $\ln(x - x_1)$ and $\ln(-x_1)$ can be grouped because the imaginary parts of the two arguments are the same and similarly for the terms in x_2 . So we get for $J(z)$:

$$\begin{aligned} J(z) &= -z \left[\int_0^1 \frac{dx}{x} \ln \left(1 - \frac{x}{x_1} \right) + \int_0^1 \frac{dx}{x} \ln \left(1 - \frac{x}{x_2} \right) \right] \\ &= z \left[\text{Li}_2 \left(\frac{1}{x_1} \right) + \text{Li}_2 \left(\frac{1}{x_2} \right) \right] . \end{aligned} \quad (9.16)$$

It can be shown, c.f. sec. 9.3, that $J(z)$ can be written using only the logarithm function whatever the value of z is:

$$J(z) = -\frac{z}{2} \begin{cases} \left(\ln \left(\frac{1-\sqrt{1-4z}}{1+\sqrt{1-4z}} \right) - i\pi \right)^2 & z \leq 1/4 \\ \ln^2 \left(\frac{i\sqrt{4z-1}-1}{i\sqrt{4z-1}+1} \right) & z > 1/4 \end{cases} . \quad (9.17)$$

So the amplitude T_1 is given by:

$$T_1 = \frac{i}{(4\pi)^2} 4m_q K_{\mu\nu} \left(g^{\mu\nu} - \frac{2p_1^\nu p_2^\mu}{M_H^2} \right) \frac{M_H^2}{2m_q^2} \times \left\{ 2 \frac{m_q^2}{M_H^2} + \left(1 - 4 \frac{m_q^2}{M_H^2} \right) J \left(\frac{m_q^2}{M_H^2} \right) \right\} . \quad (9.18)$$

For the following, we set:

$$\mathcal{F}(z) = 2z + (1-4z) J(z) \quad (9.19)$$

The function $\mathcal{F}(z)$ can be complex or real following the ratio $z = m_q^2/M_H^2$. In fig. 7, we draw the

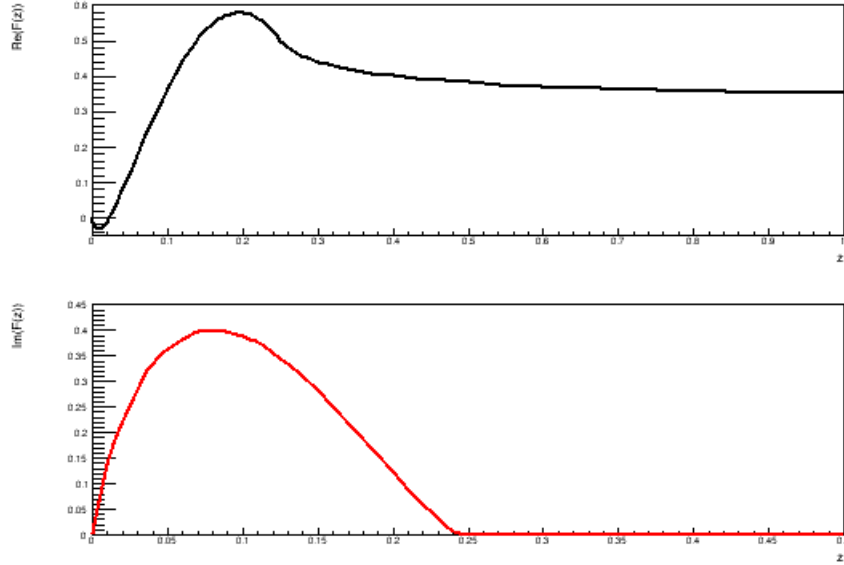


Figure 7: *Real and imaginary part of the function $\mathcal{F}(z)$ with respect to $z = m_q^2/M_H^2$*

real and imaginary parts of $\mathcal{F}(z)$ with respect to z (see sec. 9.3). It can be shown that this function has the limit $1/3$ when $z \rightarrow \infty$. To show that let us come back to eq. (9.14) which gives the integral representation of the function $J(z)$, when $z \rightarrow \infty$, the denominator cannot vanish so we can take safely the limit $\epsilon \rightarrow 0$ and write:

$$\frac{1}{1 - y^2 x(1-x)/z} \simeq 1 + y^2 x(1-x)/z .$$

So in this limit, the function $J(z)$ behaves as:

$$\begin{aligned} J(z) &\simeq \int_0^1 dx \int_0^1 y dy + \frac{1}{z} \int_0^1 dx x(1-x) \int_0^1 dy y^3 \\ &\simeq \frac{1}{2} + \frac{1}{24z}, \end{aligned} \quad (9.20)$$

and therefor the function $\mathcal{F}(z) \rightarrow 1/3$ when $z \rightarrow \infty$. Since the amplitude T_2 can be obtained from the amplitude T_1 by changing $\epsilon(p_1), p_1 \leftrightarrow \epsilon(p_2), p_2$, it is clear from eq. (9.18) that $T_2 = T_1$. So the total amplitude $T = T_1 + T_2$ is:

$$T = -\frac{i}{4\pi} \frac{\alpha_s e}{\sin \theta_w} \frac{M_H^2}{M_w} \delta^{ab} \epsilon_\mu^a(p_1) \epsilon_\nu^b(p_2) \left(g^{\mu\nu} - \frac{2p_1^\nu p_2^\mu}{M_H^2} \right) \mathcal{F} \left(\frac{m_q^2}{M_H^2} \right), \quad (9.21)$$

where the notation $\alpha_s = g_s^2/(4\pi)$ has been introduced for the strong interaction coupling. Note that in eq. (9.21), if we replace $\epsilon(p_1)$ (respectively $\epsilon(p_2)$) by p_1 (resp. p_2), the amplitude T vanishes because:

$$p_{1\mu} \left(g^{\mu\nu} - \frac{2p_1^\nu p_2^\mu}{M_H^2} \right) = 0$$

Let us now compute the modulus squared of the amplitude averaging over the initial spins and colours:

$$|\bar{T}|^2 = \frac{1}{4(N^2-1)^2} \sum_{\text{polarisations}} \sum_{\text{colours}} |T|^2$$

For the average over the initial spins, we have to compute something like:

$$\begin{aligned} S &= \sum_{\text{polarisations}} \epsilon_\mu^a(p_1) \epsilon_\nu^b(p_2) \epsilon_\rho^{c*}(p_1) \epsilon_\sigma^{d*}(p_2) \left(g^{\mu\nu} - \frac{2p_1^\nu p_2^\mu}{M_H^2} \right) \left(g^{\rho\sigma} - \frac{2p_1^\sigma p_2^\rho}{M_H^2} \right) \\ &= \delta^{ac} \delta^{bd} (-g_{\mu\rho}) (-g_{\nu\sigma}) \left(g^{\mu\nu} - \frac{2p_1^\nu p_2^\mu}{M_H^2} \right) \left(g^{\rho\sigma} - \frac{2p_1^\sigma p_2^\rho}{M_H^2} \right) \\ &= 2\delta^{ac} \delta^{bd} \end{aligned}$$

Note that we have taken $\sum_{\text{pol.}} \epsilon_\mu^a(p_1) \epsilon_\rho^{c*}(p_1) = -\delta^{ac} g^{\mu\rho}$ this is justified in this case because the replacement of $\epsilon^\mu(p_1)$ by p_1^μ ($\epsilon^\nu(p_2)$ by p_2^ν) gave zero. Now, for the average over the initial colours, we have to compute:

$$C = \sum_{a,b,c,d} \delta^{ab} \delta^{cd} \delta^{ac} \delta^{bd} = \sum_a \delta^{aa} = N^2 - 1$$

where N is the number of colours. Finally we obtain for the matrix element squared:

$$|\bar{T}|^2 = \frac{\alpha_s^2 \alpha M_H^4}{8\pi(N^2-1)(\sin \theta_w M_w)^2} \left| \mathcal{F} \left(\frac{m_q^2}{M_H^2} \right) \right|^2, \quad (9.22)$$

where the fine structure constant $\alpha = e^2/4\pi$ is introduced. So far, we considered only one quark flavour in the loop, in principle we need to sum over all the possible flavours of quarks so that eq. (9.5) becomes:

$$\sigma_H = \frac{1}{8(N^2 - 1)} \frac{\alpha_s^2 \alpha M_H^2}{(\sin \theta_w M_W)^2 S} \left(\sum_{q=d,u,s,c,b,t} \left| \mathcal{F} \left(\frac{m_q^2}{M_H^2} \right) \right|^2 \right) \times \int_{M_H^2/S}^1 \frac{dx_1}{x_1} F_g^P(x_1, M^2) F_g^P \left(\frac{M_H^2}{x_1 S}, M^2 \right) \quad (9.23)$$

In practice, we can content ourselves to keep only the top quark since the function \mathcal{F} is vanishingly small for other quark species. The scale M which appears in the partonic densities of eq. (9.23) must be taken of the order of the Higgs boson mass (M_H) because this is the only ‘‘hard’’ energy scale (much greater than Λ_{QCD}) which remains.

9.2 Function Li_2

The Li_2 function is defined as:

$$\text{Li}_2(z) = - \int_0^y dt \frac{\ln(1-t)}{t} = - \int_0^1 dt \frac{\ln(1-zt)}{t} \quad (9.24)$$

with z complex. From its definition, the function Li_2 has a cut in the complex plan on the real axis $[1, \infty[$. Furthermore, we have the following property:

$$\text{Li}_2(1) = \frac{\pi^2}{6} = \sum_{k=1}^{\infty} \frac{1}{k^2}.$$

In the case where z has an infinitesimal imaginary part $z = x \pm i\epsilon$ and a real part $x > 1$, from the definition of the function Li_2 , we can show that:

$$\text{Li}_2(x \pm i\epsilon) \stackrel{\epsilon \rightarrow 0}{=} -\text{Li}_2\left(\frac{1}{x}\right) - \frac{1}{2} \ln^2\left(\frac{1}{x}\right) + \frac{\pi^2}{3} \mp i\pi \ln\left(\frac{1}{x}\right). \quad (9.25)$$

This equation gives us the prescription for $x > 1$. More generally, if z is a complex number with a non vanishing imaginary part (it is always the case if we carefully keep track of the small imaginary part ϵ), we have the following relations:

$$\text{Li}_2\left(\frac{1}{z}\right) = -\text{Li}_2(z) - \frac{\pi^2}{6} - \frac{1}{2} \ln^2(-z) \quad (9.26)$$

$$\text{Li}_2(1-z) = -\text{Li}_2(z) + \frac{\pi^2}{6} - \ln(1-z) \ln(z). \quad (9.27)$$

9.3 Different rewriting of the function $J(z)$

We can apply the relations in the section above to simplify $J(z)$ (eq. (9.16)). Let us start with the case where $z \leq 1/4$. In this case the real parts of x_1 and x_2 are between 0 and 1. We can use eq. (9.25) and we obtain that:

$$\begin{aligned} \operatorname{Li}_2\left(\frac{1}{x_1}\right) + \operatorname{Li}_2\left(\frac{1}{x_2}\right) &= -\operatorname{Li}_2(y) - \operatorname{Li}_2(1-y) - \frac{1}{2} \ln^2(y) - \frac{1}{2} \ln^2(1-y) \\ &\quad + \frac{2\pi^2}{3} - i\pi(\ln(1-y) - \ln(y)), \end{aligned} \quad (9.28)$$

with y the real part of x_1 , $y = 1/2(1 + \sqrt{1-4z})$. Then, we can apply the relation (9.27) to the equation (9.28), this gives:

$$\begin{aligned} \operatorname{Li}_2\left(\frac{1}{x_1}\right) + \operatorname{Li}_2\left(\frac{1}{x_2}\right) &= -\frac{1}{2} \ln^2(y) - \frac{1}{2} \ln^2(1-y) + \ln(y) \ln(1-y) \\ &\quad + \frac{\pi^2}{2} - i\pi(\ln(1-y) - \ln(y)) \\ &= -\frac{1}{2} (\ln(1-y) - \ln(y))^2 + \frac{\pi^2}{2} - i\pi(\ln(1-y) - \ln(y)). \end{aligned} \quad (9.29)$$

As $0 \leq y \leq 1$, we can group the logarithms and we get:

$$\begin{aligned} \operatorname{Li}_2\left(\frac{1}{x_1}\right) + \operatorname{Li}_2\left(\frac{1}{x_2}\right) &= -\frac{1}{2} \left[\ln\left(\frac{1}{y} - 1\right) + i\pi \right]^2 \\ &= -\frac{1}{2} \ln^2\left(1 - \frac{1}{x_1}\right). \end{aligned} \quad (9.30)$$

In the case where $z > 1/4$, x_1 and x_2 are complex conjugate but with an imaginary part which is not infinitesimal. We will use the relation (9.26) to write that:

$$\operatorname{Li}_2\left(\frac{1}{x_1}\right) + \operatorname{Li}_2\left(\frac{1}{x_2}\right) = -\operatorname{Li}_2(x_1) - \operatorname{Li}_2(1-x_1) - \frac{1}{2} \ln^2(-x_1) - \frac{1}{2} \ln^2(x_1-1) - \frac{\pi^2}{3}. \quad (9.31)$$

Then, applying eq. (9.27), the sum of the dilogarithms becomes:

$$\begin{aligned} \operatorname{Li}_2\left(\frac{1}{x_1}\right) + \operatorname{Li}_2\left(\frac{1}{x_2}\right) &= -\frac{1}{2} \ln^2(-x_1) - \frac{1}{2} \ln^2(x_1-1) - \frac{\pi^2}{2} \\ &\quad + \ln(x_1) \ln(1-x_1) \\ &= -\frac{1}{2} (\ln(x_1-1) - \ln(-x_1))^2 - \frac{\pi^2}{2} \\ &\quad - \ln(x_1-1) \ln(-x_1) + \ln(x_1) \ln(1-x_1). \end{aligned} \quad (9.32)$$

Let us remark that x_1 has a real part and an imaginary part which are both positive, it lies then in the first quadrand. With the convention that the cut of the logarithm is along the negative real axis, then

the phase of a complex number in the main Riemann sheet is between $-\pi$ and π , if x_1 is parametrised like $\rho e^{i\theta}$ then $-x_1 = \rho e^{i(\theta-\pi)}$ and so the relation between the logarithms of x_1 and $-x_1$ is:

$$\ln(-x_1) = \ln(x_1) - i\pi .$$

In the same way, $1 - x_1$ has a positive real part and a negative imaginary part, so if $1 - x_1 = \rho e^{i\theta}$ then $x_1 - 1 = \rho e^{i(\theta+\pi)}$ and we have that:

$$\ln(x_1 - 1) = \ln(1 - x_1) + i\pi .$$

Using that, we write:

$$\ln(x_1) \ln(1 - x_1) = \ln(-x_1) \ln(x_1 - 1) + i\pi (\ln(x_1 - 1) - \ln(-x_1)) + \pi^2 , \quad (9.33)$$

so the sum of the two dilogarithms can be written:

$$\begin{aligned} \operatorname{Li}_2\left(\frac{1}{x_1}\right) + \operatorname{Li}_2\left(\frac{1}{x_2}\right) &= -\frac{1}{2} (\ln(x_1 - 1) - \ln(-x_1))^2 + \frac{\pi^2}{2} + i\pi (\ln(x_1 - 1) - \ln(-x_1)) \\ &= -\frac{1}{2} [\ln(x_1 - 1) - \ln(-x_1) - i\pi]^2 . \end{aligned} \quad (9.34)$$

The term $i\pi$ can be reabsorbed by writing $\ln(1-x_1)$ instead of $\ln(x_1-1)$ and remarking that $1-x_1 = x_2$ and $-x_1$ have a same sign imaginary part, then we finally get:

$$\operatorname{Li}_2\left(\frac{1}{x_1}\right) + \operatorname{Li}_2\left(\frac{1}{x_2}\right) = -\frac{1}{2} \ln^2\left(1 - \frac{1}{x_1}\right) . \quad (9.35)$$

Thus, $J(z)$ can be simplified such that only the logarithmic function is used for both cases:

$$J(z) = -\frac{z}{2} \begin{cases} \ln^2\left(\frac{\sqrt{1-4z}-1+i\epsilon}{\sqrt{1-4z}+1+i\epsilon}\right) & z \leq 1/4 \\ \ln^2\left(\frac{i\sqrt{4z-1}-1}{i\sqrt{4z-1}+1}\right) & z > 1/4 \end{cases} . \quad (9.36)$$

To conclude these technical remarks, we show how to rewrite $J(z)$ to make easy the comparison with the results which can be found in the literature. In the case $z \leq 1/4$, it is easy to show that:

$$\begin{aligned} \ln\left(\frac{\sqrt{1-4z}-1+i\epsilon}{\sqrt{1-4z}+1+i\epsilon}\right) &= \ln\left(\frac{\sqrt{1-4z}-1}{\sqrt{1-4z}+1} + i\epsilon\right) \\ &= -\ln\left(\frac{1+\sqrt{1-4z}}{1-\sqrt{1-4z}}\right) + i\pi . \end{aligned} \quad (9.37)$$

For the case $z > 1/4$, we write:

$$\ln\left(\frac{i\sqrt{4z-1}-1}{i\sqrt{4z-1}+1}\right) = \ln\left(\frac{\sqrt{1-\frac{1}{4z}}+i\sqrt{\frac{1}{4z}}}{\sqrt{1-\frac{1}{4z}}-i\sqrt{\frac{1}{4z}}}\right) . \quad (9.38)$$

Remarking that the complex number $\sqrt{1 - 1/4z} + i\sqrt{1/4z}$ has a modulus which is equal to 1 and it lies in the first quadrant, we show:

$$\begin{aligned}
\ln\left(\frac{i\sqrt{4z-1}-1}{i\sqrt{4z-1}+1}\right) &= \ln\left(\left(\sqrt{1-\frac{1}{4z}} + i\sqrt{\frac{1}{4z}}\right)^2\right) \\
&= 2 \ln\left(\sqrt{1-\frac{1}{4z}} + i\sqrt{\frac{1}{4z}}\right) \\
&= 2i \arcsin\left(\sqrt{\frac{1}{4z}}\right). \tag{9.39}
\end{aligned}$$

Then, the function $J(z)$ becomes:

$$J(z) = \frac{4z}{2} \begin{cases} -\frac{1}{4} \left(\ln\left(\frac{1+\sqrt{1-4z}}{1-\sqrt{1-4z}}\right) - i\pi\right)^2 & z \leq 1/4 \\ \arcsin^2\left(\sqrt{\frac{1}{4z}}\right) & z > 1/4 \end{cases}. \tag{9.40}$$

10 Exercises: Higgs boson decays

We consider in the following various two body decays of a Higgs boson.

10.1 Kinematics

Let the Higgs boson of mass M_H and momentum q decay into particles A and B of masses m_1 and m_2 and momenta p_1 and p_2 respectively: $H(q) \rightarrow A(p_1) + B(p_2)$. The decay rate summed over final polarisations and colours is:

$$d\Gamma = \frac{1}{2M} \frac{d^3 p_1}{(2\pi)^3 2E_1} \frac{d^3 p_2}{(2\pi)^3 2E_2} (2\pi)^4 \delta^4(q - p_1 - p_2) |\bar{T}|^2, \quad (10.1)$$

with $|\bar{T}|^2$ the invariant matrix element squared, summed over final colours and polarisations. Momentum conservation imposes $p_1 \cdot p_2 = (M_H^2 - m_1^2 - m_2^2)/2$ with $p_1^2 = m_1^2$ et $p_2^2 = m_2^2$. Thus $|\bar{T}|^2$ depends only on the external masses $|\bar{T}(m_1^2, m_2^2, M_H^2)|^2$ and the integral in eq. (10.1) can be done independently of the decay channel. Using $d^3 p_2 / 2E_2 = d^4 p_2 \delta^+(p_2^2 - m_2^2)$ and carrying out the $d^4 p_2$ integration it comes out

$$d\Gamma = \frac{1}{2M_H} \frac{|\bar{T}|^2}{(2\pi)^2} \int \frac{d^3 p_1}{2E_1} \delta^+((q - p_1)^2 - m_2^2). \quad (10.2)$$

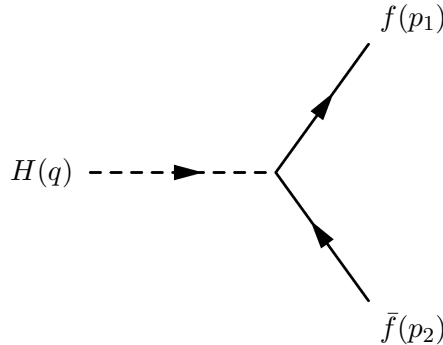
Going to the rest frame of the Higgs boson, $q = (M, 0, 0, 0)$, one finds that the argument of the δ^+ function reduces to $(M^2 - 2ME_1 + m_1^2 - m_2^2)$ independent of the angles. Since all cases we consider have $m_1 = m_2$ the expressions will simplify. Using $p_1 dp_1 = E_1 dE_1$ all integrations are easily done to get:

$$\boxed{\Gamma = \frac{1}{16\pi M_H} |\bar{T}|^2 \sqrt{1 - \frac{4m^2}{M^2}}}, \quad (10.3)$$

with m the common mass of the decay products.

10.2 Higgs decay into a fermion anti-fermion pair

This channel has only one diagram with the Higgs fermion-antifermion coupling, m_f/v given in eq. (8.29):



The corresponding amplitude T is:

$$T = -i \frac{m_f}{v} \bar{u}(p_1) v(p_2) \quad (10.4)$$

leading to:

$$\begin{aligned} |\bar{T}|^2 &= \frac{m_f^2}{v^2} (N) (Tr[\not{p}_1 \not{p}_2] - m_f^2 Tr[1]) \\ &= \frac{2 m_f^2 M_H^2}{v^2} \left(1 - \frac{4 m_f^2}{M_H^2} \right) (N) . \end{aligned} \quad (10.5)$$

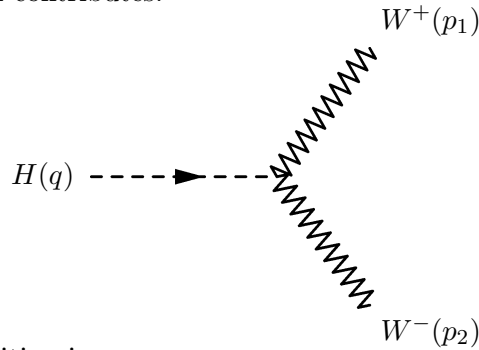
In the above result the colour factor N has been put in parentheses to indicate that, if the final fermions are quarks then we keep this factor, while if they are leptons it should be ignored. Getting rid of the vacuum expectation value v in favor of physical quantities via eq. (8.19), $1/v = e/(2 \sin \theta_w M_w)$ and $e^2 = 4\pi\alpha$ the decay rate is:

$$\boxed{\Gamma_{H \rightarrow f \bar{f}} = \frac{(N) \alpha}{8 \sin^2(\theta_w)} \frac{M_H m_f^2}{M_w^2} \left(1 - \frac{4 m_f^2}{M_H^2} \right)^{3/2}} \quad (10.6)$$

where eq. (10.3) has been used.

10.3 Higgs decay into a $W^+ W^-$ pair

Here again only one diagram contributes:



The amplitude for this transition is:

$$T = i \frac{e M_w}{\sin \theta_w} g^{\alpha\beta} \varepsilon_{\alpha}^{\lambda_1*}(p_1) \varepsilon_{\beta}^{\lambda_2*}(p_2) , \quad (10.7)$$

with $\varepsilon_{\alpha}^{\lambda}(p)$ the polarisation vector of a gauge boson and the coupling given in eq. (8.22). The sum over polarisations is done using:

$$\sum_{\lambda} \varepsilon_{\alpha}^{\lambda}(p) \varepsilon_{\beta}^{\lambda*}(p) = -g_{\alpha\beta} + \frac{p_{\alpha} p_{\beta}}{M_w^2} , \quad (10.8)$$

so that:

$$\begin{aligned}
|\bar{T}|^2 &= \left(\frac{e M_W}{\sin \theta_w} \right)^2 \left(-g_{\alpha\mu} + \frac{p_{1\alpha} p_{1\mu}}{M_W^2} \right) \left(-g^{\alpha\mu} + \frac{p_2^\alpha p_2^\mu}{M_W^2} \right) \\
&= \frac{e^2}{4 \sin^2 \theta_w M_W^2} (12 M_W^4 + M_H^4 - 4 M_W^2 M_H^2) .
\end{aligned} \tag{10.9}$$

Finally the decay rate is:

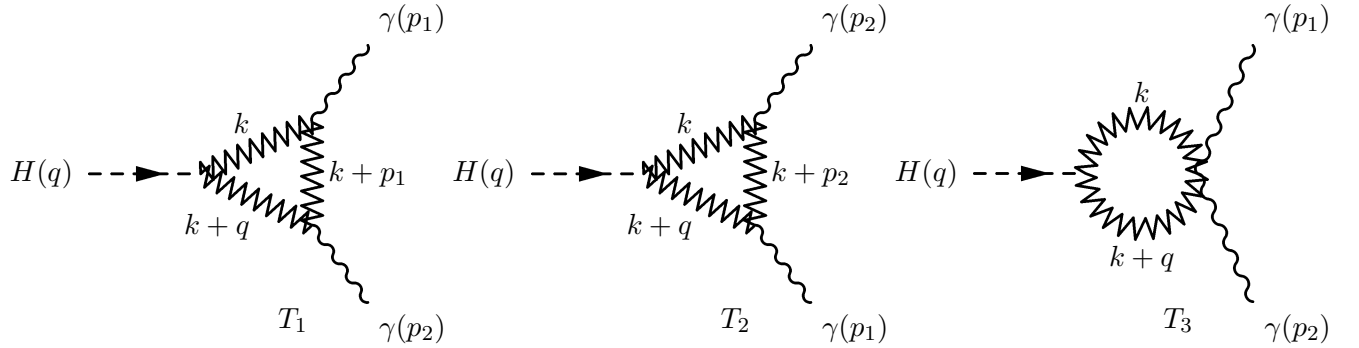
$$\boxed{\Gamma_{H \rightarrow W^+ W^-} = \frac{\alpha}{16 \sin^2(\theta_w)} \frac{M_H^3}{M_W^2} \sqrt{1 - \frac{4 M_W^2}{M_H^2}} \left(1 - 4 \frac{M_W^2}{M_H^2} + 12 \frac{M_W^4}{M_H^4} \right)} \tag{10.10}$$

10.4 Higgs decay in a $\gamma \gamma$ pair

As seen in sec. 8.4 this transition goes via two types of loop diagrams, one involving fermions and the other charged gauge bosons.

10.4.1 W boson loop

In the unitary gauge three types of diagrams contribute:



All these diagrams have a common structure, namely the HWW vertex and the two adjacent W propagators of momentum k and $k+q$ respectively. Each amplitude T_i is written as $T_i = T_i^{\mu_1 \mu_2} \varepsilon_{\mu_1}^*(p_1) \varepsilon_{\mu_2}^*(p_2)$ where we drop for simplicity the photon polarisation indices. Furthermore we introduce the tensor $\tilde{T}_i^{\mu_1 \mu_2}$:

$$T_i^{\mu_1 \mu_2} = \int \frac{d^n k}{(2\pi)^n} \tilde{T}_i^{\mu_1 \mu_2} ,$$

with $\tilde{T}_i^{\mu_1 \mu_2} = R_{\alpha_1 \alpha_2} M_i^{\mu_1 \mu_2 \alpha_1 \alpha_2}$, $R_{\alpha_1 \alpha_2}$ containing the part common to all three digrams. Applying

the Feynman rules, using the unitary gauge for the W propagators, it comes out:

$$\begin{aligned}
M_1^{\mu_1 \mu_2 \alpha_1 \alpha_2} &= (i e) \left[g^{\alpha_2 \mu_2} (k + q + p_2)^{\beta_1} + g^{\mu_2 \beta_1} (-p_2 + k + p_1)^{\alpha_2} + g^{\beta_1 \alpha_2} (-k - p_1 - k - q)^{\mu_2} \right] \\
&\quad \times (-i) \left(g_{\beta_1 \beta_2} - \frac{(k + p_1)_{\beta_1} (k + p_1)_{\beta_2}}{M_W^2} \right) \frac{1}{(k + p_1)^2 - M_W^2 + i \epsilon} \\
&\quad \times (i e) \left[g^{\beta_2 \mu_1} (k + p_1 + p_1)^{\alpha_1} + g^{\mu_1 \alpha_1} (-p_1 + k)^{\beta_2} + g^{\alpha_1 \beta_2} (-k - k - p_1)^{\mu_1} \right] \quad (10.11)
\end{aligned}$$

$$M_2^{\mu_1 \mu_2 \alpha_1 \alpha_2} = M_1^{\mu_1 \mu_2 \alpha_1 \alpha_2} (\mu_1 \leftrightarrow \mu_2, p_1 \leftrightarrow p_2) \quad (10.12)$$

$$M_3^{\mu_1 \mu_2 \alpha_1 \alpha_2} = i e^2 [g^{\alpha_1 \mu_1} g^{\alpha_2 \mu_2} + g^{\alpha_1 \mu_2} g^{\alpha_2 \mu_1} - 2 g^{\mu_1 \mu_2} g^{\alpha_1 \alpha_2}] , \quad (10.13)$$

and for the common structure of the amplitudes:

$$\begin{aligned}
R_{\alpha_1 \alpha_2} &= -i \frac{e M_W}{\sin(\theta_W)} \left(g_{\alpha_1 \alpha_2} - \frac{(k + q)_{\alpha_1} (k + q)_{\alpha_2}}{M_W^2} - \frac{k_{\alpha_1} k_{\alpha_2}}{M_W^2} + \frac{k_{\alpha_1} (k + q)_{\alpha_2} k \cdot (k + q)}{M_W^4} \right) \\
&\quad \times \frac{1}{(D_0 + i \epsilon) (D_3 + i \epsilon)} . \quad (10.14)
\end{aligned}$$

The quantities D_0 and D_3 are the denominators of propagators,

$$D_0 = k^2 - M_W^2 , \quad D_3 = (k + q)^2 - M_W^2 , \quad (10.15)$$

and we will need later,

$$D_1 = (k + p_1)^2 - M_W^2 , \quad D_2 = (k + p_2)^2 - M_W^2 . \quad (10.16)$$

The diagrams T_1 , T_2 et T_3 are highly divergent in the ultraviolet region:

$$\begin{aligned}
T_1 \text{ et } T_2 &\simeq \int d^4 k \frac{k^8}{k^6} \simeq \int dk k^5 \\
T_3 &\simeq \int d^4 k \frac{k^6}{k^6} \simeq \int dk k^3 ,
\end{aligned}$$

but working in n space-time dimensions regularizes the divergencies. Rather than evaluating these integrals by brute force we try to arrange the terms to make possible cancellations obvious in the integrands. One thus defines:

$$\begin{aligned}
T^{\mu_1 \mu_2} &= T_1^{\mu_1 \mu_2} + T_2^{\mu_1 \mu_2} + T_3^{\mu_1 \mu_2} \\
&= \int \frac{d^n k}{(2\pi)^n} \left(\tilde{T}_1^{\mu_1 \mu_2} + \tilde{T}_2^{\mu_1 \mu_2} + \tilde{T}_3^{\mu_1 \mu_2} \right) . \quad (10.17)
\end{aligned}$$

After integration on the loop momentum k the tensor $T^{\mu_1 \mu_2}$ depends only on the external momenta p_1 , p_2 and it can be parameterised as:

$$T^{\mu_1 \mu_2} = \frac{A}{p_1 \cdot p_2} p_1^{\mu_2} p_2^{\mu_1} + \frac{B}{p_1 \cdot p_2} p_1^{\mu_1} p_2^{\mu_2} + C g^{\mu_1 \mu_2} . \quad (10.18)$$

The aim is to calculate the expressions A, B and C . For this purpose we construct the following scalars:

$$\begin{aligned} g_{\mu_1 \mu_2} T^{\mu_1 \mu_2} &= A + B + n C \\ p_{1 \mu_2} p_{2 \mu_1} T^{\mu_1 \mu_2} &= p_1 \cdot p_2 (B + C) \\ p_{1 \mu_1} p_{2 \mu_2} T^{\mu_1 \mu_2} &= p_1 \cdot p_2 (A + C) , \end{aligned}$$

where the property $g_{\mu_1 \mu_2} g^{\mu_1 \mu_2} = n$ has been used since we work in n dimensions. The system of equations is easily solved to find:

$$C = \frac{1}{2(n-2)} \left(g_{\mu_1 \mu_2} T^{\mu_1 \mu_2} - \frac{p_{1 \mu_2} p_{2 \mu_1}}{p_1 \cdot p_2} T^{\mu_1 \mu_2} - \frac{p_{1 \mu_1} p_{2 \mu_2}}{p_1 \cdot p_2} T^{\mu_1 \mu_2} \right) \quad (10.19)$$

$$B = \frac{p_{1 \mu_2} p_{2 \mu_1}}{p_1 \cdot p_2} T^{\mu_1 \mu_2} - C \quad (10.20)$$

$$A = \frac{p_{1 \mu_1} p_{2 \mu_2}}{p_1 \cdot p_2} T^{\mu_1 \mu_2} - C . \quad (10.21)$$

The various contractions of the tensor $T^{\mu_1 \mu_2}$ are calculated with the help of a **form** program^{16,17}. By reconstructing systematically the quantities D_0, \dots, D_3 in the numerators and cancelling them with the denominators, we get rid of the k dependence in the numerators so that only scalar integrals have to be evaluated. There are two 3-point integrals:

$$\begin{aligned} I_{013} &= \int \frac{d^n k}{(2\pi)^n} \frac{1}{(D_0 + i\epsilon)(D_1 + i\epsilon)(D_3 + i\epsilon)} \\ I_{023} &= \int \frac{d^n k}{(2\pi)^n} \frac{1}{(D_0 + i\epsilon)(D_2 + i\epsilon)(D_3 + i\epsilon)} \end{aligned}$$

three 2-points integrals:

$$\begin{aligned} I_{03} &= \int \frac{d^n k}{(2\pi)^n} \frac{1}{(D_0 + i\epsilon)(D_3 + i\epsilon)} \\ I_{13} &= \int \frac{d^n k}{(2\pi)^n} \frac{1}{(D_1 + i\epsilon)(D_3 + i\epsilon)} \\ I_{23} &= \int \frac{d^n k}{(2\pi)^n} \frac{1}{(D_2 + i\epsilon)(D_3 + i\epsilon)} \end{aligned}$$

and four 1-point integrals:

$$\begin{aligned} I_0 &= \int \frac{d^n k}{(2\pi)^n} \frac{1}{(D_0 + i\epsilon)} & I_1 &= \int \frac{d^n k}{(2\pi)^n} \frac{1}{(D_1 + i\epsilon)} \\ I_2 &= \int \frac{d^n k}{(2\pi)^n} \frac{1}{(D_2 + i\epsilon)} & I_3 &= \int \frac{d^n k}{(2\pi)^n} \frac{1}{(D_3 + i\epsilon)} . \end{aligned}$$

¹⁶For an on line documentation on **form** see <http://www.nikhef.nl/~form/maindir/documentation/reference/online/>

¹⁷The code for the evaluation of A, B and C is found at https://lectures.laphth.cnrs.fr/standard_model/cours/hgaga.frm

Note that the last two sets of integrals would be ultraviolet divergent in 4 dimensions, but, working in n dimensions, they are regular and we can do translations on the loop momentum to evaluate them. For example:

$$I_1 = \int \frac{d^n k}{(2\pi)^n} \frac{1}{(k+p_1)^2 - M_W^2 + i\epsilon} = \int \frac{d^n k'}{(2\pi)^n} \frac{1}{(k')^2 - M_W^2 + i\epsilon} \quad \text{with } k' = k + p_1, \quad (10.22)$$

then $I_1 = I_0$. In the same way one shows that:

$$I_3 = I_2 = I_1 = I_0$$

All 2-point integrals can be written in the following form:

$$J_2 = \int \frac{d^n k}{(2\pi)^n} \frac{1}{(k^2 - M_W^2 + i\epsilon)((k+p)^2 - M_W^2 + i\epsilon)}, \quad (10.23)$$

is reduced to:

$$J_2 = \int_0^1 dx \int \frac{d^n k}{(2\pi)^n} \frac{1}{((k+px)^2 - R^2 + i\epsilon)^2}, \quad (10.24)$$

after introduction of the Feynman variable x , with $R^2 = M_W^2 - p^2 x(1-x)$. Doing the change of variable k to $l = k + px$ and using the usual formulae (see sec. 9.1) one obtains:

$$J_2 = \frac{i}{(4\pi)^{n/2}} \int_0^1 dx (R^2 - i\epsilon)^{-2+n/2} \frac{\Gamma(2-n/2)}{\Gamma(2)}. \quad (10.25)$$

Introducing ε through $n = 4 - 2\varepsilon$, and expanding around $\varepsilon = 0$, it comes out:

$$J_2 = \frac{i}{(4\pi)^{2-\varepsilon}} \frac{\Gamma(1+\varepsilon)}{\varepsilon} \left(1 - \varepsilon \tilde{I}(p^2)\right), \quad (10.26)$$

with:

$$\tilde{I}(p^2) = \int_0^1 dx \ln(M_W^2 - p^2 x(1-x) - i\epsilon). \quad (10.27)$$

The pole in ε is the consequence of the ultraviolet divergence of the 2-point functions. It turns out that, in our calculation, the 2-point integrals are all multiplied by ε which allows us to take the $\varepsilon \rightarrow 0$ limit to find finally:

$$\varepsilon J_2 = \frac{i}{(4\pi)^2}. \quad (10.28)$$

For the 3-point integrals, both I_{013} et I_{023} can be written as:

$$J_3 = \int \frac{d^n k}{(2\pi)^n} \frac{1}{(k-r_1)^2 - M_W^2 + i\epsilon} \frac{1}{k^2 - M_W^2 + i\epsilon} \frac{1}{(k+r_2)^2 - M_W^2 + i\epsilon} \quad (10.29)$$

with $r_1 = p_1$ and $r_2 = p_2$ for I_{013} , and $r_1 = p_2$ et $r_2 = p_1$ for I_{023} . Introducing the Feynman parameters and using $l = k + (r_2(1-x) - r_1 x)y$ rather than k as integration variable one finds:

$$J_3 = 2 \int_0^1 y dy \int_0^1 dx \int \frac{d^n l}{(2\pi)^n} \frac{1}{(l^2 - R^2 + i\epsilon)^3}, \quad (10.30)$$

with $R^2 = M_W^2 - y^2 x(1-x)q^2$ and $q = p_1 + p_2 = r_1 + r_2$. Integrating on l yields:

$$J_3 = -\frac{i}{(4\pi)^{n/2}} \Gamma\left(3 - \frac{n}{2}\right) \int_0^1 y dy \int_0^1 dx (R^2 - i\epsilon)^{-3+n/2}, \quad (10.31)$$

which is regular. Taking $n = 4$ and doing the y integration J_3 can be written as:

$$J_3 = -\frac{i}{(4\pi)^2} \frac{1}{M_W^2} J\left(\frac{M_W^2}{q^2}\right), \quad (10.32)$$

with the function J defined in eq. (9.16) of the previous section. The result depends only on $r_1 + r_2$ which implies $I_{013} = I_{023}$.

After contraction of the tensor $T^{\mu_1 \mu_2}$ with the photons polarisation vectors we obtain:

$$\begin{aligned} T_W &= T^{\mu_1 \mu_2} \varepsilon_{\mu_1}^*(p_1) \varepsilon_{\mu_2}^*(p_2) \\ &= \left(C g^{\mu_1 \mu_2} + \frac{A}{p_1 \cdot p_2} p_1^{\mu_1} p_2^{\mu_2} \right) \varepsilon_{\mu_1}^*(p_1) \varepsilon_{\mu_2}^*(p_2) \end{aligned} \quad (10.33)$$

one observes that the B term has disappeared as it is multiplied by 0!. The `form` code gives $A = -C$ and:

$$C = \frac{i}{(4\pi)^2} \left(e^2 \frac{e M_W}{\sin(\theta_W)} \right) \left[6 + \frac{1}{z_W} + J(z_W) \left(-12 + \frac{6}{z_W} \right) \right] \quad (10.34)$$

with $z_W = M_W^2/M_H^2$. Putting everything together it comes out:

$$\begin{aligned} T_W &= \frac{i}{(4\pi)^2} \left(e^2 \frac{e M_W}{\sin(\theta_W)} \right) \left[6 + \frac{1}{z_W} + J(z_W) \left(-12 + \frac{6}{z_W} \right) \right] \left(g^{\mu_1 \mu_2} - \frac{p_1^{\mu_1} p_2^{\mu_2}}{p_1 \cdot p_2} \right) \\ &\quad \times \varepsilon_{\mu_1}^*(p_1) \varepsilon_{\mu_2}^*(p_2) \\ &= i \frac{\alpha}{4\pi} \frac{e}{\sin(\theta_W)} \frac{M_H^2}{M_W} \mathcal{G} \left(\frac{M_W^2}{M_H^2} \right) \left(g^{\mu_1 \mu_2} - \frac{2 p_1^{\mu_1} p_2^{\mu_2}}{M_H^2} \right) \varepsilon_{\mu_1}^*(p_1) \varepsilon_{\mu_2}^*(p_2) \end{aligned} \quad (10.35)$$

where:

$$\mathcal{G}(z) = [6z + 1 + 6J(z)(1 - 2z)]$$

Some remarks are in order.

1. All ultraviolet divergences have disappeared: it was necessary to go to n dimensions in the intermediate steps of the calculation to give a mathematical meaning to individual integrals and allow for the momentum translations in the loops, but after combining all terms one takes the limit to 4 dimensions since the final result is regular;
2. $T^{\mu_1 \mu_2}$ is transverse, which means $p_{1\mu_1} T^{\mu_1 \mu_2} = p_{2\mu_2} T^{\mu_1 \mu_2} = 0$.

10.4.2 Fermion loops

This part is very similar to the calculation of Higgs boson production via gluon-gluon fusion in sec. 9 and the result eq. (9.21) can be used with appropriate changes. First the strong coupling is replaced by $e Q_f$ and α_s then becomes αQ_f^2 with $Q_f = -1, 2/3$ or $-1/3$. Since the photons are colour neutral the colour factor $Tr [T^a T^b] = \delta^{ab}/2$ becomes 1 (see eq. (9.6)). The result is:

$$T_f = -i \frac{\alpha Q_f^2 e}{2\pi \sin \theta_w} \frac{M_H^2}{M_W} \mathcal{F}(z_f) \left(g^{\mu_1 \mu_2} - \frac{2 p_1^{\mu_1} p_2^{\mu_2}}{M_H^2} \right) \varepsilon_{\mu_1}^*(p_1) \varepsilon_{\mu_2}^*(p_2), \quad (10.36)$$

with $z_f = m_f^2/M_H^2$. Eventhough heavy fermions only will contribute (Higgs coupling proportional to the fermion mass) it is necessary to recall that we have to sum over all fermions. The function \mathcal{F} is defined in eq. (9.19) and we recall it here:

$$\mathcal{F}(z) = [2z + (1 - 4z) J(z)] .$$

The amplitude for the decay of a Higgs boson into two photons is then:

$$\begin{aligned} T_f &= -i \frac{\alpha e}{2\pi \sin \theta_w} \frac{M_H^2}{M_W} \left(g^{\mu_1 \mu_2} - \frac{2 p_1^{\mu_1} p_2^{\mu_2}}{M_H^2} \right) \varepsilon_{\mu_1}^*(p_1) \varepsilon_{\mu_2}^*(p_2) \\ &\quad \times \left(\sum_l Q_l^2 \mathcal{F} \left(\frac{m_l^2}{M_H^2} \right) + N \sum_q Q_q^2 \mathcal{F} \left(\frac{m_q^2}{M_H^2} \right) \right) \end{aligned} \quad (10.37)$$

where the sum over l stands for leptons and q for quarks. In the latter case an extra factor N obviously appears from the colour sum in the loop.

10.5 Final result

The final amplitude will be the sum of the amplitudes T_f and T_W . To calculate its square one has to sum on the photon polarisation and evaluate the expression:

$$\begin{aligned} S &= \sum_{\lambda_1} \sum_{\lambda_2} \varepsilon_{\mu_1}^{\lambda_1*}(p_1) \varepsilon_{\mu_2}^{\lambda_2*}(p_2) \varepsilon_{\nu_1}^{\lambda_1}(p_1) \varepsilon_{\nu_2}^{\lambda_2}(p_2) \left(g^{\mu_1 \mu_2} - \frac{2 p_1^{\mu_1} p_2^{\mu_2}}{M_H^2} \right) \left(g^{\nu_1 \nu_2} - \frac{2 p_1^{\nu_2} p_2^{\nu_1}}{M_H^2} \right) \\ &= \left(g^{\mu_1 \mu_2} - \frac{2 p_1^{\mu_1} p_2^{\mu_2}}{M_H^2} \right) \left(g_{\mu_1 \mu_2} - \frac{2 p_{1 \mu_1} p_{2 \mu_2}}{M_H^2} \right) \\ &= 2 \end{aligned} \quad (10.38)$$

thus:

$$|\overline{T_W + T_f}|^2 = \frac{\alpha^2 e^2}{8\pi^2 \sin \theta_w} \frac{M_H^4}{M_W^2} |Y|^2 \quad (10.39)$$

with:

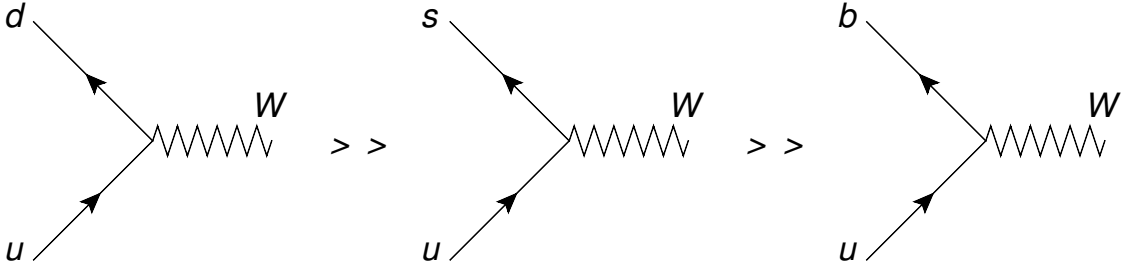
$$Y = \mathcal{G} \left(\frac{M_W^2}{M_H^2} \right) - 2 \sum_l \mathcal{F} \left(\frac{m_l^2}{M_H^2} \right) - 2N \sum_q Q_q^2 \mathcal{F} \left(\frac{m_q^2}{M_H^2} \right)$$

Using eq. (10.3), the decay rate of a Higgs boson in two photons is:

$$\Gamma_{H \rightarrow \gamma\gamma} = \frac{\alpha^3}{32 \pi^2 \sin^2(\theta_W)} \frac{M_H^3}{M_W^2} |Y|^2 \quad (10.40)$$

11 Family mixing and the Kobayashi-Maskawa matrix

The above discussion has been considerably simplified since it completely ignored mixing between the three fermion families. For example, if the coupling $u \rightarrow d + W^+$ is allowed the couplings $u \rightarrow s + W^+$ and $u \rightarrow b + W^+$ are not possible in the model. However it turns out that the transitions



are observed with the hierarchy as indicated. They can be summarised by defining a transition $u \rightarrow d'$ with d' a linear superposition of the d, s, b quarks. The quark states (u_i) and (d_i) with $i = 1, 2, 3$ for the three families constructed in the previous sections are eigenstates of the mass matrix but the charged electroweak transition is not diagonal in these states but rather it is diagonal in a (u'_i) , (d'_i) basis called the flavour basis. The two bases are related as follows:

$$u_{iL} = S_{ij}^{uL} u'_{jL}, \quad d_{iL} = S_{ij}^{dL} d'_{jL}, \quad u_{iR} = S_{ij}^{uR} u'_{jR}, \quad d_{iR} = S_{ij}^{dR} d'_{jR}, \quad i, j = 1, 2, 3. \quad (11.1)$$

Eq. (11.1) can be written in a matrix form $\mathbf{u}_L = \mathbf{S}^{uL} \mathbf{u}'_L$ and similarly for the right-handed up sector as well as the left-handed and right-handed $down$ sectors. As will be shown later the matrices $\mathbf{S}^{uL}, \mathbf{S}^{uR}, \dots$ are unitary. The quark sector of the $SU(2)_L \otimes U(1)_Y$ lagrangian is written in general¹⁸ (see eq. (5.22))

$$\mathcal{L}_F = \sum_i (\bar{u}'_{iL} \bar{d}'_{iL}) i \not{D}_{qL} \begin{pmatrix} u'_{iL} \\ d'_{iL} \end{pmatrix} + \sum_i \bar{u}'_{iR} i \not{D}_{uR} u'_{iR} + \sum_i \bar{d}'_{iR} i \not{D}_{dR} d'_{iR}, \quad (11.2)$$

so that the electroweak interactions are diagonal in the “primed” flavour basis. After symmetry breaking, the most general Yukawa lagrangian takes the form in the “primed” basis, (see eqs. (8.26), (8.27)), ignoring for the moment the H boson couplings to the fermions

$$\begin{aligned} \mathcal{L}_Y &= -\frac{v}{\sqrt{2}} \sum_{ij} (\bar{u}'_{iL} c_{ij}^u u'_{jR} + \bar{d}'_{iL} c_{ij}^d d'_{jR} + \text{h.c.}) \\ &= -\frac{v}{\sqrt{2}} (\bar{\mathbf{u}}'_L \mathbf{C}_u \mathbf{u}'_R + \bar{\mathbf{d}}'_L \mathbf{C}_d \mathbf{d}'_R + \text{h.c.}) \end{aligned} \quad (11.3)$$

¹⁸We could in fact identify flavour and mass eigenstates of the up sector and take for simplicity $\mathbf{S}^{uL} = \mathbf{S}^{uR} = \mathbf{1}$.

where the complex, 3×3 , $\mathbf{C}_u, \mathbf{C}_d$ matrices are the generalized Yukawa couplings. Including the common normalisation factor $v/\sqrt{2}$ with the \mathbf{C}_u and \mathbf{C}_d matrices, the most general such matrices can be written as a product :

$$\frac{v}{\sqrt{2}}\mathbf{C}_u = \mathbf{M}_u \mathbf{T}_u, \quad \frac{v}{\sqrt{2}}\mathbf{C}_d = \mathbf{M}_d \mathbf{T}_d \quad (11.4)$$

with \mathbf{M}_u a hermitian matrix ($\mathbf{M}_u = \mathbf{M}_u^\dagger$) and \mathbf{T}_u a unitary matrix ($\mathbf{T}_u^{-1} = \mathbf{T}_u^\dagger$). The hermitian matrix can be diagonalized by a unitary transformation, $\mathbf{M}_u = \mathbf{S}_u^{-1} \mathbf{m}_u \mathbf{S}_u = \mathbf{S}_u^\dagger \mathbf{m}_u \mathbf{S}_u$ where \mathbf{m}_u is diagonal with real eigenvalues, and similarly for the d sector. The Yukawa lagrangian reduces to the very simple diagonal form :

$$\begin{aligned} \mathcal{L}_Y &= -\bar{\mathbf{u}}_L \mathbf{m}_u \mathbf{u}_R - \bar{\mathbf{u}}_R \mathbf{m}_u \mathbf{u}_L - \bar{\mathbf{d}}_L \mathbf{m}_d \mathbf{d}_R - \bar{\mathbf{d}}_R \mathbf{m}_d \mathbf{d}_L \\ &= -\bar{\mathbf{u}} \mathbf{m}_u \mathbf{u} - \bar{\mathbf{d}} \mathbf{m}_d \mathbf{d} \end{aligned} \quad (11.5)$$

when written in terms of the mass eigenstate basis related to the original one by :

$$\begin{aligned} \mathbf{u}_L &= \mathbf{S}_u \mathbf{u}'_L, & \mathbf{u}_R &= \mathbf{S}_u \mathbf{T}_u \mathbf{u}'_R \\ \mathbf{d}_L &= \mathbf{S}_d \mathbf{d}'_L, & \mathbf{d}_R &= \mathbf{S}_d \mathbf{T}_d \mathbf{d}'_R, \end{aligned} \quad (11.6)$$

which defines the matrices $\mathbf{S}^{u_L}, \mathbf{S}^{u_R}, \dots$ introduced above. We remark that, as advertized before, the transformation from the primed basis to the unprimed one is unitary since such are the \mathbf{S}, \mathbf{T} matrices. The components of \mathbf{u} in which the mass matrix is diagonal are, by definition, the ‘‘physical’’ quark fields (u, c, t) of definite mass eigenstate (*idem* for the d sector). The same is obviously true for the Higgs couplings which are diagonal in the \mathbf{u} and \mathbf{d} bases. Having achieved a simple form for the Yukawa lagrangian we re-write now the gauge part \mathcal{L}_F in terms of these physical fields. Singling out the neutral current interactions we have

$$\begin{aligned} \mathcal{L}_F(\text{neutral current}) &= \sum_i (\bar{u}'_{i_L} i \not{D}_{u_L} u'_{i_L} + \bar{u}'_{i_R} i \not{D}_{u_R} u'_{i_R}) + d' \text{ sector} \\ &= (\bar{\mathbf{u}}'_L i \not{D}_{u_L} \mathbf{u}'_L + \bar{\mathbf{u}}'_R i \not{D}_{u_R} \mathbf{u}'_R) + \mathbf{d}' \text{ sector}, \end{aligned} \quad (11.7)$$

in which we keep only the diagonal (in $SU(2)$) part of the operator \not{D}_L . Because of the unitarity of the transformations within the left-handed bases and the right-handed bases the above lagrangian immediately reduces itself to

$$\begin{aligned} \mathcal{L}_F(\text{neutral current}) &= \bar{\mathbf{u}}_L i \not{D}_{u_L} \mathbf{u}_L + \bar{\mathbf{u}}_R i \not{D}_{u_R} \mathbf{u}_R \\ &+ \bar{\mathbf{d}}_L i \not{D}_{u_L} \mathbf{d}_L + \bar{\mathbf{u}}_R i \not{D}_{u_R} \mathbf{u}_R. \end{aligned} \quad (11.8)$$

This equation is the basis for the slogan that, in the Standard Model and in agreement with experiments, there is “no flavour-changing neutral current”, in other words the neutral current is diagonal in flavour space as well as in the mass eigenstates : it does not induce transition between the c quark and the u quark or between the b quark and the d quark for example. The case of the charged current pieces is more involved because it couples the up sector and the $down$ sector which do not transform with the same unitary matrices and, as a consequence, there is no reason for the charged current interactions to be diagonal in the basis which diagonalises the mass matrix. Indeed we have, from eqs. (11.2), (5.43):

$$\begin{aligned}\mathcal{L}_F(\text{quark charged current}) &= \frac{e}{\sqrt{2} \sin \theta_w} (\bar{\mathbf{u}}'_L \mathcal{W}^* \mathbf{d}'_L + \bar{\mathbf{d}}'_L \mathcal{W} \mathbf{u}'_L) \\ &= \frac{e}{\sqrt{2} \sin \theta_w} (\bar{\mathbf{u}}_L \mathcal{W}^* \mathbf{S}_u \mathbf{S}_d^\dagger \mathbf{d}_L + \bar{\mathbf{d}}_L \mathbf{S}_d \mathbf{S}_u^\dagger \mathcal{W} \mathbf{u}_L) \quad (11.9)\end{aligned}$$

where the last equation is obtained from eq. (11.6). The matrix $\mathbf{CKM} = \mathbf{S}_u \mathbf{S}_d^\dagger$ is the famous Cabibbo-Kobayashi-Maskawa matrix which parameterises the flavour changing content of charged current transitions, *i.e* transitions between left-handed \mathbf{up} spinors (u_L, c_L, t_L) of definite mass to \mathbf{down} spinors (d_L, s_L, b_L) of definite mass. Its matrix elements are often written as

$$\mathbf{CKM} = \begin{pmatrix} V_{ud} & V_{us} & V_{ub} \\ V_{cd} & V_{cs} & V_{cb} \\ V_{td} & V_{ts} & V_{tb} \end{pmatrix}. \quad (11.10)$$

The matrix \mathbf{CKM} is unitary, since both $\mathbf{S}_u, \mathbf{S}_d^\dagger$ are such, and its matrix elements must satisfy relations of type $V_{ub}^* V_{ud} + V_{cb}^* V_{cd} + V_{tb}^* V_{td} = 0$ or $V_{ub}^* V_{ub} + V_{cb}^* V_{cb} + V_{tb}^* V_{tb} = 1$. The determination of the V_{ij} is a very active area of particle physics phenomenology at present and it is one of the aims of the LHCb collaboration at CERN and Belle II at KEK in Japan. If V_{ud} is mainly constrained from nuclear β decays the others are essentially determined from K decays and heavy flavour decays. The 2018 edition of the particle data group¹⁹ quotes the following values

$$\begin{aligned}|V_{ud}| &= 0.97446 \pm 0.00010, & |V_{us}| &= 0.22452 \pm 0.00044, & |V_{ub}| &= (3.65 \pm 0.12)10^{-03} \\ |V_{cd}| &= 0.22438 \pm 0.00044, & |V_{cs}| &= 0.97359_{-0.00011}^{+0.00010}, & |V_{cb}| &= (4.214 \pm 0.076)10^{-02} \\ |V_{td}| &= (8.96_{-0.23}^{+0.24})10^{-03}, & |V_{ts}| &= (4.133 \pm 0.074)10^{-02}, & |V_{tb}| &= 0.999105 \pm 0.000032\end{aligned} \quad (11.11)$$

The \mathbf{CKM} matrix generalizes to three families the Cabibbo angle, $\sin \theta_C = \lambda \sim .22 \simeq V_{us}$ introduced long ago to deal with the mixing of two families. The Cabibbo-Kobayashi-Maskawa quark mixing

¹⁹ M. Tanabashi *et. al.* (Particle Data Group), Phys. Rev. **D98** (2018) 030001 (<http://pdg.lbl.gov>).

matrix is a 3×3 unitary matrix and from its definition²⁰ it depends on nine parameters which can be chosen as three real parameters and six phases. Changing the phase of u_{iL} and d_{jL} respectively by $e^{i\phi_{ui}}$ and $e^{i\phi_{dj}}$ the **CKM** matrix elements $(\mathbf{S}_u \mathbf{S}_d^\dagger)_{ij}$ becomes $e^{i(\phi_{dj} - \phi_{ui})} (\mathbf{S}_u \mathbf{S}_d^\dagger)_{ij}$. The five arbitrary phase differences can be used to absorb as many phases of the **CKM** matrix leaving one \mathcal{CP} violating phase. One should of course shift the phases of the right-handed fields and the left-handed ones by the same amount to leave the mass terms eq. (11.5) invariant. The independent parameters of the **CKM** matrix are chosen as three angles ($c_{ij} = \cos \theta_{ij}$, $s_{ij} = \sin \theta_{ij}$ with $0 < \theta_{ij} < \pi/2$) and a phase δ ($0 < \delta < 2\pi$) and one writes:

$$\begin{aligned} \mathbf{CKM} &= \begin{pmatrix} 1 & 0 & 0 \\ 0 & c_{23} & s_{23} \\ 0 & -s_{23} & c_{23} \end{pmatrix} \cdot \begin{pmatrix} c_{13} & 0 & s_{13}e^{-i\delta} \\ 0 & 1 & 0 \\ -s_{13}e^{i\delta} & 0 & c_{13} \end{pmatrix} \cdot \begin{pmatrix} c_{12} & s_{12} & 0 \\ -s_{12} & c_{12} & 0 \\ 0 & 0 & 1 \end{pmatrix} \\ &= \begin{pmatrix} c_{12}c_{13} & s_{12}c_{13} & s_{13}e^{-i\delta} \\ -s_{12}c_{23} - c_{12}s_{23}s_{13}e^{i\delta} & c_{12}c_{23} - s_{12}s_{23}s_{13}e^{i\delta} & s_{23}c_{13} \\ s_{12}s_{23} - c_{12}c_{23}s_{13}e^{i\delta} & -c_{12}s_{23} - s_{12}c_{23}s_{13}e^{i\delta} & c_{23}c_{13} \end{pmatrix}. \end{aligned} \quad (11.12)$$

This last form is not very illuminating and in view of the relative smallness of $|s_{13}| \simeq |V_{ub}| \simeq 3.57 \cdot 10^{-03}$, $|s_{23}| \simeq |V_{cb}| = 4.11 \cdot 10^{-02}$ the approximation $c_{13} \approx c_{23} \approx 1$ is justified. With $|s_{12}| \approx |V_{us}| = 0.225$, Wolfenstein introduced the convenient and often used parameterisation (see the PDG review¹⁹):

$$\mathbf{CKM} = \begin{pmatrix} 1 - \lambda^2/2 & \lambda & A\lambda^3(\rho - i\eta) \\ -\lambda & 1 - \lambda^2/2 & A\lambda^2 \\ A\lambda^3(1 - \rho - i\eta) & -A\lambda^2 & 1 \end{pmatrix}, \quad (11.13)$$

with

$$\begin{aligned} s_{12} &\approx \lambda = 0.22453 \pm 0.00044, & A &= 0.836 \pm 0.0015 \\ \rho &= 0.122_{-0.017}^{+0.018}, & \eta &= 0.355_{-0.011}^{+0.012} \end{aligned} \quad (11.14)$$

This parameterisation shows that the charged current transition, for example, of a u quark to d, s, b quarks takes place with amplitudes which are proportional to $(1 - \lambda^2/2)$, λ , $A\lambda^3(\rho - i\eta)$ respectively. The phase factor η , or equivalently δ in eq. (11.12), is responsible for \mathcal{CP} violation in the Standard Model (see appendix B, in particular B.3). The measurement of this \mathcal{CP} violating parameter, in kaon and B meson systems, for example, is of great theoretical interest in order to understand the origin of \mathcal{CP} violation and of great practical importance since it may be related to the origin of the baryon asymmetry in the universe.

²⁰A unitary matrix \mathbf{U} can be written $\mathbf{U} = \exp(i \sum_a \alpha^a T^a)$, with T^a the generators of the $SU(3)$ group for $a = 1, \dots, 8$ and $T^9 = \mathbb{1}$. The α^a are real parameters. A matrix \mathbf{U} parameterised as in eq. (11.12) is often written $\mathbf{U} = U_{23}U_{13}(\delta)U_{12}$.

A very important point is to check experimentally the unitarity of the **CKM** matrix : indeed any violation of one of the unitarity relations may indicate the existence of a new quark or a new family of quarks. Present data are consistent with the unitarity of the **CKM** matrix within a 3% accuracy.

12 Neutrinos and the Pontecorvo-Maki-Nakagawa-Sakata matrix

The absence of a **CKM** mixing matrix for the leptonic sector requires a comment. We assumed that the right-handed neutrinos decouple from the observed world. As a consequence, as mentioned above, the neutrinos ν_e, ν_μ, ν_τ remain massless even after spontaneous symmetry breaking since there are, in the lagrangian density, no terms coupling left-handed and right-handed fields like in eq. (8.26). Therefore no mass matrix can be constructed from which the “physical” neutrino states are defined. When studying the weak-current transition from charged leptons to neutrinos we are thus free to define the neutrino physical states as those for which the charged weak current is diagonal in lepton flavour.

However, recent experiments have shown that neutrinos oscillate *i.e.* they change flavour when propagating from their emission point to their detection point. This can be explained if neutrinos are massive. If one follows the same procedure as for the quarks one introduces right-handed fields and this leads to Dirac type massive neutrinos. There is another possibility which relies on the fact that, being neutral, neutrinos can be their own antiparticles and this leads to Majorana type neutrinos. In the first case the total lepton number $L = L_e + L_\mu + L_\tau$ is conserved, while, in the latter case, it is not. In this section, we deal with Dirac neutrinos, the Majorana case being treated in sec. 15.

We assume that, like quarks, the neutrinos are of Dirac type with both left-handed and right-handed components. In the flavour basis, besides the triplet of left-handed fields ν'_L one introduces a triplet of right-handed fields ν'_R , singlets under $SU(2)_L$,

$$\nu'_L = \begin{pmatrix} \nu_{eL} \\ \nu_{\mu L} \\ \nu_{\tau L} \end{pmatrix} \quad \text{and} \quad \nu'_R = \begin{pmatrix} \nu_{eR} \\ \nu_{\mu R} \\ \nu_{\tau R} \end{pmatrix}. \quad (12.1)$$

In this notation ν_{eL} is the neutrino produced by an electron in a charged current interaction and similarly for $\nu_{\mu L}$ and $\nu_{\tau L}$. Assuming the $SU(2)_L \otimes U(1)_Y$ symmetry holds true, the right handed neutrinos cannot be produced or interact in reactions mediated by gauge bosons: they do not couple to the $SU(2)_L$ gauge bosons nor to the $U(1)_Y$ boson since being neutral $y_{\nu_R} = 2e_{\nu_R} = 0$, thus they do not couple to W^\pm, Z or γ gauge bosons. They can be produced in Higgs decays but, given that the Higgs couplings are proportional to the masses, it is fair to assert that the production rate via this channel is not measurable. Their only effect is to give masses to neutrinos. The charged current

transition (eq. (5.28)) is given by the term $(g/\sqrt{2})(\bar{e}_L \mathbb{W} \nu'_L + \bar{\nu}'_L \mathbb{W}^* e_L)$, diagonal in flavour where

$$\mathbf{e}_L = \begin{pmatrix} e_L \\ \mu_L \\ \tau_L \end{pmatrix} \quad (12.2)$$

is the triplet of left-handed charged leptons. We emphasize that e_L, μ_L, τ_L are the mass eigenstates of the charged leptons. In analogy with the case of quarks, after symmetry breaking, the Dirac mass term for neutrinos is of the form

$$\mathcal{L}_{Y_D} = -\frac{v}{\sqrt{2}} \bar{\nu}'_L \mathbf{C}_\nu \nu'_R + \text{h.c.} \quad (12.3)$$

Following the steps leading from eq. (11.3) to eq. (11.6), we introduce the notation (\mathbf{M}_ν hermitian, \mathbf{T}_ν unitary),

$$\frac{v}{\sqrt{2}} \mathbf{C}_\nu = \mathbf{M}_\nu \mathbf{T}_\nu, \quad (12.4)$$

and diagonalize the hermitian matrix by the transformation $\mathbf{M}_\nu = \mathbf{S}_\nu^{-1} \mathbf{m}_\nu \mathbf{S}_\nu = \mathbf{S}_\nu^\dagger \mathbf{m}_\nu \mathbf{S}_\nu$ (\mathbf{S}_ν unitary).

Defining

$$\nu_L = \mathbf{S}_\nu \nu'_L \quad \text{and} \quad \nu_R = \mathbf{S}_\nu \mathbf{T}_\nu \nu'_R, \quad (12.5)$$

the Yukawa lagrangian becomes diagonal,

$$\Rightarrow \mathcal{L}_{Y_D} = -\bar{\nu}_L \mathbf{m}_\nu \nu_R - \bar{\nu}_R \mathbf{m}_\nu \nu_L = -\bar{\nu} \mathbf{m}_\nu \nu \quad (12.6)$$

with m_1, m_2, m_3 the three real eigenvalues of \mathbf{m}_ν and ν_1, ν_2, ν_3 the three neutrino mass eigenstates

$$\nu = \nu_L + \nu_R = \begin{pmatrix} \nu_1 \\ \nu_2 \\ \nu_3 \end{pmatrix}. \quad (12.7)$$

Then, using eq. (12.5), the charged current transition is written

$$\begin{aligned} \mathcal{L}(\text{leptonic charged current}) &= \frac{g}{\sqrt{2}} (\bar{e}_L \mathbb{W} \nu'_L + \bar{\nu}'_L \mathbb{W}^* e_L) \\ &= \frac{e}{\sqrt{2} \sin \theta_W} (\bar{e}_L \mathbb{W} \mathbf{S}_\nu^\dagger \nu_L + \bar{\nu}_L \mathbf{S}_\nu \mathbb{W}^* e_L). \end{aligned} \quad (12.8)$$

Similarly to the **CKM** mixing matrix one introduces the Pontecorvo-Maki-Nakagawa-Sakata matrix²¹ $\mathbf{PMNS} = \mathbf{S}_\nu^\dagger$ the matrix elements of which are often written as²²:

$$\mathbf{PMNS} = \begin{pmatrix} U_{e1} & U_{e2} & U_{e3} \\ U_{\mu 1} & U_{\mu 2} & U_{\mu 3} \\ U_{\tau 1} & U_{\tau 2} & U_{\tau 3} \end{pmatrix} \quad (12.9)$$

²¹In 1952, B. Pontecorvo was the first to mention the possibility of $\nu_e - \bar{\nu}_e$ oscillations. In 1962, the year when ν_μ was discovered, Ziro Maki, Masami Nakagawa and Shoichi Sakata, assuming two kinds of neutrinos proposed a "particle mixture theory of neutrino", Prog. Theor. Physics **28** (1962), 870.

²²The **PMNS** matrix appears simpler than the **CKM** one since the gauge interaction eq. (12.8) is written directly in terms of the charged lepton mass eigenstates.

where e, μ, τ refer to flavour states and 1, 2, 3 to mass eigenstates.

It is easy to check that all terms in the lagrangian density are invariant under the global phase change of all fields

$$e_L \rightarrow e^{i\lambda} e_L, \quad \nu_L \rightarrow e^{i\lambda} \nu_L, \quad \nu_R \rightarrow e^{i\lambda} \nu_R. \quad (12.10)$$

To this invariance corresponds the conservation of the total lepton number defined as $L = \sum_{\alpha} L_{\alpha}$, $\alpha = e, \mu, \tau$. It follows that such transitions as $\mu^- \rightarrow e^- + \gamma$ or $\mu^- \rightarrow e^- + e^+ + e^-$ are allowed in the model. A recent fit to available data shows that the mixing pattern is quite different from that of the quark²³

$$\begin{aligned} |U_{e1}| &= 0.800 \rightarrow 0.844, & |U_{e2}| &= 0.515 \rightarrow 0.581, & |U_{e3}| &= 0.139 \rightarrow 0.155 \\ |U_{\mu1}| &= 0.229 \rightarrow 0.516, & |U_{\mu2}| &= 0.438 \rightarrow 0.699, & |U_{\mu3}| &= 0.614 \rightarrow 0.790 \\ |U_{\tau1}| &= 0.249 \rightarrow 0.528, & |U_{\tau2}| &= 0.462 \rightarrow 0.715, & |U_{\tau3}| &= 0.595 \rightarrow 0.776. \end{aligned} \quad (12.11)$$

As for quarks, no satisfactory model can account for this mixing pattern.

The phenomenology of neutrino mixing is discussed below in the framework of Dirac neutrinos. There are several recent reviews on this topic, in particular by Nakamura and Petcov²⁴ and by Giganti, Lavignac and Zito²⁵. The case of Majorana neutrinos is discussed in sec. 15 and by Bilenky and Petcov²⁶.

12.1 Neutrino survival and oscillation

The space-time evolution of a state of given mass is ($\hbar = c = 1$)

$$|\nu_i(x)\rangle = e^{-i(Et - \vec{k}\vec{x})} |\nu_i\rangle. \quad (12.12)$$

As will be seen below it is justified to assume the neutrinos to be ultrarelativistic particles so that $E \approx k + m_i^2/2k$ and the equation becomes (x denotes now the length travelled by the neutrino)

$$|\nu_i(x)\rangle = e^{-ix(m_i^2/2k)} |\nu_i\rangle. \quad (12.13)$$

²³I. Esteban, M.C. Gonzalez-Garcia, M. Maltoni, I. Martinez-Soler, T. Schwetz, JHEP **1701** (2017) 087, arXiv:1611.01514 [hep-ph]. The variation of the coefficients is given for a 3σ range.

²⁴K. Nakamura, S.T. Petcov, in Particle Data Group (PDG), M. Tanabashi *et. al.*, Phys. Rev. **D98** (2018) 030001 (<http://pdg.lbl.gov>).

²⁵C. Giganti, S. Lavignac, M. Zito, Prog. Part. Nucl. Phys. **98** (2018) 1, arXiv:1710.00715 [hep-ex].

²⁶S.M. Bilenky, S.T. Petcov, Rev. Mod. Phys. **59** (1987) 671.

We consider a neutrino of type α produced in a charged current interaction with momentum k . It is a coherent superposition of neutrino states of definite mass²⁷,

$$|\nu_\alpha\rangle = \sum_i U_{\alpha i}^* |\nu_i\rangle, \quad \alpha = e, \mu, \tau : \quad i = 1, 2, 3. \quad (12.14)$$

The space-time evolution of this neutrino is given at a later time t and at a distance $x = t$ by

$$|\nu_\alpha(x)\rangle = \sum_i U_{\alpha i}^* e^{-ix(m_i^2/2k)} |\nu_i\rangle. \quad (12.15)$$

The probability for this neutrino, initially of flavour α , to be observed as a neutrino of flavour β at the distance x from the emission point is

$$P(\nu_\alpha \rightarrow \nu_\beta) = |\langle \nu_\beta | \nu_\alpha(x) \rangle|^2 = \sum_{i,j} U_{\alpha i}^* U_{\alpha j} U_{\beta i} U_{\beta j}^* \exp\left(ix \frac{\delta m_{ji}^2}{2k}\right), \quad (12.16)$$

where the symbol $\delta m_{ji}^2 = m_j^2 - m_i^2$. Separating the real and imaginary part of the phase factor and using the unitarity of the U matrix ($U_{\alpha i}^* U_{\beta i} = \delta_{\alpha\beta}$) this expression can be written as²⁸:

$$P(\nu_\alpha \rightarrow \nu_\beta) = \delta_{\alpha\beta} - 4 \sum_{i>j} \text{Re}(U_{\alpha i}^* U_{\alpha j} U_{\beta i} U_{\beta j}^*) \sin^2\left(x \frac{\delta m_{ij}^2}{4k}\right) + 2 \sum_{i>j} \text{Im}(U_{\alpha i}^* U_{\alpha j} U_{\beta i} U_{\beta j}^*) \sin\left(x \frac{\delta m_{ij}^2}{2k}\right), \quad (12.17)$$

For the time reversed transition $P(\nu_\beta \rightarrow \nu_\alpha)$ permuting α and β in eq. (12.16) is equivalent to permuting i and j so that it comes out

$$P(\nu_\beta \rightarrow \nu_\alpha) = \delta_{\alpha\beta} - 4 \sum_{i>j} \text{Re}(U_{\alpha i}^* U_{\alpha j} U_{\beta i} U_{\beta j}^*) \sin^2\left(x \frac{\delta m_{ij}^2}{4k}\right) - 2 \sum_{i>j} \text{Im}(U_{\alpha i}^* U_{\alpha j} U_{\beta i} U_{\beta j}^*) \sin\left(x \frac{\delta m_{ij}^2}{2k}\right), \quad (12.18)$$

which exhibits the violation of \mathcal{T} invariance due to the phase factor in the **PMNS** matrix. One finds the same result, eq. (12.18), for $P(\bar{\nu}_\alpha \rightarrow \bar{\nu}_\beta)$, exhibiting this time the \mathcal{CP} violation of the model. Then \mathcal{CPT} is conserved because $P(\nu_\beta \rightarrow \nu_\alpha) = P(\bar{\nu}_\alpha \rightarrow \bar{\nu}_\beta)$. Finally one has the sum rule, valid in the three family model

$$1 = \sum_{\nu_\beta = \nu_e, \nu_\mu, \nu_\tau} P(\nu_\alpha \rightarrow \nu_\beta) = \sum_{\bar{\nu}_\beta = \bar{\nu}_e, \bar{\nu}_\mu, \bar{\nu}_\tau} P(\bar{\nu}_\alpha \rightarrow \bar{\nu}_\beta), \quad \text{for any } \nu_\alpha, \bar{\nu}_\alpha. \quad (12.19)$$

It is important to remark that in case of a disappearance probability, $P(\nu_\alpha \rightarrow \nu_\alpha)$, the last term in the eqs. (12.17) or (12.18) disappears since terms such as $U_{\alpha i}^* U_{\alpha j} U_{\alpha i} U_{\alpha j}^*$ are real and therefore a disappearance probability cannot depend on the imaginary part of the **PMNS** matrix elements.

²⁷From eqs. (12.5), (12.9) a flavour field $\nu_{\alpha L}$ is related to the fields ν_{iL} of given masses by $\nu_{\alpha L} = \sum_i (S^\dagger)_{\alpha i} \nu_{iL} = \sum_i U_{\alpha i} \nu_{iL}$, but the state $|\nu_\alpha\rangle$ is created by the field $\bar{\nu}_{\alpha L}$, hence eq. (12.14).

²⁸We use $\cos(x\delta m_{ij}^2/2k) = 1 - 2 \sin^2(x\delta m_{ij}^2/4k)$, the factor 1 then leading to the $\delta_{\alpha\beta}$ term.

12.2 Summary of results

It turns out, as will be discussed below, that the last factor in eqs. (12.17) and (12.18) is small. Then, oscillations, as a function of x , in the probability for the neutrino to change flavour (or to remain in the same flavour) are essentially induced by the factors $\sin^2(x \delta m_{ij}^2/4k)$. For the oscillation to be seen this factor should be of $\mathcal{O}(1)$. To be quantitative, we have to inject the \hbar and c factors to make the argument of the \sin^2 factor dimensionless. One finds²⁹

$$\frac{\delta m_{ij}^2 x}{4k} \Rightarrow 1.27 10^{-18} \frac{\delta m_{ij}^2 [\text{GeV}^2] x [\text{km}]}{k [\text{GeV}]} = 1.27 \frac{\delta m_{ij}^2 [\text{eV}^2] x [\text{km}]}{k [\text{GeV}]} = 1.27 \frac{\delta m_{ij}^2 [\text{eV}^2] x [\text{m}]}{k [\text{MeV}]}, \quad (12.20)$$

where we have given this expression in terms of the units commonly used. One defines the oscillation length associated to a given mass squared difference by the condition

$$\frac{\delta m_{ij}^2 x}{4k} = \pi \quad \Rightarrow \quad x [\text{m}] = 2.47 \frac{k [\text{MeV}]}{\delta m_{ij}^2 [\text{eV}^2]} \quad \text{or} \quad x [\text{km}] = 2.47 \frac{k [\text{GeV}]}{\delta m_{ij}^2 [\text{eV}^2]}. \quad (12.21)$$

Conversely, we can use this formula to estimate the sensitivity of typical neutrino experiments to mass squared differences as shown in the table below. In some experimental conditions, a factor $(x \delta m_{ij}^2/4k)$

Source	type of ν	k [GeV]	x [km]	$\langle \delta \mathbf{m}^2 \rangle$ [eV ²]
Reactors (short baseline)	$\bar{\nu}_e$	10^{-3}	1	10^{-3}
Reactors (long baseline)	$\bar{\nu}_e$	10^{-3}	100	10^{-5}
Accelerators (short baseline)	$\nu_\mu, \bar{\nu}_\mu$	1	1	1
Accelerators (long baseline)	$\nu_\mu, \bar{\nu}_\mu$	1	10^3	10^{-3}
Atmospheric	$\nu_e, \bar{\nu}_e, \nu_\mu, \bar{\nu}_\mu$	1	10^4	10^{-4}
Sun	ν_e	10^{-2}	$1.5 10^8$	10^{-10}

Table 1: *Sensitivity in terms of δm_{ij}^2 of the different types of neutrino experiments characterised by the energy k of the neutrino and the distance x between the ν source and the detector.*

may remain small and its contribution to the oscillation pattern becomes negligible. In other cases on the contrary, it stays very large and the oscillating \sin^2 term averages out to $1/2$. These facts simplify the analysis of the oscillations as will be seen below in the discussion of several experiments. We give here the values of the parameters, with the **PMNS** matrix written as in eq. (11.12), obtained from of

²⁹In eq. (12.12) the dimensionless phase should be $-i(Et - \vec{k}\vec{x})/\hbar$, with the energy E measured in GeV and k in GeV/ c as appropriate for neutrino experiments. It can be written $-i(Ect - \vec{k}\vec{x})/(\hbar c)$, with both E and k as well as the mass measured in GeV and $[ct] = [x]$ in km if c is expressed in km/sec. We have (see the PDG tables) $\hbar c = 197.3267 10^{-21}$ GeV·km; using the approximate form eq. (12.13), the oscillation factor in eq. (12.17) becomes $\delta m_{ij}^2 [\text{GeV}^2] x [\text{km}]/(4k [\text{GeV}] \hbar c [\text{GeV}\cdot\text{km}]) = 1.27 10^{-18} \delta m_{ij}^2 [\text{GeV}^2] x [\text{km}]/k [\text{GeV}]$.

a recent global analysis of data³⁰

$$\boxed{\begin{aligned} \delta m_{21}^2 &= (6.92 - 7.91) 10^{-5} \text{ eV}^2, & \delta m_{31}^2 &= (2.392 - 2.594) 10^{-3} \text{ eV}^2 \\ \sin^2 \theta_{12} &= 0.265 - 0.346, & \sin^2 \theta_{23} &= 0.430 - 0.602, & \sin^2 \theta_{13} &= 0.0190 - 0.0239. \end{aligned}} \quad (12.22)$$

By convention the mass m_2 is chosen larger than m_1 but there are two possibilities for m_3 : either $m_1 < m_2 < m_3$, labeled *normal hierarchy*, or $m_3 < m_1 < m_2$, labeled *inverted hierarchy*. The above results are obtained assuming a *normal hierarchy*. In the other case the values of the parameters are very similar except of course for the sign of δm_{3i}^2 . For example, the best fit value for δm_{32}^2 is $2.418 10^{-3} \text{ eV}^2$ (normal hierarchy) and $\delta m_{32}^2 = -2.478 10^{-3} \text{ eV}^2$ (inverted hierarchy). There are two independent δm_{ij}^2 and given the relative smallness of δm_{21}^2 , one is justified to take $|\delta m_{32}^2| \approx |\delta m_{31}^2|$. Concerning the mass hierarchy and the \mathcal{CP} violating phase δ , they are difficult to extract because, as will be seen, they enter the observables with small coefficients. One notes that the angle θ_{13} is much smaller than the other mixing angles and small θ_{13} approximations will often be used. At present fits to data seem to indicate a value $\delta \approx 3\pi/2$, with large error bars, for both mass hierarchies and a preference for normal hierarchy.

One does not know the absolute scale of neutrino masses. If we assume $m_1 \ll m_2$ one gets $m_2 \approx 8.6 10^{-3} \text{ eV}$ and $m_3 \approx 5.1 10^{-2} \text{ eV}$, while in the inverted hierarchy case, assuming $m_3 \ll m_1$ the result is $m_1 \approx m_2 \approx 5.1 10^{-2} \text{ eV}$. One way to experimentally access the mass scale of neutrinos is through nuclear β decay which allows to give a direct limit on the $\bar{\nu}_e$ mass. For these purposes, several past and ongoing experiments study tritium decay³¹, ${}^3\text{H} \rightarrow {}^3\text{He} + e^- + \bar{\nu}_e$. The electron energy spectrum is sensitive to the neutrino mass near the upper end of the spectrum. Denoting E_0 the total energy release in the decay, the maximum value of the electron energy is $E < E_0 \approx 18 \text{ keV}$, if the neutrino is massless. A non vanishing neutrino mass will slightly reduce the bound to $E < E_0 - m_{\nu_e}$ and will modify the shape of the spectrum near this end point of the distribution. Near the end point the electron spectrum behaves as

$$dN/dE \propto E_{\nu_e} k_{\nu_e} = (E_0 - E)((E_0 - E)^2 - m_{\nu_e}^2)^{1/2}, \quad (12.23)$$

which has a non-zero derivative, in fact $-\infty$, if the neutrino is massive. The effect is very hard to measure since the rate of energetic electrons is very low. A limit established some years ago³² was

³⁰F. Capozzi, E. Lisi, A. Marrone, A. Palazzo, Prog. Part. Nucl. Phys. **102** (2018) 48, arXiv:1804.09678 [hep-ph]; see also P.F. de Salas, S. Gariazzo, O. Mena, C.A. Ternes, M. Tórtola, Front. Astron. Space Sci. **5** (2018) 36; arXiv:1806.11051 [hep-ph]; P.F. de Salas, D.V. Forero, C.A. Ternes, M. Tórtola, J.W.F. Valle, Phys. Lett. **B782** (2018) 633, arXiv:1708.01186 [hep-ph]; NuFIT webpage, <http://www.nu-fit.org/>.

³¹G. Drexlin, V. Hannen, S. Mertens, and C. Weinheimer, Adv.High Energy Phys. (2013) 293986, arXiv:1307.0101.

³²Troitsk Collaboration, V.N. Aseev *et al.* Phys. Rev **D84** (2011) 112003.

$m_{\nu_e} < 2.05$ eV at 95% c.l., quite a bit higher than the tentative scales suggested above. The KATRIN experiment which started operation in 2018, in Karlsruhe, quotes now an upper limit of 1.1 eV at 90% c.l.³³. By 2024 the collaboration expects to reach 0.2 eV (90% c.l.) or 0.35 eV (5σ). Finally astrophysical and cosmological limits are available on the sum of neutrino masses and a recent result reported by the Planck collaboration is³⁴

$$\sum_j m_j < .12 \text{ eV}, \quad (12.24)$$

but this result is model dependent. In the following we use for the **PMNS** matrix, eq. (12.9), the representation, eq. (11.12).

12.3 Survival probabilities in vacuum

Since, in experiments, both survival and oscillation probabilities can be measured we quote below the general form of these expressions for 3 flavoured neutrinos³⁵. In the analysis of results it will turn out that different approximations can be made, depending on the experimental set-up, which simplify considerably the general expressions. The reduced forms will be easily obtained from the results given in this section and the next. The simplest case is the electron survival probability, the exact expression of which is:

$$\begin{aligned} P(\nu_e \rightarrow \nu_e) = 1 & - \sin^2(2\theta_{12}) \cos^4(\theta_{13}) \sin^2\left(x \frac{\delta m_{21}^2}{4k}\right) - \sin^2(2\theta_{13}) \sin^2(\theta_{12}) \sin^2\left(x \frac{\delta m_{32}^2}{4k}\right) \\ & - \sin^2(2\theta_{13}) \cos^2(\theta_{12}) \sin^2\left(x \frac{\delta m_{31}^2}{4k}\right), \end{aligned} \quad (12.25)$$

insensitive to δ (thus $P(\nu_e \rightarrow \nu_e) = P(\bar{\nu}_e \rightarrow \bar{\nu}_e)$) and to the hierarchy of mass. The muon survival is given by:

$$\begin{aligned} P(\nu_\mu \rightarrow \nu_\mu) = 1 & - [\sin^2(2\theta_{12}) \cos^4(\theta_{23}) + \sin^2(2\theta_{23})[\cos^4(\theta_{12}) + \sin^4(\theta_{12})] \sin^2(\theta_{13})] \sin^2\left(x \frac{\delta m_{21}^2}{4k}\right) \\ & - [\sin^2(2\theta_{23}) \cos^2(\theta_{13}) \cos^2(\theta_{12}) + \sin^2(2\theta_{13}) \sin^4(\theta_{23}) \sin^2(\theta_{12})] \sin^2\left(x \frac{\delta m_{32}^2}{4k}\right) \\ & - [\sin^2(2\theta_{23}) \cos^2(\theta_{13}) \sin^2(\theta_{12}) + \sin^2(2\theta_{13}) \sin^4(\theta_{23}) \cos^2(\theta_{12})] \sin^2\left(x \frac{\delta m_{31}^2}{4k}\right) \\ & - 8J \cos(\delta) \text{COS}_{\nu_\mu} + \mathcal{O}(\sin^3(\theta_{13})), \end{aligned} \quad (12.26)$$

³³G. Drexin for the KATRIN Collaboration, 16th TAUP International Conference, Toyama, Japan, Sept. 2019.

³⁴Planck 2018 results. VI. Cosmological parameters, N. Aghanim *et al.*, in *Astronomy and Astrophysics*, 2018, arXiv:1807.06209 [astro-ph.CO].

³⁵Exact expressions in a somewhat different form are found in V. Barger, D. Marfatia, K. Whisnant, *Int. J. Mod. Phys. E***12** (2003) 569, hep-ph:0308123.

with the Jarlskog factor³⁶ J :

$$J = \frac{1}{8} \sin(2\theta_{12}) \sin(2\theta_{23}) \sin(2\theta_{13}) \cos(\theta_{13}), \quad (12.27)$$

and the expression COS_{ν_μ} :

$$\text{COS}_{\nu_\mu} = \left[\cos^2(\theta_{23}) \cos(2\theta_{12}) \sin^2 \left(x \frac{\delta m_{21}^2}{4k} \right) - \sin^2(\theta_{23}) \left(\sin^2 \left(x \frac{\delta m_{32}^2}{4k} \right) - \sin^2 \left(x \frac{\delta m_{31}^2}{4k} \right) \right) \right] \quad (12.28)$$

More precisely, in eq. (12.26), we have neglected very small terms of type $\sin^4(\theta_{13}) \sin^2(x\delta m_{21}^2/4k)$, $\sin^3(\theta_{13}) \cos(\delta)$ and $\sin^2(\theta_{13}) \cos^2(\delta)$. The τ survival probability is obtained from this equation, by exchanging $\sin^2(\theta_{23})$ and $\cos^2(\theta_{23})$ and reversing the sign of the $\cos(\delta)$ term.

12.4 Oscillation in vacuum, \mathcal{CP} asymmetries, mass hierarchy and δ

It is important to obtain the dependence on the phase δ of the oscillation probabilities as it is related to the \mathcal{CP} asymmetries and to the mass hierarchy. In fact, all oscillation probabilities have, up to a sign, the same dependence on $\sin(\delta)$ which is relatively easy to obtain. Injecting the parameterisation eq. (11.12) in the U matrices in eq. (12.16) one finds without approximations

$$\begin{aligned} P(\nu_e \rightarrow \nu_\mu) &= \sin^2(2\theta_{12}) \cos^2(\theta_{13}) [\cos^2(\theta_{23}) - \sin^2(\theta_{23}) \sin^2(\theta_{13})] \sin^2 \left(x \frac{\delta m_{21}^2}{4k} \right) \\ &+ \sin^2(2\theta_{13}) \sin^2(\theta_{23}) \sin^2(\theta_{12}) \sin^2 \left(x \frac{\delta m_{32}^2}{4k} \right) \\ &+ \sin^2(2\theta_{13}) \sin^2(\theta_{23}) \cos^2(\theta_{12}) \sin^2 \left(x \frac{\delta m_{31}^2}{4k} \right) \\ &+ 4J \cos(\delta) \text{COS} + 2J \sin(\delta) \text{SIN}, \end{aligned} \quad (12.29)$$

with

$$\text{COS} = \left[\cos(2\theta_{12}) \sin^2 \left(x \frac{\delta m_{21}^2}{4k} \right) - \sin^2 \left(x \frac{\delta m_{32}^2}{4k} \right) + \sin^2 \left(x \frac{\delta m_{31}^2}{4k} \right) \right] \quad (12.30)$$

$$\text{SIN} = \left[\sin \left(x \frac{\delta m_{21}^2}{2k} \right) + \sin \left(x \frac{\delta m_{32}^2}{2k} \right) + \sin \left(x \frac{\delta m_{13}^2}{2k} \right) \right]. \quad (12.31)$$

³⁶C. Jarlskog, Z. Phys. **C29** (1985) 491. Due to the unitarity of the **PMNS** matrix one shows that $\text{Im}(U_{\alpha i}^* U_{\alpha j} U_{\beta i} U_{\beta j}^*)$ with $\alpha \neq \beta$, $\alpha, \beta = e, \mu, \tau$, $i \neq j$, $i, j = 1, 2, 3$, is up to a sign an invariant, thus $\text{Im}(U_{e3}^* U_{e2} U_{\mu 3} U_{\mu 2}^*) = J \sin(\delta)$.

Using the sum rule eq. (12.19) or by direct calculation it comes out:

$$\begin{aligned}
P(\nu_e \rightarrow \nu_\tau) &= \sin^2(2\theta_{12}) \cos^2(\theta_{13}) [\sin^2(\theta_{23}) - \cos^2(\theta_{23}) \sin^2(\theta_{13})] \sin^2\left(x \frac{\delta m_{21}^2}{4k}\right) \\
&+ \sin^2(2\theta_{13}) \cos^2(\theta_{23}) \sin^2(\theta_{12}) \sin^2\left(x \frac{\delta m_{32}^2}{4k}\right) \\
&+ \sin^2(2\theta_{13}) \cos^2(\theta_{23}) \cos^2(\theta_{12}) \sin^2\left(x \frac{\delta m_{31}^2}{4k}\right) \\
&- 4J \cos(\delta) \text{COS} - 2J \sin(\delta) \text{SIN},
\end{aligned} \tag{12.32}$$

From the expressions given in eqs. (12.25) to (12.32) and with the help of the relations given in sec. 12.1 we can obtain all survival or oscillation probabilities of neutrinos and antineutrinos. For instance, one obtains $P(\nu_\mu \rightarrow \nu_e)$ from $P(\nu_e \rightarrow \nu_\mu)$ by reversing the sign of δ in eq. (12.29) and one derives $P(\nu_\mu \rightarrow \nu_\tau) = 1 - P(\nu_\mu \rightarrow \nu_e) - P(\nu_\mu \rightarrow \nu_\mu)$ from the sum rule. For completeness we quote it at the same level of approximation as the previous rates with the further simplification of dropping all terms proportional to $\sin^2(\theta_{13})$ in the first line:

$$\begin{aligned}
P(\nu_\mu \rightarrow \nu_\tau) &= -\frac{1}{4} \sin^2(2\theta_{23}) \sin^2(2\theta_{12}) \sin^2\left(x \frac{\delta m_{21}^2}{4k}\right) \\
&+ \sin^2(2\theta_{23}) [\cos^2(\theta_{12}) - \sin^2(\theta_{12}) \sin^2(\theta_{13})] \cos^2(\theta_{13}) \sin^2\left(x \frac{\delta m_{32}^2}{4k}\right) \\
&+ \sin^2(2\theta_{23}) [\sin^2(\theta_{12}) - \cos^2(\theta_{12}) \sin^2(\theta_{13})] \cos^2(\theta_{13}) \sin^2\left(x \frac{\delta m_{31}^2}{4k}\right) \\
&+ 4J \cos(\delta) \text{COS}_\tau + 2J \sin(\delta) \text{SIN},
\end{aligned} \tag{12.33}$$

with

$$\text{COS}_\tau = \cos(2\theta_{23}) \left[\cos(2\theta_{12}) \sin^2\left(x \frac{\delta m_{21}^2}{4k}\right) + \sin^2\left(x \frac{\delta m_{32}^2}{4k}\right) - \sin^2\left(x \frac{\delta m_{31}^2}{4k}\right) \right] \tag{12.34}$$

If one defines a measure of the \mathcal{CP} asymmetry in the oscillation $\nu_\alpha \rightarrow \nu_\beta$ by

$$\mathcal{A}(\nu_\alpha \rightarrow \nu_\beta) = P(\nu_\alpha \rightarrow \nu_\beta) - P(\bar{\nu}_\alpha \rightarrow \bar{\nu}_\beta), \tag{12.35}$$

then the following relations hold true:

$$\boxed{
\begin{aligned}
\mathcal{A}(\nu_e \rightarrow \nu_\mu) &= -\mathcal{A}(\nu_\mu \rightarrow \nu_e) = -\mathcal{A}(\nu_e \rightarrow \nu_\tau) = \mathcal{A}(\nu_\mu \rightarrow \nu_\tau) = 4J \sin(\delta) \text{SIN} \\
&= 4J \sin(\delta) \left[\sin\left(x \frac{\delta m_{21}^2}{2k}\right) + \sin\left(x \frac{\delta m_{32}^2}{2k}\right) + \sin\left(x \frac{\delta m_{13}^2}{2k}\right) \right].
\end{aligned}
} \tag{12.36}$$

Since the δm_{ij}^2 factors are not independent, $\delta m_{31}^2 = \delta m_{32}^2 + \delta m_{21}^2$, one can eliminate m_{31}^2 , for example, and obtain:

$$\text{SIN} = 4 \sin\left(x \frac{\delta m_{21}^2}{4k}\right) \sin\left(x \frac{\delta m_{31}^2}{4k}\right) \sin\left(x \frac{\delta m_{32}^2}{4k}\right) \quad (12.37)$$

$$= 4 \sin\left(x \frac{\delta m_{21}^2}{4k}\right) \sin^2\left(x \frac{\delta m_{32}^2}{4k}\right) + \mathcal{O}\left(\sin^2\left(x \frac{\delta m_{21}^2}{4k}\right)\right). \quad (12.38)$$

where the last relation is valid when $x \delta m_{21}^2/4k$ is small compared to $x \delta m_{32}^2/4k$. Coming back to the oscillation probabilities, the coefficient of the $\cos(\delta)$ piece in the equations can likewise be simplified and one finds³⁷

$$\text{COS} = 2 \sin\left(x \frac{\delta m_{21}^2}{4k}\right) \sin\left(x \frac{\delta m_{31}^2}{4k}\right) \cos\left(x \frac{\delta m_{32}^2}{4k}\right) - 2 \sin^2(\theta_{12}) \sin^2\left(x \frac{\delta m_{21}^2}{4k}\right) \quad (12.39)$$

$$= 2 \sin\left(x \frac{\delta m_{21}^2}{4k}\right) \sin\left(x \frac{\delta m_{32}^2}{4k}\right) \cos\left(x \frac{\delta m_{32}^2}{4k}\right) + \mathcal{O}\left(\sin^2\left(x \frac{\delta m_{21}^2}{4k}\right)\right). \quad (12.40)$$

Under these simplifications³⁸, and neglecting small $\sin^2(\theta_{13})$ corrections in the coefficients of terms in $\sin^2(x \delta m_{21}^2/4k)$, the oscillation probabilities for $\nu_e \rightarrow \nu_\mu$ and $\nu_e \rightarrow \nu_\tau$ take the form:

$$\begin{aligned} P(\nu_e \rightarrow \nu_\mu) &\approx \sin^2(2\theta_{12}) \cos^2(\theta_{23}) \sin^2\left(x \frac{\delta m_{21}^2}{4k}\right) + \sin^2(2\theta_{13}) \sin^2(\theta_{23}) \sin^2\left(x \frac{\delta m_{32}^2}{4k}\right) \\ &\quad + 8J \sin\left(x \frac{\delta m_{21}^2}{4k}\right) \sin\left(x \frac{\delta m_{32}^2}{4k}\right) \left[\cos(\delta) \cos\left(x \frac{\delta m_{32}^2}{4k}\right) + \sin(\delta) \sin\left(x \frac{\delta m_{32}^2}{4k}\right) \right] \end{aligned} \quad (12.41)$$

$$\begin{aligned} P(\nu_e \rightarrow \nu_\tau) &\approx \sin^2(2\theta_{12}) \sin^2(\theta_{23}) \sin^2\left(x \frac{\delta m_{21}^2}{4k}\right) + \sin^2(2\theta_{13}) \cos^2(\theta_{23}) \sin^2\left(x \frac{\delta m_{32}^2}{4k}\right) \\ &\quad - 8J \sin\left(x \frac{\delta m_{21}^2}{4k}\right) \sin\left(x \frac{\delta m_{32}^2}{4k}\right) \left[\cos(\delta) \cos\left(x \frac{\delta m_{32}^2}{4k}\right) + \sin(\delta) \sin\left(x \frac{\delta m_{32}^2}{4k}\right) \right] \end{aligned} \quad (12.42)$$

and similarly for other probabilities. The difference between normal and inverted hierarchy occurs only in the sign of the $\cos(\delta)$ coefficient, all other terms being insensitive to the sign of δm_{32}^2 . If the present experimental value of δ around $3\pi/2$ (with large error bars) is confirmed, it will be very difficult to solve the mass hierarchy problem from oscillation experiments in vacuum. More on this later.

Sometimes, it is sufficient to consider only a two neutrino system, ν_e and ν_x say, in which case the

³⁷One has also $\text{COS}_\tau = -2 \cos(2\theta_{23}) [\sin(x \delta m_{21}^2/4k) \sin(x \delta m_{32}^2/4k) \cos(x \delta m_{31}^2/4k) + \sin^2(\theta_{12}) \sin^2(x \delta m_{21}^2/4k)]$.

³⁸They are particularly useful in oscillation experiments with accelerator neutrinos. Note that one can use indifferently δm_{32}^2 or δm_{31}^2 in eqs. (12.38) and (12.40).

oscillation formulae simplify considerably:

$$\begin{aligned} P(\nu_e \rightarrow \nu_e) &= 1 - \sin^2(2\theta_{12}) \sin^2\left(x \frac{\delta m_{21}^2}{4k}\right) \\ P(\nu_e \rightarrow \nu_x) &= \sin^2(2\theta_{12}) \sin^2\left(x \frac{\delta m_{21}^2}{4k}\right) \end{aligned} \tag{12.43}$$

13 Neutrinos interactions with matter

Atmospheric (anti)neutrinos observed after crossing the earth or neutrinos produced in the sun propagate through matter and interact with it before reaching the detector. The scattering on protons, neutrons and electrons in matter will modify the oscillation patterns. This is the Mikheyev-Smirnov-Wolfenstein (MSW) effect³⁹. The important parameters in this effect are the electron density in matter and the neutrino energy. For some values of the parameters large resonance effects enhance the neutrino conversion rate compared to what is expected in vacuum.

To illustrate this point it is sufficient to consider a two-flavour model with mass eigenvectors $|\nu_1\rangle$ and $|\nu_2\rangle$ with the 1 state being the lightest one. From eq. (12.13) the evolution of the doublet of $|\nu_i(t)\rangle$ states, in vacuum, is given by ($t = x$):

$$i\frac{d}{dt} \begin{pmatrix} |\nu_1(t)\rangle \\ |\nu_2(t)\rangle \end{pmatrix} = \mathcal{H}_0 \begin{pmatrix} |\nu_1(t)\rangle \\ |\nu_2(t)\rangle \end{pmatrix} = \begin{pmatrix} m_1^2/2k & 0 \\ 0 & m_2^2/2k \end{pmatrix} \begin{pmatrix} |\nu_1(t)\rangle \\ |\nu_2(t)\rangle \end{pmatrix}, \quad (13.1)$$

with \mathcal{H}_0 the free hamiltonian. A global phase change on the $|\nu_i(t)\rangle$ states does not affect the physics but shifts the hamiltonian by a matrix proportional to the unit matrix. For instance, a phase change $im_1^2 t/2k$ on both states leads to the evolution equation:

$$i\frac{d}{dt} \begin{pmatrix} |\nu_1(t)\rangle \\ |\nu_2(t)\rangle \end{pmatrix} = \begin{pmatrix} 0 & 0 \\ 0 & \delta m^2/2k \end{pmatrix} \begin{pmatrix} |\nu_1(t)\rangle \\ |\nu_2(t)\rangle \end{pmatrix}, \quad (13.2)$$

with $\delta m^2 = m_2^2 - m_1^2$ taken to be positive. The evolution of the flavour states $|\nu_e(t)\rangle$ and $|\nu_x(t)\rangle$ ($|\nu_x(t)\rangle$ can be a combination of $|\nu_\mu(t)\rangle$ and $|\nu_\tau(t)\rangle$)⁴⁰, is easily obtained from the relation:

$$\begin{pmatrix} |\nu_e(t)\rangle \\ |\nu_x(t)\rangle \end{pmatrix} = \mathcal{R}(\theta) \begin{pmatrix} |\nu_1(t)\rangle \\ |\nu_2(t)\rangle \end{pmatrix} \quad \text{with the matrix } \mathcal{R}(\theta) = \begin{pmatrix} \cos(\theta) & \sin(\theta) \\ -\sin(\theta) & \cos(\theta) \end{pmatrix}. \quad (13.3)$$

We then have:

$$i\frac{d}{dt} \begin{pmatrix} |\nu_e(t)\rangle \\ |\nu_x(t)\rangle \end{pmatrix} = \mathcal{R}(\theta) \begin{pmatrix} 0 & 0 \\ 0 & \delta m^2/4k \end{pmatrix} \mathcal{R}^T(\theta) \begin{pmatrix} |\nu_e(t)\rangle \\ |\nu_x(t)\rangle \end{pmatrix} \quad (13.4)$$

$$= \begin{pmatrix} (\delta m^2/2k) \sin^2(\theta) & (\delta m^2/4k) \sin(2\theta) \\ (\delta m^2/4k) \sin(2\theta) & (\delta m^2/2k) \cos^2(\theta) \end{pmatrix} \begin{pmatrix} |\nu_e(t)\rangle \\ |\nu_x(t)\rangle \end{pmatrix} = \mathcal{H}_0^{\text{fl}} \begin{pmatrix} |\nu_e(t)\rangle \\ |\nu_x(t)\rangle \end{pmatrix}, \quad (13.5)$$

with $\mathcal{H}_0^{\text{fl}}$ is the free hamiltonian in the flavour basis. The interaction of neutrinos with matter can preserve or destroy the coherence of the system. In the latter case, the state of the particles (momentum and spin) is modified and it can be shown that incoherent interactions are negligible.

³⁹L. Wolfenstein, Phys. Rev. **D17** (1978) 2369; S.P. Mikheyev, A.Yu. Smirnov, Prog. Part. Nucl. Phys. **23** (1989) 41.

⁴⁰We have in mind solar neutrinos but the discussion applies to any two flavour system.

13.1 Incoherent scattering

For example, for neutrinos up to a GeV, scattering on nucleons $\nu_x + n \rightarrow x + p$ is the dominant process and the cross section⁴¹ can be parameterised as:

$$\sigma \approx 10^{-43} \left(\frac{E_\nu}{\text{MeV}} \right)^2 \text{ cm}^2, \quad (13.6)$$

with E_ν the energy in the frame where the nucleon is at rest. The scattering length of the neutrino in matter is $l_{\text{matter}} = 1/N_N\sigma$ where N_N is the number of nucleons per cm^3 . In the core of the sun, the density is 150 gr/cm^3 , so approximately 10^{26} nucleons per cm^3 . The scattering length is then:

$$l_{\text{sun}} \approx 10^{17} \left(\frac{E_\nu}{\text{MeV}} \right)^{-2} \text{ cm} \approx 10^{12} \left(\frac{E_\nu}{\text{MeV}} \right)^{-2} \text{ km}. \quad (13.7)$$

The typical energy of solar neutrinos being $.1 \text{ MeV} < E_\nu < 10 \text{ MeV}$, the corresponding scattering length is $10^{14} \text{ km} > l_{\text{sun}} > 10^{10} \text{ km}$, to be compared to the sun radius of $7 \cdot 10^5 \text{ km}$. Incoherent neutrino scattering in the sun is negligible.

The range of energy of neutrinos crossing the earth is much larger, from $.1 \text{ MeV}$ for solar neutrinos to TeV's for atmospheric or cosmic ones. At high energy the charged current ν -nucleon cross section behaves as

$$\sigma \approx 6.7 \cdot 10^{-39} \left(\frac{E_\nu}{\text{GeV}} \right) \text{ cm}^2.$$

The matter density in the earth ranges from 4 gr/cm^3 in the mantle to, on the average, 11 gr/cm^3 in the core. This leads respectively to $N_N = 2.4 \cdot 10^{24}$ to $6.6 \cdot 10^{24}$ nucleons per cm^3 . Then, the scattering length of 100 GeV neutrinos l_{earth} varies from $6 \cdot 10^6 \text{ km}$ in the mantle to $2 \cdot 10^6 \text{ km}$ in the inner core. This is to be compared to the mantle thickness of $2.9 \cdot 10^3 \text{ km}$ and the core radius of $3.4 \cdot 10^3 \text{ km}$. Thus the effect of the earth matter is negligible for neutrinos of energy up to hundreds of GeV. On the contrary, for neutrinos around 100 TeV and above the earth becomes opaque since the cross section grows linearly with energy.

13.2 Coherent scattering

Coherence of the neutrino system is preserved by forward elastic scattering of the neutrino on matter. This can go via neutral current interactions, on protons, neutrons or electrons, $\nu_{e,x} + N \rightarrow \nu_{e,x} + N$ and $\nu_{e,x} + e^- \rightarrow \nu_{e,x} + e^-$, which are universal for all neutrinos species or via charged current exchange which is specific to ν_e scattering on electrons (see fig. 15 in sec. 14.4). These interactions add a piece

⁴¹J.A. Formaggio, G.P. Zeller, Rev. Mod. Phys. **84** (2012) 1307.

to the hamiltonian which becomes

$$\mathcal{H} = \mathcal{H}_0^{\text{fl}} + \mathcal{H}_{\text{int}}^{\text{fl}} \quad (13.8)$$

where $\mathcal{H}_{\text{int}}^{\text{fl}}$ is diagonal in flavour. Implementing a phase change on the states amounts to shifting the hamiltonian by a matrix proportional to unity and one can thus subtract the universal neutral current contribution leaving the charged current one which affects only the element $\langle \nu_e | \mathcal{H}_{\text{int}}^{\text{fl}} | \nu_e \rangle = \langle \nu_e | \mathcal{H}_{\text{cc}}^{\text{fl}} | \nu_e \rangle$. This interaction is given by eqs. (2.1), (2.2) in sec. 2.1,

$$\begin{aligned} \frac{G_F}{\sqrt{2}} \bar{\psi}_e(x) \gamma_\mu (1 - \gamma_5) \psi_{\nu_e}(x) \bar{\psi}_{\nu_e}(x) \gamma^\mu (1 - \gamma_5) \psi_e(x) &= 2\sqrt{2} G_F \bar{\psi}_{e_L}(x) \gamma_\mu \psi_{\nu_{e_L}}(x) \bar{\psi}_{\nu_{e_L}}(x) \gamma^\mu \psi_{e_L}(x) \\ &= 2\sqrt{2} G_F \bar{\psi}_{\nu_{e_L}}(x) \gamma^\mu \psi_{\nu_{e_L}}(x) \bar{\psi}_{e_L}(x) \gamma_\mu \psi_{e_L}(x), \end{aligned} \quad (13.9)$$

where a Fierz transformation has been made to obtain the second line. The effective interaction hamiltonian of the neutrinos in matter is obtained by summing over all electrons in matter⁴²:

$$\begin{aligned} \mathcal{H}_{\text{cc}}^{\text{fl}} &= 2\sqrt{2} G_F \int dp_e^3 f(p_e) \langle e_L(p_e) | \bar{\psi}_{\nu_{e_L}}(x) \gamma^\mu \psi_{\nu_{e_L}}(x) \bar{\psi}_{e_L}(x) \gamma_\mu \psi_{e_L}(x) | e_L(p_e) \rangle \\ &= 2\sqrt{2} G_F \bar{\psi}_{\nu_{e_L}}(x) \gamma^\mu \psi_{\nu_{e_L}}(x) \int dp_e^3 f(p_e) \langle e_L(p_e) | \bar{\psi}_{e_L}(x) \gamma_\mu \psi_{e_L}(x) | e_L(p_e) \rangle, \end{aligned} \quad (13.10)$$

where the electron energy distribution $f(p_e)$ in matter is homogeneous, isotropic and is normalised to $\int dp_e^3 f(p_e) = 1$. Assuming the electron approximately at rest in the medium, the space components γ_i can be neglected and the combinations $\bar{\psi} \gamma_\mu \psi$ reduce to $\bar{\psi} \gamma_0 \psi = \psi^\dagger \psi$, so that

$$\begin{aligned} \mathcal{H}_{\text{cc}}^{\text{fl}} &= 2\sqrt{2} G_F \psi_{\nu_{e_L}}^\dagger(x) \psi_{\nu_{e_L}}(x) \int dp_e^3 f(p_e) \langle e_L(p_e) | \psi_{e_L}^\dagger(x) \psi_{e_L}(x) | e_L(p_e) \rangle, \\ &= \sqrt{2} G_F \psi_{\nu_{e_L}}^\dagger \psi_{\nu_{e_L}} N_e, \end{aligned} \quad (13.11)$$

with N_e the density of electrons in the medium ($N_{e_L} = N_e/2$). The evolution equation will then be of the form

$$i \frac{d}{dt} \begin{pmatrix} |\nu_e(t)\rangle \\ |\nu_x(t)\rangle \end{pmatrix} = \begin{pmatrix} (\delta m^2/2k) \sin^2(\theta) + \sqrt{2} G_F N_e & (\delta m^2/4k) \sin(2\theta) \\ (\delta m^2/4k) \sin(2\theta) & (\delta m^2/2k) \cos^2(\theta) \end{pmatrix} \begin{pmatrix} |\nu_e(t)\rangle \\ |\nu_x(t)\rangle \end{pmatrix} = \mathcal{H} \begin{pmatrix} |\nu_e(t)\rangle \\ |\nu_x(t)\rangle \end{pmatrix}. \quad (13.12)$$

Due to the charged current interaction the mass eigenstates $|\nu_i(t)\rangle$ of eq. (13.1) no longer diagonalize the hamiltonian. Let us denote ω_1 and ω_2 the eigenvalues of the above matrix and $|\nu_{m_1}(t)\rangle$ and $|\nu_{m_2}(t)\rangle$ the corresponding mass eigenstates related to the flavour states $|\nu_e(t)\rangle$ and $|\nu_x(t)\rangle$ at time t by

$$\begin{aligned} |\nu_e(t)\rangle &= \cos \theta^m |\nu_{m_1}(t)\rangle + \sin \theta^m |\nu_{m_2}(t)\rangle \\ |\nu_x(t)\rangle &= -\sin \theta^m |\nu_{m_1}(t)\rangle + \cos \theta^m |\nu_{m_2}(t)\rangle. \end{aligned} \quad (13.13)$$

⁴²M.C. Gonzalez-Garcia, M. Maltoni, Phys. Rep. **460** (2008) 1.

13.3 Matter of constant density

If N_e is independent of t , so are θ^m and the eigenvalues given by:

$$\begin{aligned}\omega_{1,2} &= \frac{G_F N_e}{\sqrt{2}} + \frac{\delta m^2}{4k} \mp \frac{1}{2} \sqrt{(\sqrt{2}G_F N_e - \cos(2\theta)\delta m^2/2k)^2 + (\sin(2\theta)\delta m^2/2k)^2} \\ &= \frac{\delta m^2}{4k} \left[\hat{A} + 1 \mp \sqrt{\sin^2(2\theta) + (\cos(2\theta) - \hat{A})^2} \right],\end{aligned}\quad (13.14)$$

with ω_i the eigenvalue of the state $|\nu_{m_i}(t)\rangle$. The important parameter \hat{A} is defined by:

$$\boxed{\hat{A} = \frac{2\sqrt{2}G_F k N_e}{\delta m^2}},\quad (13.15)$$

which is the ratio of the interaction energy in matter to the vacuum energy. The matrix \mathcal{H} in eq. (13.12) is diagonalised by $\mathcal{R}^T(\theta^m) \mathcal{H} \mathcal{R}(\theta^m) = \text{diag}(\omega_1, \omega_2)$ (see eq. (13.3)) and one finds:

$$\tan(\theta^m) = \frac{\hat{A} - \cos(2\theta) + \sqrt{\sin^2(2\theta) + (\cos(2\theta) - \hat{A})^2}}{\sin(2\theta)}\quad (13.16)$$

from which we derive (for δm^2 positive):

$$\boxed{\begin{aligned}\cos(2\theta^m) &= \frac{\cos(2\theta) - \hat{A}}{\sqrt{\sin^2(2\theta) + (\cos(2\theta) - \hat{A})^2}} \\ \sin(2\theta^m) &= \frac{\sin(2\theta)}{\sqrt{\sin^2(2\theta) + (\cos(2\theta) - \hat{A})^2}},\end{aligned}}\quad (13.17)$$

To obtain the oscillation probabilities we use eqs. (12.43):

$$\boxed{P(\nu_e \rightarrow \nu_e) = 1 - \sin^2(2\theta^m) \sin^2\left(\frac{\delta M^2 t}{4k}\right), \quad P(\nu_e \rightarrow \nu_x) = \sin^2(2\theta^m) \sin^2\left(\frac{\delta M^2 t}{4k}\right)},\quad (13.18)$$

where⁴³

$$\boxed{\delta M^2 = \delta m^2 \sqrt{\sin^2(2\theta) + (\cos(2\theta) - \hat{A})^2}}.\quad (13.19)$$

The corresponding oscillation length in matter is given by (see eq. (12.21):

$$l_{\text{mat}} = \frac{4\pi k}{\delta M^2} = \frac{2\pi}{\omega_2 - \omega_1}\quad (13.20)$$

Several cases can be distinguished assuming N_e constant in the medium (with δm^2 positive).

⁴³The physics depends only on the difference $\omega_2 - \omega_1$ and θ^m , which are functions of the difference of the diagonal elements of \mathcal{H} , in agreement with the fact that one can modify \mathcal{H} by adding to it a matrix proportional to unity.

- If $\hat{A} \ll 1$, then $\sin(2\theta^m) \approx \sin(2\theta)(1 + \hat{A} \cos(2\theta))$, $\delta M^2 \approx \delta m^2(1 - \hat{A} \cos(2\theta))$: the interaction with matter is small and the neutrino system evolves almost as in empty space, $l_{\text{mat}} \approx l_{\text{vac}}$ with a small correction;
- If $\hat{A} \gg |\cos(2\theta)|$, interaction with matter is dominant: then $\sin(2\theta^m) \approx \sin(2\theta)/\hat{A} \approx 0$ and $\cos(2\theta^m) \approx -1$, hence $\theta^m \approx \pi/2$: from eq. (13.13) the electron neutrino tends to a pure mass eigenstate $|\nu_{m_2}\rangle$, the heaviest state ($\omega_2 \approx \sqrt{2}G_F N_e$); it propagates without oscillations independent of the value of the mixing angle in vacuum;
- If $\hat{A} \approx \cos(2\theta)$, this is the resonant regime: it occurs only if $\cos(2\theta)$ is positive ($0 < \theta < \pi/4$), then $\cos(2\theta^m) \approx 0$, $\sin(2\theta^m) \approx 1$, $\theta^m \approx \pi/4$, $l_{\text{mat}} \approx l_{\text{vac}}/\sin(2\theta)$; the electron neutrino is an equal combination of $|\nu_{m_1}\rangle$ and $|\nu_{m_2}\rangle$, independent of the initial mixing angle, the amplitude of oscillations is maximal, since $\sin(2\theta^m) \approx 1$, as well as the oscillation length. For $\pi/4 < \theta < \pi/2$ there is no resonance effect possible and θ^m is always larger than $\pi/4$.

Remarks

- When applying eq. (13.11) to antineutrinos states one will obtain an extra $-\text{sign}^{44}$, thus giving a contribution $-\sqrt{2}G_F N_e$ to \mathcal{H} . Then, the sign of \hat{A} for antineutrinos is opposite to that for neutrinos. If the resonance condition $\hat{A} \approx \cos(2\theta)$ can be reached for neutrinos, it cannot occur for antineutrinos and vice-versa. For antineutrinos the resonance condition requires $\pi/4 < \theta < \pi/2$.
- The evolution of neutrinos in matter violates the \mathcal{CP} symmetry, which is obvious since matter is not \mathcal{CP} symmetric.

Application to solar neutrinos

Electron neutrinos are produced in the core of the sun where N_e can be as large as $6 \cdot 10^{25} \text{ cm}^{-3}$. It is useful to define the quantity N_{Res} by

$$N_{\text{Res}} = \frac{\delta m^2 \cos(2\theta)}{2\sqrt{2}G_F k}, \quad (13.21)$$

related to the parameter \hat{A} previously introduced by

$$\frac{N_e}{N_{\text{Res}}} = \frac{\hat{A}}{\cos(2\theta)} \quad (13.22)$$

⁴⁴ $\bar{\nu}e \rightarrow \bar{\nu}e$ scattering is obtained from $\nu e \rightarrow \nu e$ by crossing symmetry which implies a relative - sign when crossing fermions.

Taking for θ and δm^2 the values θ_{12} and δm_{21}^2 from eq. (12.22) below, one obtains

$$N_{\text{Res}}^{21} \approx .8 \cdot 10^{-6} \left(\frac{E_\nu}{\text{MeV}} \right)^{-1} \text{MeV}^3 \approx 10^{26} \left(\frac{E_\nu}{\text{MeV}} \right)^{-1} \text{cm}^{-3}, \quad (13.23)$$

so $N_{\text{Res}}^{21} \lesssim 10^{25} \text{cm}^{-3}$ for $E_\nu \gtrsim 10 \text{MeV}$. In that case, the condition $N_e \gg N_{\text{Res}}^{21}$ (equivalently $\hat{A} \gg \cos(2\theta_{12})$) is realised and the neutrino is produced in a mass eigenstate. On the contrary, neutrinos of energy $E_\nu \approx .1 \text{MeV}$ evolve as in vacuum since they satisfy $N_e \ll N_{\text{Res}}^{21}$. The range of values of θ_{12} given in eqs. (12.22), $30^\circ < \theta_{12} < .38^\circ$ implies $\cos(2\theta_{12}) > 0$ so that the resonance regime $\hat{A} \approx \cos(2\theta_{12})$ can be satisfied for neutrinos of intermediate energies. In the sun, however, N_e is a decreasing function of x , the distance from the center, and taking this effect into account requires a special treatment to which we turn in the next section. We can also consider oscillations to the third generation and estimate N_{Res}^{31} . Using the values of θ_{13} and δm_{31}^2 from eq. (12.22) one finds $N_e/N_{\text{Res}}^{31} \approx 6.10^{-3}(E_\nu/\text{MeV})$, so that $6.10^{-4} < N_e/N_{\text{Res}}^{31} < 6.10^{-2}$ in the E_ν range $[.1, 10.] \text{MeV}$, making matter effects negligible in this case. When studying oscillations in the sun, working in the 2 family oscillation model will be a good enough approximation.

Neutrinos through the earth

The electron density in the earth is much less than in the sun and it remains approximately constant in the core⁴⁵ ($N_e \approx 3.3 \cdot 10^{24} \text{cm}^{-3}$) and in the mantle ($N_e \approx 1.2 \cdot 10^{24} \text{cm}^{-3}$). It is then expected that solar neutrinos with $E_\nu < 10 \text{MeV}$ will be little affected by coherent interactions when traversing the earth. However this will not be the case for higher energy neutrinos in the GeV and multi-GeV range. Furthermore, in the 3- ν model, 13 oscillations will become important since $N_e/N_{\text{Res}}^{31} = 2\sqrt{2}G_F k / (\delta m_{31}^2 \cos(2\theta_{13}))$ can be of order 1 in the GeV range. This will be discussed later.

13.4 Matter of varying density: ν_e in the sun

When the density of electrons decreases from the core to the surface, as it is the case in the sun, the angle $\theta^m(t)$ becomes a function of $x = t$. The variation of $\theta^m(x)$ should bring a $d\theta^m(x)/dx = \theta'_m(x)$ dependence in the evolution equations of the neutrino system. From eq. (13.13) written as

$$\begin{pmatrix} |\nu_e(x)\rangle \\ |\nu_x(x)\rangle \end{pmatrix} = \mathcal{R}(\theta^m(x)) \begin{pmatrix} |\nu_{m_1}(x)\rangle \\ |\nu_{m_2}(x)\rangle \end{pmatrix}, \quad (13.24)$$

⁴⁵One assumes an equal number of neutrons and protons hence $N_p = N_e = N_N/2$, with N_N given above.

we derive

$$\begin{aligned}
i \frac{d}{dx} \begin{pmatrix} |\nu_e(x)\rangle \\ |\nu_x(x)\rangle \end{pmatrix} &= i \left(\frac{d}{dt} \mathcal{R}(\theta^m(x)) \right) \begin{pmatrix} |\nu_{m_1}(x)\rangle \\ |\nu_{m_2}(x)\rangle \end{pmatrix} + \mathcal{R}(\theta^m(x)) i \frac{d}{dt} \begin{pmatrix} |\nu_{m_1}(x)\rangle \\ |\nu_{m_2}(x)\rangle \end{pmatrix} \\
&= \mathcal{R}(\theta^m(x)) \left[\mathcal{R}^T(\theta^m(x)) i \left(\frac{d}{dt} (\mathcal{R}(\theta^m(x))) \right) + \begin{pmatrix} \omega_1(x) & 0 \\ 0 & \omega_2(x) \end{pmatrix} \right] \begin{pmatrix} |\nu_{m_1}(x)\rangle \\ |\nu_{m_2}(x)\rangle \end{pmatrix} \\
&= \mathcal{R}(\theta^m(x)) \begin{pmatrix} \omega_1(x) & i\theta'_m(x) \\ -i\theta'_m(x) & \omega_2(x) \end{pmatrix} \mathcal{R}^T(\theta^m(x)) \begin{pmatrix} |\nu_e(x)\rangle \\ |\nu_x(x)\rangle \end{pmatrix}, \tag{13.25}
\end{aligned}$$

similar to eq. (13.4) except for the off-diagonal term $i\theta'_m(x)$. If $|2\theta'_m(x)/(\omega_2(x) - \omega_1(x))| \ll 1$, then $\omega_1(x)$ and $\omega_2(x)$ will remain approximate eigenvalues of the system and the $|\nu_{m_i}(x)\rangle$ will be approximately the mass eigenstates. Intuitively, one expects this to happen if the rate of change of the electron density $(1/N_e)dN_e/dx$ is very slow compared to the oscillation length in matter. This rate of change is measured by $(1/N_e)dN_e/dx = 1/r_0$, where a large value of r_0 corresponds to a small variation of N_e and if

$$r_0/l_{\text{mat}} \gg 1, \tag{13.26}$$

with l_{mat} given by eq. (13.20), then the variation of N_e will have a small effect on the neutrino mass eigenstates. More precisely, this condition is :

$$\frac{\omega_2(x) - \omega_1(x)}{2|\theta'_m(x)|} \gg 1. \tag{13.27}$$

From eqs. (13.17) one derives

$$2\theta'_m(x) = \frac{d\hat{A}}{dx} \frac{\sin(2\theta)}{\sin^2(2\theta) + (\cos^2(2\theta) - \hat{A})^2}, \tag{13.28}$$

and from eq. (13.15) one has,

$$\frac{d\hat{A}}{dx} = \frac{\hat{A}}{r_0}. \tag{13.29}$$

Using then the relations

$$\frac{\sin^2(2\theta) + (\cos^2(2\theta) - \hat{A})^2}{\sin^2(2\theta)} = 1 + \tan^{-2}(2\theta^m), \tag{13.30}$$

the condition (13.27) can be written:

$$\boxed{\frac{1}{\hat{A}} \frac{r_0 \delta m^2}{2k} \sin^2(2\theta) (1 + \tan^{-2}(2\theta^m))^{3/2} = \frac{2\pi r_0}{l_{\text{mat}}} \frac{N_{\text{Res}}}{N_e} \tan(2\theta) (1 + \tan^{-2}(2\theta^m)) \gg 1.} \tag{13.31}$$

If this condition is satisfied the evolution of the neutrino system in matter is said to be adiabatic. The flavoured neutrinos related, at the initial time, to the mass eigenstates $|\nu_{m_i}(x_0)\rangle$ by the angle

$\theta^m = \theta^m(x_0)$ as in eq. (13.24), will be, at each point of the evolution, related to the mass eigenstates $|\nu_{m_i}(x)\rangle$ by the angle $\theta^m(x)$, until they exit from matter in vacuum, at a distance R where the mixing angle is θ and the mass eigenstates $|\nu_i\rangle$. The assumed adiabatic evolution does not mix the $|\nu_{m_1}(x)\rangle$ and $|\nu_{m_2}(x)\rangle$ states which evolve respectively to the $|\nu_1\rangle$ and $|\nu_2\rangle$ states of the vacuum when the neutrino exit from the medium. Thus, for

$$|\nu_e(x_0)\rangle = \cos(\theta^m(x_0))|\nu_{m_1}(x_0)\rangle + \sin(\theta^m(x_0))|\nu_{m_2}(x_0)\rangle, \quad (13.32)$$

at some initial time, one has at time x ,

$$|\nu_e(x)\rangle = \cos(\theta^m(x))|\nu_{m_1}(x)\rangle + \sin(\theta^m(x))|\nu_{m_2}(x)\rangle, \quad (13.33)$$

and when the neutrino reaches the surface of the sun,

$$|\nu_e(R)\rangle = \cos(\theta)|\nu_1\rangle + \sin(\theta)|\nu_2\rangle, \quad (13.34)$$

The probability to find a ν_e at the surface will be $|\langle \nu_e(R) | \nu_e(x_0) \rangle|^2$, *i.e.*:

$$\begin{aligned} P(\nu_e \rightarrow \nu_e; x_0, R) &= [\cos(\theta) \cos(\theta^m(x_0)) \langle \nu_1 | \nu_{m_1}(x_0) \rangle + \sin(\theta) \sin(\theta^m(x_0)) \langle \nu_2 | \nu_{m_2}(x_0) \rangle]^2 \\ &= \frac{1}{2}[1 + \cos(2\theta) \cos(2\theta^m(x_0))] + \text{oscillating term} \\ &\approx \sin^2(\theta) + \cos(2\theta) \cos^2(\theta^m(x_0)), \end{aligned} \quad (13.35)$$

where we have supposed that the oscillating term averages out to 0. As a special case, if at x_0 the neutrino is produced in a pure mass eigenstate $|\nu_{m_2}(x_0)\rangle$ ($\theta^m(x_0) = \pi/2$), then the neutrino will remain in this pure mass eigenstate $|\nu_{m_2}(x)\rangle$ during its propagation until it reaches the surface where $|\nu_{m_2}(R)\rangle = |\nu_2\rangle$ in vacuum. The probability to find a ν_e at the surface will then be

$$\boxed{P(\nu_e \rightarrow \nu_e; x_0, R) = \sin^2(\theta)}. \quad (13.36)$$

On the contrary, one may consider the extreme non-adiabaticity case of the evolution in matter: in that case a ν_e produced in the $|\nu_{m_2}(x_0)\rangle$ state ends up as the $|\nu_1(R)\rangle$ when exiting from the medium, and if this occurs

$$P(\nu_e \rightarrow \nu_e; x_0, R) = \cos^2(\theta). \quad (13.37)$$

in contrast with eq. (13.36). The general treatment of a non adiabatic evolution is given by Petcov⁴⁶. It is easy to check that, in the sun, the adiabaticity condition is satisfied.

⁴⁶ S.T. Petcov, Phys. Lett. **200** (1988) 373.

13.5 Neutrinos through the earth

As mentioned above, for energetic neutrinos traversing the earth N_e/N_{Res}^{21} is very large and N_e/N_{Res}^{31} may be of order 1 for $E_\nu \gtrsim 1$ GeV: indeed, in that case, $N_e \approx 1.2$ to $3.3 \cdot 10^{24} \text{ cm}^{-3}$ compared $N_{\text{Res}}^{21} \approx 10^{23} (E_\nu/\text{GeV})^{-1} \text{ cm}^{-3}$ and $N_{\text{Res}}^{31} \approx 10^{25} (E_\nu/\text{GeV})^{-1} \text{ cm}^{-3}$. It is then necessary to work with the full 3- ν model. The free hamiltonian when acting on the mass eigenstates is

$$\mathcal{H}_0 = \begin{pmatrix} m_1^2/2k & 0 & 0 \\ 0 & m_2^2/2k & 0 \\ 0 & 0 & m_3^2/2k \end{pmatrix}. \quad (13.38)$$

After a change of phase on the states it can be put in the form

$$\mathcal{H}_0 = \begin{pmatrix} 0 & 0 & 0 \\ 0 & \delta m_{21}^2/2k & 0 \\ 0 & 0 & \delta m_{31}^2/2k \end{pmatrix} \quad (13.39)$$

with $\delta m_{ij}^2 = m_i^2 - m_j^2$. Going to the flavour basis,

$$\begin{pmatrix} \nu_e \\ \nu_\mu \\ \nu_\tau \end{pmatrix} = \mathcal{U} \begin{pmatrix} \nu_1 \\ \nu_2 \\ \nu_3 \end{pmatrix}, \quad (13.40)$$

the hamiltonian is written $\mathcal{H}_0^{\text{fl}} = \mathcal{U} \mathcal{H}_0 \mathcal{U}^\dagger$ where \mathcal{U} is parameterised²⁰ as in eq. (11.12), $\mathcal{U} = U_{23} U_{13}(\delta) U_{12}$. Since the interaction in matter affects only the electron the interacting hamiltonian is written

$$\begin{aligned} \mathcal{H}^{\text{fl}} &= \mathcal{U} \begin{pmatrix} 0 & 0 & 0 \\ 0 & \delta m_{21}^2/2k & 0 \\ 0 & 0 & \delta m_{31}^2/2k \end{pmatrix} \mathcal{U}^\dagger + \begin{pmatrix} \sqrt{2} G_F N_e & 0 & 0 \\ 0 & 0 & 0 \\ 0 & 0 & 0 \end{pmatrix} \\ &= U_{23} U(\delta) \left[U_{13} U_{12} \begin{pmatrix} 0 & 0 & 0 \\ 0 & \delta m_{21}^2/2k & 0 \\ 0 & 0 & \delta m_{31}^2/2k \end{pmatrix} U_{12}^\dagger U_{13}^\dagger + \begin{pmatrix} \sqrt{2} G_F N_e & 0 & 0 \\ 0 & 0 & 0 \\ 0 & 0 & 0 \end{pmatrix} \right] U^\dagger(\delta) U_{23}^\dagger. \end{aligned} \quad (13.41)$$

Several comments are in order. The matrix U_{23} does not affect the interaction matrix which can then be multiplied by U_{23} on the left and U_{23}^\dagger on the right. Furthermore, writing $U_{13}(\delta) = U(\delta) U_{13} U^\dagger(\delta)$ with

$$U(\delta) = \begin{pmatrix} 1 & 0 & 0 \\ 0 & 1 & 0 \\ 0 & 0 & e^{i\delta} \end{pmatrix}, \quad (13.42)$$

the δ dependence can be factored out as indicated above. We know that $\delta m_{21}^2 \ll \delta m_{31}^2$ and we have seen that, in the earth, for neutrinos in the GeV range and above, the ratio $\delta m_{21}^2/2\sqrt{2}G_F N_e k$ is very

small which justifies the approximation $\delta m_{21}^2 = 0$ which is now done. This will considerably simplify the discussion⁴⁷. The hamiltonian in the flavour basis can then be written:

$$\mathcal{H}^{\text{fl}} = U_{23} U(\delta) \left[U_{13} \begin{pmatrix} 0 & 0 & 0 \\ 0 & 0 & 0 \\ 0 & 0 & \delta m_{31}^2/2k \end{pmatrix} U_{13}^\dagger + \begin{pmatrix} \sqrt{2}G_F N_e & 0 & 0 \\ 0 & 0 & 0 \\ 0 & 0 & 0 \end{pmatrix} \right] U^\dagger(\delta) U_{23}^\dagger. \quad (13.43)$$

The matrix U_{12} plays no role because of our choice $\delta m_{21}^2 = 0$, so we take $\theta_{12} = 0$, $U_{12} = 1$. Then this equation becomes:

$$\mathcal{H}^{\text{fl}} = U_{23} U(\delta) \begin{pmatrix} (\delta m_{31}^2/2k) \sin^2(\theta_{13}) + \sqrt{2}G_F N_e & 0 & (\delta m_{31}^2/4k) \sin^2(2\theta_{13}) \\ 0 & 0 & 0 \\ (\delta m_{31}^2/4k) \sin^2(2\theta_{13}) & 0 & (\delta m_{31}^2/2k) \cos^2(\theta_{13}) \end{pmatrix} U^\dagger(\delta) U_{23}^\dagger. \quad (13.44)$$

The diagonalisation of the interacting hamiltonian follows the procedure of sec. 13.3. Here one eigenvalue ω_2 is 0 while the other two, $\omega_{1,3}$, are given by

$$\omega_{1,3} = \frac{\delta m_{31}^2}{4k} \left[\hat{A} + 1 \mp \sqrt{\sin^2(2\theta_{13}) + (\cos(2\theta_{13}) - \hat{A})^2} \right], \quad (13.45)$$

identical to the eigenvalues given in eq. (13.14) with the substitution $\theta \rightarrow \theta_{13}$ and $\delta m^2 \rightarrow \delta m_{31}^2$. As in the work of M. Freund⁴⁷ \hat{A} is now

$$\boxed{\hat{A} = 2\sqrt{2}G_F N_e k / \delta m_{31}^2}. \quad (13.46)$$

The 3×3 matrix in eq. (13.44) is diagonalised via the matrix U_{13}^m and \mathcal{H}^{fl} is then written:

$$\mathcal{H}^{\text{fl}} = U_{23} U(\delta) U_{13}^m \begin{pmatrix} \omega_1 & 0 & 0 \\ 0 & 0 & 0 \\ 0 & 0 & \omega_3 \end{pmatrix} U_{13}^{m\dagger} U^\dagger(\delta) U_{23}^\dagger, \quad (13.47)$$

with the matrix U_{13}^m of the same form as U_{13} but function of the angle θ_{13}^m . This angle is given by eqs. (13.16) or (13.17) with the appropriate change of notation. Finally the matrix \mathcal{U}^m which relates the flavour eigenstates and the mass eigenstates (with eigenvalues $\omega_1, 0, \omega_3$) of the interacting theory is of the usual form

$$\mathcal{U}^m = U_{23}^m U_{13}^m(\delta) U_{12}^m = U_{23} U_{13}^m(\delta) U_{12}, \quad (13.48)$$

⁴⁷The full treatment, which is applied here in a simplified form, is given in M. Freund, Phys. Rev. **D64** (2001) 053003, [arXiv:hep-ph/0103300].

with

$$\begin{aligned}
\sin(\theta_{12}^m) &= 0, & \sin(\theta_{23}^m) &= \sin(\theta_{23}), & \delta^m &= \delta \\
\cos(2\theta_{13}^m) &= \frac{\cos(2\theta_{13}) - \hat{A}}{\sqrt{\sin^2(2\theta_{13}) + (\cos(2\theta_{13}) - \hat{A})^2}} = \frac{\cos(2\theta_{13}) - \hat{A}}{\hat{C}} \\
\sin(2\theta_{13}^m) &= \frac{\sin(2\theta_{13})}{\sqrt{\sin^2(2\theta_{13}) + (\cos(2\theta_{13}) - \hat{A})^2}} = \frac{\sin(2\theta_{13})}{\hat{C}}.
\end{aligned} \tag{13.49}$$

with

$$\hat{C} = \sqrt{\sin^2(2\theta_{13}) + (\cos(2\theta_{13}) - \hat{A})^2}. \tag{13.50}$$

To reconstruct the various ν_e transition probabilities, one needs to define the oscillating factors given by $x(\omega_i - \omega_j)/2$. They are, in the small θ_{13} approximation (see eqs. (12.22)), and using $\hat{A} < 1$:

$$\begin{aligned}
x \frac{(\omega_2 - \omega_1)}{2} &= -x \frac{\omega_1}{2} \approx -\hat{A} \frac{\delta m_{31}^2}{4k} x \\
x \frac{(\omega_3 - \omega_2)}{2} &= x \frac{\omega_3}{2} \approx \frac{\delta m_{31}^2}{4k} x \\
x \frac{(\omega_3 - \omega_1)}{2} &= x \hat{C} \frac{\delta m_{31}^2}{4k} \approx |1 - \hat{A}| \frac{\delta m_{31}^2}{4k} x.
\end{aligned} \tag{13.51}$$

The oscillation probabilities, eqs. (12.25), (12.29) and (12.32) considerably simplify because of the vanishing of θ_{12} : the only oscillating factor to be kept is $\sin^2(x(\omega_3 - \omega_1)/2) = \sin^2(x \hat{C} \delta m_{31}^2/4k)$ all others are multiplied by $\sin(\theta_{12})$ and disappear. One finds:

$$P(\nu_e \rightarrow \nu_\mu) \approx \sin^2(\theta_{23}) \frac{\sin^2(2\theta_{13})}{\hat{C}^2} \sin^2\left(x \hat{C} \frac{\delta m_{31}^2}{4k}\right), \tag{13.52}$$

Changing $\sin(\theta_{23})$ to $\cos(\theta_{23})$, one obtains $P(\nu_e \rightarrow \nu_\tau)$. In the small θ_{13} approximation $\hat{C} \approx |1 - \hat{A}|$ and

$$\boxed{P(\nu_e \rightarrow \nu_\mu) \approx \sin^2(\theta_{23}) \frac{\sin^2(2\theta_{13})}{(1 - \hat{A})^2} \sin^2\left(x(1 - \hat{A}) \frac{\delta m_{31}^2}{4k}\right)}, \tag{13.53}$$

As a result of neutrino interaction with matter, both the amplitude and the frequency of oscillations are modified.

Going beyond the $\delta m_{21}^2 = 0$ approximation leads to much more complicated expressions for the different parameters which are given in the work of Martin Freund⁴⁷. All parameters in eqs. (13.49) receive a correction proportional to $\alpha = \delta m_{21}^2/\delta m_{31}^2$. However, in a realistic and often used limit, drastic simplifications are possible. This is the case if one keeps only leading terms in α and $\sin(\theta_{13})$. In

practice if one keeps, in the probability functions, only terms up to $\mathcal{O}(\alpha^2)$, $\mathcal{O}(\sin^2(\theta_{13}))$, $\mathcal{O}(\alpha \sin(\theta_{13}))$, the only correction to the parameters in eqs. (13.49) to take into account is a modification of θ_{12} to θ_{12}^m . To derive it, we turn back to eq. (13.41) and consider, assuming now $\theta_{13} \approx 0, U_{13} \approx 1$, the diagonalisation by the matrix U_{12}^m of

$$U_{12}^m \left[U_{12} \begin{pmatrix} 0 & 0 & 0 \\ 0 & \delta m_{21}^2/2k & 0 \\ 0 & 0 & \delta m_{31}^2/2k \end{pmatrix} U_{12}^\dagger + \begin{pmatrix} \sqrt{2}G_F N_e & 0 & 0 \\ 0 & 0 & 0 \\ 0 & 0 & 0 \end{pmatrix} \right] U_{12}^{m\dagger}. \quad (13.54)$$

This is done in sec. 13.3, the only difference being here that we define ω_1 as the largest eigenvalue and ω_2 the smallest. This amounts to exchanging ω_1 and ω_2 , hence reversing the sign of the square root factor in eq (13.16). This leads to a negative θ_{12}^m , and in the large $\hat{A}_{21} = \hat{A}/\alpha \gg 1$ limit, to

$$\sin(2\theta_{12}^m) \approx -\frac{\sin(2\theta_{12})}{\hat{A}_{21}} = -\alpha \frac{\sin(2\theta_{12})}{\hat{A}}. \quad (13.55)$$

from eq. (13.17). Using this result together with eqs. (13.49) and (13.51) one reconstructs the various probability functions. All oscillatory factors now enter the formulae and, from eq. (12.29), one finds for the oscillation $\nu_e \rightarrow \nu_\mu$:

$$\begin{aligned} P(\nu_e \rightarrow \nu_\mu) \approx & \sin^2(\theta_{23}) \frac{\sin^2(2\theta_{13})}{(1-\hat{A})^2} \sin^2 \left(x(1-\hat{A}) \frac{\delta m_{31}^2}{4k} \right) + \alpha^2 \cos^2(\theta_{23}) \frac{\sin^2(2\theta_{12})}{\hat{A}^2} \sin^2 \left(x\hat{A} \frac{\delta m_{31}^2}{4k} \right) \\ & + \alpha \frac{8J \cos(\delta)}{\hat{A}(1-\hat{A})} \cos \left(x \frac{\delta m_{31}^2}{4k} \right) \sin \left(x\hat{A} \frac{\delta m_{31}^2}{4k} \right) \sin \left(x(1-\hat{A}) \frac{\delta m_{31}^2}{4k} \right) \\ & + \alpha \frac{8J \sin(\delta)}{\hat{A}(1-\hat{A})} \sin \left(x \frac{\delta m_{31}^2}{4k} \right) \sin \left(x\hat{A} \frac{\delta m_{31}^2}{4k} \right) \sin \left(x(1-\hat{A}) \frac{\delta m_{31}^2}{4k} \right). \end{aligned} \quad (13.56)$$

To obtain the terms in $\sin(\delta)$ and $\cos(\delta)$ we use respectively eqs. (12.37) and (12.39) with J as defined in eq. (12.27). We recall this expression is valid in the small $\delta m_{21}^2/\delta m_{31}^2$ and $\sin(\theta_{13})$ approximation. The effect of matter is contained in $\hat{A} = 2\sqrt{2}G_F N_e k/\delta m_{31}^2$ which changes the relative weights of the terms compared to vacuum and the magnitude of the change is energy dependent since $\hat{A} \propto k$. Taking $\alpha = 0$ one recovers a previously derived result but it is not allowed in this expression to make $\hat{A} = 0$, the vacuum limit, since the derivation was done assuming $\hat{A} = N_e \cos(2\theta_{13})/N_{\text{Res}}^{31} > \alpha$. With the present value of δm_{21}^2 this condition is, for neutrinos traversing the earth, $E_\nu > .3$ GeV. The results above thus do not apply to solar neutrinos but it does apply to atmospheric and accelerator neutrinos.

The time reversed probability $P(\nu_\mu \rightarrow \nu_e)$ is obtained from the above equation by reversing the sign of δ while for $P(\bar{\nu}_e \rightarrow \bar{\nu}_\mu)$ one reverses both the sign of \hat{A} and δ . From eq. (12.33) and the above results one can obtain the oscillation probability $P(\nu_\mu \rightarrow \nu_\tau)$ in matter which are stronger than $\nu_\mu \rightarrow \nu_e$, the

dominant term being proportional to $\sin^2(2\theta_{23})$ rather than $\sin^2(2\theta_{13})$.

• **Discussion and order of magnitude of the parameters**

We summarize here for later use the value of the parameters and the order of magnitude of the

$ \alpha $	\hat{A}	$x\delta m_{21}^2/4k$	$x\delta m_{31}^2/4k$	$x\hat{A}\delta m_{31}^2/4k$
$3 \cdot 10^{-2}$	$.125 (k/\text{GeV})$	$10^{-4} (x/\text{km})(k/\text{GeV})^{-1}$	$3.2 \cdot 10^{-3} (x/\text{km})(k/\text{GeV})^{-1}$	$4 \cdot 10^{-4} (x/\text{km})$

Table 2: Value of the parameters controlling the neutrino oscillations in the earth mantle: $|\alpha| = \delta m_{21}^2/|\delta m_{31}^2|$, $\hat{A} = 2\sqrt{2}G_F k N_e/|\delta m_{31}^2|$ with $N_e = 1.25 \cdot 10^{24} \text{ cm}^{-3}$, δm_{21}^2 is positive and $\delta m_{32}^2 \approx \delta m_{31}^2$ is assumed. The value of the masses are taken from eq. (12.22).

oscillating factors. One of the experimentally unsolved question is the mass ordering, *i.e.* is δm_{31}^2 positive or negative ? Although the derivation above was done assuming this quantity positive it also holds with $\delta m_{31}^2 < 0$ keeping $\delta m_{21}^2 > 0$. In that case, \hat{A} is also negative but the combinations α/\hat{A} and $\hat{A}\delta m_{31}^2$ remain positive. Similarly to the oscillations in vacuum the difference between the two hypothesis is the sign of the $\cos \delta$ term but this term is very small if $\delta \approx 3\pi/2$ (see eq. (13.56)). In matter however, since the magnitude of the oscillation depends on \hat{A} one can use the energy as a parameter to probe the hierarchy hypothesis. For example, all terms with a normalisation factor in $1/(1 - \hat{A})$ will be sensitive to the sign of δm_{31}^2 provided of course that the associated oscillating factor $x(1 - \hat{A})\delta m_{31}^2/4k$ be large enough so as not to compensate the normalisation otherwise one can expand $\sin(x(1 - \hat{A})\delta m_{31}^2/4k) \approx (1 - \hat{A}) \sin(x\delta m_{31}^2/4k)$ and then get back the vacuum oscillation result.

14 Neutrino experiments

In the following we discuss how the values of the **PMNS** matrix elements are extracted from data. The first experiments were "disappearance" experiments where one measured the neutrino flux of a given flavour near the emission point and compared it to the flux of neutrinos of the same flavour measured at a distance. More recently several collaborations are able to carry out "appearance" experiments where one measures, near or far from the emission point, the flux of neutrino of a flavour different from the emitted one.

The source of (anti)neutrinos are varied:

- Nuclear reactors produce $\bar{\nu}_e$ of typical energy $\langle E_{\bar{\nu}_e} \rangle \approx 3$. MeV which are measured close to the reactors ~ 100 m or ~ 1 km (Double Chooz, Daya Bay, RENO) or far away 180 km (KAMLAND).
- At accelerators, π^\pm 's produced in hadronic collisions decay predominantly in ν_μ and $\bar{\nu}_\mu$ while K^\pm 's decay also ν_e and $\bar{\nu}_e$. The average energy $\langle E_\nu \rangle \approx 1$ GeV and the flux is measured at a distance of 295 km (T2K), 735 km (MINOS), 810 km (NO ν A). For OPERA the incident neutrino energy is much higher $\langle E_{\nu_\mu} \rangle \approx 17$ GeV and the detector is 730 km away from the source. All these are long baseline experiments.
- Atmospheric neutrinos are produced in cosmic ray showers from $\pi^+ \rightarrow \nu_\mu \mu^+$ followed by $\mu^+ \rightarrow e^+ \nu_e \bar{\nu}_\mu$ (and similarly with π^-) so that they are a mixture ($\nu_\mu + \bar{\nu}_\mu$) and ($\nu_e + \bar{\nu}_e$) in proportion 2 : 1 at low energy < 1 GeV. Before being detected the neutrinos travel 1 to 30 km (above the Earth, "downward flux") or $1.3 \cdot 10^4$ km (through the Earth, "upward flux") (SNO, Super-Kamiokande).
- For the solar neutrinos, the flux from ${}^8\text{B}$ (${}^8\text{B} \rightarrow {}^7\text{Be}^* + e^+ + \nu_e$) is particularly useful. It has a relatively large energy, $1.5 \text{ MeV} < E_\nu < 15 \text{ MeV}$, and the ${}^8\text{B}$ is the only source of ν_e 's in this energy range. The neutrinos travel $1.5 \cdot 10^8$ km before being detected in mines on Earth (SNO). Previous experiments (GALLEX, GNO, SAGE) measured the flux of lower energy ν_e 's: $.1 \text{ MeV} < E_\nu < .4 \text{ MeV}$.
- Ultra-high energy or cosmic or cosmogenic neutrinos have energies in the range of 100 TeV to several PeV: they are produced by collisions of ultra-high energy cosmic rays on protons or photons, for example on photons from the Cosmic Microwave Background (CMB), and by

sources such as Active Galactic Nuclei (AGN). Their flux is very small and they require huge detectors (telescopes) to be observed (IceCube, ANTARES, KM3net, Baikal-GVD).

14.1 Nuclear reactors : KamLAND, Double-Chooz, Daya Bay, RENO

Nuclear reactors produce dominantly electron antineutrinos and, assuming three flavours, we recall that their survival probability at a distance x is from eq. (12.25),

$$\begin{aligned}
P(\bar{\nu}_e \rightarrow \bar{\nu}_e) = & 1 - \sin^2(2\theta_{12}) \cos^4(\theta_{13}) \sin^2(\delta m_{21}^2 x/4k) \\
& - \sin^2(2\theta_{13}) \sin^2(\theta_{12}) \sin^2(\delta m_{32}^2 x/4k) \\
& - \sin^2(2\theta_{13}) \cos^2(\theta_{12}) \sin^2(\delta m_{31}^2 x/4k).
\end{aligned} \tag{14.1}$$

14.1.1 Long baseline: KamLAND, δm_{21}^2 , θ_{12}

KamLAND, a long baseline experiment ($\langle x \rangle = 180$ km) with the detector in Kamioka mine in Gifu, Japan, receives $\bar{\nu}_e$'s from 56 nuclear power reactors⁴⁸. The average neutrino energy is $\langle k \rangle = 3$ MeV so that the factors $x \delta m_{31}^2/4 \langle k \rangle \approx x \delta m_{32}^2/4 \langle k \rangle \approx 190$, and integrating over the energy of the neutrino, averages the value of the factors $\sin^2(x \delta m_{31}^2/4k) \approx \sin^2(x \delta m_{32}^2/4k) \approx 0.5$. The equation above reduces to

$$\begin{aligned}
P(\bar{\nu}_e \rightarrow \bar{\nu}_e) & \approx 1 - \cos^4(\theta_{13}) \sin^2(2\theta_{12}) \sin^2(\delta m_{21}^2 x/4k) - 0.5 \sin^2(2\theta_{13}) \\
& \approx \cos^4(\theta_{13}) P^{(2)}(\bar{\nu}_e \rightarrow \bar{\nu}_e) + \sin^4(\theta_{13})
\end{aligned} \tag{14.2}$$

where one has introduced the oscillation probability in a two flavour neutrino world, eq. (12.43),

$$P^{(2)}(\bar{\nu}_e \rightarrow \bar{\nu}_e) = 1 - \sin^2(2\theta_{12}) \sin^2(\delta m_{21}^2 x/4k). \tag{14.3}$$

Taking advantage of the smallness of $\sin^2(\theta_{13})$, it is reasonable to make the further approximation (appropriate for long baseline experiments), neglecting $\sin^4(\theta_{13})$ terms,

$$\boxed{P(\bar{\nu}_e \rightarrow \bar{\nu}_e) \approx (1 - 2 \sin^2(\theta_{13})) P^{(2)}(\bar{\nu}_e \rightarrow \bar{\nu}_e)} \tag{14.4}$$

The survival probability plotted, in fig. 8, as a function of $L_0/E_{\bar{\nu}_e} = x/k$ in our notation is clearly seen in the figure from the KamLAND collaboration. One observes that the 2-neutrino best fit is very similar to the 3-neutrino one, meaning a very small value for $\theta_{13} \sim 0$. Using the 3-neutrino analysis they obtain⁴⁹:

$$\delta(m_{21}^2) = (7.54 \pm_{-0.18}^{+0.19}) 10^{-5} \text{ eV}^2, \quad \sin^2(\theta_{12}) = 0.325 \pm_{-0.039}^{+0.045}. \tag{14.5}$$

⁴⁸KamLAND collaboration, A. Gando *et al.*, Phys.Rev **D83** (2011) 052002, arXiv:1009.4771, [hep-ex].

⁴⁹Atsuto Suzuki, Eur.Phys.J. **C74** (2014) 3094, arXiv:1409.4515 [hep-ex].

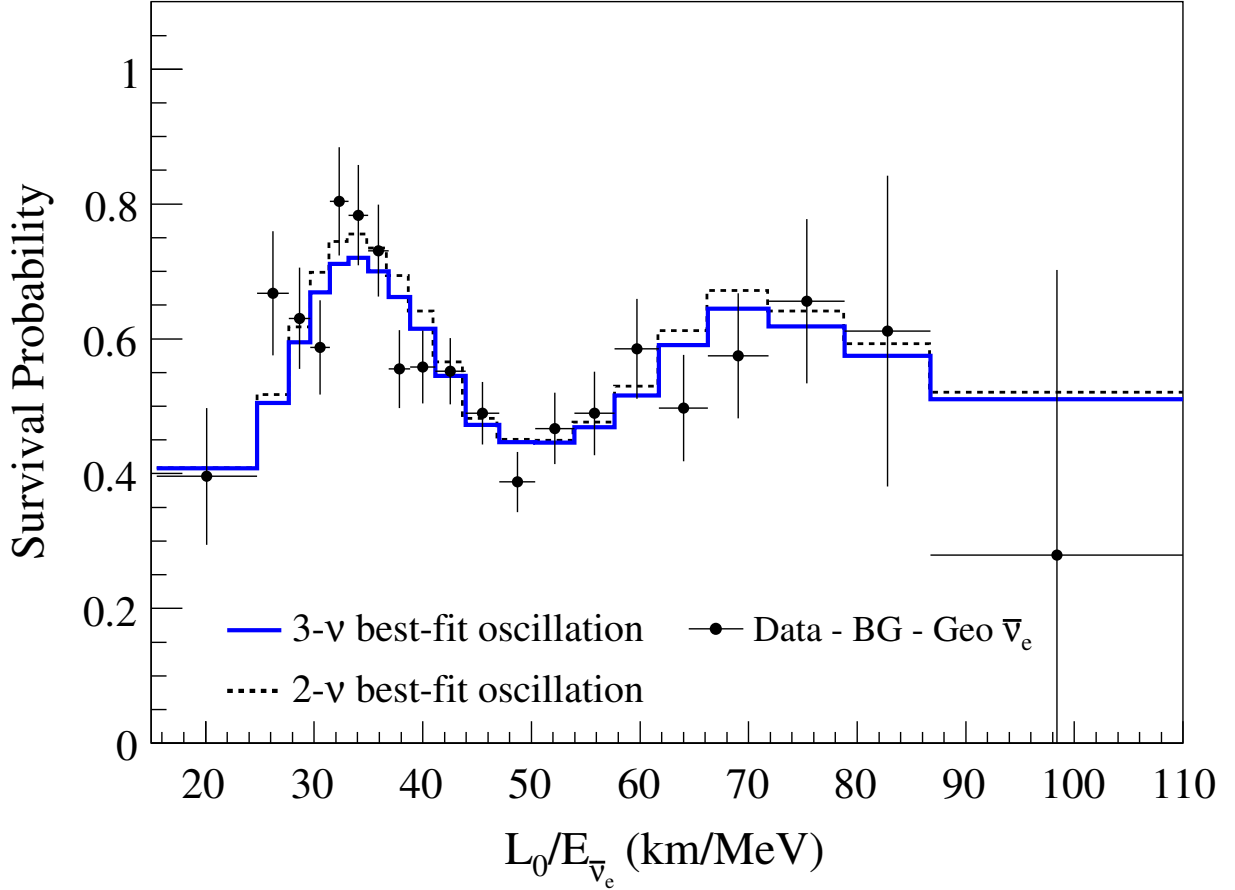


Figure 8: *KamLAND* oscillation pattern and fits in the 2ν and 3ν models.

14.1.2 Short baseline: Double-Chooz, Daya Bay, RENO, δm_{31}^2 , θ_{13}

Double-Chooz⁵⁰, Daya Bay⁵¹ and RENO⁵² are short baseline experiments. They have near detectors at a distance of typically 300 m to 600 m and far detectors at a distance of typically 1000 m to 1700 m. In these configurations the δm_{21}^2 term in eq. (14.1) becomes negligible and the oscillations are dominated by $\delta m_{31}^2 \approx \delta m_{32}^2$ terms so that the probability function reduces to (appropriate for short baseline experiments):

$$P(\bar{\nu}_e \rightarrow \bar{\nu}_e) \approx 1 - \sin^2(2\theta_{13}) \sin^2(\delta m_{32}^2 x / 4k). \quad (14.6)$$

⁵⁰Double-Chooz collaboration, C. Buck, PoS NEUTEL2015 (2015) 015.

⁵¹Daya Bay collaboration, D. Aday *et al.*, Phys. Rev. Lett. **121** (2018) 241805, arXiv:1809.02261 [hep-ex]; they use the complete expression eq. (14.1) in their fit to data.

⁵²RENO collaboration, G. Bak *et al.*, Phys. Rev. Lett. **121** (2018) 201801, arXiv:1806.00248 [hep-ex].

With the high statistics available these short baseline experiments are well suited to constrain the small θ_{13} mixing angle. For instance, the Daya Bay collaboration reports a precise determination of the angle θ_{13} , $\sin^2 2\theta_{13} = 0.0856 \pm 0.0029$. They also quote the value for the mass-squared difference for normal ordering $\delta m_{32}^2 = (2.471_{-0.070}^{+0.068}) 10^{-3} \text{ eV}^2$. Recently the result from Double Chooz⁵³ is $\sin^2 2\theta_{13} = 0.105 \pm 0.0014$.

14.2 Neutrinos from accelerators: T2K, NO ν A and OPERA ; δm_{32}^2 , θ_{23} , δ

T2K is a long baseline experiment with a muon neutrino beam with a peak energy of 0.6 GeV produced at the J-PARC (Japan Proton Accelerator Research Complex in Tokai) facility and observed in a near detector at 280 m and in the Super-Kamiokande detector at a distance $x = 295$ km from the production source. This is both a ν_μ disappearance and a ν_e appearance experiment. In 2011 the collaboration gave the first indication of ν_e appearance in a ν_μ beam⁵⁴. Based on the small number of ν_e observed, a non vanishing value of θ_{13} is obtained for the first time: $\sin \theta_{13} = .11$ with a large error however. Results analysing both ν and $\bar{\nu}$ oscillations based on a ν_μ beam generated by $7.48 10^{20}$ POT ("protons on target") and a $\bar{\nu}_\mu$ beam from $7.47 10^{20}$ POT have been published in 2017⁵⁵. Comparing $\nu_\mu \rightarrow \nu_e$ and $\bar{\nu}_\mu \rightarrow \bar{\nu}_e$ transitions is very useful to extract a precise measurement of the \mathcal{CP} violating parameter. In a simplified form ($\delta m_{31}^2 = \delta m_{32}^2$), the ν_μ survival probability is written (eq. (12.26)):

$$\begin{aligned}
P(\bar{\nu}_\mu \rightarrow \bar{\nu}_\mu) = & 1 - \sin^2(2\theta_{12}) \cos^4(\theta_{23}) \sin^2\left(x \frac{\delta m_{21}^2}{4k}\right) \\
& - [\sin^2(2\theta_{23}) \cos^2(\theta_{13}) + \sin^2(2\theta_{13}) \sin^4(\theta_{23})] \sin^2\left(x \frac{\delta m_{32}^2}{4k}\right) \\
& - 16 J \sin^2(\theta_{23}) \cos(\delta) \sin\left(x \frac{\delta m_{21}^2}{4k}\right) \sin\left(x \frac{\delta m_{32}^2}{4k}\right) \cos\left(x \frac{\delta m_{32}^2}{4k}\right),
\end{aligned} \tag{14.7}$$

and the oscillation probability is (see eq. (12.41)):

$$\begin{aligned}
P(\bar{\nu}_\mu \rightarrow \bar{\nu}_e) = & \sin^2(2\theta_{13}) \sin^2(\theta_{23}) \sin^2\left(x \frac{\delta m_{32}^2}{4k}\right) + \sin^2(2\theta_{12}) \cos^2(\theta_{23}) \sin^2\left(x \frac{\delta m_{21}^2}{4k}\right) \\
& + 8 J \sin\left(x \frac{\delta m_{21}^2}{4k}\right) \sin\left(x \frac{\delta m_{32}^2}{4k}\right) \left[\cos(\delta) \cos\left(x \frac{\delta m_{32}^2}{4k}\right) \pm \sin(\delta) \sin\left(x \frac{\delta m_{32}^2}{4k}\right) \right].
\end{aligned} \tag{14.8}$$

where the $-$ sign is for neutrino and the $+$ sign for antineutrinos.

⁵³H. de Kerret *et al.*, arXiv:1901.09445 [hep-ex].

⁵⁴T2K collaboration, K.Abe *et al.*, Phys. Rev. Lett. **107** (2011) 041801, arXiv:1106.2822 [hep-ex].

⁵⁵T2K collaboration, K.Abe *et al.*, Phys. Rev. **D 96** (2017) 092006, arXiv:1707.01048 [hep-ex].

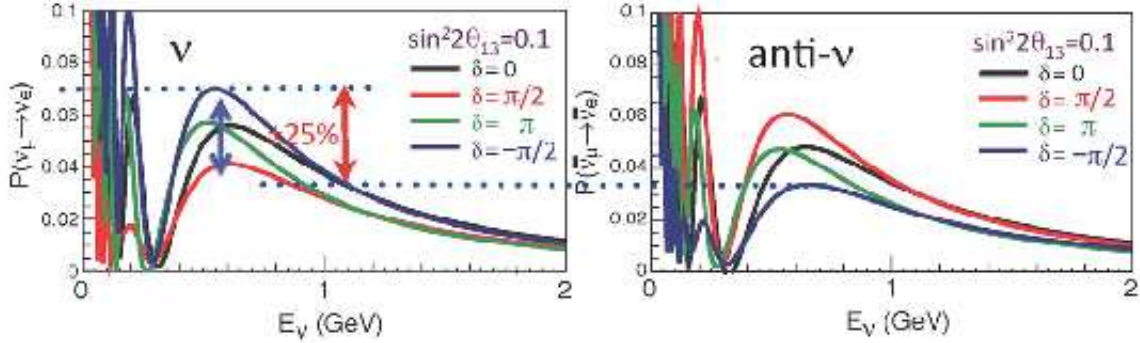


Figure 9: Comparison of the oscillation rate $\bar{\nu}_e$ in a $\bar{\nu}_\mu$ beam (right) with that of ν_e in a ν_μ beam (left) for different hypothesis on the CP violation parameter δ . Note that $\delta = -\pi/2$ in the figure corresponds to $\delta = 3\pi/2$ in the text. From Y. Oyama, for T2K Collaboration, PoS PLANCK2015 (2015) 094, arXiv:1510.07200 [hep-ex].

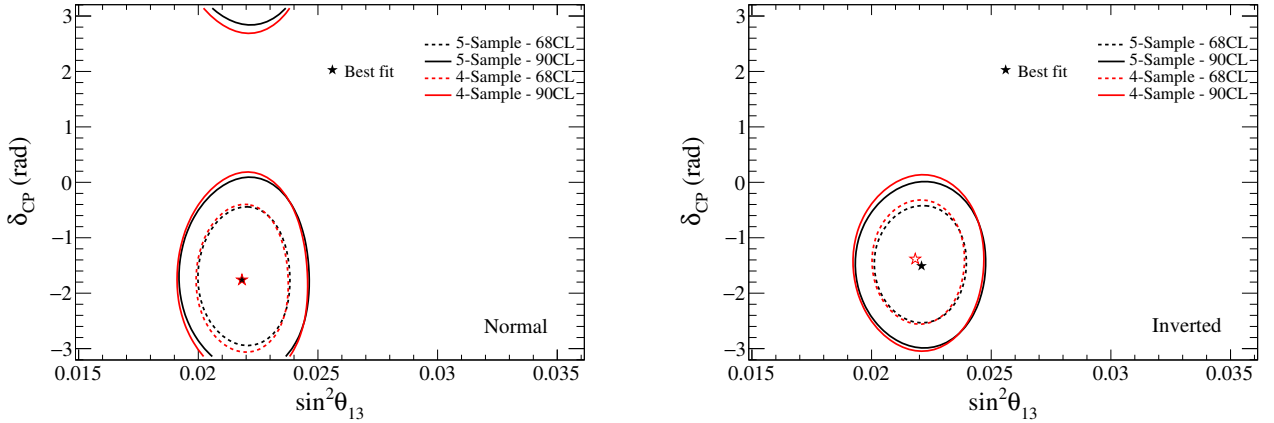


Figure 10: Joint fit of $\sin^2(\theta_{13})$ and δ to the data of appearance of ν_e in a ν_μ beam and $\bar{\nu}_e$ in a $\bar{\nu}_\mu$ beam, for both mass hierarchy hypotheses: $\Delta\chi^2$ contours using 5-sample data (black) or 4-sample data (red). Constraints from reactors data are included. δ in the text is $2\pi + \delta_{CP}$ in the figures. From T2K Collaboration, K. Abe et al., Phys. Rev. D **96** (2017) 092006, arXiv:1707.01048 [hep-ex].

For the T2K configuration, the $\sin(x\delta m_{21}^2/4k)$ term is very small (≈ 0.048) compared to $\sin(x\delta m_{32}^2/4k)$ which justifies the neglect of terms in $\sin^2(x\delta m_{21}^2/4k)$ in the coefficient of J (see eqs. (12.38) and (12.40)). Since $\sin^2(2\theta_{13}) \approx .084$ is small, we drop such terms in the coefficient of $\sin^2(x\delta m_{21}^2/4k)$ but keep them in the coefficient of $\sin^2(x\delta m_{32}^2/4k)$. The survival probabilities are dominated by the $\sin^2(2\theta_{23})\sin^2(x\delta m_{32}^2/4k)$ piece and lead to a good determination of θ_{23} and δm_{32}^2 . Based on data collected until 2016 the T2K collaboration quotes the values, at a 1σ confidence level:

$$\delta m_{32}^2 = (2.54 \pm 0.08) 10^{-3} \text{ eV}^2, \quad \sin^2(\theta_{23}) = 0.55^{+0.05}_{-0.09} \quad (14.9)$$

for normal mass ordering, and

$$\delta m_{32}^2 = (2.51 \pm 0.08) 10^{-3} \text{ eV}^2, \quad \sin^2(\theta_{23}) = 0.55 \pm_{-0.08}^{+0.05} \quad (14.10)$$

for inverted mass ordering. For this value of δm_{32}^2 and for a peak energy of .6 GeV and the base line of 295 km one finds $\cos(x \delta m_{32}^2/4k) \approx 0$ which means that the $\cos(\delta)$ term has almost no contribution to the survival or oscillation probabilities. Since it is the only term which changes sign when going from normal to inverted hierarchy, T2K is not sensitive to the sign of $\delta m_{32}^2 \approx \delta m_{31}^2$. The δ dependence of $P(\nu_\mu \rightarrow \nu_e)$ is therefore almost entirely given by the $\sin(\delta)$ piece which is

$$\begin{aligned} & -8 J \sin\left(x \frac{\delta m_{21}^2}{4k}\right) \sin^2\left(x \frac{\delta m_{32}^2}{4k}\right) \sin(\delta) \\ & \approx -\sin(2\theta_{12}) \sin(2\theta_{23}) \sin(2\theta_{13}) \cos(\theta_{13}) \sin\left(x \frac{\delta m_{21}^2}{4k}\right) \sin^2\left(x \frac{\delta m_{32}^2}{4k}\right) \sin(\delta) \\ & \approx -0.013 \sin(\delta) \end{aligned} \quad (14.11)$$

for the peak energy of 0.6 GeV. Furthermore the variation of $P(\bar{\nu}_\mu \rightarrow \bar{\nu}_e)$ as a function of δ is opposite to that of $P(\nu_\mu \rightarrow \nu_e)$. The amplitude of variation is about 0.026 when going from $\delta = \pi/2$ to $\delta = 3\pi/2$ as illustrated in fig. 9. From the oscillation data the collaboration quotes the following results, at a 1 σ confidence level, taking into account the reactor constraints on θ_{13} :

$$\begin{aligned} \delta &= 4.56 \pm_{-0.85}^{+0.81} (1.45 \pi \pm_{-0.27 \pi}^{+0.26 \pi}) \text{ for normal mass order,} \\ \delta &= 4.83 \pm_{-0.73}^{+0.68} (1.54 \pi \pm_{-0.23 \pi}^{+0.22 \pi}) \text{ for inverted mass order.} \end{aligned}$$

The correlation $\delta - \sin(\theta_{13})$ is illustrated in fig. 10. The best fit value of the \mathcal{CP} violating angle is $\delta \approx 3\pi/2$, which means $\cos(\delta) \approx 0$ and, consequently, it will be difficult to solve the hierarchy problem from any oscillation experiment in vacuum. In principle, since the neutrinos propagate through the Earth crust on a distance of about 300 km, matter effects should be taken into account when extracting the values of parameters. However, for a peak energy $E_\nu = 0.6$ GeV and a density of electrons in the Earth crust around $N_e = 8 \cdot 10^{23} \text{ cm}^{-3}$, the relevant parameter $\hat{A} = 2\sqrt{2}G_F N_e E_\nu / \delta m_{31}^2$ is very small, $\hat{A} \approx 0.05$, leading to negligible matter effects.

NO ν A is another long baseline accelerator experiment, optimised to study $\nu_\mu \leftrightarrow \nu_e$ oscillations, which started publishing results recently⁵⁶. It is a ν_μ disappearance ν_e appearance experiment for both neutrinos and antineutrinos, with a beam of peak energy $E_\nu \approx 2$ GeV from Fermilab with a far

⁵⁶NO ν A collaboration, P. Adamson, Phys. Rev. Lett. **118** (2017) 231801, arXiv:1703.03328 [hep-ex]; Jianming Bian, for the NO ν A collaboration, arXiv:1812.09585 [hep-ex].

detector 810 km away in Minnesota. With this choice of parameters, the value of $\sin^2(x\delta m_{32}^2/E_\nu)$ is near its maximum which maximizes the disappearance of ν_μ and the appearance of ν_e . NO ν A has collected an equivalent of $8.85 \cdot 10^{20}$ protons on target for neutrinos and $6.9 \cdot 10^{20}$ for antineutrinos. It should be more sensitive to matter effects than T2K with a value of $\hat{A} \approx .18$. A preliminary analysis, for normal hierarchy (with $\delta m_{31}^2 \approx \delta m_{32}^2$), yields $\delta m_{32}^2 = 2.51_{-0.08}^{+0.12} 10^{-3} \text{ eV}^2$ with a mixing angle, $\sin^2(\theta_{23}) = .58 \pm .03$.

OPERA is a τ appearance experiment : it is the only detector designed to identify τ leptons in a ν_μ beam on an event-by-event basis. The ν_μ source is the CNGS (CERN Neutrinos to Gran Sasso) beam directed at the Grand Sasso underground facility 730 km away. Compared to other accelerator experiments the ν_μ energy is very high, $\langle E_{\nu_\mu} \rangle = 17 \text{ GeV}$ to overcome the τ production threshold, $E_{th} = 3.55 \text{ GeV}$. The observed number of τ leptons is written⁵⁷

$$N_\tau = A \int_{E_{th}} \Phi_{\nu_\mu}(E) P(\nu_\mu \rightarrow \nu_\tau) \sigma_\tau^{CC}(E) \varepsilon(E) dE, \quad (14.12)$$

where A is a normalisation constant taking account of the detector mass, $\Phi_{\nu_\mu}(E)$ the neutrino flux, $\sigma_\tau^{CC}(E)$ the charged-current ν_τ cross section and $\varepsilon(E)$ the ν_τ detection efficiency. As for $P(\nu_\mu \rightarrow \nu_\tau)$ the oscillation rate given in eq. (12.33), it simplifies considerably since the $\sin^2(\delta m_{12}^2 x/4k)$ term with $\delta m_{12}^2 x/4k \approx 4.1 \cdot 10^{-3}$ gives a negligible contribution,

$$P(\nu_\mu \rightarrow \nu_\tau) \approx \sin^2(2\theta_{23}) \sin^2(\delta m_{32}^2 x/4k) \quad (14.13)$$

ignoring furthermore $\sin^2(\theta_{13})$ pieces. For the OPERA configuration the number of observed τ leptons is given⁵⁸

$$N_\tau \approx A' \sin^2(2\theta_{23}) (\delta m_{32}^2 [\text{eV}^2] L[\text{km}])^2 \int_{E_{th}} \Phi_{\nu_\mu}(E) \sigma_\tau^{CC}(E) \varepsilon(E) \frac{dE}{E^2}. \quad (14.14)$$

In 2010 the first observation of a τ lepton in a ν_μ beam⁵⁹ was made. According to the final results⁶⁰ 10 ν_τ candidate events have been reported, for an expected no oscillation background of 2 events, which allows to claim for the discovery of $\nu_\mu \rightarrow \nu_\tau$ oscillations with a significance level of 6.1σ . A value of $\delta m_{32}^2 = 2.7_{-0.6}^{+0.7} 10^{-3} \text{ eV}^2$ is obtained, consistent with the world average.

⁵⁷OPERA Collaboration, S. Dusini, AIP Conference Proc. **1666** (2015) 110003; doi: 10.1063/1.4915575.

⁵⁸In this expression the approximation $\sin(L\delta m_{32}^2/4E) \approx 1.27 \delta m_{32}^2 [\text{eV}^2] L[\text{km}]/E[\text{GeV}]$ is justified.

⁵⁹OPERA Collaboration, N. Agafonova *et al.* Phys. Lett. **B 691** (2010) 138, arXiv:1006.1623.

⁶⁰N. Agafonova *et al.* Phys. Rev. Lett. **120** (2018) 211801, arXiv:1804.04912 [hep-ex].

14.3 Atmospheric neutrinos: Super-Kamiokande ; δm_{32}^2 , θ_{23} , δ

In 1998, the collaboration provided the first experimental evidence of neutrino oscillations⁶¹. Super-Kamiokande is an underground detector of 50 kilotons of ultra-pure water located in Gifu prefecture in Japan. It records the μ^\pm and e^\pm produced in $\bar{\nu}$ and ν induced reactions. In a first analysis it is difficult to tell ν_μ (ν_e) from $\bar{\nu}_\mu$ ($\bar{\nu}_e$) so that the results are given for $\nu_\mu + \bar{\nu}_\mu$ and $\nu_e + \bar{\nu}_e$ fluxes. One distinguishes the downward going flux (zenithal angle $\theta_z \approx 0$) with the neutrinos interacting (primary vertex) in the detector after a path length of 1 to 30 km in the atmosphere, from the upward going flux (zenithal angle $\theta_z \approx \pi$) where the neutrinos, after travelling up to $1.3 \cdot 10^4$ km through the Earth, are interacting in the rocks outside Super-K producing a muon energetic enough to enter the detector⁶². In a first approximation (*e.g.* $x/k < 10^3$) one ignores the oscillation terms in $\sin(\delta m_{21}^2 x/4k)$ and take $\delta m_{32}^2 \approx \delta m_{31}^2$. The relevant rates of oscillations (in vacuum) are obtained from secs. 12.3 and 12.4:

$$\begin{aligned}
 P(\nu_e \leftrightarrow \nu_\mu) &\approx \sin^2(2\theta_{13}) \sin^2(\theta_{23}) \sin^2(\delta m_{31}^2 x/4k) \\
 P(\nu_e \rightarrow \nu_\tau) &\approx \sin^2(2\theta_{13}) \cos^2(\theta_{23}) \sin^2(\delta m_{31}^2 x/4k) \\
 P(\nu_\mu \rightarrow \nu_\tau) &\approx \sin^2(2\theta_{23}) \cos^4(\theta_{13}) \sin^2(\delta m_{31}^2 x/4k) \\
 P(\nu_e \rightarrow \nu_e) &\approx 1 - \sin^2(2\theta_{13}) \sin^2(\delta m_{31}^2 x/4k) \\
 P(\nu_\mu \rightarrow \nu_\mu) &\approx 1 - [\sin^2(2\theta_{23}) \cos^2(\theta_{13}) + \sin^2(2\theta_{13}) \sin^4(\theta_{23})] \sin^2\left(x \frac{\delta m_{31}^2}{4k}\right).
 \end{aligned} \tag{14.15}$$

One checks easily that $P(\nu_\mu \rightarrow \nu_\mu) = 1 - P(\nu_\mu \rightarrow \nu_e) - P(\nu_\mu \rightarrow \nu_\tau)$. We quote here very simplified formulae which are sufficient to understand the global features of the data but, in their analysis, the Super-K collaboration uses the full model including the \mathcal{CP} violating phase δ as well as matter effects. From eqs. (14.15) it is expected that ν_μ will fluctuate dominantly in ν_τ ($\sin^2(2\theta_{23}) \approx .99$ vs $\sin^2(2\theta_{13}) \approx .1$) and the ν_μ disappearance will be less important for downward neutrinos since they do not have time to oscillate unlike those crossing the Earth. Because of the small value of $\sin^2(2\theta_{13})$ ν_e oscillation is less effective.

The Super-K collaboration has given the most precise measurements of the atmospheric neutrino fluxes in a large energy range⁶³: $0.15 < E_\nu [\text{GeV}] < 65$ for $\nu_e + \bar{\nu}_e$ and $0.25 < E_\nu [\text{GeV}] < 2500$ for $\nu_\mu + \bar{\nu}_\mu$ (see fig. 11 which also displays model predictions with and without oscillations). At high energies, the spectrum is dominated by $\nu_\mu + \bar{\nu}_\mu$ and, for kinematical reasons, the ν_τ flux is negligible. As expected the $\nu_e + \bar{\nu}_e$ flux is globally not sensitive to oscillations while the $\nu_\mu + \bar{\nu}_\mu$ flux below 100

⁶¹Super-Kamiokande Collaboration, Y. Fukuda *et al.* Phys. Rev. Lett. **81** (1998)1562, arXiv:hep-ex/9807003.

⁶²More precisely, the downward neutrinos have $0 < \theta_z < \pi/2$ and the upward neutrinos have $\pi/2 < \theta_z < \pi$.

⁶³Super-Kamiokande collaboration, E. Richard *et al.*, Phys. Rev. **D94** (2016) 052001, arXiv:1510.08127 [hep-ex].

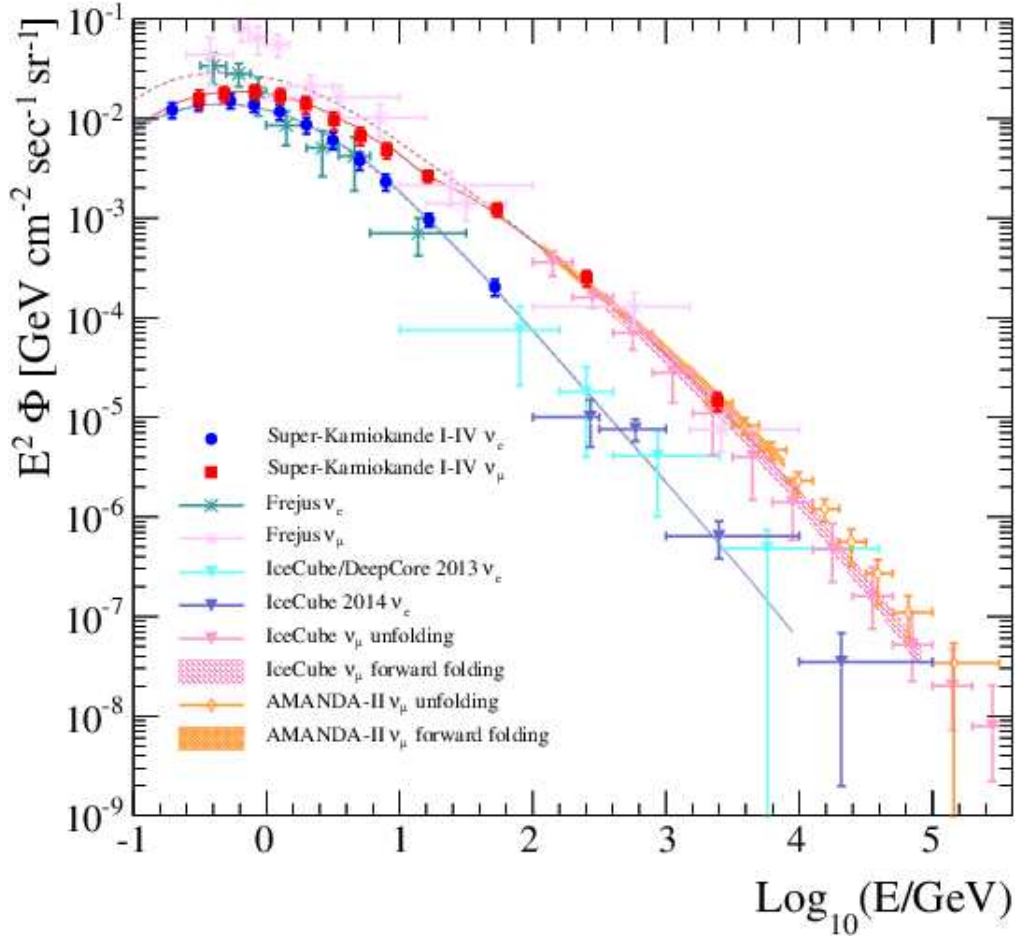


Figure 11: *Energy spectra of $\nu_e + \bar{\nu}_e$ and $\nu_\mu + \bar{\nu}_\mu$ atmospheric neutrinos by the Super-K collaboration in comparison with other measurements. The solid (dashed) lines are model predictions with (without) oscillations. From Super-Kamiokande collaboration, E. Richard et al., Phys. Rev. **D94** (2016) 052001, arXiv:1510.08127 [hep-ex].*

GeV is reduced. Above this energy the factor $(x \delta m_{31}^2 / 4k)$ is small and oscillations become irrelevant. Fig. 12 displays details of ν oscillations in the Earth. Panel b) illustrates the survival pattern of an upward ($\cos \theta_z = -1$) 4 GeV ν_μ as a function of the distance travelled in the Earth. After crossing the Earth ($x \approx 1.28 \cdot 10^4$ km) the neutrinos have undergone 3 cycles of oscillations *i.e.* $(x \delta m_{31}^2 / 4k) \approx 3\pi$. Notice that, in the model illustrated in fig. 12-b, the oscillation strength is enhanced as the muon neutrino crosses the Earth indicating a modification of the mixing angles (see eqs. (13.49)). A naive estimate of the effect of matter is obtained by calculating the factor \hat{A} , eq. (13.46):

$$\hat{A} = \frac{2\sqrt{2}G_F N_e E_\nu}{\delta m_{31}^2} \approx .1 \left(\frac{E_\nu}{[\text{GeV}]} \right), \quad \text{for } N_e \approx 1.10^{24} \text{cm}^{-3}.$$

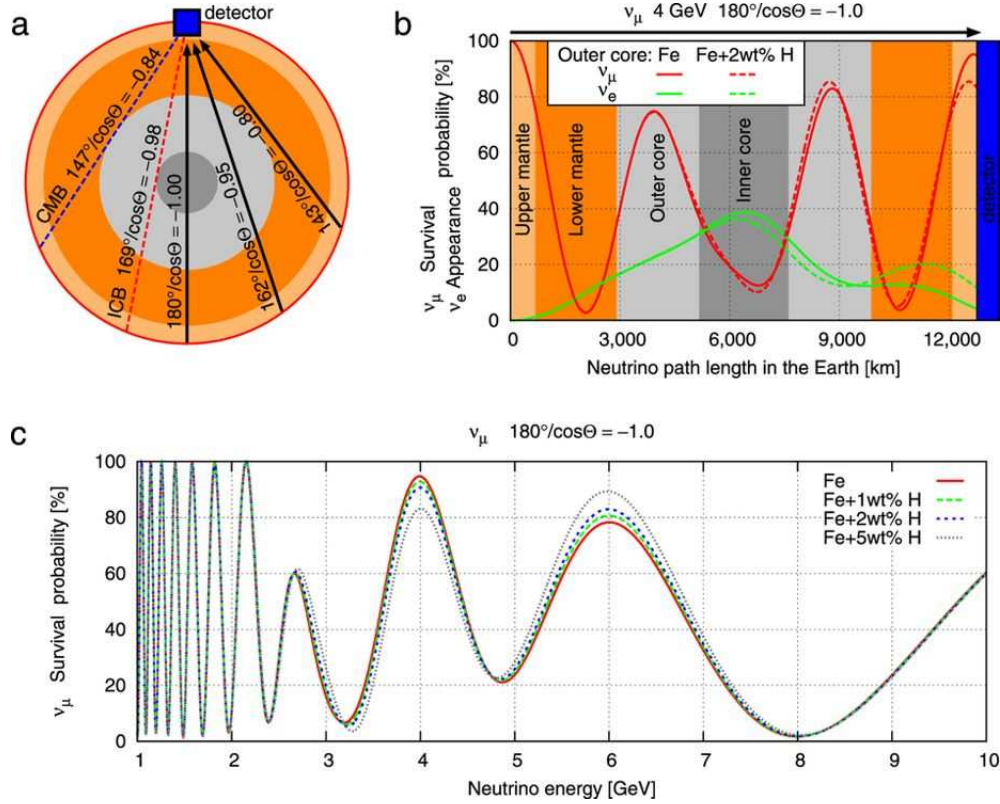


Figure 12: *Neutrino oscillation patterns in the Earth.* a) definition of the zenith angle θ , denoted θ_z in the text, and multilayer structure of the Earth; the average density of electrons in the core (grey areas) is $N_e^{core} \approx 3.3 \cdot 10^{24} \text{ cm}^{-3}$, and in the mantle (red area) $N_e^{mantle} \approx 1.2 \cdot 10^{24} \text{ cm}^{-3}$; b) survival probability of an upward ($\cos\theta = -1$) $E = 4 \text{ GeV}$ muon neutrino crossing the Earth (red) and correlated appearance probability of an electron neutrino (green); c) survival probability of an upward going muon neutrino having crossed the Earth as a function of energy. From C. Rott, A. Taketa, D. Bose, *Nature Scientific Reports*: 15225, www.nature.com/articles/srep15225.

Panel c) illustrates, as a function of energy, the survival pattern of an upward muon neutrino exiting from the Earth: because of the $1/k$ dependence of the oscillating factor, oscillations are much more rapid at low energy. In data, an average over a large energy range is performed so that the oscillating factor $\sin^2(x\delta m_{31}^2/4k)$ reduces to .5.

The distribution of events as a function of the zenith angle is given in fig. 13: for events labelled "Multi-GeV μ -like" (middle panel) the increase in the number of events when $\cos\theta_z$ decreases from 1 to 0 is due to the increase of the effective thickness of the atmosphere, then at $\cos\theta_z = -1$ the oscillations reduce the $\nu_\mu + \bar{\nu}_\mu$ flux by a factor 2 compared to the no oscillation expectation. Concerning ν_e 's, the disappearance (left panels) is much less pronounced. One notices however that energetic upgoing

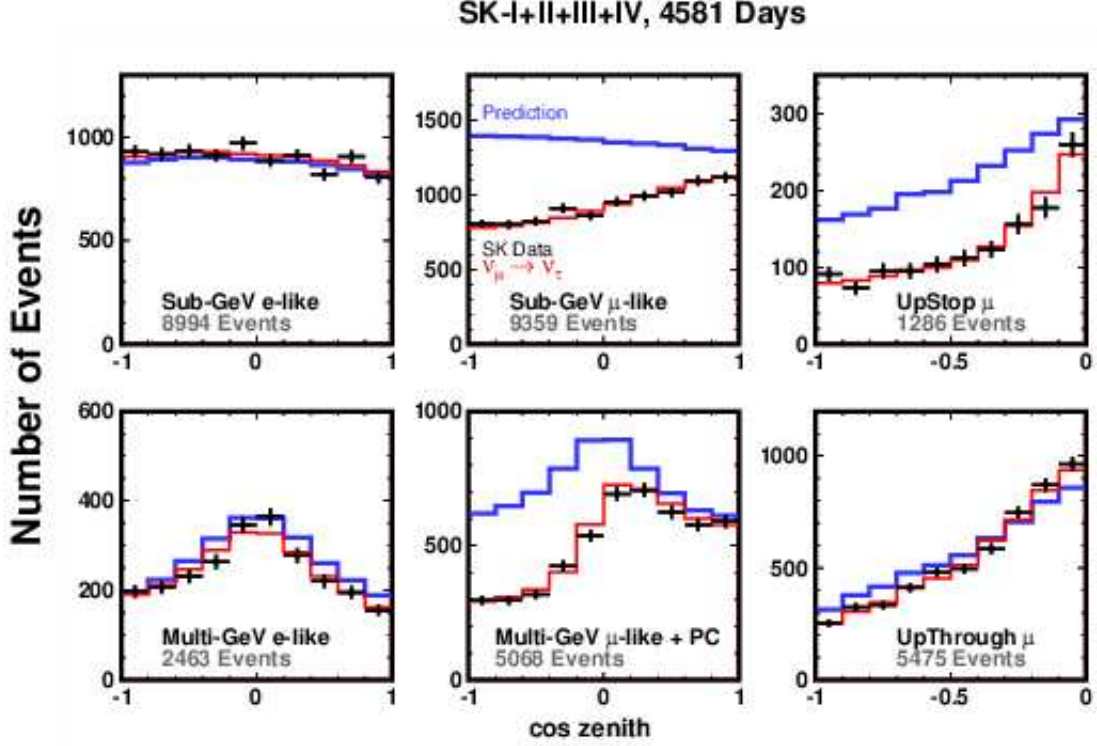


Figure 13: *Superkamiokande zenithal oscillations* : “Sub-GeV” refers to events with $E_{vis} < 1.33$ GeV while “Multi-GeV” refers to neutrinos with $E_{vis} > 1.33$ GeV. The 4 left most panels have a reconstructed vertex in the SK detector while the 2 right most panels show the sample of upward-going muons produced by neutrinos in the rock surrounding the detector. The blue lines show the non-oscillated prediction and the red lines the oscillated ones. From R. Wendell for the Super-Kamiokande collaboration, *arXiv:1412.5234 [hep-ex]*.

(anti)neutrinos are less suppressed than downgoing ($\cos \theta_z \approx 1$) ones: at high energy the atmospheric $\nu_\mu + \bar{\nu}_\mu$ flux is much larger than the $\nu_e + \bar{\nu}_e$ flux and, furthermore, between 2 and 10 GeV the $\nu_\mu + \bar{\nu}_\mu$ to $\nu_e + \bar{\nu}_e$ resonant enhancement in the Earth is possible as discussed in sec. 13.3. The resonant enhancement is sensitive to the sign of δm_{31}^2 and affects ν_e 's for normal hierarchy and $\bar{\nu}_e$'s for inverted hierarchy. Separating neutrinos from antineutrinos would allow to determine the sign of δm_{31}^2 . For this purpose the collaboration is constructing ν_e and $\bar{\nu}_e$ enriched samples.

In recent analyses of their data⁶⁴, keeping the δ dependence and matter effects as in eq. (13.56), for example, the Super-Kamiokande collaboration constrains several mixing parameters. The analyses are constrained, *i.e.* fixing $\sin^2(\theta_{13})$, or unconstrained. In the latter case the best fit for normal hierarchy gives $\sin^2(\theta_{13}) = .008^{+0.025}_{-0.005}$ and:

$$\delta m_{31}^2 = (2.63^{+0.10}_{-0.21}) 10^{-3} \text{eV}^2, \quad \sin^2(\theta_{23}) = 0.588^{+0.030}_{-0.062}, \quad \delta = 3.84^{+2.00}_{-2.14} \quad (1.22\pi^{+0.63\pi}_{-0.68\pi}), \quad (14.16)$$

⁶⁴Super-Kamiokande collaboration, K. Abe *et al.*, Phys.Rev. **D97** (2018) 072001, arXiv:1710.09126 [hep-ex].

while, fixing $\sin^2(\theta_{13}) = 0.0210 \pm 0.0011$ (from the Daya Bay, RENO and Double-Chooz) the results are:

$$\delta m_{31}^2 = (2.53_{-0.12}^{+0.22}) 10^{-3} \text{eV}^2, \quad \sin^2(\theta_{23}) = 0.425_{-0.037}^{+0.046}, \quad \delta = 3.14_{-1.35}^{+2.67} \quad (\pi_{-0.43\pi}^{+0.85\pi}). \quad (14.17)$$

Very similar numbers are obtained for the inverted hierarchy hypothesis but the data indicate a weak preference for the normal mass hierarchy. One observes that, when constraining θ_{13} , the θ_{23} angle is in the first octant $\theta_{23} < \pi/4$ but, for the other case, θ_{23} is in the second octant $\theta_{23} > \pi/4$ ⁶⁵. This illustrates the strong correlations between parameters as shown by eqs. (14.15), as well as the difficulty to obtain a precise determination of the mixing angles.

The upper end of the $\nu + \bar{\nu}$ spectra in fig. 11 do not play any role in the physics of oscillations but, as will be seen in sec. 14.5, they carry information on cosmic sources.

The parameters δm_{32}^2 and $\sin^2(\theta_{23})$ are often called atmospheric oscillation parameters.

14.4 Solar neutrinos: SNO ; δm_{12}^2 , θ_{12}

Since the mid sixties solar neutrinos presented a nagging problem : the measured flux⁶⁶ was two to three time smaller than the predicted one by the standard solar neutrino model⁶⁷. Several explanations were proposed to account for this discrepancy⁶⁸ but now it has been shown that the correct explanation lies in the incoherent interactions of neutrinos with matter in the sun.

According to the standard solar neutrino model, the production modes of neutrinos are given in fig. 14.

The most abundant one is

$$p + p \rightarrow D + e^+ + \nu_e \quad (14.18)$$

with $.1 \text{ MeV} < E_\nu < .4 \text{ MeV}$. The flux has been observed by the "Gallium" experiments, GALLEX⁶⁹, SAGE⁷⁰ and GNO⁷¹, via the transition Gallium to Germanium $\nu_e + {}^{71}\text{Ga} \rightarrow e^- + {}^{71}\text{Ge}$, with a threshold of $.233 \text{ MeV}$. They all show a deficit of ν_e 's compared to the model, roughly $\phi_{obs}(\nu_e)/\phi_{mod}(\nu_e) \approx .54$. Later on, the SNO (Sudbury Neutrino Observatory) collaboration measured the neutrino flux from the

⁶⁵If $\theta_{23} \approx \pi/4$ the interchange $\theta_{23} \rightarrow \pi/2 - \theta_{23}$ leads to almost degenerate predictions for the observables, see eqs. (14.15).

⁶⁶Homestake experiment, R. Davis *et al.*, Phys. Rev. Lett. **12** (1964) 302.

⁶⁷J.N. Bahcall, *et al.*, Phys. Rev. Lett. **17** (1966) 398; J.N. Bahcall, A.M. Serenelli, S. Basu, Astrophys.J. **621** (2005) L85.

⁶⁸Bruno Pontecorvo suggested in 1977 neutrino oscillations as the most reasonable explanation for the observed ν_e deficit, Dubna Report E10545, 1977; S.M. Bilenky, B. Pontecorvo, Comments Nuc. Part. Phys. **7** (1977) 149.

⁶⁹GALLEX Collaboration, W. Hampel *et al.*, Phys. Lett. **B447** (1999) 127.

⁷⁰SAGE Collaboration, J.N. Abdurashitov *et al.*, Phys. Rev. **C80** (2009) 015807.

⁷¹GNO Collaboration, M. Altmann *et al.*, Phys. Lett. **B616** (2005) 174; GALLEX + GNO, F. Kaether *et al.*, Phys. Lett. **B685** (2010) 47.

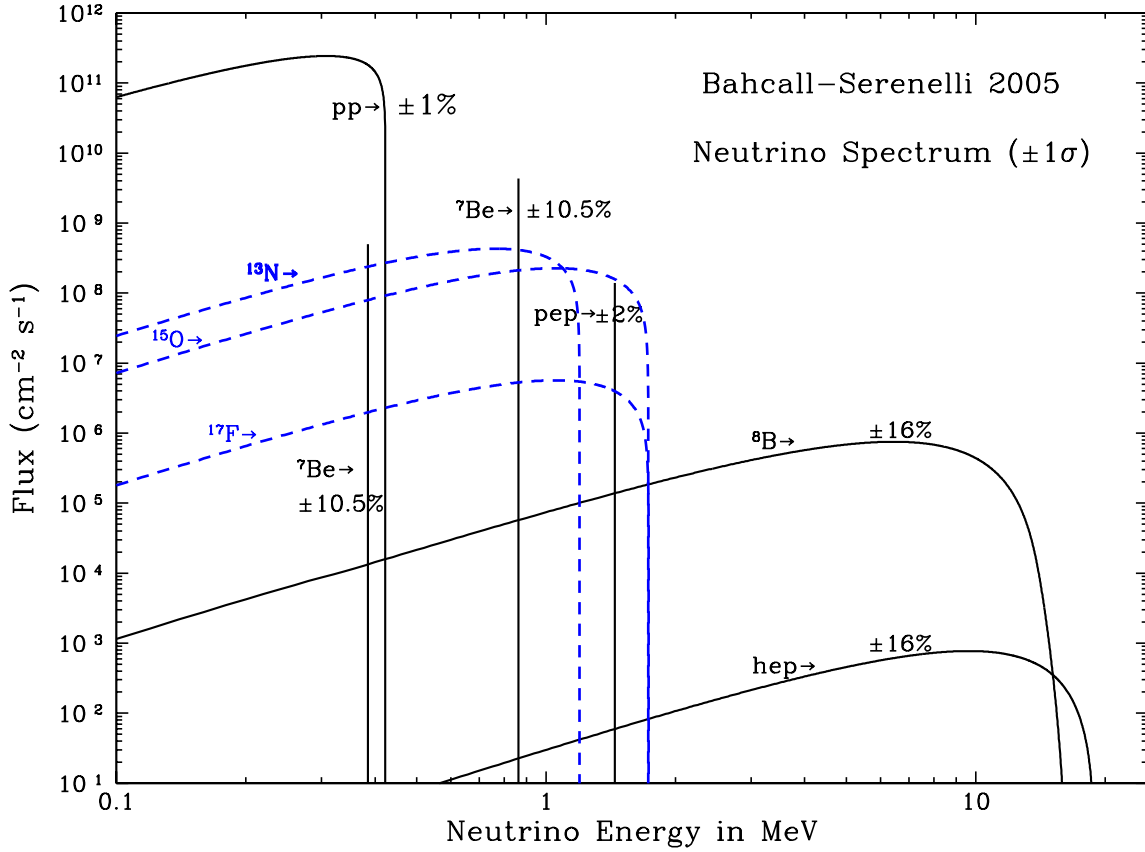


Figure 14: *The solar neutrino spectrum from the sun (from J.N. Bahcall, A.M. Serenelli, S. Basu, Astrophys.J. **621** (2005) L85).*

8B decay into an excited beryllium state:

$$^8B \rightarrow ^8Be^* + e^+ + \nu_e. \quad (14.19)$$

It is essentially the only ν_e source in the energy range $1.5 \text{ MeV} < E_{\nu_e} < 15 \text{ MeV}$ but the solar ν_e 's can convert to ν_μ 's and ν_τ 's on their way to the detector. The SNO collaboration⁷² in Canada conducted an elaborate study of 8B solar neutrinos. SNO is a detector using 1000 tons of ultra-pure heavy water (D_2O) surrounded by an ultra-pure water (H_2O) shield. Three types of reactions are studied

$$\begin{aligned} \nu_e + D &\rightarrow p + p + e^-, && \text{via charged current (CC)} \\ \nu_x + D &\rightarrow p + n + \nu_x, && \text{via neutral current (NC)} \\ \nu_x + e^- &\rightarrow \nu_x + e^-, && \text{elastic scattering (ES),} \end{aligned} \quad (14.20)$$

⁷²SNO collaboration, B. Aharmim *et al.*, Phys. Rev. **C88** (2013) 025501, arXiv:1109.0763 [nucl-ex].

where ν_x stands for ν_e , ν_μ or ν_τ . The Cherenkov light emitted by the electron in the final state is used to detect the first and third reactions and the second one is seen via the emission of a photon of 6.25 MeV emitted in the capture of the neutron on deuterium. The first reaction (CC), mediated by a W boson exchange, is only sensitive to electron neutrino while the second one (NC), mediated by Z boson exchange, receives an equal contribution from all three flavours

$$\sigma^{NC}(\nu_e) = \sigma^{NC}(\nu_\mu) = \sigma^{NC}(\nu_\tau) \quad (14.21)$$

For the third one, ν_e has a higher cross section since it can go both by charged or neutral current as shown in fig. 15, and one has with a good approximation

$$\sigma^{ES}(\nu_\mu) = \sigma^{ES}(\nu_\tau) \approx 0.156 \sigma^{ES}(\nu_e) \quad (14.22)$$

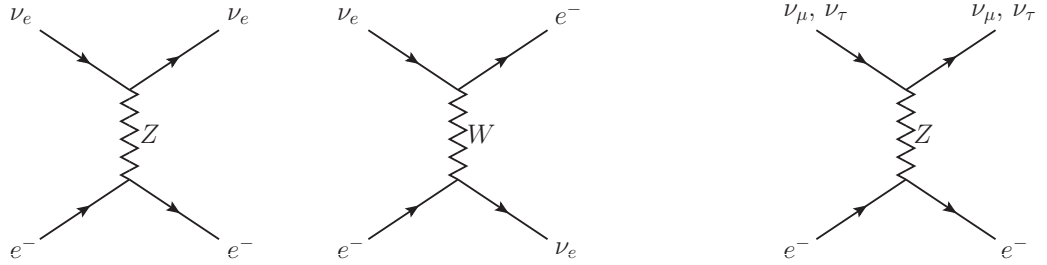


Figure 15: *Feynman diagrams for the elastic diffusion of a neutrino on an electron: on the left for ν_e , on the right for ν_μ or ν_τ .*

The collaboration measures the flux of neutrinos in the various channels and finds (in units of $10^6 \text{ cm}^{-2} \text{ s}^{-1}$)

$$\begin{aligned} \phi^{CC} = \phi(\nu_e) &= 1.76_{-0.05}^{+0.06} \text{ (stat.)}_{-0.09}^{+0.09} \text{ (syst.)} \\ \phi^{ES} = \phi(\nu_e) + 0.156 (\phi(\nu_\mu) + \phi(\nu_\tau)) &= 2.39_{-0.23}^{+0.24} \text{ (stat.)}_{-0.12}^{+0.12} \text{ (syst.)} \\ \phi^{NC} = \phi(\nu_e) + \phi(\nu_\mu) + \phi(\nu_\tau) &= 5.09_{-0.43}^{+0.44} \text{ (stat.)}_{-0.43}^{+0.46} \text{ (syst.)} \end{aligned} \quad (14.23)$$

The result of ϕ^{NC} is in very good agreement with the Standard Solar Neutrino Model⁷³. From these results the collaboration derives (in the same units)

$$\phi(\nu_\mu) + \phi(\nu_\tau) = 3.41_{-0.45}^{+0.45} \text{ (stat.)}_{-0.45}^{+0.48} \text{ (syst.)}, \quad (14.24)$$

⁷³A.S. Brun, S. Turck-Chièze, J.P. Zahn, *Astrophys. J.* **525** (2001) 1032; J.N. Bahcall, M.H. Pinsonneault, S. Basu, *Astrophys. J.* **555** (2001) 990.

which is clear evidence for the disappearance of solar ν_e 's. In later stages, the SNO collaboration improved the detection efficiency of neutrons by adding an array of ${}^3\text{He}$ proportional counters in the D_2O volume and they obtain the most precise estimate of active neutrino flux (in units of $10^6 \text{ cm}^{-2} \text{ s}^{-1}$)

$$\begin{aligned}\phi^{NC} &= 5.25^{+0.16}_{-0.16} \text{ (stat.) }^{+0.11}_{-0.13} \text{ (syst.)} \\ \frac{\phi(\nu_e)}{\phi^{NC}} &= .317 \pm 0.016 \text{ (stat.) } \pm 0.009 \text{ (syst.)}, \quad \text{at } E_\nu = 10 \text{ MeV, independent on } E_\nu. \quad (14.25)\end{aligned}$$

Because SNO observes ν_e and $\nu_\mu + \nu_\tau$ only, neither the mixing angle θ_{23} nor the \mathcal{CP} violating phase play a role (see eqs. (12.25), (12.29), (12.32)). Furthermore, given the distance involved, $1.5 \cdot 10^9 \text{ km}$, the argument of the oscillating factors are so large that the corresponding \sin^2 terms reduce to $1/2$. In vacuum, the ν_e survival rate is then

$$\begin{aligned}P(\nu_e \rightarrow \nu_e) &= 1 - \frac{1}{2} \sin^2(2\theta_{12}) \cos^4(\theta_{13}) - \frac{1}{2} \sin^2(2\theta_{13}) \\ &= \sin^4(\theta_{13}) + (1 - \frac{1}{2} \sin^2(2\theta_{12})) \cos^4(\theta_{13}) \approx 1 - \frac{1}{2} \sin^2(2\theta_{12}), \quad (14.26)\end{aligned}$$

where the last approximate equality is a consequence of the smallness of θ_{13} . It is then justified to use a two neutrino model. Assuming the validity of the oscillation model in vacuum to explain the SNO data, one would obtain

$$\frac{\phi(\nu_e)}{\phi^{NC}} \approx 1 - \frac{1}{2} \sin^2(2\theta_{12}) \approx 0.56, \quad (14.27)$$

in contradiction with the SNO result of 0.317. The obvious conclusion is that neutrinos interact with matter in the sun.

• Neutrinos in the sun

The electron density in the sun is parameterised as⁷⁴

$$N_e(x) = N_e(x_0) \exp\left(\frac{x - x_0}{r_0}\right) \quad (14.28)$$

with $N_e(0) \approx 6 \cdot 10^{25}$ and $r_0 \approx .1 R_\odot \approx .7 \cdot 10^5 \text{ km}$ (valid for $x_0 \gtrsim .05 R_\odot$). If one uses for δm^2 and θ the values δm_{21}^2 and θ_{12} given by eq.(12.22) the adiabaticity condition eq. (13.31) will be satisfied if

$$\frac{1}{\hat{A}} \frac{r_0 \delta m_{12}^2}{2E_\nu} \sin^2(2\theta_{12}) \approx 2.7 \cdot 10^4 \left(\frac{E_\nu}{\text{MeV}}\right)^{-2} \gg 1, \quad (14.29)$$

where \hat{A} is taken from eq. (13.15). The inequality is satisfied for the SNO range of $5 \text{ MeV} < E_\nu < 15 \text{ MeV}$. Besides \hat{A} remaining large (see secs. 13.3 and 13.4) one is justified to assume that the

⁷⁴J.N. Bahcall, Neutrino Astrophysics, Cambridge University Press, 1989.

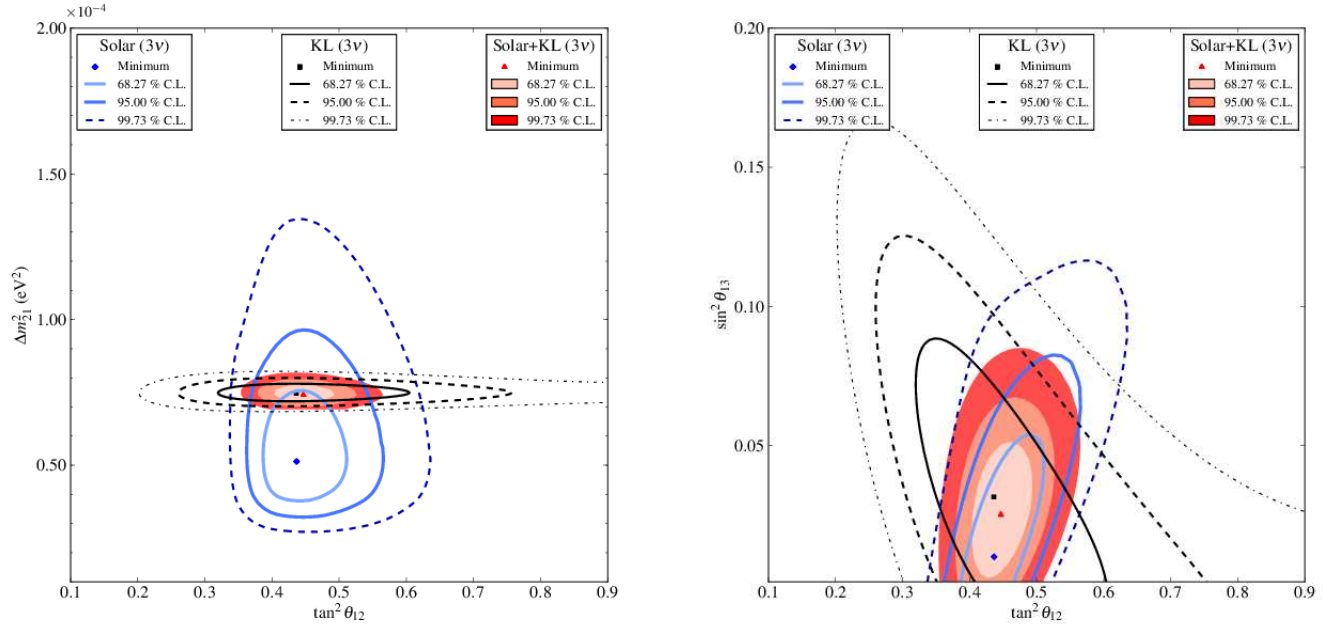


Figure 16: *Three flavour neutrino oscillation analysis : the blue lines are obtained using all solar neutrino experiments, the black ones are from KamLAND data and the colored potatoes are from a joint analysis. (From SNO collaboration, B. Aharmim et al., Phys. Rev. **C88** (2013) 025501, arXiv:1109.0763 [nucl-ex].)*

neutrino is produced as the heaviest mass eigenstate and will emerge from the sun in a $|\nu_2\rangle$ state with a probability $P(\nu_e \rightarrow \nu_e; x_0, R) = \sin^2(\theta_{12})$ as in eq. (13.36). Being a pure eigenstate of the vacuum it will propagate without oscillation to Earth and will give

$$\frac{\phi(\nu_e)}{\phi_{NC}} = \sin^2(\theta_{12}) \approx .325, \quad (14.30)$$

in good agreement, within errors, with the experimental result of eq. (14.25). Based on their flux measurements the SNO collaboration performs a two flavour and a three flavour neutrino oscillation analysis. However SNO data alone are not sufficient to give tight constraints on the parameters δm_{12}^2 , θ_{12} so an analysis is performed using also other solar data as well as KamLAND reactor data. Fig. 16 shows the constraints provided by SNO alone as well as various combinations of data. The best fit to the joint data, in the three flavour analysis, yields:

$$\delta m_{21}^2 = (7.46^{+0.20}_{-0.19}) 10^{-5} \text{eV}^2, \quad \tan^2 \theta_{12} = 0.443^{+0.030}_{-0.025}, \quad \sin^2 \theta_{13} = (2.49^{+0.20}_{-0.32}) 10^{-2}, \quad (14.31)$$

in very good agreement with eq. (12.22). Coming back to the case of low energy neutrinos from

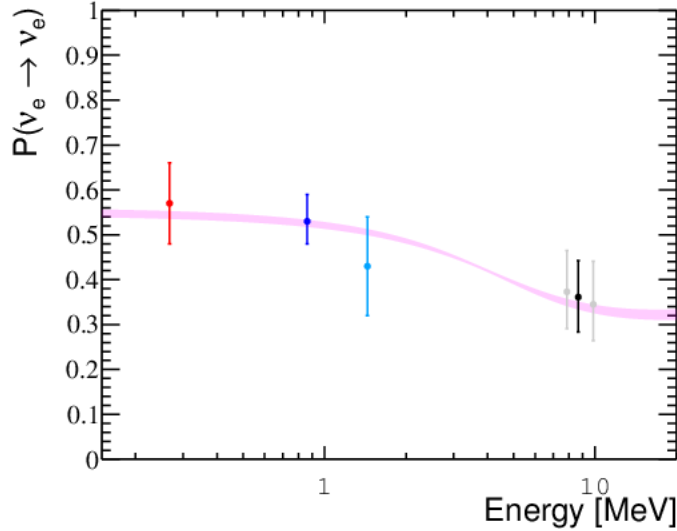


Figure 17: Summary of solar ν_e survival probabilities as a function of the average neutrino energy. ν_e 's produced in the pp reactions eq. (14.18): red point; in the ${}^7\text{Be} + e^- \rightarrow {}^7\text{Li} + \nu_e$ channel: blue point; in the $p + e^- + p \rightarrow D + \nu_e$ channel: light blue point; in the ${}^8\text{B}$ channel eq. (14.19): black and grey points. The band is the theoretical prediction from the standard solar model with the MSW effect. The figure is from Borexino Collaboration, M. Agostini et al., arXiv:1709.00756 [hep-ex].

reaction eq. (14.18), the adiabatic condition is still verified but, in this case, the resonance condition cannot be satisfied since $\hat{A} < \cos(2\theta_{12})$, or equivalently $N_e(x_0) < N_{\text{Res}}$, and interaction with matter becomes weaker. One expects from eq. (13.35) to have a larger ratio for $\phi(\nu_e)/\phi^{NC}$ as is found by the collaborations GALLEX, GNO, SAGE and Borexino. In fact, for $E_\nu \approx .2$ MeV, one finds $N_e/N_{\text{Res}} \approx .1$ from eq. (13.23) and, with a good approximation, the ν_e 's should propagate as in vacuum with the result $P(\nu_e \rightarrow \nu_e) = .56$ as in eq. (14.27) (see fig. 17).

The parameters δm_{21}^2 and θ_{12} are sometimes referred to as solar oscillation parameters and indexed with the symbol \odot .

14.5 Ultra-high energy or cosmic neutrinos

It is expected that, in the multi-TeV energy range and above, neutrinos from astrophysical or cosmic origin, will dominate over the atmospheric neutrinos. They can be produced in violent phenomena such as those occurring in Active Galactic Nuclei (AGN) or in collisions of ultra-high energy (UHE) cosmic rays on nucleons or photons, in particular photons from the cosmic microwave background (CMB). Neutrinos produced in a supernova event or in the merging of stars or black holes are expected to have energies in the MeV/GeV range. Unlike other cosmic messengers such as cosmic rays or photons the

universe is transparent to neutrinos⁷⁵. Cosmic rays (protons, nuclei) are deflected by extra-galactic and galactic fields so that it is not possible to identify the source which produced them. They also lose energy when scattering on CMB photons, gas and dust. Concerning photons, if their energy is high enough, they are absorbed on their way to Earth by e^+e^- pair production on CMB to UV

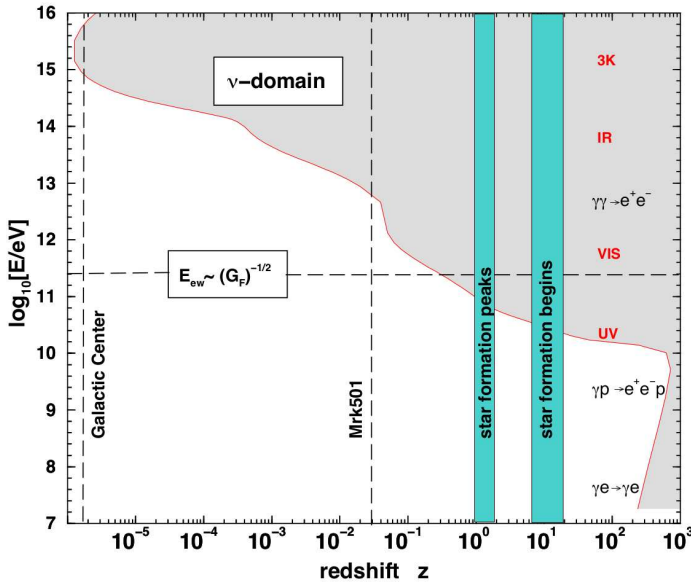


Figure 18: *The photon horizon. Photons emitted in the grey domain do not reach the Earth because of annihilation into e^+e^- pairs. A redshift $z = 1$ corresponds to a distance of 14 Gly from the Earth. From J.G. Learned, K. Mannheim, *Annual Rev. Nuc. Part. Sci.* **50** (2000) 679.*

background photons via $\gamma_{HE} + \gamma_{bkgrd} \rightarrow e^+ + e^-$. The threshold for such a process is obtained by solving the constraint $(p_{\gamma_{HE}} + p_{\gamma_{bkgrd}})^2 > 4m_e^2$. Because of their high density ($\sim 400 \text{ cm}^{-3}$) the CMB photons ($E_{\gamma_{CMB}} \approx .23 \text{ meV}$) are particularly efficient in this respect cutting the high energy photon flux above 10^{15} eV : even those emitted nearby in the galactic center do not reach the Earth, as seen in Fig. 18. This figure illustrates the depth of the photon horizon as a function of the photon energy: for example a 10^{12} eV photon emitted by an object with a redshift $z = .1$ (*i.e.* roughly 1 Gly away) is absorbed before reaching the Earth. On the contrary, neutrinos are expected to travel undisturbed once they are emitted.

However the flux of UHE neutrinos is very low and to observe them requires huge detectors such as the km^3 IceCube detector⁷⁶ at the South Pole, the projected KM3NET⁷⁷ with a volume of 5 km^3 in the Mediterranean Sea which builds up on the ANTARES telescope⁷⁸ or the Giga Volume Detector⁷⁹ (GVD) which is an upgrade of the Lake Baikal experiment. As neutrino cross sections increase with

⁷⁵ The "Glashow resonance", *i.e.* the reaction $\bar{\nu}_e + e^- \rightarrow W^- \rightarrow X$ should affect the $\bar{\nu}_e$ flux above $E_{\bar{\nu}_e} > 6.3 \cdot 10^{15} \text{ eV}$.

⁷⁶ IceCube collaboration, *Science* **342** (2013) no. 6161.

⁷⁷ KM3NET Collaboration, Maarten De Jong, *PoS NEUTEL2015* (2015) 055

⁷⁸ ANTARES Collaboration, Maurizio Spurio, *PoS NEUTEL2015* (2015) 054.

⁷⁹ BAIKAL-GVD Collaboration, A.D. Avrorin *et al.* (2015), DOI: 10.1142/9789814663618_0019.

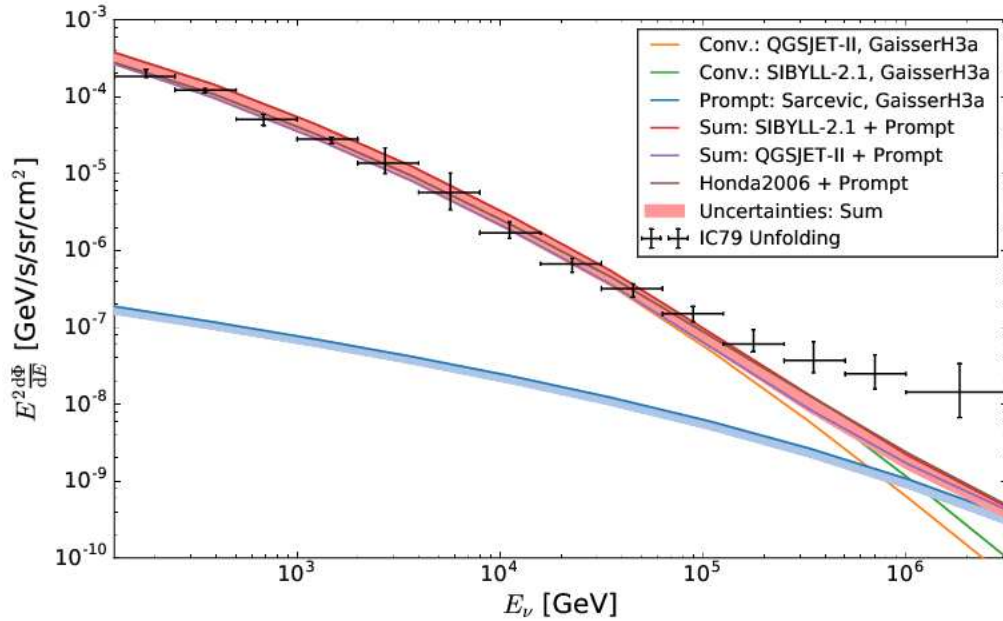


Figure 19: *The high energy $\nu_\mu + \bar{\nu}_\mu$ flux in IceCube, [arXiv:1705.07780].*

energy the Earth will become opaque to neutrinos for $E_\nu > 100$ TeV. The UHE neutrinos will then be searched for in the downward neutrino fluxes, but, in that case, the cosmic ray shower background will be enormous and must be vetoed.

IceCube recently extended the measurement of the $\nu_\mu + \bar{\nu}_\mu$ flux above the domain shown in Fig. 11, up to more than 2 PeV⁸⁰. The results are displayed in Fig. 19 where a hardening of the spectrum is observed above 100 TeV. Using a parameterisation of the cosmic ray flux and models of interactions of cosmic rays with the atmosphere they estimate the flux of atmospheric neutrinos : model and observation are in very good agreement up to around 100 TeV, energy above which the atmospheric neutrino flux falls below the data. The excess is interpreted as the flux of "astrophysical neutrinos" *i.e.* neutrinos directly emitted by sources such as AGN or produced in collisions of cosmic rays with dust, gaz or CMB photons.

On 22 September 2017 a high-energy neutrino-induced muon track event was detected by IceCube: the muon energy loss was estimated at 23.7 ± 2.8 TeV corresponding to a probable parent neutrino energy of 290 TeV (event labelled IceCube-170922A)⁸¹. Furthermore the reconstructed neutrino direction appeared to be pointing at the known blazar TXS 0506+56 (redshift $z = .3365$). An automatic alert was activitated and led to the subsequent observation of very high energy gamma rays by the

⁸⁰IceCube collaboration, M.G. Aarsten et. al., EPJ **C77** (2017) 692, [arXiv:1705.07780].

⁸¹IceCube collaboration, M.G. Aarsten et. al. Science **361** (2018) 347, [arXiv:1807.08794].

Fermi-LAT satellite and the MAGIC telescope by this blazar in a flaring state. Radio, optical, and X-ray observations were carried out and pointed to an increase of radio emission and variability in months before the alert and of X-ray emission a week after⁸².

This event is interesting as it is, at present, the only example of an identified neutrino emission from a blazar.

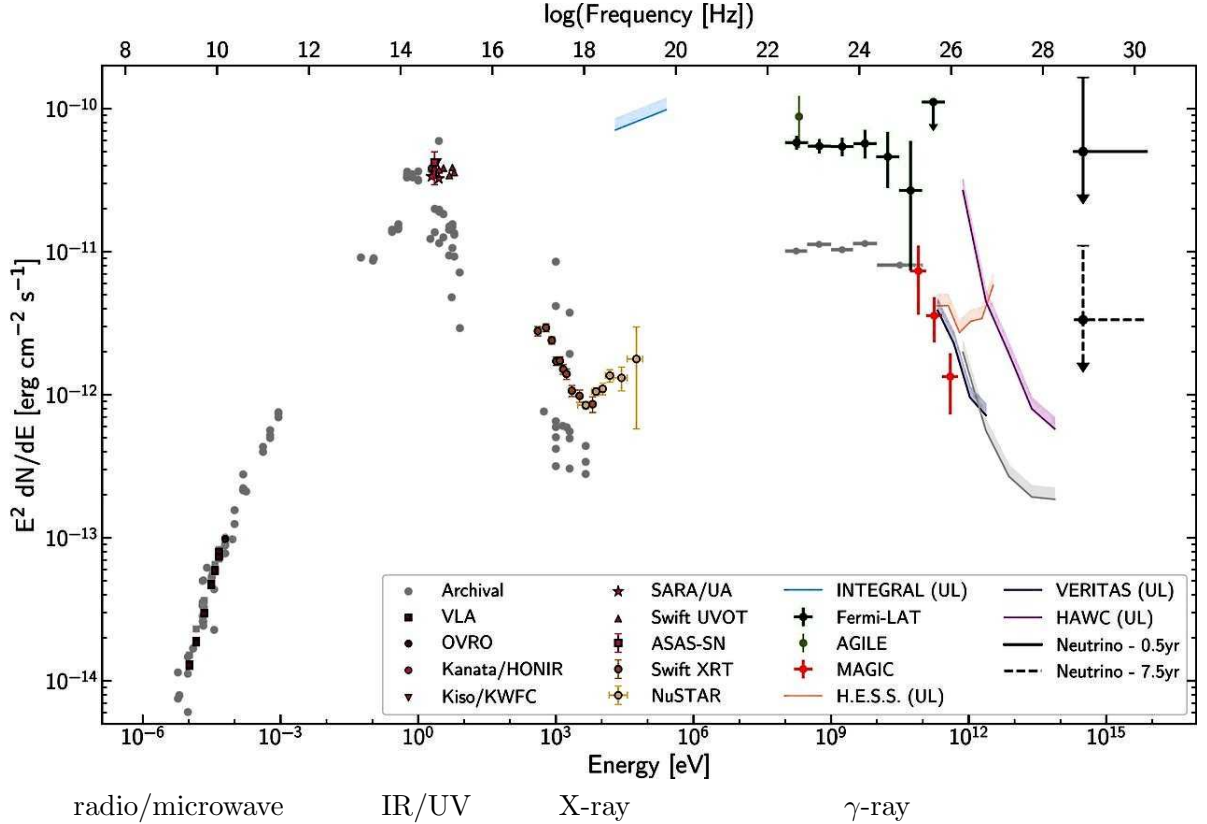


Figure 20: *Spectral energy density of blazar TXS 0506+056 in a multi-messenger, multi-wave length analysis*⁸². The rightmost two points are representative of $\nu_\mu + \bar{\nu}_\mu$ flux upper limits that produce on average one detection like IceCube-170922A over a period of 0.5 year (solid black line) or 7.5 years (dashed black line) assuming a spectrum of $dN/dE \propto E^{-2}$ at the most probable neutrino energy (311 TeV).

• Example of multi-messenger constraints on astrophysical ν emission

Fig. 20 shows the spectral energy density (SED) of TXS 0506+056 from radio to γ -ray energies as well as the upper limit of the neutrino contribution⁸³. The characteristic two-peak structure of AGN

⁸²Science **361** (2018) no.6398, eaat1378,[arXiv:1807.08816].

⁸³For a review on multi-messenger studies of blazars see M. Böttcher, [arXiv:1901.04178].

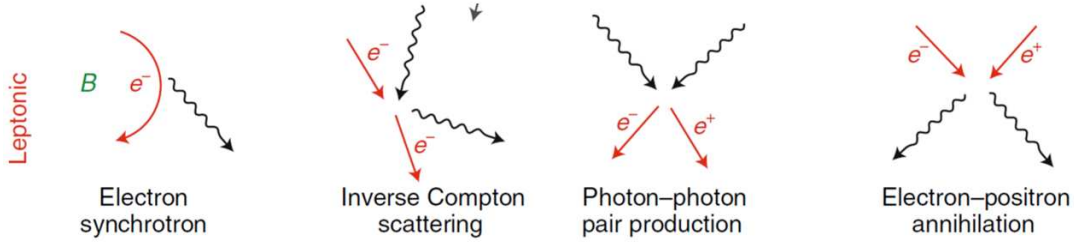


Figure 21: *The dominant reactions in the leptonic model of AGN*

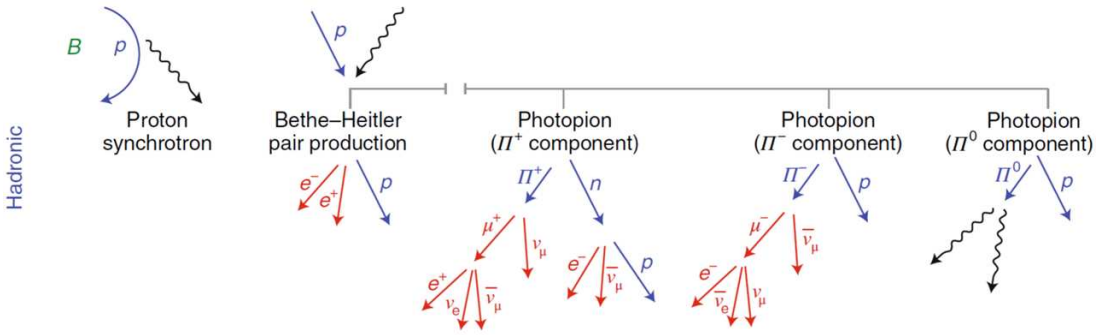


Figure 22: *The dominant reactions in the hadronic model of AGN.*

spectra is clearly visible⁸⁴. The first peak is due to bremsstrahlung emission by relativistic electrons in the AGN jet but different models are used to explain the second peak. In leptonic models, Fig. 21, it is due to scattering of low energy bremsstrahlung photons on electrons producing them (synchrotron-self-Compton) or, more generally, to inverse Compton scattering; in this class of models protons in the jet are not accelerated to high enough energy to contribute to radiative energy even though they carry most of the kinetic energy of the jet. In hadronic models, Fig. 22, on the contrary, protons reach energies high enough to initiate photoproduction reactions on bremsstrahlung photons and produce pions. In more details one has the photoproduction of π^0 via

$$\gamma + p \rightarrow \pi^0 + p \quad \text{followed by} \quad \pi^0 \rightarrow \gamma + \gamma$$

and also production of π^\pm , *e.g.*

$$\begin{aligned} \gamma + p &\rightarrow \pi^+ n, & \gamma + p &\rightarrow \pi^+ + \pi^- + \pi^0 + p \\ \pi^\pm &\rightarrow \mu^\pm + \nu_\mu, & \mu^\pm &\rightarrow e^\pm + \nu + \bar{\nu} \end{aligned}$$

Hadronic models then imply, from charged pion decays, the production of ν_e 's and ν_μ 's carrying on the average 5% of the energy of the initiating proton. Knowing the energy of the neutrino detected on

⁸⁴An AGN consists typically in a supermassive rotating black hole in the center ($10^6 M_\odot$ to $10^{10} M_\odot$), an accretion disk, clouds of ionized gas, a dust ring, two jets extending on 10^2 's of parsecs and lobes extending on 100^2 's of parsecs.

Earth it is then possible to estimate, after taking account of the relevant boost factor, the energy of the proton in the frame of the emission zone. An important feature is that hadronic models predict also the emission, from neutral pion decays, of ultra energetic photons in the same energy range as that of the neutrinos, namely hundreds of TeV. If these photons escape from the emission zone they are not seen on Earth because of e^+e^- pair production which would cut-off their flux (see the "photon horizon" cut-off on Fig. 18). Most of the ultra-high energy photons however are expected to be absorbed by e^+e^- pair creation in the emission zone and the e^\pm 's radiate, create electromagnetic cascades ending in the UV, X-ray or soft gamma regimes. In conclusion, in this model, the rate of emission of neutrinos is strongly constrained by the spectral energy density in the UV and X-ray range, but no very high energy photons are expected to be seen in association with ν 's observations. A model of SED spectra of TXS 0506+056 is shown in Fig. 23 : it is seen that the hadronic component

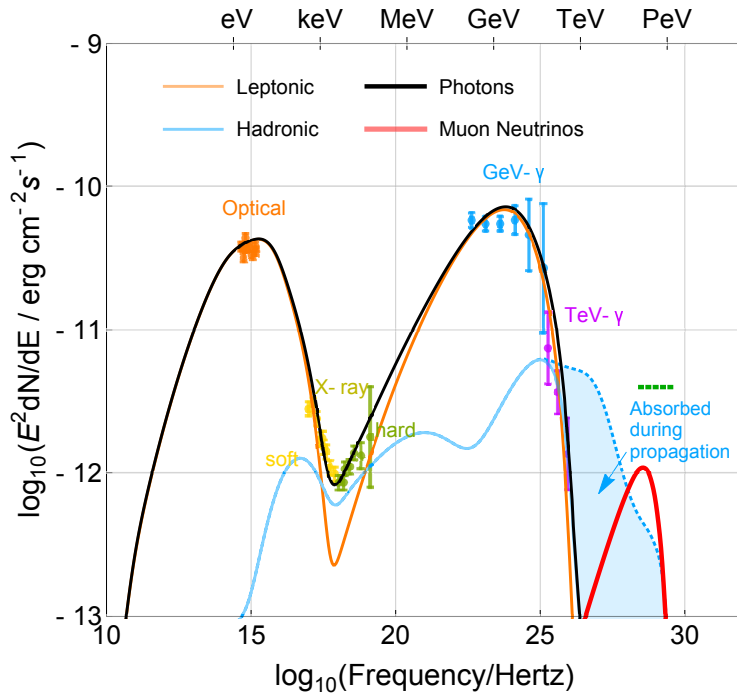


Figure 23: Spectral energy density of blazar TXS 0506+056 in the model of Shan Gao, A. Fedynitch, W. Winter, M. Pohl, *Nat. Astron.* **3** (2019) 88, [arXiv:1807.04275]. The red curve indicates the neutrino contribution assuming one ν_μ observation in 180 days. The emission of GeV γ rays is dominated by leptonic processes. The blue area shows the domain of absorption, by e^+e^- pair creation, of UHE photons on their way to Earth.

gives a major contribution to the spectral energy density in the X-ray range.

The above discussion illustrates how a multi-messenger analysis can constrain models and thereby help understand the physics of astrophysical objects.⁸⁵

Coming back to neutrinos IceCube can, to some extent, determine the neutrino flavor. Using this

⁸⁵No neutrinos have been observed in correlation with the detection of gravitational waves emitted in the merging of black holes or neutron stars: ANTARES, IceCube and the Pierre Auger Observatory, *Astrophys.J.* **850** (2017) L35, [arXiv:1710.05839]; IceCube collaboration [arXiv:1908.07706].

possibility and taking into account oscillations, the observations will then give precious information on the flavor composition in the production zone which in turn helps distinguish between production models⁸⁶.

14.6 Problems?

The three neutrino oscillation model can account, at present, for almost all data. However two collaborations, LSND⁸⁷ and MiniBooNE⁸⁸, claim results in strong disagreement with the above experiments. To add to the confusion LSND results are not confirmed by KARMEN⁸⁹ where very similar technics are used. MiniBooNE considers $\nu_\mu \rightarrow \nu_e$ and $\bar{\nu}_\mu \rightarrow \bar{\nu}_e$ in short baseline experiments with $.2 < E_\nu [\text{GeV}] < 1.25$ and a ratio x/E_ν in the range $.25 < x/E_\nu [m/\text{MeV}] < 2.5$. In a 2-neutrino oscillation model involving a sterile neutrino, the oscillations are best fitted with the parameters $[\delta m^2, \sin^2(2\theta)] = [3.14 \text{ eV}^2, 0.002]$ for ν 's, and $[0.043 \text{ eV}^2, 0.88]$ for $\bar{\nu}$'s. MiniBooNE results are summarised saying that "the data are consistent with neutrino oscillations in the $0.01 < \delta m^2 [\text{eV}^2] < 1.0$ range" and they "have some overlap with the evidence for antineutrino oscillations from LSND".

In the last few years, the $\bar{\nu}_e$ flux from nuclear reactors has raised a puzzle. In short baseline experiments ($10 < x [\text{m}] < 100$) there is a 6% deficit in the observed $\bar{\nu}_e$ compared to model expectations: this is the Reactor Antineutrino Anomaly (RAA)⁹⁰. Several explanations have been proposed. In a recent study the Daya Bay collaboration⁹¹ observes correlations between the time evolution of the fuel in the core (the composition in U and Pu isotopes varies with time) and changes in the $\bar{\nu}_e$ flux and energy spectrum. A detailed study of these correlations shows a 7.8% discrepancy between the observed and predicted ^{235}U yields which suggests that this isotope is the main contributor to the RAA.

An alternative explanation has been to assume a fourth (sterile) neutrino to account for the $\bar{\nu}_e$ deficit in short baseline nuclear reactor experiments. This is illustrated in Fig. 24 which shows that short and very short (less than 10 m) baseline reactor measurements are not sensitive to the three family neutrino parameters as given in eqs. (12.22), but would be affected by a fourth neutrino according the disappearance probability (see eq. (14.3)):

$$P(\bar{\nu}_e \rightarrow \bar{\nu}_e) = 1 - \sin^2(2\theta_{14}) \sin^2\left(\frac{x \delta m_{41}^2}{4k}\right).$$

⁸⁶IceCube collaboration, M.G. Aartsen *et al.*, *Astrophys.J.* **809** (20158) 98, [arXiv:1507.03991].

⁸⁷LSND collaboration, A. Aguilar *et al.*, *Phys. Rev.* **D64** (2001) 112007.

⁸⁸MiniBooNE collaboration, A. A. Aguilar-Arevalo, arXiv:1207.4809 [hep-ex]; *Phys. Rev. Lett.* **110** (2013) 161801; arXiv:1303.2588 [hep-ex].

⁸⁹KARMEN collaboration, B. Armbruster *et al.*, *Phys. Rev.* **D65** (2002) 112001.

⁹⁰G. Mention *et al.*, *Phys. Rev.* **D83** (2011) 073006, arXiv:1101.2755 [hep-ex].

⁹¹Daya Bay collaboration, F. P. An *et al.*, *Phys. Rev. Lett.* **118** (2017) 251801, arxiv:1704.01082 [hep-ex].

Nouvelle oscillation vers un neutrino stérile ?

- Pas de couplage par interaction faible → Visible uniquement par effet d'oscillation

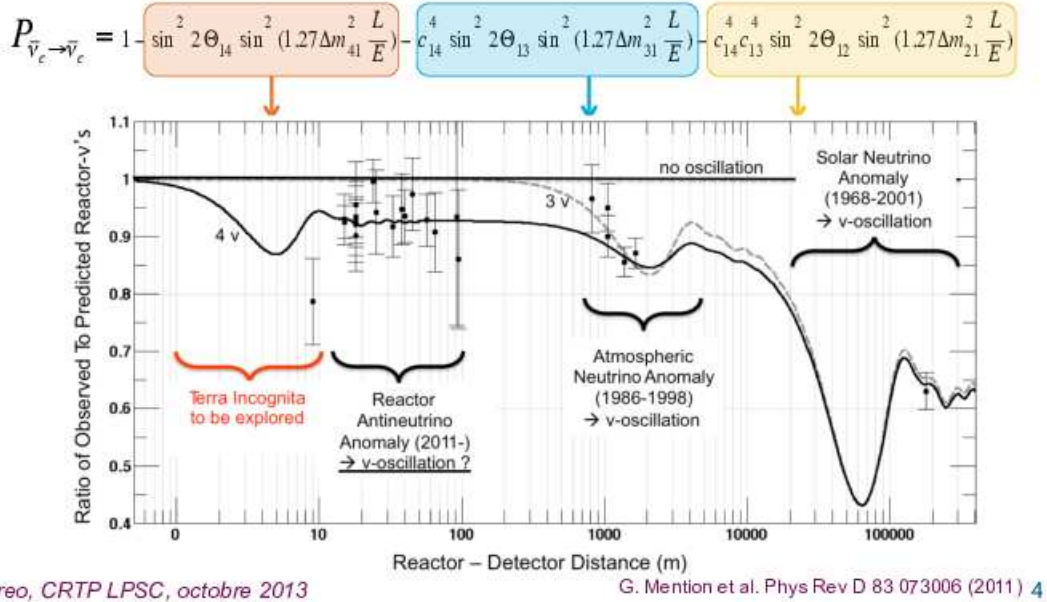


Figure 24: The figure illustrates the range of various oscillation parameters as a function the reactor-detector distance: a sterile neutrino with parameters as given in the text does not affect long baseline experiments, from the 2013 presentation of STEREO experiment by S. Kox et al., on the site lpsc.in2p3.fr/trac/nuetrino/wiki/.

The best global fit⁹² to short baseline $\bar{\nu}_e$ disappearance is obtained with δm_{41}^2 of the order of 1. eV² and $\sin^2(2\theta_{14}) \approx .1$. To further test the hypothesis of a sterile neutrino several experiments with very short baseline are taking data. DANSS⁹³ is located at a nuclear reactor in Russia with detectors at 10,7 m and 12,7 m from the core while the NEOS collaboration⁹⁴ has been taking data at a nuclear reactor in Korea at a distance of around 24 m from the core. More recently STEREO⁹⁵ at ILL

⁹²J. Kopp et al, JHEP 1305:050 (2013); see also C. Giunti, X. P. Ji, M. Laveder, Y. F. Li and B. R. Littlejohn, JHEP 1710 (2017) 143, arXiv:1708.01133 [hep-ph]; M. Dentler et. al., JHEP 1711 (2017) 099, arxiv:1709.04294 [hep-ph].

⁹³DANSS collaboration, I. Alekseev et. al., JINST 11 (2016) P11011, arXiv:1606.02896 [physics.ins-det]; arXiv:1804.04046 [hep-ex].

⁹⁴NEOS collaboration, Y.J. Ko et. al., Phys. Rev. Lett. 118 (2017) 121802, arXiv:1610.05134 [hep-ex].

⁹⁵STEREO collaboration, N. Allemandou, et. al., arXiv:1804.09052 [physics.ins-det]; Phys. Rev. Lett. 121 161801

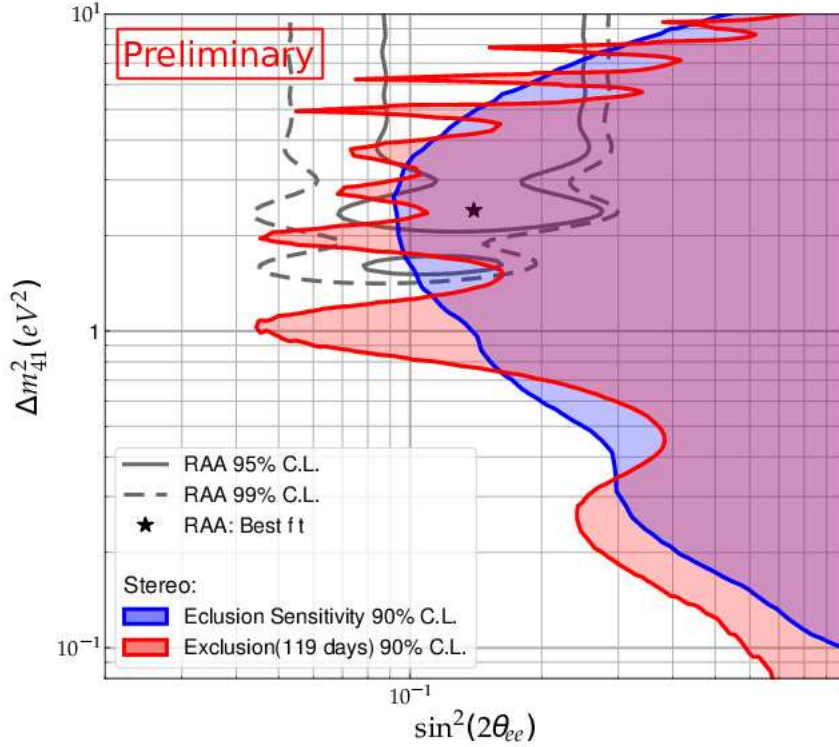


Figure 25: *Exclusion contour in the parameter space $\delta m_{41}^2, \sin^2(2\theta_{14}) \equiv \sin^2(2\theta_{ee})$. The RAA contours are taken from G. Mention et al.⁹⁰ and the RAA best fit is marked by \star . From STEREO publications⁹⁵.*

Grenoble, a high flux reactor using a 93% enriched ^{235}U with no time evolution on the ν_e flux, has a segmented detector taking data at distances between 9 and 11 m from the core. In PROSPECT⁹⁶, at the High Flux Isotope Reactor at Oak Ridge National Laboratory, the detector is 7.4 m from the core. All these experiments reduce the domain of sterile neutrino parameters obtained in previous reactor data⁹⁰ or global fits⁹² and already exclude some best fits, as illustrated in Fig. 25 from the STEREO collaboration: the best RAA fit is already excluded at 99% C.L. More data are being accumulated and could reduce further the allowed domain of $\theta_{14}, \delta m_{41}^2$.

14.7 Neutrinos: conclusions

The work for more precision on the determination of neutrino oscillation parameters is continuing. The present experiments will increase the precision even more and this is crucial for the determination

(2018), arXiv:1806.02096 [hep-ex]; L. Bernard arXiv:1905.11896 [hep-ex]].

⁹⁶PROSPECT collaboration, J. Ashenfelter et al., arXiv:1809.02784 [hep-ex].

of the \mathcal{CP} violating phase. This will also help settle the ambiguity of the neutrino mass hierarchy. For example, recent global fits³⁰ indicate that normal hierarchy, in the 3ν model, is favoured over inverted hierarchy at a 3σ level and the \mathcal{CP} phase is constrained at the same level by $.87 < \delta/\pi < 1.94$. There remains the ambiguity in the mixing angle θ_{23} which is near the maximum mixing value ($\sin(2\theta_{23}) \approx 1$), but in which octant ($\theta_{23} \leq \pi/4$ or $\theta_{23} \geq \pi/4$)? Measuring these parameters with precision will be a long process: for example the DUNE collaboration⁹⁷ expects to measure δ to better than 20° and

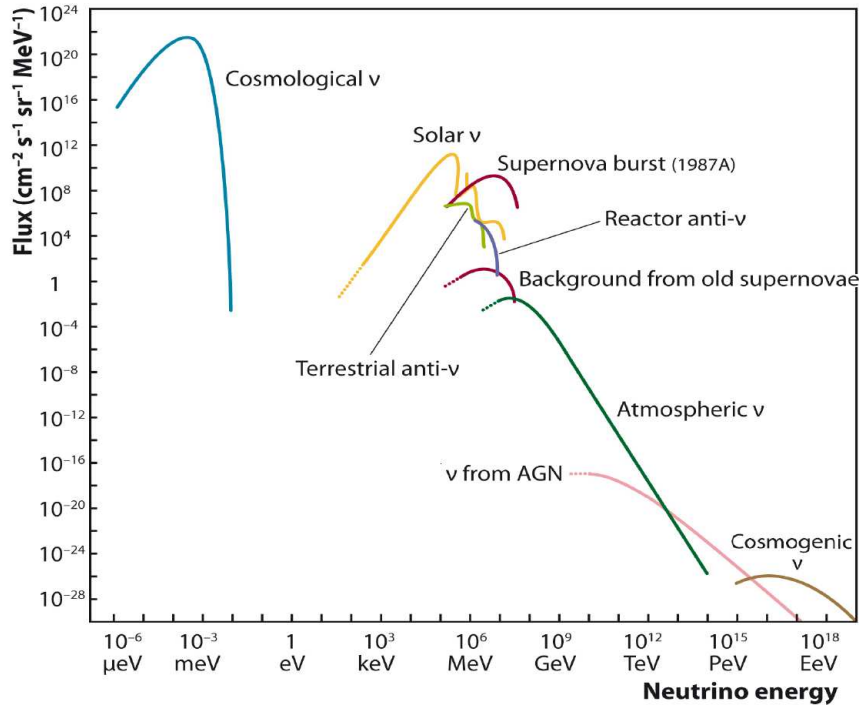


Figure 26: *The measured or expected flux of neutrinos originating from different sources, from C. Spiering, Eur. Phys. J. **H37** (2012) 515, [arXiv:1207.4952]. The range in energy covers 24 orders of magnitude, from μeV to EeV*

resolve the θ_{23} octant with a 5σ significance after 10 years of running. The absolute mass scale of neutrinos is not settled yet although (model dependent) cosmological constraints become stronger and stronger. Also, are neutrinos of Dirac type or of Majorana type (see next section)? Finally there remains the question: are sterile neutrinos necessary? On this last topic progress is soon expected thanks to the future very short baseline reactor data. Despite these open questions, neutrinos are on the verge of becoming useful messengers which will contribute to the understanding of astrophysical

⁹⁷For the DUNE collaboration, N. Grant, PoS(NuFact2017) 052 (2017). DUNE is a long base line oscillation experiment (1300 km) with a highly pure ν_μ beam from FERMILAB and 4 10kt Liquid Argon Time Projection Chambers deep underground in South-Dakota, expected to start operation in 2026.

phenomena and objects such as gamma-ray bursts, supernovae remnants, quasars, blazars, \dots ⁹⁸. As an illustration, in Fig. 26 is summarized in a semi-quantitative way the flux of neutrinos associated to different sources. Notice that there is more than 36 orders of magnitude between the solar neutrino flux and the expected cosmogenic flux.

Neutrinos may also be a signal of dark matter annihilation in the universe⁹⁹.

⁹⁸Astro2020 Science White Paper: Cosmology and Fundamental Physics, K.N. Abazajian *et al.*, arXiv:1903.04333, [astro-ph].

⁹⁹M. Chianese, arXiv:1907.11926, [hep-ph].

15 Majorana neutrinos

A Majorana fermion is a fermion which transforms into itself when applying the charge conjugation operator : a Majorana fermion is its own antiparticle. This is the case if we choose, in eq. (2.6), to identify the operators :

$$b(p) \equiv d(p), \quad b^\dagger(p) \equiv d^\dagger(p) \quad (15.1)$$

so that:

$$\psi^M(x) = \int \frac{d^3p}{(2\pi)^3 2\omega} \left[b(p) u(p) e^{-ip \cdot x} + b^\dagger(p) v(p) e^{ip \cdot x} \right]. \quad (15.2)$$

In the case of a "left-handed" neutrino eq. (3.23),

$$\psi_L(x) = \int \frac{d^3p}{(2\pi)^3 2\omega} \left[b_L(p) u_L(p) e^{-ip \cdot x} + b_R^\dagger(p) v_R(p) e^{ip \cdot x} \right], \quad (15.3)$$

we have using eqs. (B.12) in the appendix, $u_L^c = v_L$, $v_R^c = u_R$,

$$\begin{aligned} \psi_L^c(x) &= \int \frac{d^3p}{(2\pi)^3 2\omega} \left[b_R(p) u_R(p) e^{-ip \cdot x} + b_L^\dagger(p) v_L(p) e^{ip \cdot x} \right] \\ &= \psi_R(x) \end{aligned} \quad (15.4)$$

and defining a Majorana neutrino by

$$\psi^M(x) = \psi_L(x) + \psi_L^c(x), \quad (15.5)$$

one has indeed,

$$\boxed{(\psi^M(x))^c = \psi^M(x)}, \quad (15.6)$$

which satisfies the Majorana condition. A Majorana neutrino has both left-handed and a right-handed components which are related by the \mathcal{C} transformation. A mass for a Majorana neutrino is generated very simply from a term in the lagrangian density such as

$$\bar{\psi}_L^c(x) \psi_L(x) + \bar{\psi}_L(x) \psi_L^c(x) \equiv \bar{\psi}^M(x) \psi^M(x). \quad (15.7)$$

without introduction of an extra right-handed component.

15.1 Majorana mass term for neutrinos

Coming back to the Standard Model with three generations, we recall that we have defined, eq. (12.1),

$$\nu'_L = \begin{pmatrix} \nu_{e_L} \\ \nu_{\mu_L} \\ \nu_{\tau_L} \end{pmatrix},$$

a triplet of left-handed neutrino flavour eigenstates. A Yukawa mass term is defined by¹⁰⁰,

$$\mathcal{L}_{Y_M} = -\frac{1}{2}(\overline{\nu}'^c \mathbf{M} \nu'_L + \overline{\nu}'_L \mathbf{M}^\dagger \nu'^c) \quad (15.8)$$

where \mathbf{M} is a 3×3 complex matrix. One shows first that this matrix is symmetric, $\mathbf{M} = \mathbf{M}^T$. Indeed, from eq. (B.11) in the appendix, and using $i\gamma_2^T = i\gamma_2$,

$$\begin{aligned} \overline{\nu}'^c \mathbf{M} \nu'_L &= \nu'^T i\gamma_2 \gamma_0 \mathbf{M} \nu'_L \\ &= -\nu'^T \mathbf{M}^T \gamma_0 i\gamma_2 \nu'_L = \nu'^T i\gamma_2 \gamma_0 \mathbf{M}^T \nu'_L \end{aligned} \quad (15.9)$$

where the second line is obtained from the first by transposition with a change of sign due to the anticommutation of fermions, which proves the symmetry property of the mass matrix. The complex matrix \mathbf{M} is diagonalised by the matrix \mathbf{S}

$$\mathbf{M} = \mathbf{S}^T \mathbf{m} \mathbf{S}, \quad (15.10)$$

with \mathbf{m} is diagonal with real eigenvalues. Plugging this expression in \mathcal{L}_{Y_M} , the mass term is written

$$\begin{aligned} \mathcal{L}_{Y_M} &= -\frac{1}{2}(\overline{\nu}'^c \mathbf{M} \nu'_L + \overline{\nu}'_L \mathbf{M}^\dagger \nu'^c) = -\frac{1}{2}(\nu'^T i\gamma_2 \gamma_0 \mathbf{S}^T \mathbf{m} \mathbf{S} \nu'_L + \nu'^\dagger \gamma_0 \mathbf{S}^\dagger \mathbf{m} \mathbf{S}^* i\gamma_2 \nu'^*) \\ &= -\frac{1}{2}(\overline{\nu}'^c \mathbf{m} \nu'_L + \overline{\nu}'_L \mathbf{m} \nu'^c), \end{aligned} \quad (15.11)$$

where we have defined

$$\nu'_L = \mathbf{S} \nu'_L \quad \Leftrightarrow \quad \nu'^* = \mathbf{S}^* \nu'^* \quad \Leftrightarrow \quad \nu'^\dagger = \nu'^\dagger \mathbf{S}^\dagger. \quad (15.12)$$

The Yukawa mass term can then be simplified to

$$\mathcal{L}_{Y_M} = -\frac{1}{2} \overline{\nu} \mathbf{m} \nu = -\frac{1}{2} \sum_i m_i \overline{\nu}_i \nu_i \quad (15.13)$$

with $\nu = \nu_L + \nu_L^c$, a triplet of Majorana neutrinos diagonalising the mass term. This shows that one could, in principle, give a mass to neutrinos solely from left-handed neutrinos.

To generate in the Standard Model a mass term by spontaneous symmetry breaking, coupling a left-handed neutrino to its conjugate ν_L^c and a $SU(2)$ scalar doublet field Φ , we turn to sec. 8.3. However a possible candidate like $\overline{\psi}_{e_L} \tilde{\Phi} \nu_L^c$ is not acceptable since is not a singlet under $SU(2)_L \otimes U(1)_Y$: $\overline{\psi}_{e_L} \tilde{\Phi}$ is indeed a singlet but ν_L is a $SU(2)_L$ doublet with a non-vanishing y quantum number. One could introduce a more complicated structure¹⁰¹,

$$\mathcal{L}_{Y_M} = c \overline{\psi}_{e_L} \tilde{\Phi} (\tilde{\Phi} \overline{\psi}_{e_L})^c, \quad (15.14)$$

¹⁰⁰Note the factor 1/2, compared to a Dirac mass term, because ν' and $\overline{\nu}'$ contain the same degrees of freedom.

¹⁰¹S. Weinberg, Phys. Rev. Lett. **43** (1979) 1566.

which after symmetry breaking gives a mass to neutrinos of order $m_\nu \simeq c v^2 \simeq c G_F^{-1}$. Since this term has dimension 5, the coupling c is necessarily of the form $1/\Lambda$, with Λ a large scale introduced to keep the neutrinos very light. But this interaction is not renormalizable and it would require the introduction of new particles to render the theory finite in analogy with what is done to go from the Fermi model to the Standard Model. Therefore, it seems difficult to generate massive neutrinos without introducing new degrees of freedom.

15.2 Neutrino masses and the see-saw mechanism

We restrict the discussion to a one generation model and postulate a very massive right-handed neutrino singlet, N_R , under the gauge group (sterile neutrino since non-interacting with gauge bosons). The Yukawa lagrangian is assumed to have both a Dirac mass term (arising from the usual symmetry breaking mechanism with a scalar field doublet) and a Majorana mass term, coupling the right-handed neutrino to its charge conjugate, of the following form,

$$\begin{aligned}\mathcal{L}_Y &= -m_D \overline{N_R} \nu_L - \frac{1}{2} M_R \overline{N_R} N_R^c + \text{h.c.} \\ &= -\frac{1}{2} (\overline{\nu_L^c} \overline{N_R}) \begin{pmatrix} 0 & m_D \\ m_D & M_R \end{pmatrix} \begin{pmatrix} \nu_L \\ N_R^c \end{pmatrix} + \text{h.c.},\end{aligned}\quad (15.15)$$

where we have used $\overline{\nu_L^c} N_R^c = \overline{N_R} \nu_L$ to recover the first line from the matrix expression of the second one. We assume $m_D \ll M_R$, m_D being of the order of the electroweak symmetry breaking scale and M_R much larger (of the order of a grand unification scale?). The symmetric mass matrix can be diagonalised and, taking into account the hierarchy of the two mass scales, one finds eigenvalues approximately equal to $-m_D^2/M_R$ and M_R . To make both eigenvalues positive we rather write

$$\begin{pmatrix} 0 & m_D \\ m_D & M_R \end{pmatrix} \approx \begin{pmatrix} i & \rho \\ -i\rho & 1 \end{pmatrix} \begin{pmatrix} \rho^2 M_R & 0 \\ 0 & M_R \end{pmatrix} \begin{pmatrix} i & -i\rho \\ \rho & 1 \end{pmatrix}\quad (15.16)$$

with $\rho = m_D/M_R \ll 1$, so that the eigenstates of the mass matrix are

$$\begin{aligned}\nu_{1L} &= i(\nu_L - \rho N_R^c) \\ N_{1L} &= \rho \nu_L + N_R^c \simeq N_R^c,\end{aligned}\quad (15.17)$$

and the Yukawa term can be written

$$\begin{aligned}\mathcal{L}_Y &= -\frac{1}{2} (\overline{\nu_{1L}^c} \overline{N_{1L}}) \begin{pmatrix} \rho^2 M_R & 0 \\ 0 & M_R \end{pmatrix} \begin{pmatrix} \nu_{1L} \\ N_{1L}^c \end{pmatrix} + \text{h.c.} \\ &= -\frac{1}{2} \rho^2 M_R \overline{\nu_1} \nu_1^c - \frac{1}{2} M_R \overline{N_1} N_1^c,\end{aligned}\quad (15.18)$$

after introducing the Majorana neutrinos

$$\nu_1 = \nu_{1L} + \nu_{1L}^c, \quad N_1 = N_{1L} + N_{1L}^c. \quad (15.19)$$

To summarize, from a light left-handed "Dirac" neutrino and a heavy right-handed "Majorana" neutrino, the symmetric mass matrix of type eq. (15.15), can be diagonalised leading to two Majorana neutrinos, a light one, ν_1 with mass $\rho^2 M_R$, and a heavy one with mass M_R . The light left-handed neutrino ν_{1L} has a small mixing component with the heavy neutrino which could in principle be produced at the LHC, if its mass is not too high.

The procedure above can be generalised to the three generations of the Standard Model. One of the simplest way (type I see-saw) is to introduce three right-handed heavy neutrinos, N_{Ri} , singlets under the gauge group, similar to what is done for charged leptons, and add in the Yukawa Lagrangian, besides the term coupling to the scalar doublet field Φ , a Majorana mass term for the N_{Ri} 's:

$$\mathcal{L}_Y = -\frac{1}{2} \sum_{i=1,2,3} M_{Ri} \overline{N_{Ri}^c} N_{Ri} - \sum_{\substack{\alpha=e,\mu,\tau \\ i=1,2,3}} c_{\alpha i} \overline{\psi}_{\alpha L} \tilde{\Phi} N_{Ri} + \text{h.c.} . \quad (15.20)$$

The second term $c_{\alpha i}(\overline{\nu}_L \Phi^0 - \overline{e}_L \Phi^-) N_{Ri}$, after symmetry breaking, generates Dirac mass parameters $m_{D\alpha i} = c_{\alpha i} v / \sqrt{2}$. The Yukawa term can be written in a matrix form identical to eq. (15.15) where

$$(\nu_L^T \ N_R^{cT}) = (\nu_{L_e}^T \ \nu_{L_\mu}^T \ \nu_{L_\tau}^T \ N_{R1}^{cT} \ N_{R2}^{cT} \ N_{R3}^{cT}) \quad (15.21)$$

is the transpose of a six-component spinor and the mass matrix

$$\mathcal{M} = \begin{pmatrix} 0 & m_D \\ m_D^T & M_R \end{pmatrix} \quad (15.22)$$

is a 6×6 matrix constructed from the 3×3 matrix m_D with elements $m_{D\alpha i}$ and M_R a 3×3 diagonal matrix with elements M_{Ri} . This symmetric matrix \mathcal{M} can be diagonalised yielding 3 light eigenvalues of order

$$m_\nu \simeq -m_D M_R^{-1} m_D^T \quad (15.23)$$

and 3 heavy ones. The associated eigenstates are Majorana neutrinos. Introducing these mass eigenstates in the charged current interactions term will yield a **PMNS** mixing matrix exactly as before, in the case of Dirac neutrinos. There is a difference however since it is not allowed to rotate away the phases of the neutrino fields¹⁰²: the phase of a Majorana neutrino is fixed by the condition

¹⁰²J. Bernabeu, P. Pascual, Nucl. Phys. **B228** (1983) 21; S.T. Petcov, Adv. High Energy Phys. 2013 (2013) 852987, arXiv:1303.5819 [hep-ph] .

$\nu_i^c = \mathcal{C}\gamma_0\nu_i^* = \nu_i$. In the expression of the charged current lagrangian, eq. (12.8), only the phases of the charged lepton fields can be changed, $e_{\alpha L} \rightarrow e^{-i\phi_{e\alpha}} e_{\alpha L}$, so that the **PMNS** matrix elements $(\mathbf{S}_\nu^\dagger)_{\alpha j}$ become $e^{-i\phi_{e\alpha}} (\mathbf{S}_\nu^\dagger)_{\alpha j}$ (see the discussion after eq. (11.11)). These three arbitrary phases are used to absorb three phases of the **PMNS** matrix, which can be written in the form, see eq. (11.12),

$$\mathbf{PMNS} = \begin{pmatrix} c_{12}c_{13} & s_{12}c_{13} & s_{13}e^{-i\delta} \\ -s_{12}c_{23} - c_{12}s_{23}e^{i\delta} & c_{12}c_{23} - s_{12}e^{i\delta}s_{23} & s_{23}c_{13} \\ s_{12}s_{23} - c_{12}c_{23}e^{i\delta} & -c_{12}s_{23} - s_{12}c_{23}e^{i\delta} & c_{23}c_{13} \end{pmatrix} \begin{pmatrix} 1 & 0 & 0 \\ 0 & e^{i\alpha_1} & 0 \\ 0 & 0 & e^{i\alpha_2} \end{pmatrix}, \quad (15.24)$$

with three angles and three phases: the \mathcal{CP} phase δ and the 2 Majorana phases $0 < \alpha_1 < 2\pi$ and $0 < \alpha_2 < 2\pi$. The pattern of oscillations of Majorana neutrinos is the same as that of Dirac neutrinos since the combination which controls the change of flavour (see eq. (12.9)),

$$U_{\alpha i} U_{\alpha j}^* U_{\beta i}^* U_{\beta j},$$

in eq. (12.17) is independent of the form of the **PMNS** matrix, eqs. (11.12) or (15.24), and it is not possible from the study of oscillations to distinguish Majorana from Dirac neutrinos.

If one considers a global phase change on all left-handed fields

$$\nu'_{iL}(x) = e^{i\Lambda} \nu_{iL}(x) \quad \Leftrightarrow \quad \chi'_{iL}(x) = e^{i\Lambda} \chi_{iL}(x); \quad l'(x) = e^{i\Lambda} l(x), \quad (15.25)$$

the gauge interaction part remains invariant but this is not the case for the Yukawa term in the lagrangian since the right-handed fields are not independent and one has

$$\overline{\nu}'_L(x) = e^{i\Lambda} \overline{\nu}_L(x). \quad (15.26)$$

Invariance under the global phase change eq. (15.25) is associated to lepton number conservation $L = L_e + L_\nu + L_\tau$. In the presence of a Yukawa mass term, the invariance is lost and the lepton number is not conserved: it is possible to have nuclear transitions with emission of two electrons without neutrino

$$(A, Z) \rightarrow (A, Z + 2) + e^- + e^-, \quad (15.27)$$

i.e. a neutrinoless double-beta decay $\{0\nu\beta\beta\}$. This is illustrated in fig. 27. In a first beta decay in a nucleus, a $\overline{\nu}_e$ is produced which turns into a ν_e via the Majorana Yukawa mass term eq. (15.8) followed by the reaction $\nu_e + n \rightarrow e^- + p$. The rate of transition is minute : proportional the $G_F^4 m_\nu^2$ the fourth power of Fermi constant and the square of the neutrino mass ! Several experiments (CUORE¹⁰³,

¹⁰³CUORE Collaboration, K. Alfonso *et al.*, Phys. Rev. Lett. **115** (2015) 102502.

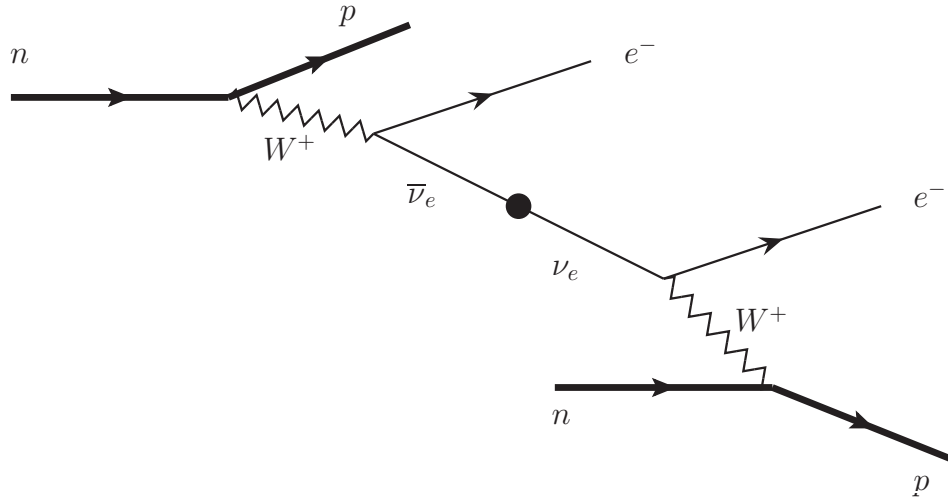


Figure 27: $\{0\nu\beta\beta\}$ decay: neutrinoless double-beta decay.

NEMO¹⁰⁴, KamLAND-Zen¹⁰⁵, SNO+¹⁰⁶, SuperNEMO¹⁰⁷) have searched, are searching or will search for this process which is essentially the unique signature of the Majorana nature of the neutrinos¹⁰⁸.

¹⁰⁴NEMO Collaboration, R. Arnold *et al.*, Phys. Rev. **D89** (2014) 111101.

¹⁰⁵KamLAND-Zen Collaboration, A. Gando *et al.*, Phys. Rev. Lett. **110** (2013) 062502.

¹⁰⁶SNO+ Collaboration, S. Andringa, *et al.*, Adv. High Energy Phys. **2016** (2016) 6194250, arXiv:1508.05759 [physics.ins-det].

¹⁰⁷NEMO-3 Collaboration, R. Arnold *et al.*, Phys. Rev. **D92** (2015) 072011.

¹⁰⁸For a review on neutrinoless double β decay, see Stefano Dell’Oro *et al.*, Adv. High Energy Phys. **2016** (2016) 2162659, arXiv:1601.07512 [hep-ph].

16 Conclusions

Putting all together, the lagrangian which contains the dynamics of particle physics, as described by the Standard Model, is decomposed into (not including gauge fixing terms)

$$\mathcal{L} = \mathcal{L}_{QCD} + \mathcal{L}_G + \mathcal{L}_F + \mathcal{L}_S + \mathcal{L}_Y$$

where each piece has been previously defined. If one attempts to count the number of parameters we arrive at:

- $SU(3)$ (QCD) gauge invariance: 1 coupling g_s or α_s which is rather precisely determined by an enormous amount of data in deep-inelastic scattering, proton-proton, proton-antiproton or more generally hadron-hadron collisions, $e^+ + e^- \rightarrow jets$ as well as, at low energy, hadronic τ decays¹⁹ : $\alpha_s(M_Z^2) = 0.1181 \pm 0.0011$ in the \overline{MS} renormalisation scheme with 5 active flavours.

- $SU(2)_L \otimes U(1)_Y$ gauge invariance: two couplings g, g' , and the weak mixing angle θ_w : in fact one coupling e , the charge of the proton/electron and the angle because of the relation $g \sin \theta_w = g' \cos \theta_w = e$. One has $\alpha = 1/(137.035999139 \pm 0.000000031)$ and $\sin \theta_w = M_W/M_Z$ with $M_W = 80.385 \pm 0.015$ GeV, $M_Z = 91.1876 \pm 0.0021$ GeV.

- spontaneous symmetry breaking from \mathcal{L}_S : two parameters μ and h or rather the vacuum expectation value v and h determined, for example, from $v = M_W \sin \theta_w / \sqrt{\pi \alpha}$ and $h = 0.5 M_H^2 / v^2$ with $M_H = 125.09 \pm 0.24$ GeV¹⁰⁹.

- Yukawa couplings in \mathcal{L}_Y : nine couplings, i.e. one coupling per lepton and quark species and four CKM parameters for the mixing between quark generations. The Yukawa couplings are determined from the masses $m_e = 0.510998946$ MeV, $m_\mu = 105.6583745$ MeV, $m_\tau = 1.7768$ GeV, $m_u = 2.2$ MeV, $m_d = 4.7$ MeV, $m_s = 96$ MeV, $m_c = 1.27$ GeV, $m_b = 4.18$ GeV, $m_t = 173.2$ GeV. Massive neutrinos of Dirac type require seven new parameters.

There are thus 25 parameters assuming Dirac neutrinos (27 with Majorana neutrinos), most of them related to the fermions, which is not a satisfactory situation for a minimal model! However the model is strongly constrained since there are no less than 68 vertices of various types expressed in terms of the above parameters. Any persistent deviation from the predicted values in the Standard Model will indicate new physics. Checking experimentally the value of these couplings is one of the tasks of particle physicists.

¹⁰⁹Combined Measurement of the Higgs Boson Mass with the ATLAS and CMS Experiments, G. Aad, et al., arXiv:1503.07589.

The large number of parameters has prompted an intensive continuing search for higher hidden symmetries such as supersymmetry, for example, and Minimal Supersymmetric Standard Models and Next-to-Minimal Supersymmetric Standard Models and \dots have been constructed. The very unfortunate situation is that in such models the number of fields is more than doubled compared to the Standard Model as no supersymmetric multiplets can be filled with only known particles. Furthermore, while in principle supersymmetry breaking can in turn trigger electroweak symmetry breaking, one does not know yet how supersymmetry is dynamically broken. Thus one is led to describe it in a effective way which requires many more parameters than in the Standard Model. It seems that, at present, the remedy is worse than the disease but there are still hopes

Appendices

A Properties of γ^μ matrices

In Dirac representation γ^μ matrices are defined by:

$$\gamma^0 = \begin{pmatrix} \mathbb{1}_2 & 0 \\ 0 & -\mathbb{1}_2 \end{pmatrix}, \quad \gamma^i = \begin{pmatrix} 0 & \tau^i \\ -\tau^i & 0 \end{pmatrix}, \quad (\text{A.1})$$

where the τ^i are the Pauli matrices:

$$\tau^1 = \begin{pmatrix} 0 & 1 \\ 1 & 0 \end{pmatrix}, \quad \tau^2 = \begin{pmatrix} 0 & -i \\ i & 0 \end{pmatrix}, \quad \tau^3 = \begin{pmatrix} 1 & 0 \\ 0 & -1 \end{pmatrix}, \quad (\text{A.2})$$

The Pauli matrices are hermitian and they satisfy:

$$\left[\frac{\tau_i}{2}, \frac{\tau_j}{2} \right] = i \epsilon_{ijk} \frac{\tau_k}{2}, \quad \text{Tr}(\tau_i \tau_j) = 2 \delta_{ij} \quad (\text{A.3})$$

The matrices γ^μ have the following properties:

$$\gamma^0 \gamma^{\mu\dagger} \gamma^0 = \gamma^\mu, \quad \gamma^{0^2} = \mathbb{1}_4, \quad \gamma^{i^2} = -\mathbb{1}_4, \quad \sum_{\mu} \gamma_{\mu} \gamma^{\mu} = 4 \mathbb{1}_4, \quad \mu = 0, 1, 2, 3. \quad (\text{A.4})$$

They satisfy anticommutation relations:

$$\{\gamma^\mu, \gamma^\nu\} = 2 g^{\mu\nu} \mathbb{1}_4. \quad (\text{A.5})$$

The matrix γ_5 is defined by:

$$\gamma_5 = \gamma^5 = i \gamma^0 \gamma^1 \gamma^2 \gamma^3 \quad \gamma^5 = \begin{pmatrix} 0 & \mathbb{1}_2 \\ \mathbb{1}_2 & 0 \end{pmatrix}. \quad (\text{A.6})$$

It anticommutes with γ^μ matrices:

$$\{\gamma^5, \gamma^\nu\} = 0, \quad \mu = 0, 1, 2, 3. \quad (\text{A.7})$$

One proves easily:

$$\begin{aligned} & \bullet \quad \gamma_{\mu} \gamma_{\alpha} \gamma^{\mu} = -2 \gamma_{\alpha} \\ & \bullet \quad \gamma_{\mu} \gamma_{\alpha} \gamma_{\beta} \gamma^{\mu} = 4 g_{\alpha\beta} \mathbb{1}_4 \\ & \bullet \quad \gamma_{\mu} \gamma_{\alpha} \gamma_{\beta} \gamma_{\delta} \gamma^{\mu} = -2 \gamma_{\delta} \gamma_{\beta} \gamma_{\alpha}. \end{aligned} \quad (\text{A.8})$$

For the evaluation of traces of products $\gamma^\alpha \gamma^\beta \dots$ one has the following relations :

$$\begin{aligned}
\text{Tr}(\gamma^\alpha \gamma^\beta) &= 4 g^{\alpha\beta} \\
\text{Tr}(\gamma^\alpha \gamma^\beta \gamma^\delta \gamma^\lambda) &= 4 [g^{\alpha\beta} g^{\delta\lambda} - g^{\alpha\delta} g^{\beta\lambda} + g^{\alpha\lambda} g^{\beta\delta}] \\
\text{Tr}(\gamma^\alpha \gamma^\beta \dots) &= 0 \quad \text{for an odd number of matrices} \\
\text{Tr}(\gamma^5 \gamma^\alpha \gamma^\beta \dots) &= 0 \quad \text{for an odd number of } \gamma^\alpha \text{ matrices} \\
\text{Tr}(\gamma^5 \gamma^\alpha \gamma^\beta) &= 0 \\
\text{Tr}(\gamma^5 \gamma^\alpha \gamma^\beta \gamma^\delta \gamma^\lambda) &= -4i \epsilon^{\alpha\beta\delta\lambda},
\end{aligned} \tag{A.9}$$

where $\epsilon^{\alpha\beta\delta\lambda}$ is the totally antisymmetric tensor under permutation of its indices with $\epsilon^{0123} = +1$. One has $\epsilon_{\alpha\beta\delta\lambda} = -\epsilon^{\alpha\beta\delta\lambda}$ and in particular $\epsilon_{0123} = -1$. A useful relation is:

$$\epsilon_{\mu\nu\alpha\beta} \epsilon^{\rho\sigma\alpha\beta} = -2(\delta_\mu^\rho \delta_\nu^\sigma - \delta_\nu^\rho \delta_\mu^\sigma) \tag{A.10}$$

There exists other representations due to Weyl and to Majorana which satisfy the relations eq. (A.5) to eq. (A.9). In general, when doing calculations, the explicit form of γ^μ matrices is not necessary.

B Charge conjugation \mathcal{C} , space reflection \mathcal{P} , time reversal \mathcal{T}

B.1 Charge conjugation \mathcal{C}

A fermion (electron) of charge e obeys the Dirac equation

$$((i\partial_\mu - eA_\mu)\gamma^\mu - m)\psi = 0. \quad (\text{B.1})$$

Looking for a plane wave solution of type eq. (2.6) we obtain

$$\begin{aligned} (\not{p} - e\not{A} - m)u_\alpha(p) &= 0, \quad \text{for positive energy solutions,} \\ (\not{p} + e\not{A} + m)v_\alpha(p) &= 0, \quad \text{for negative energy solutions,} \end{aligned}$$

which suggests to interpret the negative energy solution as a positive energy one with charge $-e$, *i.e.* the antiparticle (positron). The wave function of the positron should thus satisfy the same equation as the electron with an opposite charge

$$((i\partial_\mu + eA_\mu)\gamma^\mu - m)\psi^c = 0. \quad (\text{B.2})$$

The solution ψ^c can be constructed in the following way. From the first equation above one has

$$(-(i\partial_\mu + eA_\mu)\gamma^{\mu*} - m)\psi^* = 0. \quad (\text{B.3})$$

We look for ψ^c under the form

$$\boxed{\psi^c = \mathcal{C}\gamma^0\psi^*}, \quad (\text{B.4})$$

where \mathcal{C} is a 4×4 matrix. Then eq. (B.3) yields after multiplication on the left by $\mathcal{C}\gamma^0$:

$$(\mathcal{C}\gamma^0)(-(i\partial_\mu + eA_\mu)\gamma^{\mu*} - m)(\mathcal{C}\gamma^0)^{-1}\psi^c = 0, \quad (\text{B.5})$$

and, if one finds a matrix \mathcal{C} such that:

$$(\mathcal{C}\gamma^0)\gamma^{\mu*} = -\gamma^\mu(\mathcal{C}\gamma^0), \quad (\text{B.6})$$

then we recover eq. (B.2). In our representation of γ_μ matrices, we have

$$\gamma^{\mu*} = \gamma^\mu, \quad \mu = 0, 1, 3; \quad \gamma^{\mu*} = -\gamma^\mu, \quad \mu = 2, \quad (\text{B.7})$$

so that the choice of the real matrix

$$\boxed{(\mathcal{C}\gamma^0) = i\gamma^2} \Leftrightarrow \boxed{\mathcal{C} = i\gamma^2\gamma^0} \quad (\text{B.8})$$

satisfy the condition (B.6) which is equivalent to:

$$\gamma_2 \gamma_\mu \gamma_2 = \gamma_\mu^* \quad (\text{B.9})$$

Using the relations eqs. (A.4) and (A.5), it is easy to prove

$$\mathcal{C} = -\mathcal{C}^{-1} = -\mathcal{C}^\dagger = -\mathcal{C}^T \quad \text{and} \quad \mathcal{C} \gamma^5 \mathcal{C}^{-1} = \gamma^5 \Leftrightarrow \gamma_2 \gamma_5 \gamma_2 = \gamma_5. \quad (\text{B.10})$$

Under charge conjugation, the wave function ψ which satisfies eq. (B.1) becomes

$$\boxed{\psi^c = \mathcal{C} \gamma^0 \psi^* = \mathcal{C} \bar{\psi}^T = i \gamma^2 \psi^* \quad \Leftrightarrow \quad \bar{\psi}^c = i \psi^T \gamma_2 \gamma_0,} \quad (\text{B.11})$$

solution of eq. (B.2).

Let us first discuss free massless chiral spinors, eqs. (3.28) and (3.30), important in the construction of the Standard Model. The application of \mathcal{C} parity yields:

$$\begin{aligned} (u_L)^c(p) &= \mathcal{C} \gamma_0 u_L^*(p) = i \gamma_2 u_L^*(p) = \sqrt{\omega} i \gamma_2 \begin{pmatrix} \chi_L^* \\ -\chi_L^* \end{pmatrix} = -\sqrt{\omega} \begin{pmatrix} \chi_R \\ \chi_R \end{pmatrix} = v_L(p) \\ (u_R)^c(p) &= \mathcal{C} \gamma_0 u_R^*(p) = i \gamma_2 u_R^*(p) = \sqrt{\omega} i \gamma_2 \begin{pmatrix} \chi_R^* \\ \chi_R^* \end{pmatrix} = \sqrt{\omega} \begin{pmatrix} -\chi_L \\ \chi_L \end{pmatrix} = v_R(p), \end{aligned} \quad (\text{B.12})$$

and thus, the \mathcal{C} operator transforms the wave-function of a positive energy spinor (electron) into the wave-function of a negative energy one (positron) of the same helicity (similar relations exist for $(v_L)^c$ and $(v_R)^c$). Recalling the definition of $\psi_L(x)$, eq. (3.23),

$$\psi_L(x) = \int \frac{d^3 p}{(2\pi)^3 2\omega} \left[b_L(p) u_L(p) e^{-ip \cdot x} + d_R^\dagger(p) v_R(p) e^{ip \cdot x} \right]$$

its \mathcal{C} transformed is:

$$(\psi_L)^c(x) = \int \frac{d^3 p}{(2\pi)^3 2\omega} \left[d_R(p) u_R(p) e^{-ip \cdot x} + b_L^\dagger(p) v_L(p) e^{ip \cdot x} \right], \quad (\text{B.13})$$

which destroys a right-handed antifermion with wave-function $u_R(p)$ and creates a left-handed fermion with $v_L(p)$. Equivalently, in a compact form, if one writes $\psi_L = (1 - \gamma^5)\psi/2$, its charge conjugate is:

$$(\psi_L)^c = i \gamma^2 \psi_L^* = \frac{1 + \gamma^5}{2} i \gamma^2 \psi^* = \frac{1 + \gamma^5}{2} \psi^c = (\psi^c)_R, \quad (\text{B.14})$$

a right-handed wave-function. Likewise the \mathcal{C} conjugate of a right-handed wave-function is left-handed

$$(\psi_R)^c = \frac{1 - \gamma^5}{2} \psi^c = (\psi^c)_L. \quad (\text{B.15})$$

Going back to the general case, it is easy to show that under \mathcal{C} parity the helicity projection operators satisfy:

$$i\gamma_2 \Sigma^{\pm*}(s) = i\gamma_2 \frac{(1 \pm \gamma_5 \not{s}^*)}{2} = \frac{(1 \pm \gamma_5 \not{s})}{2} i\gamma_2 = \Sigma^{\pm}(s) i\gamma_2,$$

and the energy projection operators satisfy:

$$i\gamma_2 \Lambda^{\pm*}(p) = i\gamma_2 \frac{\pm \not{p}^* + m}{2} = \frac{\mp \not{p} + m}{2} i\gamma_2 = \Lambda^{\mp}(p) i\gamma_2,$$

where one has used the relations eq. (B.7). Thus, a solution of the Dirac equation of positive (resp. negative) energy and given helicity becomes a solution of negative (resp. positive) energy of the same helicity:

$$i\gamma_2 \Sigma^{\pm*}(s) \Lambda^{\pm*}(p) \psi^*(p, x) = \Sigma^{\pm}(s) \Lambda^{\mp}(p) \psi^c(p, x), \quad (\text{B.16})$$

It is useful to list the transformation of fermion bilinears under \mathcal{C} . They easily derived from eqs.(B.9) to (B.11), remembering the $-$ sign (due to Fermi statistics) when transposing the expressions to obtain the right hand-side, and one finds:

$$\begin{aligned} \overline{\psi}_2^c(x) \psi_1^c(x) &= \overline{\psi}_1(x) \psi_2(x), \\ \overline{\psi}_2^c(x) \gamma^5 \psi_1^c(x) &= \overline{\psi}_1(x) \gamma^5 \psi_2(x), \\ \overline{\psi}_2^c(x) \gamma^\nu \psi_1^c(x) &= -\overline{\psi}_1(x) \gamma^\nu \psi_2(x), \\ \overline{\psi}_2^c(x) \gamma^\nu \gamma^5 \psi_1^c(x) &= \overline{\psi}_1(x) \gamma^\nu \gamma^5 \psi_2(x). \end{aligned} \quad (\text{B.17})$$

B.2 Space reflection \mathcal{P}

The space reflection, or parity transformation is defined by :

$$x_0 \rightarrow x'_0 = x_0, \quad \mathbf{x} \rightarrow \mathbf{x}' = -\mathbf{x}. \quad (\text{B.18})$$

The transformation is parameterised in the following way

$$x'^\nu = a^\nu_\mu x^\mu \quad \text{with} \quad a^\nu_\mu = \begin{pmatrix} 1 & 0 & 0 & 0 \\ 0 & -1 & 0 & 0 \\ 0 & 0 & -1 & 0 \\ 0 & 0 & 0 & -1 \end{pmatrix}. \quad (\text{B.19})$$

Knowing $\psi(x_0, \mathbf{x})$ satisfying the free Dirac equation, we look for the form of the solution obtained under a space reflection. We write

$$\psi'(x_0, \mathbf{x}') = \psi'(x_0, -\mathbf{x}) = \mathcal{P} \psi(x_0, \mathbf{x}), \quad \text{thus} \quad \psi(x_0, \mathbf{x}) = \mathcal{P}^{-1} \psi'(x_0, -\mathbf{x}) \quad (\text{B.20})$$

From the free Dirac equation

$$(i\frac{\partial}{\partial x^\mu}\gamma^\mu - m)\psi(x_0, \mathbf{x}) = 0, \quad (\text{B.21})$$

we obtain, using

$$\frac{\partial}{\partial x^\mu} = \frac{\partial}{\partial x'^\nu} \frac{\partial x'^\nu}{\partial x^\mu} = \frac{\partial}{\partial x'^\nu} a_\mu^\nu, \quad (\text{B.22})$$

$$(i\frac{\partial}{\partial x^\mu}\gamma^\mu - m)\mathcal{P}^{-1}\psi'(x_0, \mathbf{x}') = (i\frac{\partial}{\partial x'^\nu} a_\mu^\nu \gamma^\mu - m)\mathcal{P}^{-1}\psi'(x_0, \mathbf{x}') = 0, \quad (\text{B.23})$$

which leads to

$$(i\frac{\partial}{\partial x'^\nu} a_\mu^\nu \mathcal{P}\gamma^\mu\mathcal{P}^{-1} - m)\psi'(x_0, \mathbf{x}') = 0. \quad (\text{B.24})$$

If we find a matrix \mathcal{P} such that $a_\mu^\nu \mathcal{P}\gamma^\mu = \gamma^\nu\mathcal{P}$, then $\psi'(x_0, \mathbf{x}')$ will be a solution. Such a matrix should commute with γ^0 and anticommute with $\vec{\gamma}$. Obviously

$$\boxed{\mathcal{P} = e^{i\phi}\gamma^0} \quad (\text{B.25})$$

has such a property. Thus

$$\psi'(x_0, \mathbf{x}') = e^{i\phi}\gamma^0\psi(x_0, \mathbf{x}), \quad \bar{\psi}'(x_0, \mathbf{x}') = e^{-i\phi}\psi^\dagger(x_0, \mathbf{x}). \quad (\text{B.26})$$

Note that the parity operator reverses the fermion helicity. Thus a massless left-handed fermion becomes right-handed:

$$\begin{aligned} \mathcal{P}\psi_L(x_0, \mathbf{x}) &= \gamma_0 \frac{1 - \gamma_5}{2} \psi(x_0, \mathbf{x}) \\ &= \frac{1 + \gamma_5}{2} \psi'(x_0, \mathbf{x}') = \psi'_R(x_0, \mathbf{x}') \end{aligned} \quad (\text{B.27})$$

(where for simplicity we ignore an irrelevant phase). In terms of Dirac spinors one has:

$$\gamma_0 u(\mathbf{p}) = u(-\mathbf{p}), \quad \gamma_0 v(\mathbf{p}) = -v(-\mathbf{p}), \quad (\text{B.28})$$

as can be immediatly verified from eqs (3.12). It is easy to check the behavior of the fermion bilinears under a parity transformation:

$$\begin{aligned} \overline{\psi}'_2(x_0, \mathbf{x}')\psi'_1(x_0, \mathbf{x}') &= \overline{\psi}_2(x_0, \mathbf{x})\psi_1(x_0, \mathbf{x}), \quad \text{a scalar} \\ \overline{\psi}'_2(x_0, \mathbf{x}')\gamma^5\psi'_1(x_0, \mathbf{x}') &= -\overline{\psi}_2(x_0, \mathbf{x})\gamma^5\psi_1(x_0, \mathbf{x}), \quad \text{a pseudoscalar} \\ \overline{\psi}'_2(x_0, \mathbf{x}')\gamma^\nu\psi'_1(x_0, \mathbf{x}') &= a_\mu^\nu\overline{\psi}_2(x_0, \mathbf{x})\gamma^\mu\psi_1(x_0, \mathbf{x}), \quad \text{a vector} \\ \overline{\psi}'_2(x_0, \mathbf{x}')\gamma^\nu\gamma^5\psi'_1(x_0, \mathbf{x}') &= -a_\mu^\nu\overline{\psi}_2(x_0, \mathbf{x})\gamma^\mu\gamma^5\psi_1(x_0, \mathbf{x}), \quad \text{a pseudovector or axial vector} \end{aligned} \quad (\text{B.29})$$

B.3 Variance and invariance of the lagrangien under \mathcal{C} and \mathcal{CP}

From the above discussion, it is easy to obtain the transformation properties of the lagrangien. The easiest case is that of QED:

$$\mathcal{L}_{QED} = \bar{\psi}(x)(i\cancel{\partial} - e\cancel{A}(x) - m)\psi(x). \quad (\text{B.30})$$

Under \mathcal{P} all vectors such as $x'_\mu, \partial'_\mu, A'_\mu(x')$ transform as $a'_\mu x_\nu, a'_\mu \partial_\nu, a'_\mu A_\nu(x)$ and $\bar{\psi}'(x_0, \mathbf{x}')\gamma^\mu\psi'(x_0, \mathbf{x}') \rightarrow a'_\nu \bar{\psi}(x_0, \mathbf{x})\gamma^\nu\psi(x_0, \mathbf{x})$ so that

$$\bar{\psi}'(x')(i\cancel{\partial}' - e\cancel{A}'(x') - m)\psi'(x') \quad (\text{B.31})$$

reduces to the lagrangien above. The transformation is also very simple under \mathcal{C} . The $U(1)$ gauge transformation, $\psi'(x) \rightarrow \exp(-ie\alpha(x))\psi(x)$, implies $\psi^c(x) \rightarrow \exp(ie\alpha(x))\psi^c(x)$ and the $U(1)$ gauge invariance of \mathcal{L}_{QED} leads to $A'_\mu(x) = -A_\mu(x)$ (use eqs. (B.17) to prove the invariance). For the derivative term it is a bit more tricky since

$$\begin{aligned} \bar{\psi}^c(x) i\cancel{\partial} \psi^c(x) &= \bar{\psi}^c(x) i\gamma^\mu \overrightarrow{\partial}_\mu \psi^c(x) = \psi^T(x)\gamma_0 i\gamma^{\mu*} \overrightarrow{\partial}_\mu \psi^*(x) \\ &= -\psi^\dagger(x) \overleftarrow{\partial}_\mu i\gamma^{\mu\dagger} \gamma_0 \psi(x) = -\psi^\dagger(x) \overleftarrow{\partial}_\mu \gamma_0 i\gamma^\mu \psi(x) \\ &= \bar{\psi}(x) i\gamma^\mu \overrightarrow{\partial}_\mu \psi(x) = \bar{\psi}(x) i\cancel{\partial} \psi(x). \end{aligned} \quad (\text{B.32})$$

One goes from the first to the second line by transposing the expression keeping in mind the - sign for the anticommutation of the fermions and from the second line to the last one by a partial integration neglecting, as usual, a total derivative. This proves the invariance of the QED lagrangian under \mathcal{C} , \mathcal{P} and therefore \mathcal{CP} transformations.

On the contrary a theory with an interaction term of the form $\bar{\psi}(x)\gamma^\mu(1 - \gamma_5)\psi(x)$ is not invariant under \mathcal{C} or \mathcal{P} since this term becomes, up to an overall sign, $\bar{\psi}(x)\gamma^\mu(1 + \gamma_5)\psi(x)$ (use eqs. (B.17) and (B.29)), and one can say that there is maximum violation of these symmetries. However it is invariant under \mathcal{CP} . The case of the Standard Model with three generations is a bit more subtle. Consider the charged current piece eq. (11.9) written in the mass eigenstate basis. Denoting \mathbf{V} the **CKM** matrix, with $\mathbf{V}_{ij} = v_{ij}$, $\mathbf{V}_{ji}^\dagger = v_{ij}^*$, the charged current is written:

$$\begin{aligned} \mathcal{L}_F(\text{charged current}) &= \frac{e}{\sqrt{2} \sin \theta_w} [\bar{\mathbf{u}}_L W_\mu^* \gamma^\mu \mathbf{V} \mathbf{d}_L + \bar{\mathbf{d}}_L \mathbf{V}^\dagger W_\mu \gamma^\mu \mathbf{u}_L] \\ &= \frac{e}{\sqrt{2} \sin \theta_w} [v_{ij} \bar{u}_L^j W_\mu^* \gamma^\mu d_L^i + v_{ij}^* \bar{d}_L^j W_\mu \gamma^\mu u_L^i] \\ &= \frac{e}{2\sqrt{2} \sin \theta_w} [v_{ij} \bar{u}^i W_\mu^* \gamma^\mu (1 - \gamma_5) d^j + v_{ij}^* \bar{d}^j W_\mu \gamma^\mu (1 - \gamma_5) u^i], \end{aligned} \quad (\text{B.33})$$

where the index i, j run over the number of fermion generations. If ψ is in the fundamental representation of the unitary group \mathbf{G} , with generators τ^a the generators operating on the ψ^c fields are τ^{a*} and the conjugate of the gauge boson is $\mathbf{W}_\mu^c = -W_\mu^a \tau^{a*} = -\mathbf{W}_\mu^*$, so that $W_\mu \leftrightarrow -W_\mu^*$ under \mathcal{C} parity (with the definition of W_μ given after eq. (5.43)). Under charge conjugation, \mathcal{L}_F becomes:

$$\begin{aligned} \mathcal{L}_F^{\mathcal{C}}(\text{charged current}) &= \frac{e}{2\sqrt{2}\sin\theta_W} [v_{ij}\bar{u}^{ci} W_\mu^{c*} \gamma^\mu (1 - \gamma_5) d^{cj} + v_{ij}^* \bar{d}^{cj} W_\mu^c \gamma^\mu (1 - \gamma_5) u^{ci}] \\ &= \frac{e}{2\sqrt{2}\sin\theta_W} [v_{ij}\bar{d}^j W_\mu \gamma^\mu (1 + \gamma_5) u^i + v_{ij}^* \bar{u}^i W_\mu^* \gamma^{\mu*} (1 + \gamma_5) d^j], \end{aligned} \quad (\text{B.34})$$

where we have used eqs. (B.17). If we do furthermore a \mathcal{P} transformation on this expression we obtain:

$$\mathcal{L}_F^{\mathcal{CP}}(\text{charged current}) = \frac{e}{2\sqrt{2}\sin\theta_W} [v_{ij}\bar{d}^j W_\mu \gamma^\mu (1 - \gamma_5) u^i + v_{ij}^* \bar{u}^i W_\mu^* \gamma^{\mu*} (1 - \gamma_5) d^j], \quad (\text{B.35})$$

since, following eqs. (B.29), the term in $W_\mu \gamma^\mu$ is invariant while $W_\mu \gamma^\mu \gamma_5$ changes sign. This is identical to eq. (B.33) except for the $v_{ij} \leftrightarrow v_{ij}^*$ factors interchanged between the two terms of the expression: if the **CKM** matrix were real then the lagrangian would be invariant under \mathcal{CP} , in other words the phase of the **CKM** matrix is at the origin of \mathcal{CP} violation in the Standard Model since all other terms in the lagrangian are invariant under \mathcal{CP} .

B.4 Time reflection \mathcal{T}

The time-reflection transformation takes the coordinate $x = (x_0, \mathbf{x})$ to $x' = (-x_0, \mathbf{x})$. This transformation can be written

$$x'^\nu = a_\mu^\nu x^\mu \quad \text{with} \quad a_\mu^\nu = \begin{pmatrix} -1 & 0 & 0 & 0 \\ 0 & 1 & 0 & 0 \\ 0 & 0 & 1 & 0 \\ 0 & 0 & 0 & 1 \end{pmatrix}. \quad (\text{B.36})$$

Denoting $\psi'(x') \equiv \psi'(-x_0, \mathbf{x})$ the free time-reflected wave function, we attempt to construct it under the form

$$\psi'(x') = \mathcal{T}\psi^*(x), \quad \Rightarrow \quad \psi^*(x) = \mathcal{T}^{-1}\psi'(x'), \quad (\text{B.37})$$

where \mathcal{T} is a 4×4 constant matrix and $\psi(x)$ is the solution of the free Dirac equation with

$$\left(-i\frac{\partial}{\partial x_\mu}\gamma^{\mu*} - m\right)\psi^*(x) = 0, \quad \Rightarrow \quad \left(-i\frac{\partial}{\partial x'_\nu}a_\mu^\nu\gamma^{\mu*} - m\right)\mathcal{T}^{-1}\psi'(x') = 0. \quad (\text{B.38})$$

Multiplying to the left by \mathcal{T} we obtain

$$\left(-i\frac{\partial}{\partial x'_\nu}a_\mu^\nu\mathcal{T}\gamma^{\mu*}\mathcal{T}^{-1} - m\right)\psi'(x') = 0, \quad (\text{B.39})$$

and $\psi'(x')$ will be a solution of the Dirac equation, *i.e.* will satisfy

$$(i\frac{\partial}{\partial x'_\nu}\gamma^\nu - m)\psi'(x') = 0, \quad (\text{B.40})$$

if we find a matrix such that

$$a'_\mu \mathcal{T} \gamma^{\mu*} \mathcal{T}^{-1} = -\gamma^\nu. \quad (\text{B.41})$$

Recalling that $\gamma^{\mu*} = \gamma^\mu$ for $\mu = 0, 1, 3$ and $\gamma^{2*} = -\gamma^2$, the above conditions reduce to $\mathcal{T}\gamma^i = \gamma^i\mathcal{T}$ for $i = 0, 2$ and $\mathcal{T}\gamma^j = -\gamma^j\mathcal{T}$, $j = 1, 3$. The matrix

$$\mathcal{T} = i\gamma^1\gamma^3 \quad (\text{B.42})$$

satisfies the required conditions and we have thus

$$\boxed{\psi'(-x_0, \mathbf{x}) = i\gamma^1\gamma^3\psi^*(x_0, \mathbf{x})} \quad (\text{B.43})$$

the solution for the free wave function evolving backward in time. For an interacting fermion in QED, under time reversal the potential $A'^\mu(x')$ is related to $A^\mu(x)$ by $A'^0(x') = A^0(x)$, $A'^i(x') = -A^i(x)$, since the current reverses sign when the arrow of time is reversed and under this condition we can show that QED is invariant under time reversal.

Combining the symmetries \mathcal{P} and \mathcal{T} one can construct the wave function of an electron evolving backward in space-time,

$$\begin{aligned} \psi^{\mathcal{PT}}(-x) &= \mathcal{PT}\psi(x) = \gamma^0[i\gamma^1\gamma^3\psi^*(x)] \\ &= \gamma^5 i\gamma^2\psi^*(x) \\ &= \gamma_5\psi^c(x), \end{aligned} \quad (\text{B.44})$$

where we introduced the wave-function of the positron via eq. (B.11), Thus the wave function of a (right-handed) positron is that of a (left-handed) electron moving backward in space-time (up to an irrelevant phase factor).

C Feynman rules of the Glashow-Weinberg-Salam model

C.1 Propagators

Massless spin 1 boson (Feynman gauge)

$$\begin{array}{c} \text{~~~~~} \\ \text{k} \end{array} \qquad -i \frac{g^{\mu\nu}}{k^2 + i\epsilon} \qquad (\text{C.1})$$

Massive spin 1 boson

$$\begin{array}{c} \text{~~~~~} \\ \text{k} \end{array} \qquad -i \frac{g^{\mu\nu} - k^\mu k^\nu / M^2}{k^2 - M^2 + i\epsilon} \qquad (\text{C.2})$$

Fermion

$$\begin{array}{c} \text{-----} \\ \text{p} \end{array} \qquad i \frac{\not{p} + m}{p^2 - m^2 + i\epsilon} \qquad (\text{C.3})$$

Massive spin 0 boson

$$\begin{array}{c} \text{-----} \\ \text{k} \end{array} \qquad \frac{i}{k^2 - m^2 + i\epsilon} \qquad (\text{C.4})$$

C.2 Vertices

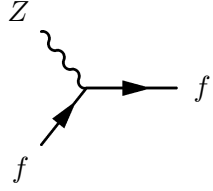
Fermion-fermion- γ vertex

$$\begin{array}{c} \gamma \\ \text{~~~~~} \\ \text{f} \text{-----} \text{f} \\ \text{f} \text{-----} \end{array} \qquad -i Q_e e \gamma^\mu \qquad (\text{C.5})$$

Fermion-fermion- W^\pm vertex

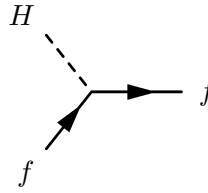
$$\begin{array}{c} W^\pm \\ \text{~~~~~} \\ \text{f} \text{-----} \text{f} \\ \text{f} \text{-----} \end{array} \qquad -i \frac{e}{2\sqrt{2} \sin \theta_w} \gamma^\mu (1 - \gamma^5) \qquad (\text{C.6})$$

Fermion-fermion- Z vertex



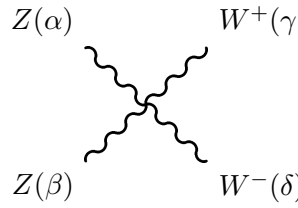
$$-i \frac{e}{2 \sin \theta_w \cos \theta_w} \gamma^\mu \left[\left(I_3^f - 2 Q_f \sin^2 \theta_w \right) - I_3^f \gamma^5 \right] \quad (\text{C.7})$$

Fermion-fermion- H vertex



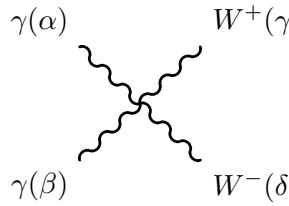
$$-i \frac{e}{2 \sin^2 \theta_w} \frac{m_f}{M_w} \quad (\text{C.8})$$

Z - Z - W^+ - W^- vertex



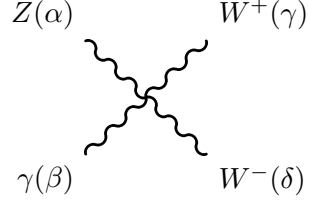
$$i e^2 \frac{\cos^2 \theta_w}{\sin^2 \theta_w} \left[g^{\alpha\delta} g^{\beta\gamma} + g^{\alpha\gamma} g^{\beta\delta} - 2 g^{\alpha\beta} g^{\gamma\delta} \right] \quad (\text{C.9})$$

γ - γ - W^+ - W^- vertex



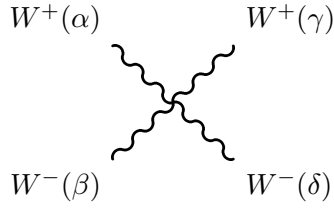
$$i e^2 \left[g^{\alpha\delta} g^{\beta\gamma} + g^{\alpha\gamma} g^{\beta\delta} - 2 g^{\alpha\beta} g^{\gamma\delta} \right] \quad (\text{C.10})$$

Z - γ - W^+ - W^- vertex



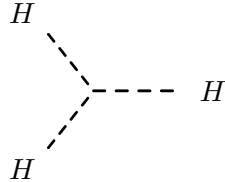
$$i e^2 \frac{\cos \theta_w}{\sin \theta_w} \left[g^{\alpha\delta} g^{\beta\gamma} + g^{\alpha\gamma} g^{\beta\delta} - 2 g^{\alpha\beta} g^{\gamma\delta} \right] \quad (\text{C.11})$$

W^+ - W^- - W^+ - W^- vertex



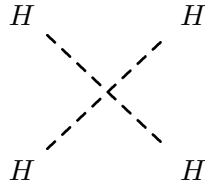
$$i \frac{e^2}{\sin^2 \theta_w} \left[g^{\alpha\delta} g^{\beta\gamma} + g^{\alpha\gamma} g^{\beta\delta} - 2 g^{\alpha\beta} g^{\gamma\delta} \right] \quad (\text{C.12})$$

H - H - H vertex



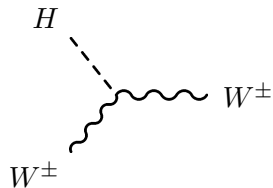
$$-i \frac{3}{2} \frac{e}{\sin \theta_w} \frac{M_H^2}{M_W} \quad (\text{C.13})$$

H - H - H - H vertex



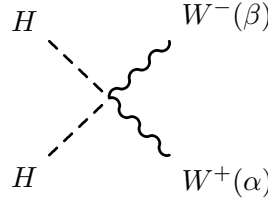
$$-i \frac{3}{4} \frac{e^2}{\sin^2 \theta_w} \frac{M_H^2}{M_W^2} \quad (\text{C.14})$$

H - W^+ - W^- vertex



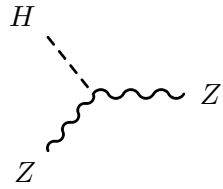
$$i \frac{e}{\sin \theta_w} M_W g^{\alpha\beta} \quad (\text{C.15})$$

H - H - W^+ - W^- vertex



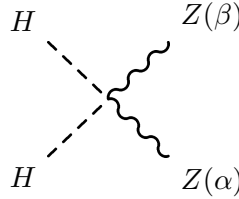
$$i \frac{e^2}{2 \sin^2 \theta_w} g^{\alpha\beta} \quad (\text{C.16})$$

H - Z - Z vertex



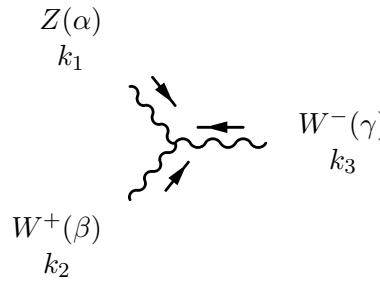
$$i \frac{e}{\sin \theta_w \cos \theta_w} M_Z g^{\alpha\beta} \quad (\text{C.17})$$

H - H - Z - Z vertex



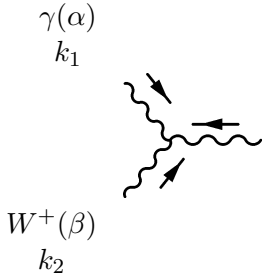
$$i \frac{e^2}{2 \sin^2 \theta_w \cos^2 \theta_w} g^{\alpha\beta} \quad (\text{C.18})$$

Z - W^+ - W^- vertex



$$i e \frac{\cos \theta_w}{\sin \theta_w} \left[g^{\alpha\beta} (k_1 - k_2)^\gamma + g^{\beta\gamma} (k_2 - k_3)^\alpha + g^{\gamma\alpha} (k_3 - k_1)^\beta \right] \quad (\text{C.19})$$

γ - W^+ - W^- vertex



$$i e \left[g^{\alpha\beta} (k_1 - k_2)^\gamma + g^{\beta\gamma} (k_2 - k_3)^\alpha + g^{\gamma\alpha} (k_3 - k_1)^\beta \right] \quad (\text{C.20})$$